

Propagation of drought through groundwater systems

Illustrated in the Pang (UK) and
Upper-Guadiana (ES) catchments

Promotor: Prof. dr. ir. R. A. Feddes,
Hoogleraar in de bodemnatuurkunde, agrohydrologie
en het grondwaterbeheer,
Wageningen Universiteit

Co-Promotor: dr. ir. H. A. J. van Lanen,
Universitair hoofddocent bij de leerstoelgroep
Hydrologie en kwantitatief waterbeheer,
Wageningen Universiteit

Samenstelling Promotiecommissie:

Ass. Prof. dr. L. M. Tallaksen, University of Oslo, Noorwegen
Prof. dr. ir. M. F. P. Bierkens, Universiteit Utrecht
dr. ir. C. Maas, Kiwa Water Research/Technische Universiteit Delft
Prof. dr. ir. P. A. Troch, Wageningen Universiteit

ELISABETH PETERS

PROPAGATION OF DROUGHT THROUGH
GROUNDWATER SYSTEMS

ILLUSTRATED IN THE PANG (UK) AND
UPPER-GUADIANA (ES) CATCHMENTS

PROEFSCHRIFT

ter verkrijging van de graad van doctor
op gezag van de rector magnificus
van Wageningen Universiteit,
prof. dr. ir. L. Speelman,
in het openbaar te verdedigen
op dinsdag 2 december 2003
des namiddags te vier uur in de Aula.

*Nation shattered,
mountains and rivers stay*

Tu Fu, 757 AD

Peters, E.
Propagation of drought through groundwater systems
Illustrated in the Pang (UK) and Upper-Guadiana (ES) catchments
Dissertation Wageningen Universiteit, Wageningen 2003
ISBN 90-5808-980-0
Copyright © E. Peters, 2003.
Photo cover © Corbis/TCS.

Abstract

Peters, E., 2003. *Propagation of drought through groundwater systems - Illustrated in the Pang (UK) and Upper-Guadiana (ES) catchments*. Ph.D. thesis, Wageningen University, The Netherlands. 203 pp.

The transformation of droughts as a result of the propagation through groundwater systems is examined by comparing droughts in time series of groundwater recharge, levels and discharge. The groundwater system was simulated mostly as a reservoir, characterised by a reservoir coefficient j (d). Different aquifer characteristics were simulated using a range of j -values. A groundwater system causes attenuation and increasing persistence in the discharge. The attenuation decreases the drought severity, whereas the increasing persistence makes the cumulative probability distribution of both drought duration and severity steeper. This means that recharge and discharge from fast responding catchments (small j) have a large number of relatively unsevere droughts, whereas slowly responding catchments have fewer droughts, but a larger probability of severe droughts. To evaluate the overall performance of the groundwater system with respect to drought, a new performance criterion has been introduced. This criterion shows that groundwater reservoirs with intermediately fast response ($j \approx 200$ d) have the lowest overall performance. The highest overall performance occurs for slowly responding systems. The influence of the characteristics of the recharge has been examined by using recharge from two catchments: the sub-humid Pang catchment (UK) and the semi-arid Upper-Guadiana catchment (ES). The most important difference between the two catchments with respect to the propagation of drought is the difference in seasonality. The strong seasonality for the Pang prevents the pooling of droughts. For the semi-arid catchment, the increase in the number of severe droughts as a result of the propagation through the groundwater system was much higher and thus the overall performance was much lower. For the Pang catchment, a physically based groundwater flow model was used to examine the spatial distribution of drought. After normalising the groundwater levels with the standard deviation, the variations in the persistence dominate the drought behaviour in the groundwater levels. Thus the cumulative probability distribution close to the stream was less steep than at the interflaves. Finally, non-linearity in the groundwater level-discharge relationship increases the drought duration and, for most droughts, the severity.

Index words: drought, groundwater, simulation, synthetic data, extreme events

Voorwoord

De zomer van 2003 was een van de heetste en droogste zomers sinds lange tijd. Bosbranden, een sterke toename in het aantal sterfgevallen onder ouderen, schade aan land- en tuinbouw en problemen met de elektriciteitsvoorziening zijn slechts enkele van de vele problemen die het gevolg waren van de droogte. Tegen deze achtergrond kreeg het afronden van mijn proefschrift een extra betekenis.

Nu rest mij slechts het bedanken van al diegenen die dit onderzoek mogelijk gemaakt en ondersteund hebben. In de eerste plaats gaat mijn dank uit naar Henny van Lanen die deze studie mogelijk gemaakt heeft. Ondanks een overvolle agenda wist hij toch altijd tijd te vinden om over droogte na te denken. Mijn oprechte dank daarvoor. Mijn dank gaat ook uit naar Reinder Feddes, die met name in de laatste fase een sturende rol heeft gespeeld. Verder ben ik veel dank verschuldigd aan de leden van de begeleidingsgroep Paul Torfs, George Bier, Jos van Dam, Eric Querner en Toon Leijnse. Met name Paul Torfs was als buurman van onschatbare waarde bij alle mogelijke (wiskundige) problemen. George Bier zou ik willen bedanken voor zijn hulp met de modellering van de verzadigde grondwaterstroming en Jos van Dam voor zijn hulp met SWAP. Also I would like to especially thank Rafal Wójcik for his help on Nearest Neighbour Resampling. Aan de studenten die meegewerkt hebben: Rosalie Franssen, Arwen Looijaard en Mechteld ter Horst, mijn hartelijke dank. Natuurlijk ook mijn kamergenoten Marc Hoffmann, Ruben IJpelaar en Shaakeel Hasan wil ik graag bedanken. Met name Marc ben ik veel dank verschuldigd voor zijn vriendschap, zijn hulp met vele praktisch problemen en natuurlijk voor zijn hulp met L^AT_EX. Roel Dijkema wil ik graag bedanken voor zijn hulp in the Pang. Verder wil ik alle andere collega's op de Nieuwlanden bedanken voor hun steun en interesse en de prettige werkomgeving die ze mij geboden hebben.

Ook buiten de vakgroep hebben velen geholpen. Specifiek gaat mijn dank uit naar Hans Gehrels, Eddy Moors en Joop Kroes, maar ook naar al die anderen die gedurende conferenties en workshops commentaar en hulp geleverd hebben. Finally I would like to thank Ladislav Holko for his helpful discussions on base flow separation.

During the first two years of my PhD, I worked in the framework of the ARIDE project. Afterwards I was involved in the ASTHyDA project. Hereby I would like to thank all the members of the ARIDE and ASTHyDA teams for the in-

teresting discussions, stimulating questions and useful comments. Also I would like to thank Joaquin Cruces and Luis Martinez, who made it possible for me to spend three weeks in Santander and get acquainted with the model of the Upper-Guadiana catchment. Special thanks are due to Javier Álvarez and Pedro Fernandez for facilitating the data supply for the Upper-Guadiana catchment from CEDEX. At CEH (UK), Dick Bradford provided the same service. For that and all his help with supervising the students, many thanks.

I am very grateful to the many institutions that have provided the data that have made this study possible. For providing data for the Pang catchment acknowledgements are due to the following institutions:

- The UK Meteorological Office through the British Atmospheric Data Centre for the meteorological data.
- The Environment Agency (England and Wales) for the flow data.
- The Centre for Ecology and Hydrology (former Institute of Hydrology) for spatial data and groundwater level observation data.
- The Institute for Terrestrial Ecology for the land use data.

For providing the information and data for the Upper-Guadiana catchment and the simulations of the SIMPA model, I am greatly indebted to CEDEX.

The research presented in this thesis was carried out under the Programme of the Wageningen Institute of Environment and Climate Research (WIMEK-SENSE) and the FRIEND project, which is part of UNESCO's International Hydrological Programme. In part this work was carried out in the framework of the ARIDE project (Assessment of the Regional Impact of Droughts in Europe) and of the ASTHyDA project (Analysis, Synthesis and Transfer of Knowledge and Tools on Hydrological Droughts Assessment through a European Network). For the ARIDE project support was given by the European Commission under contract no. ENV4-CT97-0553 and for the ASTHyDA project under no. EVK1-2001-00166.

Promoveren doe je niet alleen op je werk, maar dat neem je ook mee naar huis. Daarom wil ik mijn familie en vrienden bedanken voor hun niet aflatende interesse en steun. Ria en Jaap, Paul en Nelleke en Anne, bedankt voor jullie interesse, steun en vriendschap. Mam, pap, voor alles, bedankt. Robert, je weet wel waarvoor... Bedankt.

Contents

List of frequently used symbols	xv
1 Introduction	1
1.1 An anatomy of drought	1
1.2 Main themes and gaps in drought research	2
1.3 Concept of groundwater drought	4
1.4 Thesis objective	7
1.5 Thesis outline	7
2 Description of the Pang and Upper-Guadiana catchments	9
2.1 Pang catchment	9
2.1.1 Introduction	9
2.1.2 Climate	9
2.1.3 Geology	10
2.1.4 Hydrogeology	14
2.1.5 Soils	16
2.1.6 Land use	17
2.1.7 Hydrology	18
2.2 Upper-Guadiana catchment	21
2.2.1 Climate	21
2.2.2 Soils	21
2.2.3 Land use	23
3 Groundwater drought	25
3.1 Causes and effects of groundwater drought	25
3.2 Groundwater drought research	27
3.3 Propagation of drought through groundwater systems	28

3.4	Drought event definition	31
3.5	Summary and conclusions	33
4	Propagation of individual droughts through the groundwater system - an analytical approach using synthetic recharge	35
4.1	Introduction	36
4.2	Definition of drought events	37
4.3	The propagation of a drought in a linear reservoir	39
4.4	Recharge and discharge	41
4.4.1	Definition of the recharge	41
4.4.2	Derivation of the discharge	42
4.5	Derivation of drought duration and deficit	44
4.5.1	Threshold level	44
4.5.2	Duration and deficit	45
4.6	Results	48
4.6.1	Recharge	48
4.6.2	Discharge	49
4.7	Discussion	51
4.7.1	Influence of the drought event definition	51
4.8	Conclusions	53
5	Propagation of individual droughts through the groundwater system using recharge simulated observed meteorological data from two contrasting climatic regimes	59
5.1	Introduction	59
5.2	Data and methods	60
5.3	Results	61
5.4	Conclusions	64
6	Propagation of drought through groundwater systems - drought distribution and performance criteria for the Pang catchment	65
6.1	Introduction	66
6.2	Description of data and methods	67
6.2.1	Generating synthetic data	68

6.2.2	Simulation of groundwater recharge and discharge . . .	69
6.2.3	Drought event definition	72
6.3	Return periods and performance	73
6.3.1	Return periods	73
6.3.2	Performance	74
6.4	Results	77
6.4.1	Distribution of droughts	77
6.4.2	Performance	78
6.5	Discussion	82
6.6	Conclusions	84
7	Sensitivity analysis and validation of the linear reservoir concept	87
7.1	Influence of recharge characteristics on the frequency distribution of drought	87
7.1.1	Simulation of recharge for the Upper-Guadiana	88
7.1.2	Comparison of droughts for the Pang and Upper-Guadiana	89
7.2	Non-linearity versus linearity of the groundwater reservoir . . .	94
7.2.1	Simulation of discharge from a non-linear reservoir . . .	94
7.2.2	Results	96
7.3	Validation of the propagation of drought through a linear reservoir using data from the Pang catchment	100
7.3.1	Approach	100
7.3.2	Estimation of the reservoir coefficient j	101
7.3.3	Results for droughts in recharge and base flow	103
7.3.4	Results from the frequency distribution	103
7.4	Conclusions	105
8	Spatial aspects of drought in a groundwater catchment	107
8.1	Introduction	107
8.2	Simulation of the spatial distribution of groundwater recharge, levels and discharge for the Pang	108
8.2.1	Derivation of droughts	109

8.3	Results	110
8.4	Discussion	117
8.5	Conclusions	122
9	Summary and conclusions	125
9.1	Conclusions	125
9.2	Recommendations for future research, perspectives	131
	Samenvatting	134
A	Simulation of recharge for the Pang catchment with the SWAP model	143
A.1	Simulation of the recharge	143
A.1.1	Calculation Procedure	143
A.1.2	Description of the input	145
A.2	Recharge results	149
B	Simulation of recharge for the Upper-Guadiana catchment with the SIMPA model	153
B.1	Simulation of the recharge	153
B.2	Recharge results	154
C	Separation of base flow from streamflow using groundwater levels - illustrated for the Pang catchment (UK)	157
C.1	Introduction	158
C.2	Derivation of the filter equations	159
C.3	Data and methods	162
C.4	Parameter estimation	165
C.5	Results	166
C.6	Comparison of base flow separation methods	170
C.6.1	BFI filter	170
C.6.2	Boughton filter	171
C.6.3	Kliner and Kněžek filter	173
C.7	Discussion	174
C.8	Conclusions	176

D Description of the groundwater flow model for the Pang catchment	179
D.1 Definition of the groundwater flow model	179
D.1.1 Hydrogeological schematisation and discretisation	179
D.1.2 Input data MODFLOW	181
D.2 Calibration	184
D.2.1 Input for PEST	184
D.2.2 Results of the calibration and validation	187
D.3 Simulated hydraulic heads and discharge	188
Bibliography	191
Curriculum Vitae	201

List of frequently used symbols

Symbol	Description	Dimension	Applied unit
A	$\sqrt{(1/j)^2 + (2\pi\omega)^2}$ in Equation (4.12)	T^{-1}	d^{-1}
A_f	surface area contributing to fast runoff	L^2	m^2
a	parameter in Equation (C.1)	$L^{3-3b}T^b$	$m^{3-3b}s^b$
a	parameter in Equation (7.1)	$L^{1-b}T^b$	$mm^{1-b}month^b$
B	$\arcsin(\frac{-2\pi\omega}{A})$ in Equation (4.12)	-	-
b	parameter indicating non-linearity	-	-
C	parameter in Equation (C.8)	-	-
C_r	capillary rise flux	$L T^{-1}$	$mm d^{-1}$
c	drought criterion	-	-
ET	evapotranspiration flux	$L T^{-1}$	$mm d^{-1}$
ET_{pot}	potential evapotranspiration flux	$L T^{-1}$	$mm d^{-1}$
ET_a	actual evapotranspiration flux	$L T^{-1}$	$mm d^{-1}$
f_d	drought fraction	-	-
f_t	crop factor	-	-
H	groundwater level	L	m
h	soil water pressure head	L	cm
I_m	information content	-	-
I_s	infiltration flux	$L T^{-1}$	$mm d^{-1}$
j	reservoir coefficient	T	d
$j(q)$	reservoir coefficient in Equation (7.1)	T	d
j_i	equivalent reservoir coefficient	T	d
K	parameter in Correia loss function	-	-
k	hydraulic conductivity	$L T^{-1}$	$m d^{-1}$
k	recession constant in Equation (C.8)	-	-
kD	transmissivity	L^2T^{-1}	m^2d^{-1}
L	drought duration	T	varying
L_m	duration of multi-year drought	T	varying
L_w	duration of within-year drought	T	varying
l	distance between streams	L	m
M	length of a time series	T	varying
m_t	number of days in month t	-	-
N	number of years	-	-
n	number of droughts/observations	-	-
P	precipitation flux	LT^{-1}	$mm d^{-1}$
P_s	stemflow flux	LT^{-1}	$mm d^{-1}$
P_t	throughfall flux	LT^{-1}	$mm d^{-1}$
p	performance	-	-
$p_{D,10}$	performance in Equation (6.16)	-	-
$p_{D,Cor}$	performance in Equation (6.18)	-	-
$p_{D,yr}$	performance in Equation (6.14)	-	-

Symbol	Description	Dimension	Applied unit
Q	discharge	L^3T^{-1}	m^3s^{-1}
q	discharge	LT^{-1}	varying
Q_f	direct runoff ('fast')	L^3T^{-1}	m^3s^{-1}
Q_i	interflow	L^3T^{-1}	m^3s^{-1}
Q_o	overland flow	L^3T^{-1}	m^3s^{-1}
Q_s	base flow ('slow')	L^3T^{-1}	m^3s^{-1}
R	recharge flux	LT^{-1}	$mm\ d^{-1}$
R_0	long term average recharge flux	LT^{-1}	$mm\ d^{-1}$
R^2	model efficiency	-	-
R_{JJA}^2	model efficiency in June, July, August	-	-
R_i	indirect recharge flux	LT^{-1}	$mm\ d^{-1}$
R_p	discharge at bottom of root zone	LT^{-1}	$mm\ d^{-1}$
$r\nu$	scaled vulnerability	-	-
S	storage	L^3 or L	m^3 or mm
S_f	storage for 'fast' runoff component	L	m^3d^{-1}
S_L	sustainability index (Equation (6.11))	T^{-1}	$month^{-1}$
S_r	soil moisture storage in root zone	L	mm
S_s	specific storage	L^{-1}	m^{-1}
S_s	storage for 'slow' runoff component	L^3	m^3d^{-1}
S_y	specific yield	-	-
$T(x)$	return period for x	T	years
t	time	T	varying
U_r	root water uptake flux	LT^{-1}	$mm\ d^{-1}$
w	weight in objective function	varying	varying
$X(c)$	shape factor to determine threshold	-	-
α	reliability	-	-
β	$\frac{1}{j(q)b}$ in Equation (7.2)	T^{-1}	d^{-1}
γ	resilience	T^{-1}	$month^{-1}$
ε_d	maximum discretisation error	%	%
θ	soil moisture content	-	-
λ	average number of droughts per year	T^{-1}	a^{-1}
μ	storage coefficient	-	-
ν	vulnerability	varying	varying
$\pi 1$	no. of exceedances	-	-
$\pi 2$	deviation from the annual minimum	varying	varying
ϕ	objective function	varying	varying
ω	frequency	T^{-1}	d^{-1}
Operators			
AC	autocorrelation coefficient	-	-
$B_s(x)$	bias	$\dim[x]$	$\text{unit}[x]$
D	drought deficit	$\dim[x]T$	varying
Dc	decrease of x compared to average	$\dim[x]$	$\text{unit}[x]$
Dm	deficit of multi-year drought	$\dim[x]T$	varying
D_{norm}	normalised drought deficit	T	d
	normalised using σ		
D_{rel}	relative drought deficit	-	-

Symbol	Description	Dimension	Applied unit
	fraction of the annual recharge or discharge		
D_w	drought deficit of within-year drought	$\text{dim}[x]T$	varying
$F(x)$	cumulative distribution function of x	-	-
$f(x)$	probability density function of x	$\text{dim}[x^{-1}]$	$\text{unit}[x^{-1}]$
I	drough intensity	$\text{dim}[x]$	$\text{unit}[x]$
$r(x)$	rank of x	-	-
$s(x)$	severity function	-	-
$\mu(x)$	average of x	$\text{dim}[x]$	$\text{unit}[x]$
$\sigma(x)$	standard deviation of x	$\text{dim}[x]$	$\text{unit}[x]$
ρ	cross correlation coefficient	-	-
\bar{x}	average of x	$\text{dim}[x]$	$\text{unit}[x]$
Subscripts			
b	beginning		
Cor	Correia		
cp	critical point below which ET is reduced		
d	drought		
e	end		
f	direct runoff ('fast')		
fc	field capacity		
max	maximum		
n	normal or average situation		
norm	normalised		
r	root zone		
rel	relative		
s	base flow ('slow')		
T	threshold to determine droughts		
tr	point below which no runoff occurs		
wp	wilting point		
yr	year		

Chapter 1

Introduction

1.1 An anatomy of drought

Drought is one of the main weather-related disasters, but has a significantly different character from other types of disasters. It is a slow, creeping event, for which neither the beginning nor the end may be clearly defined (Wilhite, 1999). Yet, it causes extensive damage throughout the world. The Federal Emergency Management Agency (1995) estimates the annual cost of droughts in the United States at \$6-8 billion, which is more than the cost of either floods or hurricanes (National Drought Mitigation Center, 2003). In developed humid and sub-humid areas the damage caused by droughts is mainly monetary, whereas in developing areas with (semi-) arid climates, drought threatens the very livelihood of people. However, improved monitoring and management of the water resources and understanding of the development of droughts can mitigate the impact of droughts. For example, improved forecasting and monitoring of drought parameters and early warning considerably reduced the impact of the 1994-95 drought in the South African Development Community (SADC) countries (Garanganga, 1999).

Although drought is an ancient concept, it is not easily defined. Drought is a complex phenomenon, with manifests itself in different parts of the hydrological system and at different spatial and temporal scales. To different people, droughts have different meanings. For example, to a farmer a drought may occur when during the growing season the amount of soil moisture is insufficient (Illston and Basara, 2003). For a manager of a surface water reservoir, a drought occurs when the amount of streamflow is insufficient to keep reservoir levels and outflow at a required level, while a villager in southern Africa experiences drought when his well dries up (Calow *et al.*, 1999). From an ecological point of view, a drought occurs mainly when the amount of precipitation is significantly less than the expected amount. For example, for natural vegetation in the arid zone of California a single year without precipitation is not exceptional. Only when it lasts for several years in a row, it is a drought (Clark, 1993). Because of these and many other different interpretations of drought it is extremely difficult to arrive at a common definition of drought. This is possibly one of the great obstacles for drought research (Beran and Rodier,

1985; Yevjevich, 1967).

In this thesis the following definitions will be used, which closely follow the definitions given in the recent textbook on hydrological drought by Tallaksen and van Lanen (2004). A *permanent* low availability of precipitation, moisture or water is not called a drought but *aridity*¹. Also downward *trends* in water availability are not droughts but are called *desiccation*, *aridification* or *desertification*. Another important definition is the difference between low flow and drought. *Low flows* are the annually recurring low streamflows in areas with a clear seasonality. Following the definition by Beran and Rodier (1985) droughts are viewed in this thesis as ‘a decrease in water availability in a particular period over a particular area’.

Classification of droughts Droughts are commonly classified into four categories (Figure 1.1), which are mostly based on different parts of the hydrological cycle. Droughts generally start with a lack of precipitation, possibly in combination with high evapotranspiration, resulting from the natural variability of the weather. This is called a *meteorological drought*. The meteorological drought causes a lack of soil moisture, which is called a *soil moisture drought* and which affects agricultural crops and/or the natural vegetation. The soil moisture drought is also frequently called *agricultural drought*. A lack of precipitation may also cause low streamflows: the *streamflow drought*. The soil moisture drought causes a decrease in the amount of recharge, which in turn causes lower groundwater levels and decreasing groundwater discharge to the surface water system, which is a *groundwater drought*. Both the streamflow drought and the groundwater drought are part of the *hydrological drought* in Figure 1.1. The *socio-economic drought* expresses the deficit of water as an economic good and addresses the damage caused by all the different types of drought.

1.2 Main themes and gaps in drought research

Although droughts have not been studied as extensively as floods, the amount of research on drought is substantial. Because a full review of drought research is beyond the scope of this study, only an overview of the main topics will be presented. Drought research can roughly be divided in three categories:

- drought frequency analysis;
- regionalisation of drought;

¹Some authors use the term *dryness* to describe a permanent low availability of water, for example Deutscher Verband Für Wasserwirtschaft und Kulturbau (1998).

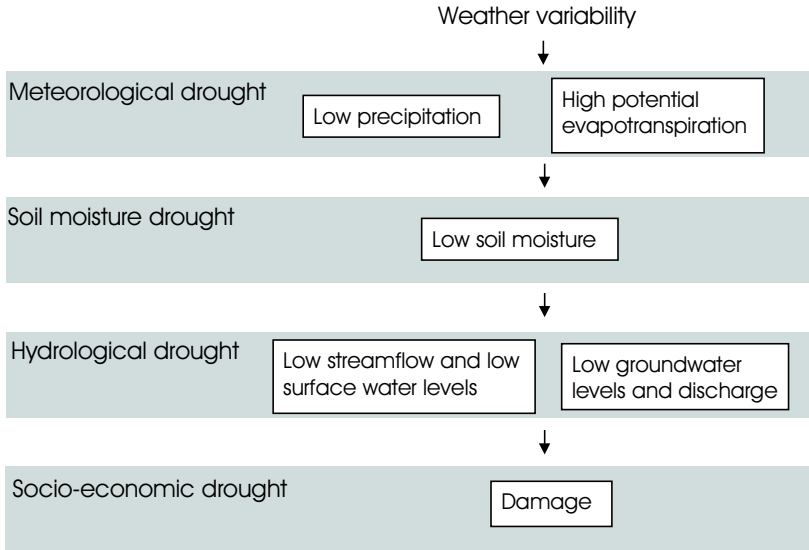


Figure 1.1: Drought classification after Hisdal *et al.* (2004) and National Drought Mitigation Center (2003)

- and drought management (monitoring, prediction and mitigation).

Drought frequency analysis includes the estimation of the return period of historical droughts and the estimation of future drought risks for the design of structures and for water management (Sharma, 1998; Tallaksen, 2000; Klemeš, 2000; Kjeldsen *et al.*, 2000; Hisdal *et al.*, 2002). Historically, this was a purely statistical activity, however more recently there have been attempts to derive distribution functions for the annual minimum flow based on the exponential recession curve of the outflow from groundwater reservoirs (Gottschalk and Perzyna, 1989; Gottschalk *et al.*, 1997).

The *regionalisation of drought* covers both the analysis of regional aspects of drought and the estimation of drought characteristics at ungauged sites. The estimation of drought characteristics at the ungauged site is usually divided in two steps: first, the delineation of homogeneous areas and second, relating drought characteristics to catchment characteristics like catchment area, precipitation characteristics, soil characteristics, drainage density and geology using multiple regression techniques (Demuth *et al.*, 2004; Smakhtin, 2001). These studies show that geology is an important factors, since groundwater discharge is the main component of streamflow during dry periods (Demuth *et al.*, 2004).

For *drought management* attention is focused on mitigation of droughts by early-warning systems and developing pro-active water management to replace reactive disaster-management. The most well-developed example of a drought early warning system is probably the drought monitor in the USA (Svoboda *et al.*, 2002). Another example is the worldwide monitoring of vegetation health indices using AVHRR data (Kogan, 2002). Historically, this type of research was more concerned with meteorological and agricultural drought, but now it includes all parts of the hydrological system. Recently this type of research has also been extended to include drought prediction on longer time-scales (long-range forecasting) by seeking relationships between large-scale weather patterns and drought. The most well-researched relation or teleconnection is probably between the El Niño-Southern Oscillation (ENSO) phenomenon and below average precipitation in large parts of southern Asia and Australia (Chiew and McMahon, 2002; Caruso, 2002). Other relationships are for example sought with the North Atlantic Oscillation Index (NAOI) (Stahl, 2001) and the North Atlantic Sea Surface Temperature (Lloyd-Hughes, 2002).

Gaps in drought research Panu and Sharma (2002) have analysed the field of drought research and have identified three areas where drought research shows gaps: first, the relation between crop yield and soil moisture deficit, second, the regional aspect of drought and third, forecasting of start and end of droughts. However, other authors have identified additional gaps in drought research. Robins *et al.* (1997) and Calow *et al.* (1999) note that the logical propagation of drought through the catchment has been studied insufficiently, especially for areas, which are dominated by groundwater. Leonard (1999) also notices the lack of understanding of the propagation of the temporal variability of the climate in groundwater. In fact, according to van Lanen and Peters (2000) drought in groundwater explicitly has hardly been investigated at all. Another area, which has been investigated insufficiently, is the interaction and possible feedback between land surface and atmosphere during drought (Delworth and Manabe, 1989; McNab and Karl, 1991). This may be important because a land surface, dried out as a result of drought, may provide insufficient moisture for subsequent rainfall, thus making a drought persistent. Finally, Smakhtin (2001) concludes his review of low flow hydrology with the remark that the understanding of the different low-flow generating mechanisms in the catchment remains rather limited at the moment.

1.3 Concept of groundwater drought

The reason for the limited interest in droughts in groundwater may be understood from the different concepts of groundwater drought that occur in different publications and which appear to have changed over time. Changes

possibly occurred because of the increasing exploitation and over-exploitation of groundwater systems (Custodio, 2000; Foster, 2000), but also because several severe droughts in the recent past have exacerbated the problems with, often already stressed, groundwater resources. Examples of such events are the 1988-92 drought in the UK (Marsh *et al.*, 1994; Bryant *et al.*, 1994) and the 1991-93 drought in Southern Africa (Garanganga, 1999; Calow *et al.*, 1999).

The conventional concept of drought in groundwater (Day and Rodda, 1978; Shiva, 1991; Calow *et al.*, 1999), which is oriented towards groundwater management, is illustrated well by the discussion of the 1975-76 drought in the UK by Day and Rodda (1978)². First, the authors state that, under natural conditions, a drought will not affect groundwater very much, because after a short while the discharge from the aquifer becomes so low that the aquifer is in effect no further emptied and the groundwater levels reach a kind of minimum level. Only abstractions can cause the water level to fall below this minimum level. This implies that only abstractions can cause a groundwater drought. Second, below this minimum level is a large static water reserve, the 'static storage', which can be used in periods of drought for river augmentation. They state, however, that great care is needed in locating the abstraction wells for such a scheme.

Although the concept, illustrated using the example of Day and Rodda (1978), may hold for some aquifers, in others it can be misleading as already noted by Yevjevich (1968). First, natural droughts can affect groundwater, because the concept that the groundwater system will stop discharging relatively quickly can be wrong. Lewis *et al.* (1993) note that base flow from Chalk aquifers in the UK was larger than expected during drought. In fact because of its reliability, many communities rely on base flow during drought. Moreover, discharge to, for example, deeper layers or the sea in case of coastal aquifers may continue during drought. The second point is the use of the 'static storage' for river augmentation. Use of this water, as Day and Rodda themselves state, means that it has to be replenished in the winter afterwards. If this fails to happen, large volumes of water will have to be supplied to keep the river flowing all through the following year. And depending on the scale of the abstractions, the groundwater levels may take years to recover. Moreover, when using this 'static storage', the negative impact of low groundwater levels, like for example salt water intrusion, is ignored. Day and Rodda (1978) considered this acceptable, as they figure that the possibility of recurrence for such a severe event as the 1975-76 drought is remote. The future has proven them to be wrong, as already in 1988 to 1992 an even more severe drought occurred in large parts (especially

²This concept is related to the misleading concept of 'safe yield', in which it is considered sustainable to abstract an amount of water equal to the groundwater recharge, without considering, for example, the impact on groundwater discharge (Sophocleous, 1997; Bredehoeft, 1997, 2002; Kendy, 2003). Both concepts view the groundwater system as a static reservoir, rather than a dynamic part of the hydrological cycle.

the east and the south) of the UK. During this drought, groundwater levels fell below their apparent minimum level, also in boreholes largely unaffected by human activity (Bryant *et al.*, 1994).

An opposing concept of groundwater drought views the groundwater system as an integral part of the hydrological system ('dynamic storage') and groundwater droughts as the effect of the temporal variability of the weather on groundwater (Figure 1.1). Because of the short-comings in the conventional concept on groundwater, nowadays the concept of groundwater drought as a result of the temporal variability of the weather is used increasingly (Chang and Teoh, 1995; Eltahir and Yeh, 1999; White *et al.*, 1999).

A second important question for defining groundwater drought is whether it should have any negative impacts (on society or the environment) before it is to be called a drought. Especially for groundwater this question is relevant, as droughts in groundwater are often 'invisible' (Swistock, 2002). For example, Calow *et al.* (1999) define groundwater drought as 'a situation where groundwater sources fail as a direct consequence of drought'. Guerrero-Salazar and Yevjevich (1975) define a drought in general when supply cannot meet the demand.

A third issue relevant for the concept of groundwater drought, is the variable that should be used to quantify it. For groundwater, the total amount of water available is difficult to define. And even if it can be defined, in most groundwater systems, negative impacts of storage depletion can be felt, long before the total storage is depleted (van Lanen and Peters, 2000; Calow *et al.*, 1999). So, most often groundwater drought is defined by the decrease of the groundwater level (Chang and Teoh, 1995; Eltahir and Yeh, 1999). However, groundwater storage, or groundwater recharge (Marsh *et al.*, 1994) or discharge (Peters *et al.*, 2001) can and have also been used to define or quantify a groundwater drought.

In this thesis, groundwater droughts are defined as *a decrease in water availability (with or without a negative impact) caused by the variability of the weather*. Analysis of the additional impact of exploitation is beyond the scope of the present study. For this readers are referred to Peters and van Lanen (2001) and van Lanen and Peters (2002). In this thesis, a drought will be defined with respect to the natural fluctuation, irrespective of whether or not such a drought has any socio-economic or environmental consequences and groundwater levels, recharge and discharge will be used to analyse groundwater droughts.

1.4 Thesis objective

In this thesis, the propagation of the drought in the groundwater system will be examined. Hence, the central objective of this thesis is to answer the following question:

‘How do droughts change as a result of their propagation through groundwater systems and how does this transformation depend on the characteristics of the climate and the groundwater system?’

The secondary objective is to develop the concept of groundwater drought further and to examine how groundwater droughts should be defined.

1.5 Thesis outline

The outline of the thesis is as follows:

- In Chapter 2 the catchments of the Pang and Upper-Guadiana will be described. The Pang catchment is described in more detail than the Upper-Guadiana, because it will be used more extensively.
- In Chapter 3 the concept of groundwater drought is discussed, as well as the drought event definition used to derive the actual drought events from the time series of groundwater recharge, levels and discharge.
- In Chapter 4 the propagation of an individual drought through groundwater will be examined using an analytical approach. The flow and storage in an aquifer will be approximated by a range of linear reservoirs. For the recharge a synthetic signal will be used.
- In Chapter 5 the results of Chapter 4 will partly be validated by using recharge from the Pang and Upper-Guadiana catchments as input to a range of linear reservoirs.
- In Chapter 6, instead of the propagation of an individual drought, the propagation of the frequency distribution of droughts will be investigated. Therefore long time series of recharge for the Pang catchment will be simulated. Again, a range of linear reservoirs is used to simulate the groundwater system. The simulated drought distributions will be used to introduce a new way of expressing the performance of groundwater systems with respect to drought.

- In Chapter 7 the validity of the results and assumptions in Chapters 4, 5 and 6 will be investigated. First, by examining the assumption of linearity that was used to simulate the groundwater flow by means of a non-linear model. Second, by comparing the results for the semi-arid Upper-Guadiana catchment to those of the Pang catchment for the results of Chapter 6. Third, by examining the drought propagation for the Pang catchment using observed data. Because the base flow is not observed, it will be estimated using a new method based on observations of streamflow and groundwater levels.
- In Chapter 8 some *spatial* aspects of drought in groundwater recharge, levels and discharge will be analysed and discussed. For this purpose the groundwater flow in the Pang catchment was simulated using a numerical groundwater flow model (MODFLOW).

The thesis will be completed by the summary, conclusions and opportunities for further research in Chapter 9. Because some of the chapters are based on papers, which have previously been published elsewhere, some minor repetitions will occur.

Chapter 2

Description of the Pang and Upper-Guadiana catchments

2.1 Pang catchment

2.1.1 Introduction

The Pang catchment is a softly undulating, rural catchment some 25 km south of Oxford (UK) (Figure 2.1). The River Pang is a tributary to the River Thames. The area of the surface water catchment of the Pang is approximately 170 km². The Pang is a groundwater catchment, meaning that groundwater flow is the dominant runoff generating process. The groundwater catchment is mostly larger than the surface water catchment and can change in shape and size over time (Bradford, 2002). In Figure 2.1 an overview of the catchment is given. The altitude ranges from approximately 40 mAMS L (m Above Mean Sea Level) near the outlet to over 230 mAMS L at the surface water divide in the northwest.

2.1.2 Climate

The Pang catchment has a sub-humid climate with an average annual precipitation P of around 690 mm a⁻¹ in the period 1960-1997. P varies little throughout the year (Figure 2.2). Minimum average monthly P is 45 mm in July, the maximum is 70 mm in December. The interannual variation in P is moderate. In the period of analysis 1960-1997, the minimum annual P was 350 mm in 1975 and the maximum 880 mm in 1976 (hydrological years from October to September). On the high ground, P is somewhat higher than in the valleys: just over 700 mm a⁻¹ compared to around 600 mm a⁻¹. The potential evapotranspiration ET_{pot} has a smaller interannual variability than P , but a larger within-year variability. The average annual ET_{pot} from grass is 520 mm a⁻¹. Maximum ET_{pot} occurred in 1975 with 644 mm, minimum in 1987 with 465 mm. Maximum monthly average ET_{pot} is 92 mm in July, minimum monthly average is 8.9 mm in December (Figure 2.2).

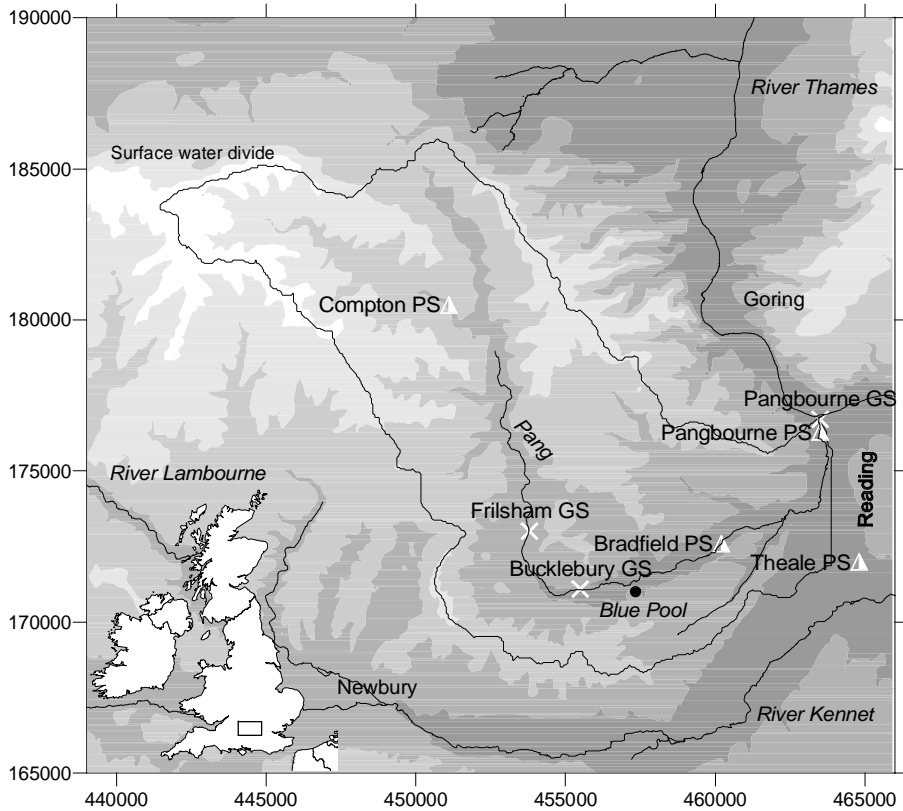


Figure 2.1: Overview of the Pang catchment (coordinates of the British National grid (m), PS: Pumping Station, GS: Gauging Station, greyscale indicates altitude (lighter is higher))

2.1.3 Geology

The main geologic feature in the area is the syncline known as the London Basin. Apart from this major tectonic structure the area is relatively free of faults (Sherlock, 1960). The catchment lies at the north-western edge of this syncline, which strikes approximately east-west in this area. Because of this, the layers are tilted slightly and progressively younger layers surface to the south (Figure 2.3). The most important deposits are from the Upper Cretaceous (the Chalk). In the south these deposits are covered by mostly clayey sediments from the Tertiary (Figure 2.3 and 2.4). Table 2.1 gives an overview of the deposits found in the area. In the following part the most important ones will be discussed. The description is largely based on Institute of Geological Sciences and Thames Water Authority (1978) and Sherlock (1960). A new

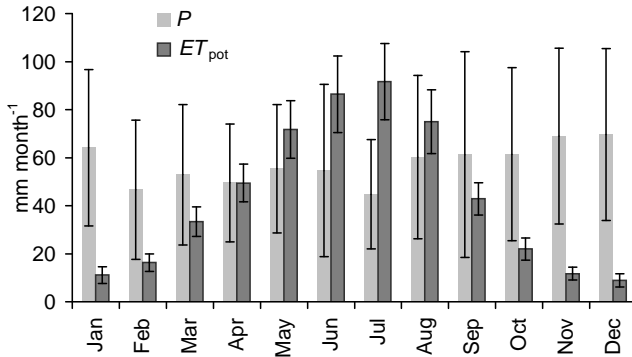


Figure 2.2: Average monthly precipitation P and potential evapotranspiration ET_{pot} for the Pang catchment for the period 1960-1997. ET_{pot} is calculated according to Penman-Monteith (Feddes and Lenselink, 1994) with crop resistance r_s is 70 s m^{-1} (error bars indicate standard deviation).

lithostratigraphy for the area is being developed (Bradford, 2002; Schürch and Buckley, 2002), but here the old, more familiar names will still be used.

Gault At the end of the Lower Cretaceous the Gault was deposited. The Gault consists of stiff blue-grey clay and marl. It is 30-70 m thick and it thickens from west to east. The base of the Gault is fairly flat, as the Lower Greensand has filled up all the depressions which existed at that time. The Gault acts as the hydrological base for the Pang catchment.

Upper Greensand The transition between the Gault and the Upper Greensand forms the boundary between the Lower and the Upper Cretaceous. The Upper Greensands are the continuation of the Gault deposits but in more shallow water, which caused them to be more sandy. The Greensand consists of glauconitic, micaceous, fine-grained sands and sandstones and is locally silty (Allen *et al.*, 1997).

Chalk As the transgression phase, which had already been active during the Lower Cretaceous flooded more and more land, less terrigenous material became available and instead of the sand and clays of the Greensands, calcareous material was deposited. This material was to become the soft white limestone called ‘chalk’. The term ‘Chalk’ is used when referring to the Chalk Group (i.e. in a stratigraphic sense, Table 2.1) while ‘chalk’ refers to the material (Allen *et al.*, 1997; Schürch and Buckley, 2002). This chalk forms the Lower, Middle and Upper Chalk which are the dominant deposits in the catchment.

The *Lower Chalk* is more argillaceous than the other two Chalk formations

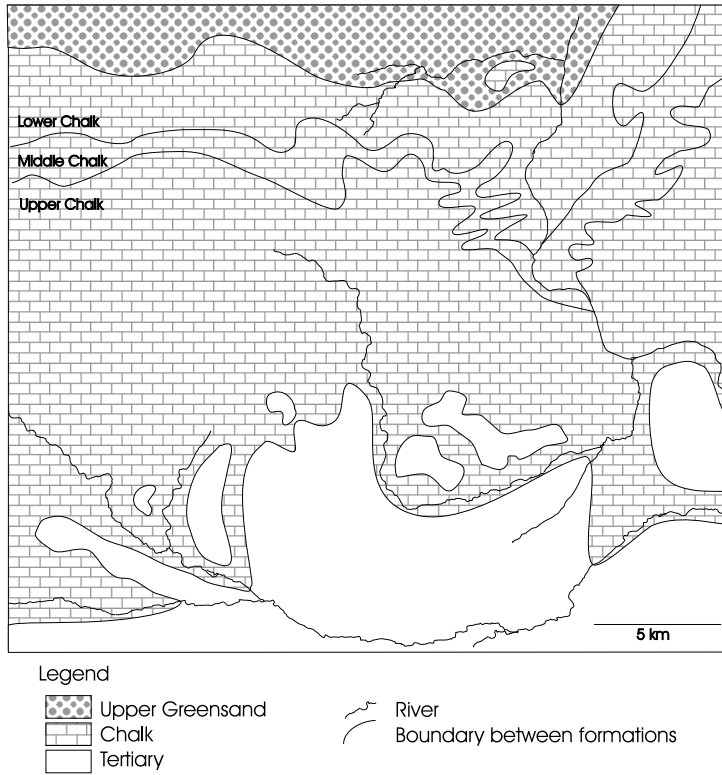


Figure 2.3: Simplified geological map of the Pang catchment showing the outcrop of major geological formations. Valleys fillings are not included.

and contains no flint. The clay content of the Lower Chalk decreases from bottom to top. It contains two hard beds. Locally a bed of very compact chalk named the Marl Rock, which is traceable by a line of strong springs (possibly the springs which are found to the north of the catchment), is found about 15-18 m above the base of the Lower Chalk. Above this bed a similar hard bed is found, the Totternhoe Stone. The total layer is 60-75 m thick with a maximum thickness of 90 m in the Lambourn area. Its top is defined by the hard nodular Melbourn Rock which can be up to 5 m thick. The *Middle Chalk* is less argillaceous than the Lower Chalk with flints in the upper part. It is 45-60 m thick. Its top is marked by a hard nodular band, the Chalk Rock (up to 8 m thick). The *Upper Chalk* is a very pure white homogeneous chalk with regularly spaced bands of nodular and tabular flint. Its clay content is lower than the clay contents of the Lower or Middle Chalk. The Upper Chalk is up to 105 m thick and crops out extensively on the Chalk dip-slopes.

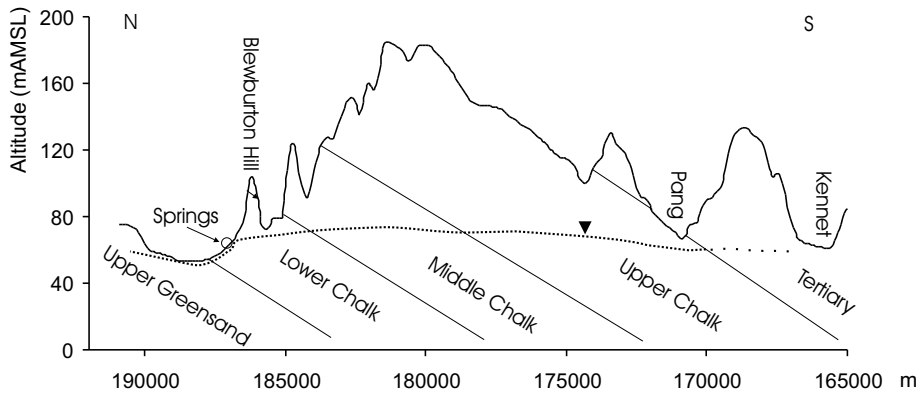


Figure 2.4: North-South cross section through the Pang catchment along a line with x-coordinate 454700 m in Figure 2.1.

Table 2.1: Stratigraphic table of formations known to be present in the Pang catchment.

Era	Period	Epoch	Formations	Composition and thickness	
KENOZOIC	QUATERN.	Holocene	Alluvium		
		Pleistocene	Fluvial sands and gravels ^a Plateau Gravels Clay-with-flints		
	TERTIARY	Pliocene			
		Miocene			
		Oligocene			
		Eocene	Bagshot Beds	sand, silt, clay	44-70 m
			London Clay	stiff clay	0-90 m
Reading Beds	sand, silt, clay		4-30 m		
Palaeocene					
MESOZOIC	CRETACEOUS	Upper Cretaceous	Upper Chalk	pure chalk, flints	0-105 m
			Middle Chalk	transitional	45-60 m
			Lower Chalk	argillaceous chalk	60-75 m
		Upper Greensand	sand and sandstone	10-50 m	
		Lower Cretaceous	Gault	clay and marly clay	30-70 m
			Lower Greensand	sand and sandstone	

^aThis comprises several formations near the Kennet and Thames

Tertiary deposits In the catchment different Tertiary deposits can be found. They can be subdivided into the Reading Beds, London Clay and the Bagshot Beds (Table 2.1). These are all deposited in the Eocene. They are only found in the southern part of the catchment, where they lie at the surface.

The Reading Beds consist of a variable sequence of sands, silts and clays, deposited by rivers. The clays are mottled and plastic and dominate in the upper part, the sands are light-coloured with thin bands of flint pebbles. The Reading Beds are followed by a layer of 0-90 m of London Clay. It is mostly a uniform, stiff, dark or blue-grey marine clay. The Bagshot Beds comprise a variable sequence of sands, clays and silts that outcrop intermittently along the southern edge of the catchment area.

Quaternary On the Chalk outcrop the Clay-with-flints occurs, which consists of clay, angular flints and flint-pebbles. The angular flints are the insoluble residues left by solution of chalk containing flints. The clay and the flint pebbles are derived from the waste of Eocene deposits which capped the Chalk and decayed there. In the area also 'high-level gravels' occur, on the old geological maps called Plateau Gravels. More recently, a good many of these patches have been classified in more detail, but some still remain unclassified. These unclassified high-level gravels still retain their old name for lack of a better one. It is possible that the Plateau Gravels include material of different origin. During the Quaternary also alluvium and fluvial sands and gravels were deposited in this area. They are found in the valleys of the rivers. Alluvium is up to 3 m thick and floors most river valleys. It consists mainly of clay and silt. The fluvial sands and gravels, up to 8 m thick, include flood plain and river terrace deposits of various ages and heights in the valleys of the River Thames and its tributaries.

2.1.4 Hydrogeology

In this paragraph the properties of the most important aquifers in the Pang catchment will be described. The Chalk has the largest outcropping area in the area (Figures 2.3 and 2.4). It is by far the most important aquifer. Immediately below the Chalk the Upper Greensand is found, which is assumed to be an important aquifer too, although both the thickness and outcropping area are considerably less than the Chalk. Hydraulic continuity between the Upper Greensand and the overlying Chalk is thought to be limited over much of the area due to the clayey nature of the Lower Chalk (Rushton *et al.*, 1989). The Gault acts everywhere as an aquiclude, separating the Chalk and Upper Greensand from the deeper Lower Greensand and forming the hydrological base. The London Clay confines the Chalk aquifer in the south of the model area. Hence the Chalk aquifer is partly confined and partly unconfined.

Chalk aquifer The Chalk is referred to as a dual porosity or dual permeability medium, depending on the amount of flow which is expected to occur in the chalk matrix and fissures. In a classic dual porosity aquifer the matrix pores provide the storage and fractures provide the permeable pathways to permit flow (Downing *et al.*, 1993). The fissuring is generally considered to be well developed along the lines of the valleys and poorly developed on the higher ground forming the ridges. Possible reasons for the development of this pattern are local variations in the Chalk, increased dissolution because of more intense groundwater flow and the effect of periglacial weathering (Younger, 1989). How the pattern has developed exactly is still under dispute (Younger, 1989; Bloomfield, 1996).

In the vertical the highest amount of fissuring is observed in the zone of water table fluctuation where the movement of groundwater can enhance the aperture of fractures by dissolution. Deeper within the Chalk the frequency, appearance and apertures of fractures decline due to increasing overburden and a general reduction in circulating groundwater and hence dissolution. The most important flow zones are concentrated near the top of the Chalk, with little flow deeper than 50 m below groundwater levels or below the top of the confined Chalk (Owen and Robinson, 1978). The fissuring is especially well developed in hard grounds like the Chalk Rock. Schürch and Buckley (2002) show that these hard grounds provide a significant amount of the total flow towards boreholes. In general, transmissivity values in the top layer range between 50 and 1300 m²d⁻¹, corresponding to a permeability of around 1 to 35 m d⁻¹ (Table 2.2). The higher values in the range occur both in the valleys containing streams and dry valleys and the lower values in the higher part of the area. Also at the edges of areas with Tertiary deposits the fissuring seems to be well developed, probably as a result of acid runoff from the Tertiary clays.

Table 2.2: Properties of the different Chalk strata: hydraulic conductivity k , porosity, pore size and specific yield S_y .

	k (m d ⁻¹)	Porosity ³ (%)	Pore size ³ (μ m)	S_y ⁴ (-)
Upper Chalk	1 to 35 ¹	38.8 \pm 5.8	0.65 \pm 0.14	0.003 to 0.05
Middle Chalk	2 to 5 ²	31.4 \pm 6.6	0.53 \pm 0.14	Unknown
Lower Chalk	1 ²	31.4 \pm 6.6	0.22 \pm 0.11	Unknown

¹(Price *et al.*, 1977; Younger, 1989; Rushton *et al.*, 1989; Allen *et al.*, 1997) ²(R.B. Bradford, Pers. Comm.) ³(Bloomfield *et al.*, 1995) ⁴(Rushton *et al.*, 1989)

The specific yield S_y is very small because of the very fine-grained nature of the matrix, which retains most of its saturated water content under gravity. S_y varies regionally; in the valleys S_y is higher than near the water divide (Downing *et al.*, 1993). In the catchment, S_y is up to 0.05 in river valleys,

whereas in the higher parts of the area the average S_y is about 0.003 (Rushton *et al.*, 1989). The Chalk has a high total porosity. Values as high as 50% can occur. In Table 2.2 the average values for the three strata are listed. The average Upper Chalk porosity is consistently higher than that of the Middle Chalk and Lower Chalk.

Upper Greensand aquifer The Upper Greensand has a limited outcropping area and therefore receives little direct recharge (Figure 2.3). It only appears at the surface near the northern escarpment. The flow in this area is both intergranular and through fractures depending on the degree of cementation (Allen *et al.*, 1997). The permeability of the Upper Greensand is assumed to be greater than the permeability of the Lower Chalk (Institute of Geological Sciences and Thames Water Authority, 1978). The groundwater head fluctuations are generally smaller in the Upper Greensands than in the Chalk and follow approximately the same annual cycle.

2.1.5 Soils

Many soil types occur in the catchment, however only five of these soils occur in more than 5% of the area, together covering nearly 70% of the total area (Soil Survey of England and Wales, 1983). The description will concentrate on these soils. In Table 2.3 a short overview is given. ‘Drift’ in this table is a general term referring to deposits left by water, wind or glacial processes during the Pleistocene and Holocene, including among others Plateau Gravels and Clay-with-flints.

Table 2.3: Dominant soil types in the Pang catchment.

Name	Coverage (%)	Substrate	Soil depth (to substrate)	Position in landscape
Hornbeam	21.92	Plateau drift over Chalk	> 150 cm	High ground
Wickham	15.37	Drift over Tertiary clay	110 cm	Slopes and lower areas
Andover	14.03	Chalk	25 cm	Steep slopes
Coombe	12.02	Chalky drift and Chalk	80 cm	Dry valleys
Frilsham	6.26	Drift over Chalk	60 cm	River valleys

Hornbeam soils are developed in plateau drift and are predominantly found on the higher grounds. They are often associated with Clay-with-flints deposits (Klinck *et al.*, 1998). Land use is mainly arable land. These soils are deep fine

loamy over clayey soils with slowly permeable subsoils and slight seasonal water logging. They can be very flinty and sometimes well drained. Hornbeam is a brown soil, in which pedogenic processes have produced brownish or reddish subsurface horizons.

Wickham soils are developed on drift over Tertiary clays. These soil types can be found in the south of the catchment where Tertiary deposits cover the Chalk. Land use is predominantly grassland and deciduous forest. It is a slowly permeable, seasonally waterlogged, fine loamy over clayey soil. The texture can vary from coarse loamy over clayey to fine silty over clayey. Similar more clayey or permeable soils with slight waterlogging can also be classified as Wickham. Mottles are prominently developed above 40 cm depth.

Andover soils are developed on the steep slopes on the Chalk. Land use is both tilled land and grassland. These soils are shallow, well drained, calcareous, silty soils over chalk on slopes and crests; deep calcareous and non-calcareous fine silty soils in valley bottoms. Just west of the River Thames on the (very) steep slopes these soils are called Upton. In these shallow soils the only significant pedogenic process has been the formation of an organic-enriched mineral surface horizon (A horizon). Chalk can be found within 30 cm depth and these soils are still very calcareous.

Coombe soils are developed on chalky drift and chalk and can predominantly be found in the dry valleys. Land use is mainly tilled land and some grassland. They are deep, well drained, calcareous, fine silty soils. At valley sides these soils can be shallow in places. Coombe soils also are brown soils (like Hornbeam), but with a weathered calcareous subsoil.

Frilsham soils are developed in river valleys on drift over chalk and can be found downstream of the Coombe soils. Land use is mainly tilled land and grassland. This is a well drained mainly fine loamy soil over chalk, sometimes calcareous, with significant clay enrichment in the subsurface horizon.

In the remaining 30% of the catchment area, there are several soil types. In the Pang, Thames and Kennet valleys soils developed on river alluvium occur. In the north are soils developed on a more argillaceous chalk (e.g. Wantage on Lower Chalk) and in the south are some acid soils developed on Plateau Gravels.

2.1.6 Land use

The region is part of the Berkshire Downs, which is classified as an 'Area of Outstanding Natural Beauty'. In the catchment are only small villages. Land cover nowadays consists of tilled land, grass and forest (Table 2.4). On the

Chalk hills, grass and tilled land predominate. Forest occurs mainly in the southern part of the catchment or more specific on the Wickham soil series. Deciduous forest is more common than coniferous forest. Traditionally cereals (spring barley, winter wheat and winter barley) form the most important crop in the area (Thompson *et al.*, 1981). Sheep, with some cattle and pigs in the lower areas, can be found on the pastures. But now there are even pigs (outdoor pig farming) on the upper parts of the catchment. However, problems concerning outdoor pig farming in a Chalk area are not to be expected with respect to water quantity but rather with respect to soil erosion, increased sediment load in the streams and a higher probability of groundwater contamination.

Table 2.4: Land use in the Pang catchment in 1995.

Land use type	Surface area (%)
Water	0.08
Grassland	34.9
Deciduous forest	12.2
Coniferous forest	2.2
Tilled land	43.5
Urban	5.3
Inland bare ground	1.9

2.1.7 Hydrology

The unconfined aquifer of the West Berkshire Downs forms a groundwater system extending from the River Kennet near Newbury to the River Thames between Goring and Reading. The Pang catchment lies at the eastern edge of this area and the Pang drains to the Thames at Pangbourne. The other rivers in the area (e.g. Lambourn and the Winterbourne, a small intermittent tributary to the Lambourn) drain to the River Kennet (Figure 2.1).

The average discharge Q of the Pang is $0.61 \text{ m}^3\text{s}^{-1}$ over the period 1968-1998. The upstream part of the Pang (above Bucklebury) is intermittent. The upper reaches of the Pang drain the Chalk aquifer only during periods with high groundwater levels, thereby intercepting groundwater that otherwise would flow eastwards to the Thames. The lower reaches of the Pang cut through the overlying Tertiary deposits and drain the Upper Chalk directly. However, in some reaches of the groundwater level can be below the stream level (Figure 2.4). From the south several intermittent Tertiary streams, which drain the superficial Tertiary deposits, discharge into the Pang.

An important feature, which influences the local hydrology is the variability in the location of the rise of the Pang (Bradford, 2002). In very wet years,

the valleys near Compton (Figure 2.1), which are usually dry, may conduct water. In very dry years, the rise of the Pang may be much further downstream (even below Frilsham GS), which means that the groundwater flow north of the rise of the Pang can go directly to the Thames. Other local controls include springs which appear on several places in the catchment. In the north of the catchment are springs, which rise where the Lower Chalk surfaces at the base of the escarpment. These springs might be caused by preferential flow paths over hard grounds like the Marl Rock. Springs also appear on the edge of the Tertiary deposits, which confine the Chalk aquifer south of Bucklebury. The most important one is the Blue Pool, a complex of springs which has an estimated discharge of $0.2 \text{ m}^3\text{s}^{-1}$. The pond derives its name from the bluish-green colour of the water, which may be caused by glauconite. The outflow from these springs is rather constant and traditionally has been used for growing water cress. It is not known whether the flow of the springs has been enhanced by installing boreholes. Also there appears to be fast flow paths between swallow holes near Bucklebury and the Blue Pool (Banks *et al.*, 1995).

Groundwater features The groundwater divide of the Pang is not coincident with the surface water divide (Bradford, 2002). The groundwater divide to the south-west (at Newbury) lies about 5 km outside the surface boundary. However, on the northern side (at Didcot) the groundwater boundary lies within the surface water divide. Moreover the location of the groundwater divide is not constant in time, but changes with the position of the rise of the Pang.

In Figure 2.5 an example of the groundwater levels in the Chalk aquifer in the Pang catchment is given. These are values for 1995, which was a rather wet year. The interpolation, which is solely based on information from boreholes, is unreliable along the edges due to insufficient data. From this picture we can clearly see that the Thames is a dominant influence on the groundwater flow, whereas the Pang has only a limited influence. The Kennet has no influence on the groundwater flow in the Chalk aquifer because of the low conductivity of the Tertiary deposits which separate it from the Chalk aquifer.

Abstractions of groundwater There are a number of small, private boreholes in the Pang catchment, but larger scale groundwater abstraction for the public water supplies did not begin until the mid-1960s. The main pumping stations within the catchment are situated at Compton in the northern part of the catchment and at Bradfield and Pangbourne in the southern part of the catchment (Figure 2.1). Abstractions from Bradfield have remained constant at about $1250 \text{ m}^3\text{d}^{-1}$ since it came into production in 1964. Abstractions from Pangbourne are about $38\,750 \text{ m}^3\text{d}^{-1}$. Abstractions from Compton, which began in 1965 to supply Didcot (a fast growing town to the north of the Pang catchment), gradually increased to about $14\,000 \text{ m}^3\text{d}^{-1}$ (licensed output 13 600

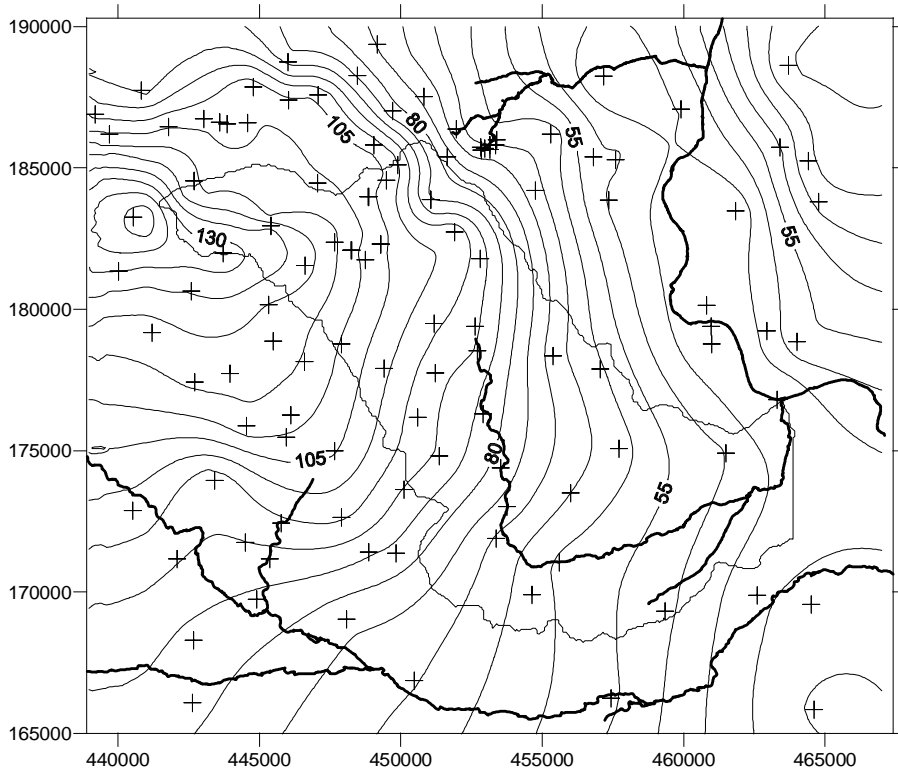


Figure 2.5: Average groundwater levels (mAMS) in 1995 in the Pang catchment. Contours based on groundwater levels only.

m^3d^{-1}) by the mid-1980s. The abstractions at Compton were decreased in the beginning of the 1990s. They have been replaced to Gatehampton at the other side of the River Thames just south of Goring where they could benefit from induced riverbank infiltration. The reduction of abstractions in Compton contributed to the return of the flow in the upper reaches of the River Pang. Other licensed abstractions in the area are situated at Cleeve (license $16\,200\ \text{m}^3\text{d}^{-1}$) and Woods Farm ($3700\ \text{m}^3\text{d}^{-1}$), which are both near Goring and Theale (Figure 2.1) (Charalambous *et al.*, 1995). Abstractions from Theale occurred from 1974 to 1992 with a maximum of about $5500\ \text{m}^3\text{d}^{-1}$ between 1977 and 1984.

The Pang and the adjacent Lambourn were chosen to augment the Thames during low flows (West Berkshire Groundwater Scheme). This scheme was operated in 1975-76 and during the drought of 1990 (Headworth *et al.*, 1983; Estrela *et al.*, 2000a).

2.2 Upper-Guadiana catchment

For the Upper-Guadiana catchment only recharge is simulated and used, so the description of the catchment is limited to the surface area (climate, soils and land use). The catchment of the Upper Guadiana, which is located in the central part of Spain, covers a total area of around 16 000 km² (about 28% of the total catchment area of the Guadiana River). This includes 17 tributaries (Figure 2.6). The catchment covers five aquifer units of which three units cover most of the area, i.e. the Sierra de Altomira, the Mancha Occidental and the Campo de Montiel (Figure 2.6). The altitude differences are moderate: 600 mAMSL near the outlet to 1100 mAMSL in the highest parts. The central area, the Mancha Occidental, which is a filled-in basin, is quite flat. The areas to the north (Sierra de Altomira) and south (Campo de Montiel) are slightly hilly.

2.2.1 Climate

The Upper Guadiana catchment has a semi-arid climate. The average precipitation P varies between 350 mm a⁻¹ in the Mancha Occidental to 580 mm a⁻¹ in the Campo de Montiel. P shows a clear inter-annual variability. The lowest precipitation record in the period 1940 to 1997 was 242 mm in hydrological year 1949 (October-September) and the highest 697 mm in 1969. The coefficient of variation CV is 0.257, compared to 0.141 for the Pang catchment. A large part of the annual P falls in a limited number of days, usually in storms. The spatial variability of P is very high. Average monthly P and standard deviation for the Mancha Occidental unit are shown in Figure 2.7. The pattern for the other aquifer units is similar, although the annual totals are larger (Estrela *et al.*, 2000b). During the summer months rainfall is scarce. In July and August, average monthly P is 10 and 19 mm respectively. Potential evapotranspiration ET_{pot} is calculated from monthly values of the temperature using the Thornthwaite method (Ruiz García, 1998; Peters *et al.*, 2001). ET_{pot} , which almost reaches 960 mm a⁻¹ on average for the whole basin, clearly exceeds P . Within the basin it varies from 870 to 1030 mm a⁻¹ (Estrela *et al.*, 2000b). A distinct peak in ET_{pot} can be recognised in the summer months (Figure 2.7). On average P exceeds ET_{pot} only in the period November-February.

2.2.2 Soils

The main soil type occurring in the Upper Guadiana catchment is the Cambisol (Ruiz García, 1998). A B-horizon with beginning soil formation is the only diagnostic feature that all Cambisols have in common (Driessen and Dudal,

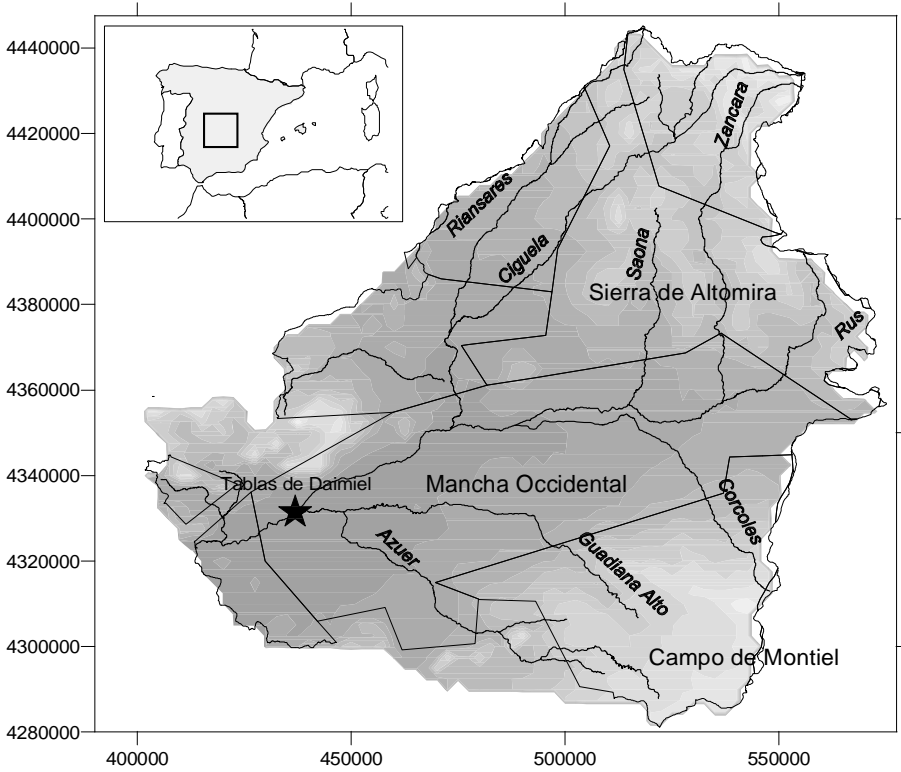


Figure 2.6: Overview of the catchment of the Upper-Guadiana with the major aquifer units (e.g. Mancha Occidental) and rivers (e.g. Azuer) indicated. Coordinates according to Spanish National grid (m).

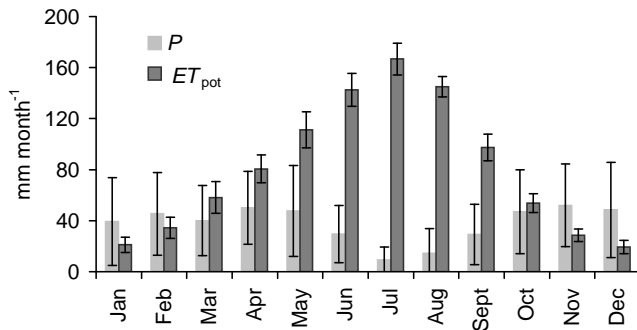


Figure 2.7: Average monthly precipitation P and potential evapotranspiration ET_{pot} (Thornthwaite method) for the Mancha Occidental aquifer unit (error bars indicate standard deviation).

1991). In the Upper-Guadiana catchment, the soil texture is loamy to clayey with the highest clay content in the A-horizon. The Cambisols generally make good agricultural land and are intensively used.

Luvisols, the second main soil type in the catchment, are characterized by their argic B-horizon. This implies that this horizon has a distinctly higher clay content than the overlaying A horizon. The soil texture of Luvisols is clayey and they have a granular or crumb surface soils that are porous and well aerated. Along the rivers in the west part of the catchment we find the gleyic Solonchak soil type. The gleyic Solonchaks have salic properties and occur where the water table is at shallow depth. The texture of the gleyic Solonchaks found in the Upper-Guadiana catchment is sandy clay loam, so moderately fine-textured soils. In the west of the Campo de Montiel at the places where the Triassic (clays, marls and gypsum) outcrops, we find Vertisols. Vertisols are soils having 30% or more of swelling clay in all horizons to a depth of at least 50 cm (the upper 18 cm are allowed to be mixed). They have a fine texture and poor internal drainage. At last we find a few small areas with eutric Fluvisols in the north and middle of the catchment. These are medium- and fine-textured soils with a base saturation of 50% or more, developed in fluvial, lacustrine or marine deposits.

2.2.3 Land use

Till the beginning of the 1970s land use in the catchment of the Upper Guadiana consisted mainly of dryland farming of cereals and vines. A small part of the land (less than 300 km²) was irrigated by ‘norias’, a traditional irrigation system of Arabic design (Estrela *et al.*, 2000a). An estimated 60 Mm³a⁻¹ of groundwater was abstracted in this way. In the beginning of the 1970s abstractions increased dramatically, especially in the central part of the Mancha Occidental aquifer. The total irrigated area reached 1000 km² by the mid 1980s, mostly at the expense of dry land farmed areas or wetlands. Although the irrigated area does not cover more than 25% of the surface area of the La Mancha aquifer, the effects on the hydrological system are profound. Because of the lowering of the groundwater levels many wetlands decreased in size or disappeared altogether. The most important one being the Tablas de Daimiel, which is located near the outlet of the Upper-Guadiana basin (Figure 2.6).

Initially the irrigated areas were planted with a wide mixture of crops like cereals, maize, vegetables, fruits, vines and industrial crops (Estrela *et al.*, 2000a). But in the 1990s there has been an important shift to vines, because they require less water than, for example, vegetables or maize. And that made it possible to reduce annual abstractions from the maximum of 600 Mm³a⁻¹ in mid-1980s to 200-300 Mm³a⁻¹ in the present situation. In the remainder

of the catchment the main land use types are dry land farming (cereals, vines and olives predominantly) and semi-natural vegetation (Campo de Montiel).

Chapter 3

Groundwater drought

3.1 Causes and effects of groundwater drought

In this thesis (Section 1.3), a groundwater drought was defined as resulting from the natural variability of the weather, which usually means a decrease in precipitation, possibly in combination with a high evapotranspiration. Below, the causes and consequences of groundwater drought are examined in some more detail.

In Figure 3.1 the hydrological cycle under natural conditions (without abstractions or irrigation) is presented. Ignoring for the moment uptake of groundwater (saturated store) by vegetation directly U_r or through capillary rise C_r and indirect recharge R_i , a groundwater drought can be caused by either a decrease in recharge R or an increase in base flow Q_s . A decrease in R can be caused in several ways: most importantly by a decrease in the amount or effectiveness of precipitation P (Wilhite, 1999), but also by an increase in evapotranspiration ET . Low effectiveness of P can occur, for example, when P intensity is very high, thus increasing the amount of overland flow and decreasing the infiltration. Overland flow and interflow can also increase because of a decrease in infiltration capacity. The infiltration capacity of the soil can decrease because of water repellency or crust forming, but also because the topsoil is frozen. Compaction of the subsoil ('plough pan') may increase interflow. Low effectiveness of the precipitation can also occur as a result of low precipitation intensity, which increases evaporation of intercepted water. The timing of P can be important in monsoon type climates (Wilhite, 1999). An increase in evapotranspiration can be caused by a high evaporative demand from the atmosphere, but also by changes in the vegetation (e.g. increase in rooting depth). An increase in base flow does not usually occur within the time frame of a drought.

So far, two processes have not been discussed: uptake of groundwater by vegetation (directly from groundwater or through capillary rise) and indirect recharge. These processes are especially important in semi-arid or arid environments. Uptake of groundwater by vegetation is important when it occurs over extensive areas with shallow groundwater levels or in semi-arid areas where the recharge

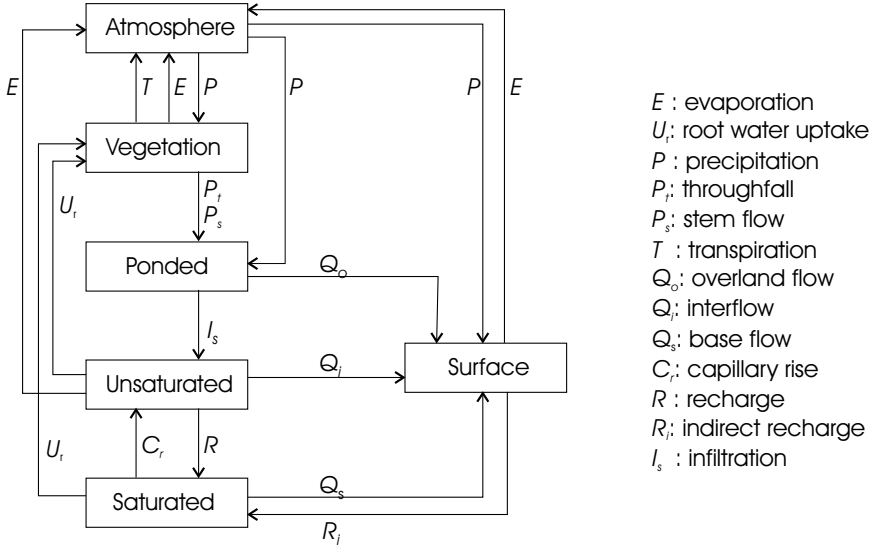


Figure 3.1: Schematic view of the hydrological cycle. ‘Atmosphere’ represents all water stored in the atmosphere, ‘Vegetation’ is the water stored in and on the vegetation, ‘Pondered’ represents the water on the land surface, before infiltrating into the soil, ‘Unsaturated’ is the moisture stored in the unsaturated zone and ‘Saturated’ in the saturated, ‘Surface’ is all water stored in the surface water system, like streams, rivers and lakes.

is so low that the transpiration losses from even a small area of vegetation is important for the water balance. Examples of the first situation are deltaic areas like the Netherlands or Bangladesh. An example of the second situation is the Upper-Guadiana catchment, where groundwater is evaporated in the wetlands (Tablas de Daimiel) near the outlet (Figure 2.6). Within a catchment, indirect recharge will seldom be a process, which causes or aggravates drought. Mostly it will allow some of the water that was previously lost to groundwater, to be infiltrated later. Indirect recharge, which is imported from outside the catchment, is subject to the same temporal variability and thus the same droughts as precipitation. Under natural conditions most soil and vegetation characteristics do not change quickly and will thus rather result in a trend in the groundwater levels (e.g. desiccation or desertification) than a drought (Section 1.1). An exception to this could be the occurrence of fire, which in itself is often a result of drought.

Groundwater droughts show a wide variety of consequences. In the strict sense (van Lanen and Peters, 2000), groundwater droughts cause decreased groundwater levels and decreased outflow to the surface water system Q_s . The decrease in groundwater levels has a multitude of secondary effects, such as: increased

cost of pumping for abstractions, drying up of wells, intrusion of salt water from the sea (Melloul and Collin, 2002) or from deeper layers, loss of crop yield or increased stress for natural vegetation because of decreased transpiration (Schneider, 2001), increased land subsidence, changes in water quality and thus damage to terrestrial or aquatic ecosystems. Of course, depending on the local conditions also other effects may occur. However, for deep groundwater levels the effects may be limited and that is probably another reason why groundwater drought has received little attention in the past. The decreased outflow to the surface water system mostly has the same effect as a streamflow drought. However, especially water quality may suffer, even though sufficient water is available in the stream (Caruso, 2002).

3.2 Groundwater drought research

A large part of the research on groundwater drought deals with the management of groundwater resources for abstraction, for example in southern Africa (Calow *et al.*, 1999), in the Pacific (White *et al.*, 1999), in the UK (Wyness *et al.*, 1994), in Ohio (Chang and Kleopa, 1991) and in Florida (Ahn, 2000). Other studies look at specific aspects of droughts. Price *et al.* (2000) look at the outflow mechanism from the unsaturated zone of the Chalk during low flow and drought conditions. They pose that the high base flow from the Chalk during drought (Lewis *et al.*, 1993) is caused by residual outflow from the surface of the fissures of the unsaturated Chalk. Warren (1994) and Bradford (2000) notice that several mildly severe dry winters with low recharge can cause a serious groundwater drought. They use the phrase ‘winter drought’ to describe anomalously dry winters. Please note that the term ‘winter drought’ usually describes streamflow droughts caused by below-zero temperatures.

Kašpárek and Novický (1997) and Querner and van Lanen (2001) use physically based models to study the effects of drought and mitigation measures on drought. Kašpárek and Novický (1997) and Zaidman *et al.* (2001) note the slow response of a groundwater catchment to drought and the persistency of a drought once it has been established. Chang and Teoh (1995) study the regional character of groundwater drought.

Considering the small volume of research on groundwater drought, it would be very useful if knowledge gained in the study of streamflow droughts could be applied to groundwater drought. Indeed, streamflow during drought is often mainly derived from groundwater. However, the end of streamflow droughts is probably determined more by direct runoff components like surface runoff and interflow, implying that streamflow droughts generally end before groundwater droughts.

3.3 Propagation of drought through groundwater systems

The propagation of drought through groundwater is illustrated in Figure 3.2 taking data from the Pang catchment. From top to bottom, this figure shows the precipitation P at Yattendon station (daily and 3-monthly moving average) (Appendix A), the soil moisture storage in the root zone S_r , the groundwater level H in a representative borehole (SU47/141 in Figure D.4) and the observed streamflow Q at Pangbourne gauging station (Figure 2.1). The soil moisture storage in the root zone was simulated with NUTDAY (Chapter 6). The streamflow contains both groundwater discharge and direct runoff (Section 2.1.7). Because the component groundwater discharge is larger than the direct runoff (Bradford, 2002), the streamflow is plotted last in the propagation.

In Figure 3.2, four droughts A, B, C and D with different characteristics are indicated. Because of the strong non-linearities in the hydrological cycle, these droughts with different characteristics propagate differently. Drought A is a normal summer drought, with around average P , but high ET and low values of S_r , H and Q during summer. In fact, because of the influence of the evapotranspiration ET , a dry period occurs every year in S_r , H and Q . Drought B is a drought with low P during the previous winter. This means that a relatively small decrease in P during summer, results in a serious drought in H and Q . Drought C is the most severe drought in P and S_r in Figure 3.2. However, because the preceding winter was reasonably wet, its effects are limited in H and Q . However, the period following this drought is also relatively dry resulting in a prolonged drought in H and Q up to drought D. These examples show clearly how variable individual drought events are. And although it is possible to explain each individual event, this provides little information on the drought propagation in general.

From the existing studies on the propagation of drought through groundwater, the most relevant is that by Eltahir and Yeh (1999). The authors examine the propagation of drought through the groundwater system using observed data from Illinois (US). Eltahir and Yeh (1999) observe a tendency for an increase in the persistence and severity of droughts as the droughts propagate through the groundwater system. Marani *et al.* (2001) show that this change in persistence and severity can partly be related to the non-linearity in the groundwater-discharge relationship (groundwater rating curve) as a result of changes in drainage density with changing groundwater levels. Other studies of the propagation of drought through groundwater are White *et al.* (1999) and Changnon *et al.* (1988). White *et al.* (1999) show that droughts in rainfall accumulated over 60 to 120 months can be used as an indicator for droughts in groundwater lenses on small coral islands.

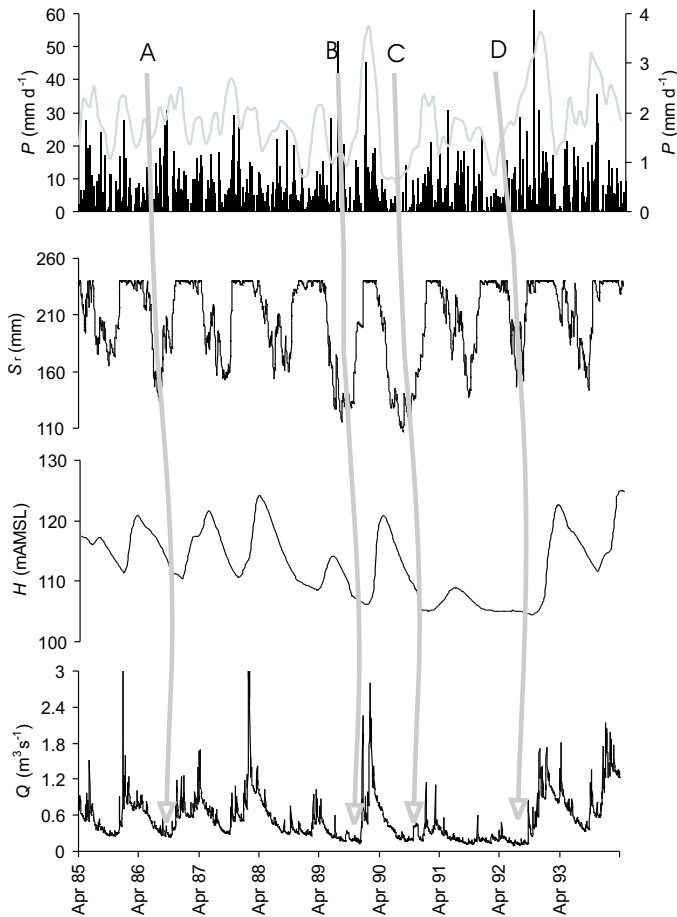


Figure 3.2: Illustration of the propagation of drought through the Pang catchment with precipitation P , soil moisture storage in the root zone S_r , groundwater level H and streamflow Q . Propagation of the four droughts A, B, C and D is indicated by the arrows.

It is useful to split and analyse the question of the propagation of drought through groundwater in two separate questions:

- How do the characteristics of a time series change as a result of the propagation through groundwater?
- How do the drought characteristics depend on the characteristics of the time series?

The changes in the time series as a result of the propagation through groundwater are illustrated in Figure 3.2. Both the soil and groundwater system act as a low-pass filter to the precipitation adding memory to the signal and decreasing the high-frequency components (Delworth and Manabe, 1989; Entekhabi, 1994). As a result of the flow through the groundwater system the persistence of the signal increases, the amplitude or variance decreases and the skewness changes from positively skewed for precipitation and recharge to a more normal distribution for groundwater levels and groundwater discharge. However, it is not well known how the changes caused by the groundwater system depend on the characteristics of the groundwater system. For surface water this has been examined extensively using the unit hydrograph theory (Sherman, 1932; Dooge, 1973; Rodriguez-Iturbe and Valdez, 1979). For groundwater, a similar theoretical framework is missing (Marani *et al.*, 2001).

An extensive investigation on how droughts depend on the characteristics of a time series has been carried out by Millan and Yevjevich (1971). The authors examined the influence of time series length, truncation level, autocorrelation and skewness on the maximum drought duration (longest negative run length) and the maximum drought severity (largest negative run-sum) in the time series. Millan and Yevjevich (1971) showed that both the maximum drought duration and severity increase with increasing threshold, time series length and persistence. Increasing skewness decreased the maximum drought duration and severity only slightly. Sharma (1998) on the other hand showed that both increasing skewness and persistence increase the drought severity and duration. The author states that ‘the effect of skewness on the extremal drought durations cannot be regarded as insignificant, contrary to the existing belief in hydrological literature’. It is not clear what causes the difference in response to skewness between Millan and Yevjevich (1971) and Sharma (1998).

The influence on drought of long-term persistence in time series, which is also called the ‘Joseph effect’ or Hurst phenomenon (Bras and Rodriguez-Iturbe, 1985) has long been debated. *Increasing short-term persistence* clearly increases the maximum drought duration and decreases the number of droughts (Fernández and Salas, 1999; Douglas *et al.*, 2002). However, Klemeš *et al.* (1981) found only little influence of *long-term dependence* for planning of reservoir capacity. Pelletier and Turcotte (1997), however, did find an increasing probability for severe droughts when long-term dependence was taken into account. These difference may be explained by differences in time horizon, which was shorter for Klemeš *et al.* (1981) than for Pelletier and Turcotte (1997).

Combining the answers to the two separate questions discussed above, should provide a first idea of how droughts change as a result of the propagation through groundwater. According to the increase in persistence, drought duration and severity should increase and the number of droughts should decrease. However, the decrease in variance suggests that drought severity should de-

crease. The influence of skewness is very unclear. Overall, it is difficult to predict how the total distribution of drought severity and duration will change as a result of the propagation through a groundwater reservoir.

3.4 Drought event definition

Up to now, within this thesis the concept of a groundwater drought has been discussed, but it has not been discussed how actual drought events can be derived from time series of groundwater recharge, levels and discharge. The derivation of the drought events from the relevant time series is a key step in any analysis, as the results may depend strongly on the drought event definition used. Some drought event definitions are specifically developed for one type of variable (for example precipitation), but many can be applied to any time series. A review of the full range of drought event definitions used in literature is beyond the scope of this study. For recent reviews see Hisdal and Tallaksen (2000) and Hisdal *et al.* (2004).

Two well-known methods, which can be used to derive drought events from time series like groundwater recharge, levels and discharge are: the annual minimum approach and the threshold level approach. In the first method, a time series is divided in annual periods (calendar or hydrological years) and for each annual period the minimum is selected (Figure 3.3), providing the so-called Annual Minimum Series (AMS). The relative level of the minimum, compared to the minima of other years is a measure for the severity of the drought. The drought has no duration and multi-year droughts (droughts lasting more than one year) are not possible. The example in Figure 3.3a illustrates that for a time series with a large interannual variability, in some year the minimum can be higher than the maximum in other years. Also, it shows an example of a drought which stretches over two years (multi-year drought), but which is identified twice by the AMS method.

The threshold level approach is derived from the runs or crossing theory, which was first developed by Rice (1954) and further developed by Cramer and Leadbetter (1967) according to Bras and Rodriguez-Iturbe (1985). One of first applications to drought was by Yevjevich (1967). For a summary of the method see Bras and Rodriguez-Iturbe (1985), p 240-261. In Figure 3.3b an example of the application of the method is given. The collection of values below the threshold is called the Partial Duration Series (PDS). The drought severity is usually defined by the drought deficit D . However, the drought duration L or drought intensity I can also be used. The example shows how different the PDS can be from the AMS. In this case, the number of droughts is much smaller for the PDS and variation in drought severity is much larger. A clear advantage of this method over the AMS method is the possibility to identify multi-year

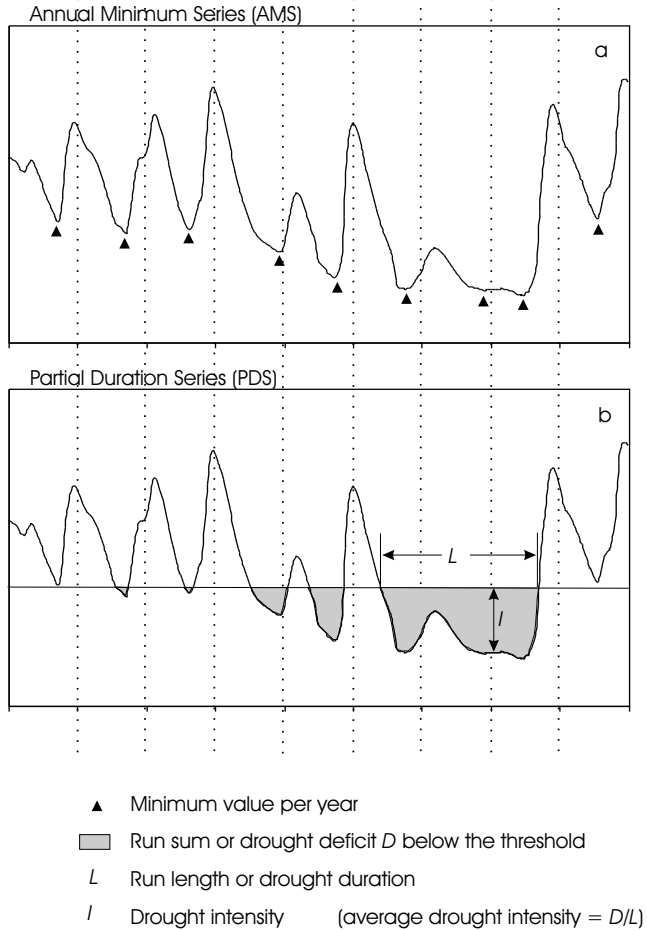


Figure 3.3: Two different ways of defining drought events: a) Annual Minimum Series and b) Partial Duration Series.

droughts. As that is expected to be particularly important for groundwater, the threshold level approach was used to define groundwater droughts. The threshold level approach will be applied to groundwater recharge, levels and discharge. Drought deficit will be used as the main identifier for drought severity. For the groundwater recharge and discharge the deficit is a volume or water depth, however for *groundwater levels* it is expressed as [LT].

The threshold for defining the droughts can be derived in many different ways. The method, which is used most frequently, is to derive the threshold from exceedance probabilities. For example, the groundwater level which is exceeded

70% of the time can be used as threshold level. Common thresholds are the 50 to the 95-percentile. However for time series with many zeros, for example recharge or river discharge in arid regions, thresholds as low as the 20-percentile may have to be used (Santos and Goncalves-Henriques, 1999). Generally, with increasing skewness a lower exceedance percentile is selected. In Chapter 4, a new way of deriving the threshold level is introduced which does not need to be changed as a result of changes in the skewness or the number of zeros in the time series.

In Figure 3.3, the threshold level is constant in time. However, also a time varying threshold can be used (Hisdal *et al.*, 2001; Zaidman *et al.*, 2001). When using a variable threshold, anomalies or atypical flows rather than droughts are derived. Instead of using a variable threshold, other authors remove seasonality before analysing the drought occurrence (Eltahir and Yeh, 1999; McNab and Karl, 1991). Analysing anomalies rather than droughts means that anomalies can occur in wet periods. It depends on the purpose of the analysis whether this is suitable or not. An advantage of analysing anomalies rather than droughts is that it is usually easier to see relations between different variables in one area or over a larger area. A disadvantage is that often anomalies are not really what one is interested in operationally. For example, a wet season with relatively low precipitation is in many cases mainly important because of the potential for drought it causes for the drier season afterwards. In this thesis droughts are analysed rather than anomalies.

Please note that in the remainder of this thesis the term ‘drought’ is often used to describe the events derived using the threshold level approach, rather than events which are commonly called drought (see also Section 4.2).

3.5 Summary and conclusions

Groundwater droughts are mainly caused by a decrease in the amount and effectiveness of the precipitation, possibly in combination with a high evapotranspiration. The effectiveness of the precipitation can decrease because of an increase or decrease in the precipitation intensity or a change in the soil or vegetation. The main effects of groundwater drought are lowered groundwater levels and decreased outflow to the surface water system, however these cause a range of secondary effects.

The limited amount of research on groundwater drought is mainly concentrated on groundwater management for abstractions. Some studies show the integrating influence of the groundwater system, which increases the persistence of the droughts. An illustration of the propagation of drought through the groundwater system with data from the Pang catchment shows the large variability

in droughts. Although the behaviour of each individual drought event can be explained, it is difficult to derive more general conclusions on how droughts change as a result of the propagation through the groundwater system. A hypothesis of how droughts change might also be build with the knowledge of how a time series changes as a result of a propagation through a groundwater system and the knowledge of how droughts depend on the characteristics of the time series from which they are derived. However, because it is only partly understood how droughts depend on time series characteristics, especially when different changes are combined, the hypothesis is very limited. It is only clear that the number of droughts will decrease and that the persistence (duration) of the droughts will increase.

In the last part of this chapter, the approach used to derive droughts from time series of groundwater recharge, levels and discharge is described, which is the threshold level approach.

Chapter 4

Propagation of individual droughts through the groundwater system - an analytical approach using synthetic recharge¹

Abstract

The effect of drought on groundwater levels and discharge is often complex and poorly understood. Therefore the propagation of a drought from groundwater recharge to discharge and the influence of aquifer characteristics on the propagation was analysed by tracking a drought in recharge through a linear reservoir. The recharge was defined as a sinusoid function with a period of one year. The decrease in recharge due to drought was simulated by multiplying the recharge during one year with a drought fraction between 0 and 1, which represents a decrease in the recharge of 100 to 0%, respectively. The droughts were identified using the threshold level approach with a threshold, which is constant in time. For this case analytical formulations were derived, which express the drought duration and deficit in the groundwater discharge in terms of the decrease in recharge, the reservoir coefficient that characterises aquifer properties and the height of the threshold level. The results showed that the delay in the groundwater system caused a shift of the main part of the decrease in recharge from the high flow to the low flow period. This resulted in an increase in drought deficit for discharge compared to the drought deficit for recharge. Also the development of multi-year droughts caused an increase in drought deficit. The attenuation in the groundwater system caused a decrease in drought deficit. In most cases the net effect of these processes was an increase of drought deficit as a result of the propagation through groundwater. Only for small droughts the deficit decreased from recharge to discharge. The amount of increase or decrease depends on the reservoir coefficient and the severity of the drought. Under most conditions a maximum in the drought deficit occurred for a reservoir coefficient of around 200 days.

¹This chapter is based on the paper 'Peters, E., P.J.J.F. Torfs, H.A.J. van Lanen and G. Bier, 2003. Propagation of drought through groundwater - a new approach using linear reservoir theory. *Hydrological Processes* **17**(15): 3023-3040. DOI:10.1002/hyp.1274.'

Keywords: drought, low flows, groundwater, extreme events, analytic expressions, deficit, run theory, threshold level approach

4.1 Introduction

Natural droughts are recurring phenomena, which affect all components of the water cycle (Wilhite, 2000). When a drought affects groundwater, it is called a groundwater drought. Natural droughts can be classified into meteorological, agricultural and hydrological droughts, where hydrological droughts include both streamflow and groundwater droughts (Hisdal *et al.*, 2001). Like the other types of natural drought, groundwater droughts are caused by low precipitation possibly in combination with high evapotranspiration. Groundwater droughts develop only slowly from meteorological droughts. A deficit in precipitation (meteorological drought) can result in a recharge deficit, which in turn causes lowered groundwater levels and a deficit in groundwater discharge (McNab and Karl, 1991; Changnon, 1987; van Lanen and Peters, 2000). Another cause of groundwater drought is abstraction, which may enhance naturally occurring droughts, but in case of overexploitation may create groundwater droughts (van Lanen and Peters, 2000; Acreman *et al.*, 2000; Foster, 2000; Custodio, 2000). The consequences of groundwater drought are diverse. The direct effects are lower groundwater levels and a decrease of the groundwater flow to riparian areas, springs and streams. For shallow groundwater, capillary rise to the vegetation will decrease, which may affect wetlands and crop yield negatively. Also well yields may decrease and shallow wells may even dry up (Calow *et al.*, 1999). One of the most irreversible effects of prolonged groundwater drought, is the slow intrusion of salt water.

To date, little research has been devoted to the occurrence and propagation of drought in groundwater. Yet, from regression analyses relating drought in streamflow to catchment properties, it is well known that geology is one of the main factors influencing hydrological drought (Vogel and Kroll, 1992; Zecharias and Brutsaert, 1988). Recently however, the interest in groundwater drought has increased (Robins *et al.*, 1997; White *et al.*, 1999; Gottschalk *et al.*, 1997), also in connection with climate change (Leonard, 1999). Recent research includes work from Price *et al.* (2000), who propose outflow from storage in the unsaturated zone as the source of larger-than-expected groundwater discharge from chalk aquifers during drought. Marani *et al.* (2001) analysed the influence of geomorphic controls on groundwater discharge and in particular the influence on the behaviour of floods and droughts. A recent attempt to analyse the propagation of droughts from recharge to groundwater discharge by Peters *et al.* (2001) revealed several problems. A main difficulty is the lack of understanding of the way aquifer characteristics influence the propagation of

droughts through groundwater. Therefore this study aims to investigate systematically how droughts are propagated from recharge to groundwater levels and discharge, and to evaluate how this propagation depends on aquifer characteristics. To keep the analysis transparent, a synthetic recharge function was defined and the groundwater system was simulated as a linear reservoir with a reservoir coefficient representing the aquifer characteristics. These choices enabled the derivation of analytical expressions, which express the drought duration and deficit in terms of the decrease in recharge and the reservoir coefficient.

4.2 Definition of drought events

Although most people have quite a strong notion about what a drought is, no precise common definition of drought exists. Therefore it is important to start with a description of how droughts will be defined in this paper. Central in most definitions of drought is the concept of a water deficit over a limited period of time (up to several years), but extended in space (Dracup *et al.*, 1980; Beran and Rodier, 1985; Wilhite and Glantz, 1985; McNab and Karl, 1991; Hisdal *et al.*, 2001; National Drought Mitigation Center, 2003). In this paper the term ‘drought’ is used to describe events which are selected from a time series using the threshold level approach, which was first described by Yevjevich (1967) (Figure 4.1). This definition has three major consequences:

1. droughts can only occur during periods, which have a low water availability in the absolute sense and not during periods, which are only dry relative to the normal situation,
2. permanent low water availability is not called drought but ‘aridity’, and
3. not only extreme events are called droughts but all events, which have a low availability of water. These are often called ‘minor droughts’ or ‘non-extreme events’ (Hisdal *et al.*, 2002).

This definition of droughts is close to the meaning of the expression ‘low flow’, which is often used for streamflow (Smakhtin, 2001).

The threshold level approach is based on the theory of runs or crossing theory, which studies the statistical properties of runs above and below a given threshold level (Bras and Rodriguez-Iturbe, 1985). The threshold level approach is also called Peak Over Threshold approach (POT) and the series of events below the threshold are called the Partial Duration Series (PDS). For any hydrologically relevant variable x (e.g. recharge, discharge, groundwater

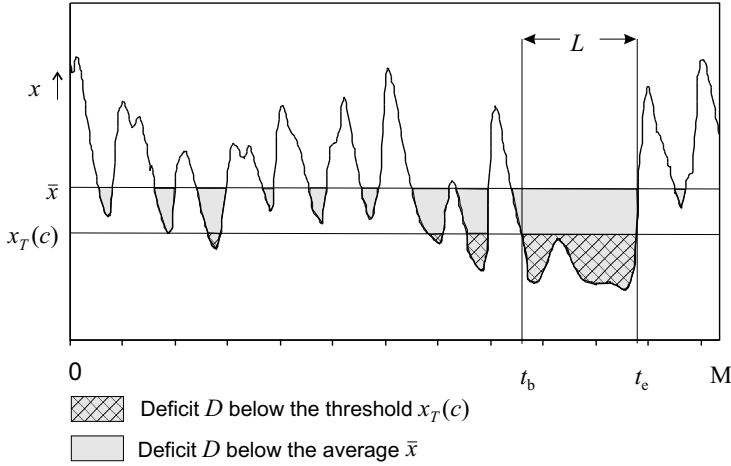


Figure 4.1: Illustration of the threshold level approach and the definition of the threshold level $x_T(c)$ for a time series of variable x with average \bar{x} of length M containing four droughts, where c is the drought criterion, L is drought duration and t_b and t_e are start and end time of the drought.

levels or storage) the deficit D or run sum below the threshold for a particular drought is calculated as:

$$D = \int_{t_b}^{t_e} (x_T - x(t)) dt \quad (4.1)$$

where t_b and t_e are the start and end date of the drought and x_T is the threshold (Figure 4.1). Please note that $x(t_b) = x(t_e) = x_T$ and that $x(t) < x_T$ for $t_b < t < t_e$. The duration L is calculated as:

$$L = t_e - t_b \quad (4.2)$$

An important step is the determination of an appropriate threshold level x_T . The threshold can be a naturally occurring threshold, for example the streamflow rate below which ships can no longer navigate a river or the level below which no groundwater can be extracted from a specific well. However, in many cases, no natural threshold is available and therefore the threshold is derived from observations. The most commonly used method is the percentile approach, which means that a percentile (e.g. 70 or 80-percentile) from the cumulative frequency distribution is chosen as threshold. However using the threshold level approach for data which contain many zeros or which are highly skewed (e.g. recharge or discharge from intermittent streams) is problematic. Solutions to this problem, which are presented in literature, namely use of

a very low percentile (e.g. 20-percentile by Santos and Goncalves-Henriques (1999)), use of only part of the data (e.g. only winter) or using annual data, are not suitable for this study, because they all would require using different event definitions in one analysis. This would make comparisons between drought deficits very difficult. Therefore a new approach to derive threshold levels is introduced, which is based on relating the total deficit below the threshold to the total deficit below the average. The total deficit below a threshold is the sum of the deficits of all droughts below this threshold or in other words the sum of the Partial Duration Series. This is illustrated in Figure 4.1. Thus the threshold function $x_T(c)$ can be defined as follows:

$$\int_0^M (x_T(c) - x(t))_+ dt = c \int_0^M (\bar{x} - x(t))_+ dt \quad (4.3)$$

where:

$$x_+ = \begin{cases} x & \text{if } x \geq 0 \\ 0 & \text{if } x < 0 \end{cases}$$

M is the length of the time series and c is the *drought criterion*, which determines the height of the threshold level. The drought criterion c is the ratio of the deficit below the threshold to the deficit below the average. If $c = 1$ the threshold level is equal to the average \bar{x} . If $c = 0$ the threshold level is equal to the minimum of x . \bar{x} is the average of variable x , which is calculated as $\bar{x} = \frac{1}{M} \int_0^M x(t) dt$. This definition of the threshold also ensures that the total drought deficit decreases with decreasing amplitude of $x(t)$, something which is not necessarily true when the threshold is determined with percentiles.

4.3 The propagation of a drought in a linear reservoir

An overview of the approach used to analyse the propagation of droughts from recharge to discharge is presented in Figure 4.2. A description of the recharge and the derivation of the discharge will be presented later. The groundwater system or aquifer was approximated by a linear reservoir. The discharge rate from the linear reservoir is given by:

$$q = \frac{1}{j} S \quad (4.4)$$

where q is the discharge rate [LT^{-1}], S is the storage of the reservoir [L] and j is the reservoir coefficient [T]. According to non-linear drainage theory (Krajenhof van de Leur, 1962; Rorabaugh, 1964; Ritzema, 1994), the reservoir coefficient j can be interpreted, in specific cases, as $j = \mu l^2 / \pi^2 k D$, where μ is

the storage coefficient [-], l is the distance between streams [L] and kD is the transmissivity [L^2T^{-1}]. This interpretation is valid for horizontal flow in an isotropic medium between parallel drains. For naturally drained aquifers, a more general interpretation is the response time ($\mu l^2/kD$) (Birtles and Wilkinson, 1975). Values of j of 1 to 20 or 30 d are generally applicable to artificially drained fields and values of 300 to 2000 d to discharge from aquifers (Vereniging Voor Landinrichting, 1992).

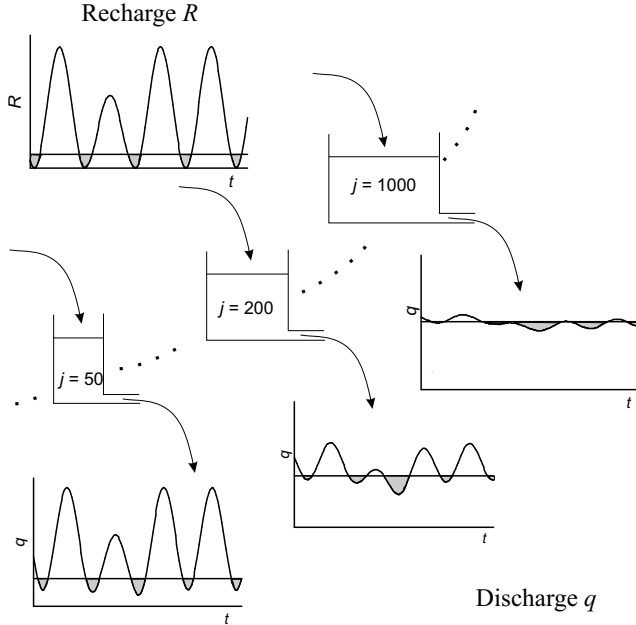


Figure 4.2: Schematic overview of the procedure followed to analyse the propagation of drought through groundwater. The sinusoid recharge function serves as input to the linear reservoir, which is characterised by the reservoir coefficient j (in days).

Combining Equation (4.4) with the equation for the conservation of mass results in the following ordinary, first-order, non-homogeneous differential equation:

$$\frac{dq(t)}{dt} = \frac{1}{j} (R(t) - q(t)) \quad (4.5)$$

where $R(t)$ is the recharge rate [LT^{-1}]. As groundwater is approximated by a linear reservoir, the principle of superposition can be used to analyse the propagation of a drought through the reservoir. Let the recharge rate $R(t)$ be composed of two parts, namely the normal recharge rate $R_n(t)$ and the decrease in recharge rate due to drought $R_d(t)$ then:

$$R(t) = R_n(t) - R_d(t) \quad (4.6)$$

From the principle of superposition it follows that discharge rate can also be written as:

$$q(t) = q_n(t) - q_d(t) \quad (4.7)$$

where $q_n(t)$ is the normal discharge and $q_d(t)$ is the decrease in discharge as a result of the decrease in recharge. The total decrease in recharge Dc_R c.q. discharge Dc_q is:

$$Dc_R = \int_{-\infty}^{\infty} R_d(t) dt \quad (4.8)$$

As groundwater is simulated as a linear reservoir, the transient discharge from the reservoir and the storage in the reservoir (represented by the level) are identical, except for a scaling factor and dead storage. From now on only the discharge will be analysed, but the analysis would have been identical for the reservoir storage or groundwater level. For more complicated reservoirs, like natural aquifers, the relationship between storage and discharge may not be trivial and a separate analysis may be required (Chapter 8).

4.4 Recharge and discharge

4.4.1 Definition of the recharge

The next step is to define the recharge function in Equation (4.6). This recharge function should be simple enough to allow the derivation of an analytical expression, but should also be sufficiently realistic to allow a meaningful analysis. The recharge is described by a sinusoidal shape, which represents annually recurring recharge (Figure 4.2). The normal recharge rate is defined as follows:

$$R_n(t) = R_0 (1 + \sin(2\pi\omega t)) \quad (4.9)$$

where R_0 [LT^{-1}] is the long-term average recharge rate and ω [T^{-1}] is the frequency of the recharge. The dry period is defined as a single year with decreased recharge. The decrease in the recharge is defined as:

$$R_d(t) = \begin{cases} (1 - f_d)R_n(t) & \text{for } \frac{3}{4\omega} \leq t < \frac{7}{4\omega} \\ 0 & \text{for } t < \frac{3}{4\omega} \text{ and } t \geq \frac{7}{4\omega} \end{cases} \quad (4.10)$$

where f_d [-] is the *drought fraction*, which determines the amount of decrease in the recharge. For all examples in this article, ω is $1/365 \text{ d}^{-1}$ and R_0 is 0.685 mm d^{-1} (250 mm a^{-1}), an amount of recharge which is common in sub-humid climates like the UK or the Netherlands. The drought fraction specifies the ratio between the recharge in the drought year and the recharge in an average year. For example, for $f_d = 0.4$ the $R(t)$ in the drought year is $0.4R_n(t)$. An example of the recharge for $f_d = 1$ (no drought) and $f_d = 0.4$ is

given in Figure 4.3. The sinusoidal function assumes a systematic sequence of periods with low recharge (summer or dry season) and high recharge (winter or wet season). The defined recharge function in combination with the event definition with a threshold which is constant in time, implies that a drought will occur each year.

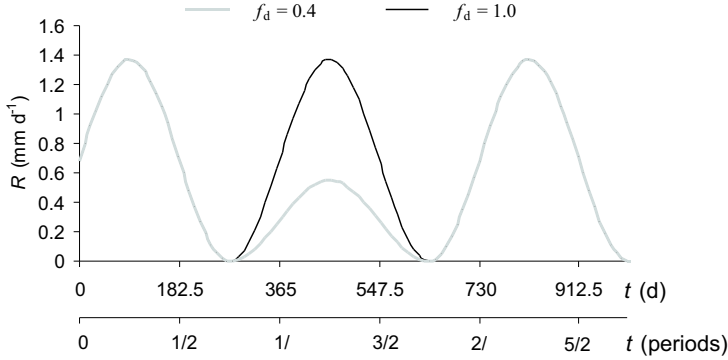


Figure 4.3: Recharge functions R for $f_d = 1.0$ and $f_d = 0.4$ for the time expressed both in days and periods of the sine function (ω is the frequency).

The selected definition of recharge limits the analysis in two ways. First, this type of recharge with a clearly seasonal recharge peak each year, mainly occurs in humid or sub-humid climates. For arid or semi-arid climates the recharge would be much more erratic. Secondly, the analysis is limited to droughts which originate in the wet period, as mainly the recharge during the peak (wet season) is decreased (Figure 4.3). However it is expected that this type of drought is especially important for groundwater (Warren, 1994; Seely, 1999).

4.4.2 Derivation of the discharge

From Equation (4.9) and (4.10) and Equation (4.5) and (4.7) the discharge rate can be derived. The normal discharge rate $q_n(t)$ is:

$$q_n(t) = R_0 \left(1 + \frac{1}{jA} \sin(2\pi\omega t + B) \right) \quad (4.11)$$

where:

$$A = \sqrt{(1/j)^2 + (2\pi\omega)^2}$$

$$B = \arcsin\left(\frac{-2\pi\omega}{A}\right)$$

The decrease in discharge rate $q_d(t)$ due to a decrease in the recharge rate is:

$$q_d(t) = \begin{cases} 0 & \text{for } t < \frac{3}{4\omega} \\ (1 - f_d) q_n(t) - R_0\left(1 - \frac{1}{(jA)^2}\right)(1 - f_d)e^{-\frac{t}{j} + \frac{3}{4\omega j}} & \text{for } \frac{3}{4\omega} \leq t < \frac{7}{4\omega} \\ R_0\left(1 - \frac{1}{(jA)^2}\right)(1 - f_d)e^{-\frac{t}{j} + \frac{3}{4\omega j}}(e^{\frac{1}{\omega j}} - 1) & \text{for } t \geq \frac{7}{4\omega} \end{cases} \quad (4.12)$$

These equations can easily be verified by inserting $R(t)$ and $q(t)$ in Equation (4.5). The discharge $q(t)$ is illustrated in Figure 4.2 for $f_d = 0.6$, $c = 0.1$ and three values of the reservoir coefficient ($j = 50$, $j = 200$ and $j = 1000$ d). The decrease in discharge $q_d(t)$ is presented in Figure 4.4 for $f_d = 0.6$. Please note that the term jA can also be written as: $\sqrt{1 + (2\pi\omega j)^2}$. This term combines the effect of the response time of the groundwater reservoir defined by the reservoir coefficient with the frequency of the recharge. From $q_n(t)$ (Equation (4.11)) it can be seen that the transition through the linear reservoir results in an amplitude magnification (attenuation) of $\frac{1}{jA}$ and a phase shift (delay) of B . This is illustrated well in Figure 4.4. For increasing reservoir coefficients the maximum in the decrease comes later (delay) and less high (attenuation), the right tail becomes heavier and the duration increases. Of course, the total amount of decrease is identical, irrespective of the reservoir coefficient. In the following we will examine how the attenuation and delay interact with the drought event definition to form the drought duration and deficit.

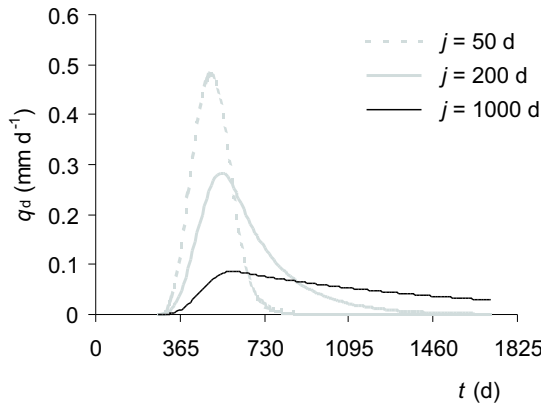


Figure 4.4: Decrease in discharge $q_d(t)$ as a result of a decrease in the recharge ($f_d = 0.6$).

4.5 Derivation of drought duration and deficit

4.5.1 Threshold level

In this section expressions describing the duration and deficit of the drought will be derived. First, however, an expression for the threshold level will be derived according to the event definition defined previously (Equation (4.3)). The threshold is derived from the normal situation, i.e. for $R_n(t)$ and $q_n(t)$. In Appendix 4.A the derivation of the threshold for the recharge R_T and the discharge q_T is described. The thresholds are:

$$R_T(c) = R_0 + R_0 X(c) \quad (4.13)$$

$$q_T(c) = R_0 + \frac{R_0 X(c)}{jA} \quad (4.14)$$

where $X(c)$ is a shape function that only depends on the drought criterion c and which transforms the drought criterion based on the deficit (Equation (4.3) and Figure 4.1) to a threshold level. $X(c)$ is presented as a function of the drought criterion c in Figure 4.5.

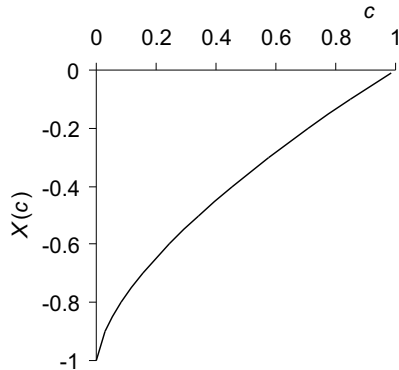


Figure 4.5: Shape function $X(c)$ as a function of the drought criterion c , for the threshold in the recharge and discharge (Equations (4.13) and (4.14)).

4.5.2 Duration and deficit

Recharge

With the expression for the threshold level (Equation (4.13)), the duration and deficit of the droughts in the recharge (recharge droughts) can be calculated. In Figure 4.6 this is illustrated for two possible situations. For $f_d = 0.6$ the reduction in recharge is not very large and the peak at 456 d ($\frac{5}{4\omega}$) still exceeds the threshold. Two droughts result with identical duration and deficit ($Dw1_R$ and $Dw2_R$). Both droughts last less than one year (within-year drought). However, when the peak in the recharge remains lower than the threshold (e.g. for $f_d = 0.15$), one drought with a duration of more than one year results (multi-year drought, here two-year drought with deficit Dm_R). This has to be taken into account when calculating the deficit and duration of the droughts. The duration L_R and deficit D_R of the recharge droughts are determined according to Equations (4.1) and (4.2). When determining the times of intersection between the recharge function and the constant R_T , we have to consider in which part of the recharge function the intersections will be, namely whether it is in the drought part ($\frac{3}{4\omega} \leq t < \frac{7}{4\omega}$ d) or not. For the two-year drought both times of intersection are in the normal part R_n of the recharge. For the two within-year droughts one of the intersections will be in the normal part and the other one in the drought part (Figure 4.6).

The times of intersection t_e and t_b for the first within-year drought and the two-year drought are:

$$t_b = \frac{1}{2\omega} - \frac{1}{2\pi\omega} \arcsin(X(c)) \quad (4.15)$$

$$t_e = \begin{cases} \frac{1}{\omega} + \frac{\arcsin X_{R,d}(c)}{2\pi\omega} & \text{for the first within-year drought} \\ \frac{1}{\omega} + \frac{\arcsin X(c)}{2\pi\omega} & \text{for two-year drought} \end{cases} \quad (4.16)$$

where:

$$X_{R,d}(c) = \frac{R_T(c) - f_d R_0}{f_d R_0} = \frac{X(c) + 1 - f_d}{f_d} \quad (4.17)$$

For the second within-year drought, t_e and t_b are exchanged. The duration of the recharge droughts L_R is:

$$L_R(c) = \begin{cases} \frac{1}{2\omega} + \frac{1}{2\pi\omega} [\arcsin X(c) + \arcsin(X_{R,d}(c))] & \text{for within-year droughts} \\ & (Lw1_R \text{ and } Lw2_R) \\ [3\pi + 2 \arcsin X(c)] / 2\pi\omega & \text{for two-year droughts} \\ & (Lm_R) \end{cases} \quad (4.18)$$

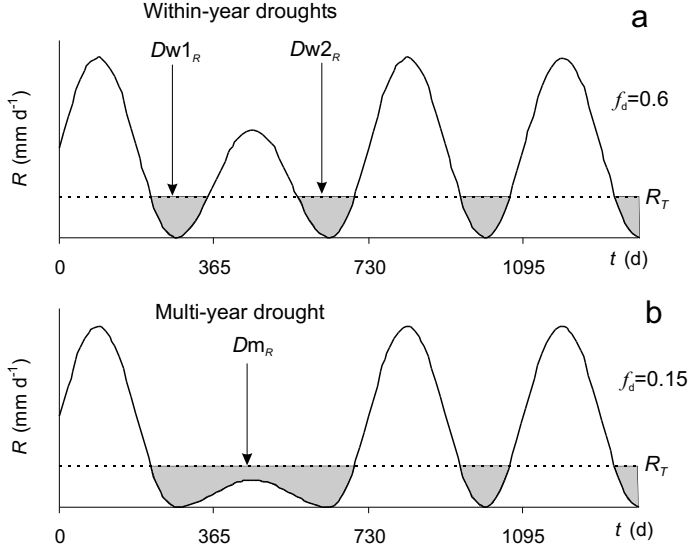


Figure 4.6: Recharge drought below threshold R_T ($c = 0.3$) for drought fraction $f_d = 0.6$ (a) and for $f_d = 0.15$ (b). $Dw1_R$ and $Dw2_R$ are the drought deficit for the first and second within-year drought, Dm_R is the drought deficit for the multi-year drought (two-year here) (Equations (4.1) and (4.19)). Please note: The additions w (for within-year drought) and m (for multi-year drought) have been added to distinguish between within-year and multi-year droughts.

Where $Lw1_R$ and $Lw2_R$ refer to the drought duration in the recharge of the first and second within-year drought and Lm_R to the deficit of the multi-year drought. Using Equation (4.15) and (4.16) for t_b and t_e respectively the following relations are derived for the deficit of the recharge drought D_R :

$$D_R(c) = \begin{cases} \frac{cR_0}{2\pi\omega} + \frac{f_d R_0}{2\pi\omega} \left[\sqrt{1 - (X_{R,d}(c))^2} + X_{R,d}(c) \arcsin(X_{R,d}(c)) + \frac{\pi}{2} X_{R,d}(c) \right] & \text{for within-year droughts} \\ & (Dw1_R \text{ and } Dw2_R) \\ \frac{cR_0}{\pi\omega} + \frac{f_d R_0}{\omega} X_{R,d}(c) & \text{for two-year droughts} \\ & (Dm_R) \end{cases} \quad (4.19)$$

Where $Dw1_R$ and $Dw2_R$ refer to the drought deficit in the recharge of the first and second within-year drought and Dm_R to the deficit of the multi-year drought (Figure 4.6).

Discharge

For the discharge the decrease is no longer limited to the period between $t = \frac{3}{4\omega}$ and $t = \frac{7}{4\omega}$, but it becomes longer as was illustrated in Figure 4.4. This means that the times of intersection of the drought in the discharge (discharge drought) can no longer be determined analytically, as it is not known beforehand in which part of the discharge function the intersection will be (part 1: $t < \frac{3}{4\omega}$, part 2: $\frac{3}{4\omega} \leq t < \frac{7}{4\omega}$, part 3: $t \geq \frac{7}{4\omega}$). The example in Figure 4.7 shows that the deficit is spread out over at least three separate droughts. The main drought is the two-year drought lasting from approximately 300 to 860 d. For this example the start of the drought t_b is in part 2 of the discharge function and the end of the drought t_e is in part 3 (Equation (4.12)). For a somewhat smaller reservoir coefficient or a higher threshold, however, the start of the drought will be in part 1 of the discharge. As no analytical solution is possible, the times of intersection are determined numerically. With the numerical approximation of the times of intersection, duration L_q and deficit D_q of discharge droughts are determined according to Equations (4.2) and (4.1). The integral in Equation (4.1) is expanded analytically to arrive at an expression for D_q . Depending on the part the drought starts and ends in, different expressions result. An example of the expressions derived for D_q is presented in Appendix 4.B.

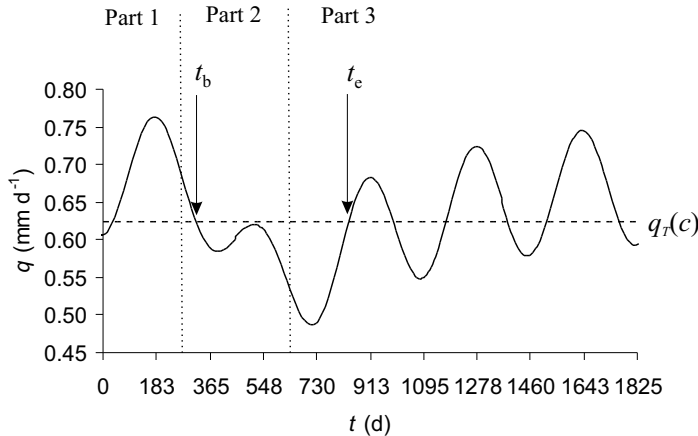


Figure 4.7: Drought derived from the discharge ($j = 500$ d). The times t_b and t_e denote the start and end of the drought respectively. Part 1 to 3 denote the three parts of the discharge as defined in Equations (4.7), (4.11) and (4.12).

4.6 Results

4.6.1 Recharge

In Figure 4.8 the duration L_R and deficit D_R of the recharge droughts are presented as a function of the drought fraction f_d and the drought criterion c . The total decrease in recharge DC_R (Equation (4.8)) is added for comparison in Figure 4.8b. The discontinuity in the lines is caused by the transition from one within-year to a two-year drought. When the peak in the recharge during the drought no longer exceeds the threshold, the deficits $Dw1_R$ and $Dw2_R$ are summed to form one drought with deficit Dm_R (Figure 4.6). If the sum (duration or deficit) of the two within-year droughts would have been presented, the lines would have been continuous. Obviously, L_R increases with increasing drought criterion c and decreasing drought fraction f_d , with the major increase for the change from within-year droughts to two-year droughts (Figure 4.8a). For two-year droughts, L_R no longer depends on the drought fraction at all, because the start and end are only determined by the normal recharge R_n . This is illustrated in Figure 4.6.

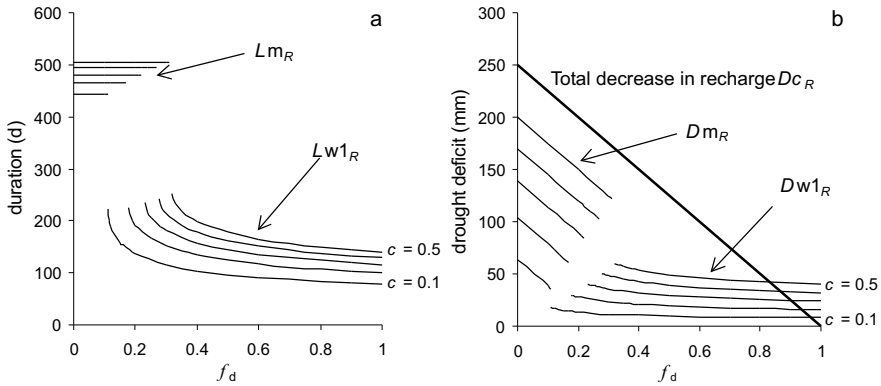


Figure 4.8: Recharge drought duration L_R (a) and deficit D_R (b) for 5 values of the drought criterion c : $c = 0.1$ to $c = 0.5$ (step 0.1). Also presented in figure B is the total decrease in recharge DC_R according to Equation (4.8).

Generally the drought deficit D_R is much smaller than the actual decrease in recharge DC_R (Figure 4.8b). Only for very small droughts ($f_d \approx 1$) D_R is larger because D_R cannot become smaller than the deficit in a normal year ($f_d = 1$). For small droughts D_R is rather insensitive to the drought fraction f_d . For long droughts (multi-year droughts), on the other hand, D_R is linearly related to the drought fraction f_d and thus is parallel to DC_R . This is evident from the equations for D_R (Equation (4.19), Dm_R).

4.6.2 Discharge

In Figure 4.9 an example of the results for the drought deficit D_q is presented from which the most important processes will be explained. Please note that the x-axis has a logarithmic scale. In Figure 4.9 three symbols are shown, which are labelled $Dw1_q$, $Dw2_q$ and Dm_q . These are the deficits for the first within-year drought ($Dw1$), for the second within-year drought ($Dw2$) and for the multi-year drought (Dm) (see also Figure 4.6). Also the deficit of the associated recharge drought D_R is indicated. D_R is practically identical to the deficit of the discharge drought for reservoirs with a very small reservoir coefficient ($j \approx 1$), therefore D_R has not been indicated in the overview in Figure 4.11, which will be presented later. Overall we see a slight decrease in D_q for the first within-year drought ($Dw1_q$), a rise in D_q for the second within-year drought ($Dw2_q$) and a combination of sudden discontinuous increases ('jumps') and a decrease between the jumps for the multi-year droughts (Dm_q).

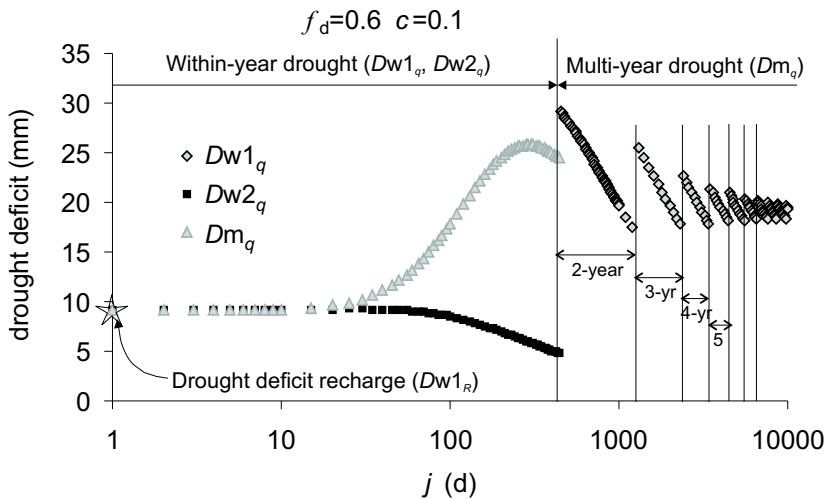


Figure 4.9: Deficit of the discharge droughts D_q as a function of the reservoir coefficient j for drought fraction $f_d = 0.6$ and drought criterion $c = 0.1$ for two within-year droughts ($Dw1_q$ and $Dw2_q$) and one multi-year drought (Dm_q) (Figure 4.6). Also presented is the deficit of the recharge drought $Dw1_R$ for $f_d = 0.6$ and $c = 0.1$.

The decrease of $Dw1_q$ is caused by the increasing attenuation with increasing reservoir coefficient j (Figure 4.4). The increase of $Dw2_q$ is the result of the delay of the decrease in discharge $q_d(t)$ (Dc_q). The main part of Dc_q shifts from the wet to dry season with increasing j (Figure 4.4). For reservoir coefficients of up to $j = 290$ d the net effect of attenuation and delay is an increase in $Dw2_q$. For larger reservoir coefficients, the decrease in q due to attenuation becomes larger than the increase caused by the delay and therefore D_q decreases. For

multi-year droughts (Dm_q), every discontinuity ('jump') represents the addition of another year to the duration of the drought (Figures 4.7 and 4.9). The decrease in deficit in between the 'jumps' is again caused by the attenuation as explained earlier. The large number of discontinuities shows how long the droughts become for very large reservoir coefficients (> 10 years for $j > 10000$ d). These droughts are so long because the decrease in the recharge is followed by average recharge conditions (Figure 4.2) and this assumption becomes increasingly unlikely for longer droughts. In reality the droughts would have been ended by wetter than normal recharge conditions.

In Figure 4.10 the drought duration (L_q) for the example in Figure 4.9 is presented. This shows that the duration of the discharge droughts L_q only increases with increasing reservoir coefficient, which means that discharge droughts last longer than recharge droughts. The duration of the second within-year drought is larger than of the first within-year drought, because the second drought is affected more by the decrease in recharge. The major increase in duration ('jump') is caused by the transitions from within-year droughts to multi-year droughts.

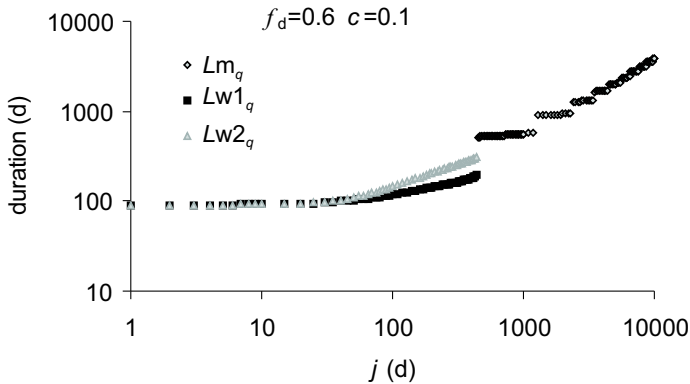


Figure 4.10: Duration of the discharge droughts L_q as a function of the reservoir coefficient j for drought fraction $f_d = 0.6$ and drought criterion $c = 0.1$ for two within-year droughts ($Lw1_q$ and $Lw2_q$) and one multi-year drought (Lm_q).

In Figure 4.11 an overview is presented for discharge droughts deficits with a decrease in recharge of 20% ($f_d = 0.8$) to 80% ($f_d = 0.2$) for two drought criteria: $c = 0.1$ and $c = 0.3$. The influence of the drought criterion will be discussed in the following section. Please recall that the deficit in the recharge is practically identical to the deficit for $j = 1$ (Figure 4.9). The general pattern as explained for the specific case with $f_d = 0.6$ and $c = 0.1$ (Figure 4.9) is

evident in most examples. Only for $f_d = 0.8$ no multi-year droughts develop and as a consequence the drought deficit becomes very low for large reservoir coefficients. The increase in drought deficit with increasing drought severity (decreasing drought fraction f_d) is much smaller for small reservoir coefficients (from 8.4 for $f_d = 0.8$ to 13.4 mm for $f_d = 0.2$ ($c = 0.1$)) than for large reservoir coefficients (from 0.8 for $f_d = 0.8$ to 98 mm for $f_d = 0.2$ ($c = 0.1$)). Obviously, multi-year droughts develop for smaller reservoir coefficients in case of more severe droughts (f_d small) and higher thresholds (c large). For most of the examples presented in Figure 4.11 the deficit has a maximum. The average reservoir coefficient, where the maximum occurs, is $j = 205$ d (range: 140-290 d).

4.7 Discussion

The results of the numerical experiment presented in Figures 4.9, 4.10 and 4.11 have been tested partially using real data by Peters and van Lanen (2003)(Chapter 5). Instead of a synthetic recharge signal, they used recharge based on observed meteorological data as input for a linear reservoir. Their results confirm the main results of this paper. Both in sub-humid and semi-arid climate types a maximum in the discharge deficit occurs for intermediately large reservoir coefficients.

The results presented here can also be interpreted for a single reservoir or aquifer (for one value of j). A small decrease in the recharge translates into an even smaller drought in the discharge or no drought at all. A large decrease in the recharge translates into a large drought in the discharge.

The way in which the drought (decrease in the recharge R_d , Equations (4.6) and (4.10)) is simulated influences the results. In this paper, the decrease in recharge was defined in the wet season and the decrease shifts to the dry season as a result of the delay of the reservoir. This causes the drought deficit to be larger in the discharge than in the recharge. Of course, it can easily be deduced that if the main decrease in recharge is in the dry season, then the delay would cause the decrease in discharge to shift in the direction of the wet season and this would result in a decrease in deficit with increasing reservoir coefficient. However, in most cases a decrease in recharge during the dry season is hardly possible due to the physical processes determining the formation of recharge.

4.7.1 Influence of the drought event definition

Several aspects of the drought event definition influence the calculated drought duration and deficit. The influence of the height of the threshold level is

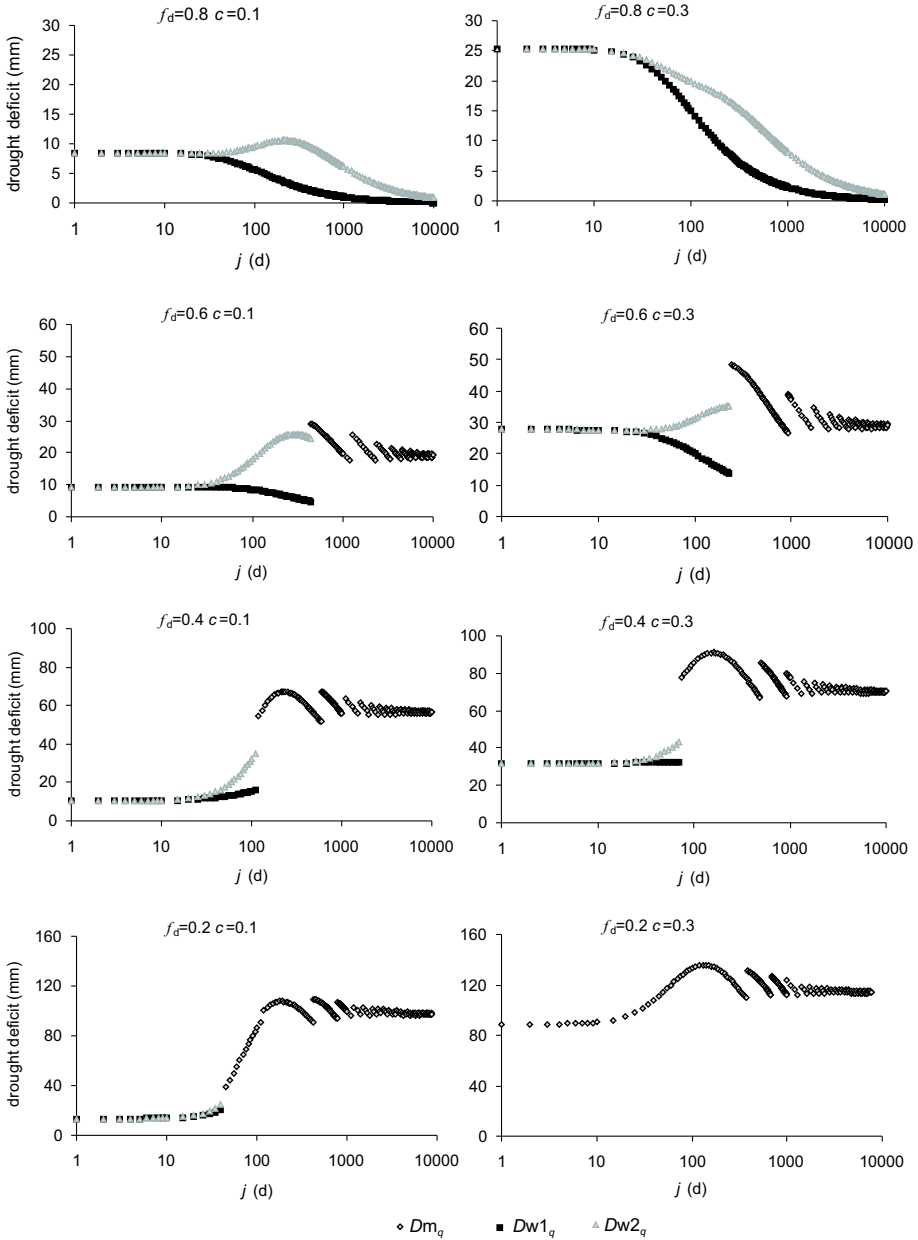


Figure 4.11: Deficit of the discharge drought D_q for several values of the drought fraction f_d and drought criterion c . Explanation of symbols see Figure 4.9.

straightforward (Figure 4.11): for a higher threshold level ($c = 0.3$) the drought duration and deficit are larger than for a lower threshold level ($c = 0.1$). For higher threshold levels, multi-year discharge droughts develop for less severe recharge droughts and for lower reservoir coefficients. A consequence of using a constant threshold as drought event definition is the fact that the drought deficit is not always a good measure for the overall decrease in recharge or discharge (Figure 4.8). Because only the part below the threshold is analysed, deviations during normally high recharge are not taken into account. Thus, if the main interest is in volumes of water rather than water levels, this approach can be misleading. Therefore in some cases a different drought event definition is used, for example for reservoir management (Montaseri and Adeloey, 1999).

The type of event definition has a more profound influence on the results than the height of the threshold level. If a variable threshold had been used instead of a threshold, which is constant in time, the results for the recharge would have been like the decrease in recharge DC_R in Figure 4.8b and the results for the discharge would have been like q_d (Figure 4.4). If a threshold had been chosen, which is constant in time and identical for all reservoir coefficients, the deficit volume would be largest for the recharge and for the groundwater discharge of the fastest responding groundwater systems (Figure 4.2). Instead of the threshold level approach, also the annual n-day minimum discharge, which is a commonly used measure for streamflow drought frequency analysis (Smakhtin, 2001), could have been used as drought event definition. In Figure 4.12 the minimum discharge is presented as a function of the reservoir coefficient for different drought fractions. As expected, the minimum discharge increases with increasing reservoir coefficient and decreases with drought severity. The increase in minimum discharge with the reservoir coefficient is far from linear. In Figure 4.13 the decrease in minimum recharge compared to the minimum recharge for the normal discharge q_n is presented. This shows that for a reservoir coefficient of about 225 d the minimum discharge decreases most compared to the normal situation for the full range of drought fractions. This is close to the value of 205 d for which, on average, the maximum in the deficit occurs (Figure 4.11).

4.8 Conclusions

The simple approach that was used to simulate the propagation of droughts through a groundwater system was found to provide a clear overview of the effects of the propagation through a groundwater reservoir (namely attenuation and delay) on recharge drought. The approach, which consisted of a combination of a synthetic recharge function with a linear reservoir, enabled the analysis of a wide range of reservoir coefficients (aquifer characteristics)

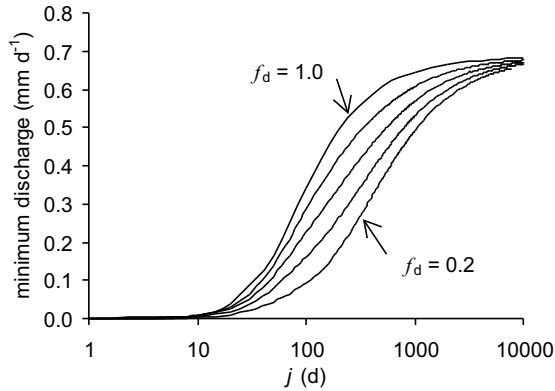


Figure 4.12: Minimum discharge for several values of the drought fraction: $f_d = 0.2$ to $f_d = 1.0$ (step 0.2) ($f_d = 1$ means no drought, normal recharge).

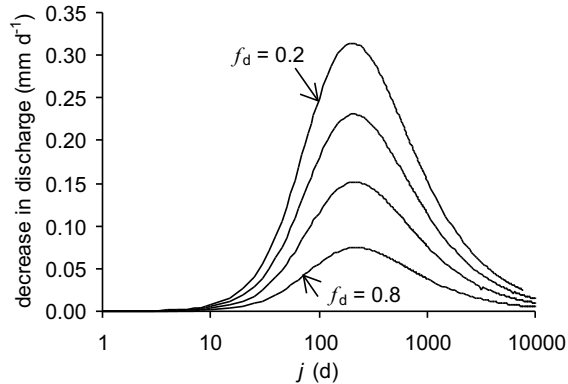


Figure 4.13: Decrease in minimum discharge with respect to the normal minimum discharge as a function of the reservoir coefficient, for several values of the drought fraction: $f_d = 0.2$ to $f_d = 0.8$ (step 0.2).

and drought severities. Although the effects of a reservoir (attenuation and delay) on inputs are well known, the effect of the propagation of a recharge drought (defined using a constant threshold) through a groundwater system is less straightforward and depends on the interaction of the attenuation and delay with the drought event definition. The analyses resulted in the following conclusions:

1. The *main effect of the attenuation* is a decrease of the deficit of discharge droughts compared to recharge droughts. The decrease in the drought deficit is caused by a decrease in the amplitude of the discharge compared to the recharge function. The drought duration remains practically constant or increases slightly.
2. The *main effect of the delay* is an increase in the duration and deficit of the discharge drought. As the main decrease in recharge was defined in the high flow period, the decrease in recharge shifted from the wet season in the direction of the following dry season.
3. A *combined, secondary effect* of the attenuation and delay is the development of multi-year droughts.

The net effect of these three effects on the duration and deficit of the groundwater discharge drought depends on the amount of decrease of the recharge and on aquifer characteristics represented by the reservoir coefficient. In most cases the deficit and duration of the discharge drought were larger than the deficit and duration of the recharge drought. Only for small droughts (20% decrease in recharge during one year) the deficit of the discharge drought was smaller. The amount of deficit increase from a recharge to a discharge drought depends on the reservoir coefficient, on the severity of the drought and on the height of the threshold level. In most cases, the largest increase in deficit occurred for groundwater systems with a reservoir coefficient of around 200 d. The increase in deficit was generally larger for more severe droughts and for lower threshold levels.

Acknowledgements The research in this paper was in part carried out in the framework of the ARIDE project (Assessment of the Regional Impact of Droughts in Europe). Support has been given by the European Commission under contract no. ENV4-CT97-0553. The research was carried out under the Programme of the Wageningen Institute of Environment and Climate Research (WIMEK-SENSE).

Appendix 4.A Derivation of the threshold level

The threshold is derived from the normal situation, i.e. for $R_n(t)$ and $q_n(t)$. The derivation is based on the deficit and duration of one cycle ($\frac{1}{\omega}$ or 365 d). Based on the event definition (Equation (4.3)), the following equation defines the threshold for the recharge (R_T):

$$\int_{t_b(R_T)}^{t_e(R_T)} (R_T - R(t))dt = c \int_{t_b(R_0)}^{t_e(R_0)} (R_0 - R(t))dt \quad (4.20)$$

Where t_b and t_e are the times of intersection between the threshold level and the recharge function (left-hand side) and the average recharge and the recharge function (right-hand side) respectively. For the threshold (R_T) t_b and t_e enclose the period where $R(t) < R_T$. The times of intersection follow from equating the recharge $R(t)$ to the threshold:

$$R_T = R_0 (1 + \sin(2\pi\omega t)) \quad (4.21)$$

This results in:

$$\begin{aligned} t_b &= \frac{1}{2\omega} - \frac{1}{2\pi\omega}(\arcsin(X_R)) \\ t_e &= \frac{1}{\omega} + \frac{1}{2\pi\omega}(\arcsin(X_R)) \end{aligned} \quad (4.22)$$

where:

$$X_R = \frac{(R_T - R_0)}{R_0}$$

The times of intersection for the average are $\frac{1}{2\omega}$ and $\frac{1}{\omega}$. Substituting $R(t)$ in Equation (4.20) results in:

$$\int_{t_b}^{t_e} (R_T - R_0 - R_0 \sin(2\pi\omega t))dt = c \int_{\frac{1}{2\omega}}^{\frac{1}{\omega}} (-R_0 \sin(2\pi\omega t))dt \quad (4.23)$$

The left hand side of Equation (4.23) is (please note that: $\cos(\arcsin(x)) = \sqrt{1 - x^2}$):

$$(R_T - R_0) \left(\frac{1}{2\omega} + \frac{1}{\pi\omega}(\arcsin(X_R)) \right) + \frac{R_0}{\pi\omega} \left(\sqrt{1 - X_R^2} \right) \quad (4.24)$$

The right hand side of Equation (4.23) is:

$$\frac{cR_0}{\pi\omega} \quad (4.25)$$

Combining the solution of the right hand side and left hand side, results after rewriting in:

$$\sqrt{1 - X_R^2} + X_R \arcsin X_R + X_R \frac{\pi}{2} = c \quad (4.26)$$

This means that the dimensionless number X_R , which was defined above, depends only on the drought criterion c in the drought event definition. The number X_R defined by Equation (4.26) is from now on denoted as the function $X(c)$. X_R is used to refer to the dimensionless number. The function $X(c)$ can be derived numerically. In Table 4.1 some relevant values for $X(c)$ are listed.

Table 4.1: Values of X as a function of drought criterion c

Drought criterion c	$X(c)$
0.1	-0.778
0.2	-0.649
0.3	-0.541
0.4	-0.447
0.5	-0.360

It is also possible to derive an expression for the threshold based on percentiles. Comparison of the two thresholds results in the following: $c = 0.1$ is equal to Q78, $c = 0.2$ is Q72, $c = 0.3$ is Q68, $c = 0.4$ is Q65 and $c = 0.5$ is Q62 (Q78 is the flow which is equalled or exceeded 78% of the time). Figure 4.5 gives $X(c)$ as a function of c . Thus for the threshold R_T the following equation holds:

$$R_T(c) = R_0 + R_0 X(c) \quad (4.27)$$

In the same way the threshold for the discharge (q_T) can be derived. This results in the following expression for the threshold for the discharge:

$$q_T(c) = R_0 + \frac{R_0 X(c)}{jA} \quad (4.28)$$

Appendix 4.B Derivation of the deficit for the discharge

To arrive at analytical expressions for the deficit, several possibilities with regard to the timing of the intersection have to be taken into account. An overview of the different possibilities is presented below:

1. $t_b < \frac{3}{4\omega}$ and $\frac{3}{4\omega} \leq t_e < \frac{7}{4\omega}$
2. $t_b < \frac{3}{4\omega}$ and $t_e \geq \frac{7}{4\omega}$
3. $\frac{3}{4\omega} \leq t_b < \frac{7}{4\omega}$ and $\frac{3}{4\omega} \leq t_e < \frac{7}{4\omega}$
4. $\frac{3}{4\omega} \leq t_b < \frac{7}{4\omega}$ and $t_e \geq \frac{7}{4\omega}$

As an example the deficit for the first option is presented.

$$D_q = \int_{t_b}^{\frac{3}{4\omega}} (q_T - q(t)) dt + \int_{\frac{3}{4\omega}}^{t_e} (q_T - q(t)) dt = D_{q,I} + D_{q,II} \quad (4.29)$$

where:

$$D_{q,I} = (q_T - R_0) \left(\frac{3}{4\omega} - t_b \right) + \frac{R_0}{2\pi\omega j A} \left[\cos \left(\frac{3}{2}\pi + B \right) - \cos(2\pi\omega t_b + B) \right] \quad (4.30)$$

$$D_{q,II} = (q_T - f_d R_0) \left(t_e - \frac{3}{4\omega} \right) + j R_0 \left(1 - \frac{1}{(jA)^2} \right) (1 - f_d) e^{\frac{3}{4\omega j}} \left(e^{-\frac{t_e}{j}} - e^{-\frac{3}{4\omega j}} \right) \\ + \frac{f_d R_0}{2\pi\omega j A} \left[\cos(2\pi\omega t_e + B) - \cos \left(\frac{3}{2}\pi + B \right) \right] \quad (4.31)$$

Please note that $\cos \left(\frac{3}{2}\pi + B \right) = \sin(B) = \frac{-2\pi\omega}{A}$.

Chapter 5

Propagation of individual droughts through the groundwater system using recharge simulated with observed meteorological data from two contrasting climatic regimes¹

Abstract

It is well known that the groundwater system might affect hydrological droughts significantly. So, to investigate drought in groundwater, recharge was simulated for two climatically contrasting regimes (semi-arid: Upper-Guadiana (ES) and sub-humid: Pang (UK)) and used as input for a linear reservoir model to simulate groundwater discharge. The groundwater system is characterised by a reservoir coefficient. The groundwater discharge was simulated for a range of reservoir coefficients for each of the two recharge regimes. For the semi-arid regime, multi-year droughts occur more often than for the sub-humid regime, because for the semi-arid regime the seasonal component in the recharge is much weaker and more irregular. For the semi-arid regime the effect of the groundwater system is mainly to pool erratically occurring dry months into prolonged groundwater droughts.

Key words drought; low flow; groundwater; Spain; UK; simulation

5.1 Introduction

It is commonly known that different climatic regimes show different sensitivity to meteorological drought. Both drought frequency and severity (deficit) are higher for arid and semi-arid regions than for sub-humid regions (Pandey and Ramasastri, 2001). The sensitivity to hydrological drought (streamflow and

¹This chapter is based on the paper 'Peters, E. and H.A.J. van Lanen, 2003. Propagation of drought in groundwater in semi-arid and sub-humid climatic regimes. In: *Hydrology of the Mediterranean and Semi-Arid Regions*, E. Servat, W. Najem, C. Leduc and A. Shakeel (eds.), IAHS Publication no. 278, p. 312-317.'

groundwater drought) also depends on the physical characteristics of a catchment, as they determine the response to the climatic conditions. For streams with a high proportion of baseflow (high BFI), the vulnerability of a region to hydrological drought is largely determined by its hydrogeology, because the flow during drought is often mainly derived from underground storage. However, it is unclear yet how droughts are influenced by groundwater systems in detail and how the differences in meteorological droughts between different climatic regimes are propagated through the groundwater system. This propagation is investigated in this chapter by simulating recharge and groundwater discharge and analysing the droughts in the recharge and groundwater discharge for two climate types, namely a semi-arid climate (Spain) and a sub-humid climate (UK).

5.2 Data and methods

Recharge was simulated from observed meteorological data for two catchments in Europe. These are the Upper-Guadiana catchment in Spain (1940 - 1996) and the Pang catchment in the UK (1960 - 1997). The catchments are described in Chapter 2. For the Upper-Guadiana the recharge was calculated with the SIMPA model and described in Appendix B. For the Pang catchment the recharge was calculated with the SWAP model for a limited number of physiographic units, i.e. different combinations of precipitation, soil and land use (Appendix A). For the Upper-Guadiana and the Pang catchment a spatially averaged recharge was calculated (Peters *et al.*, 2001). The groundwater system was simulated using a linear reservoir. The size and delay of the reservoir are characterised by the reservoir coefficient j (d). Although the recharge was calculated for two specific catchments, the discharge was not simulated for the Upper-Guadiana or Pang catchment itself, but for a range of hypothetical catchments with a range of reservoir coefficients from 10 to 10 000 d. This implies that the propagation of droughts through the groundwater system was investigated for a wide range of aquifer characteristics for both climatic regimes. The drought events in both the recharge (recharge droughts) and the groundwater discharge (discharge droughts) were defined using the threshold level approach (Chapters 3 and 4). Drought duration is defined as the period of time when the recharge or discharge falls below the threshold until the threshold is crossed again. The drought deficit is the integrated area below the threshold. The threshold level was determined using the method described in Chapter 4, which uses the total deficit below the threshold to determine the height of the threshold.

5.3 Results

The key to understanding the effect of a groundwater system on droughts is to understand how the delay and attenuation caused by the storage in an aquifer affect the discharge droughts. Figure 5.1a shows the simulated recharge for the Upper-Guadiana catchment and the discharge for an aquifer with $j = 316$ d for 1987 to 1995. As expected the discharge is smoothed and delayed compared to the recharge. Figure 5.1b shows the deviation below the threshold, i.e. when the recharge or discharge is lower than the threshold. For recharge and discharge the threshold was calculated to be 0.0066 and 0.022 mm d⁻¹, respectively. The recharge below the threshold is bounded at the upper end, because the recharge in the SIMPA model concept cannot be below zero. These figures show a very important additional effect of the propagation through the groundwater system, namely an increased pooling of the droughts. The period from 1988 to 1994 is characterised by a series of years with below average recharge with only one clear recharge drought at the end of 1994. However it resulted in an extremely severe and prolonged discharge drought.

Figure 5.2 shows the drought deficit for the major drought in Figure 5.1 (1992-1994) for a range of reservoir coefficients j . This shows how a range of aquifers with different characteristics would respond to the same recharge drought. For $j = 1$ d the deficit of the recharge drought is plotted. The arrow indicates the aquifer with $j = 316$ d presented in Figure 5.1. From the duration it is clear for which values of j droughts are merged, namely the jumps around $j = 70$ and 1000 d. Thus generally, the amount of pooling increases with increasing reservoir coefficient. For very large j the discharge drought deficit is smaller because of the attenuation (Chapter 4).

Figure 5.3 shows recharge and discharge ($j = 316$ d) and the deviation below the threshold for the recharge and discharge for sub-humid conditions (Pang catchment recharge) for the period 1969-1979. This period shows only single-year droughts in both recharge and discharge. In fact, in the total period 1960-1997 only one multi-year drought occurs for the sub-humid climate of the Pang. Because of the strong, regular seasonal component of the Pang recharge as compared to the Upper-Guadiana, pooling of the droughts and thus multi-year droughts are much less common.

Figure 5.4 shows the deficits of three droughts, namely the droughts in 1972, 1973 and 1974, for a range of reservoir coefficients (compare with Figure 5.1). The whole period 1970 to 1974 showed below average recharge (Figure 5.3a). However, none of the summers in 1972, 1973 or 1974 showed a large recharge deficit (Figure 5.3b). But in the discharge for an aquifer with $j = 316$ d, the 1973 drought formed the fifth largest drought in the period 1960 to 1997. The 1974 drought shows for $j < 200$ d the typical behaviour of a short, unsevere

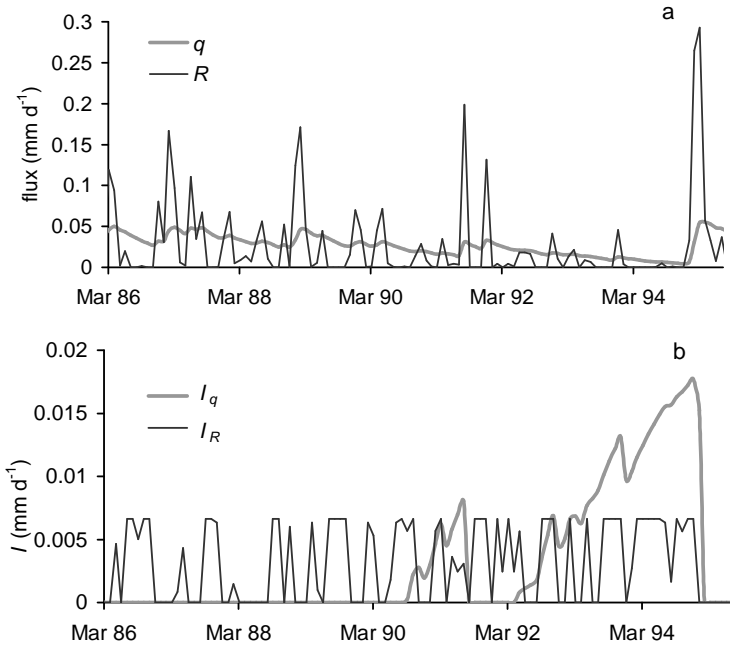


Figure 5.1: Recharge, groundwater discharge and droughts in a semi-arid region: a) simulated recharge R for the *Upper-Guadiana* catchment and discharge q for an aquifer with $j = 316$ d and b) drought intensity for the recharge I_R and groundwater discharge I_q .

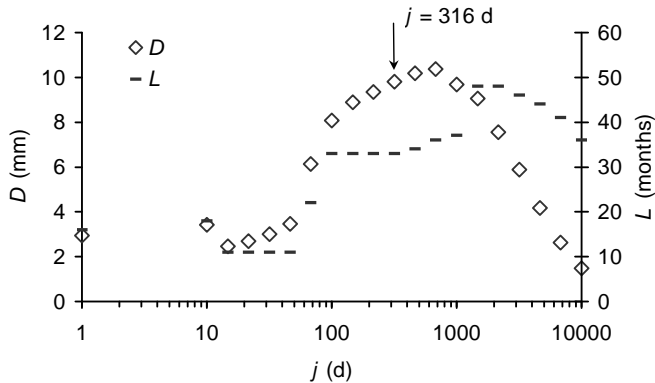


Figure 5.2: Drought deficit D and duration L of the recharge drought in 1994 for the *Upper-Guadiana* catchment (plotted for $j = 1$ d) and discharge drought in 1992-1994 for a wide range of aquifer characteristics ($j = 10$ to 10 000 d). The arrow indicates the aquifer conditions in Figure 5.1.

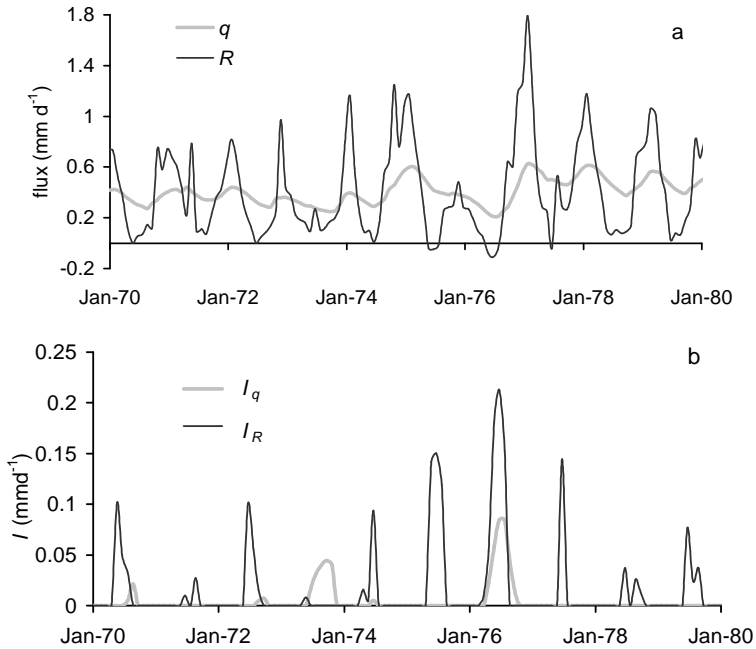


Figure 5.3: Recharge, groundwater discharge and droughts in a sub-humid region: a) simulated recharge R for the *Pang* catchment and discharge q for an aquifer with $j = 316$ d and b) drought intensity for the recharge I_R and groundwater discharge I_q .

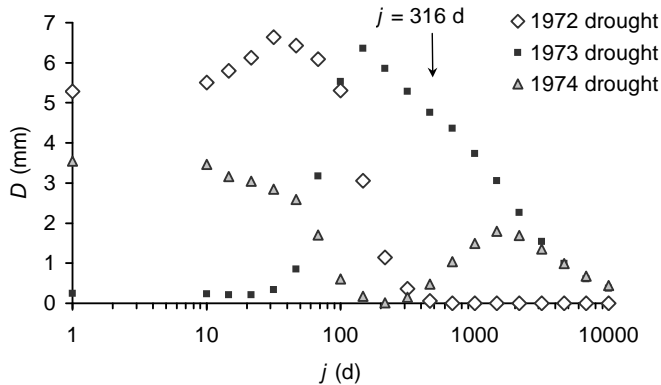


Figure 5.4: Drought deficit D of the recharge droughts in 1972, 1973 and 1974 for the *Pang* catchment (plotted for $j = 1$ d) and discharge drought in the same years for a wide range of aquifer characteristics ($j = 10$ to 10 000 d). The arrow indicates the aquifer conditions in Figure 5.3.

drought, which means a lower deficit in the groundwater discharge as compared to the recharge (Figure 5.4). This is caused by the attenuation in the aquifer and thus the larger the attenuation, the lower the deficit in the groundwater discharge. The 1972 drought basically shows the same behaviour, only for aquifers with $j = 10$ to 100 d the deficit increases slightly going from recharge to discharge. This increase is the result of the delay caused by the aquifer. This can be understood as follows. In this sub-humid climate, the majority of the recharge occurs during winter and spring. A decrease in recharge during this period does not usually cause a drought in the recharge, because the recharge is still above the threshold. However, due to the delay caused by the aquifer, the decrease in recharge spreads over a longer period and thus affects the discharge during the following summer (low-flow period) (Chapter 4). The 1973 drought shows this effect very strongly, as it is a relatively wet summer in recharge (7 mm more than average) following on a dry winter (57 mm less than average). The relatively large deficit in the discharge drought in 1974 for $j > 200$ d is also caused by this effect. Because of the less pronounced seasonal cycle in the Upper-Guadiana, this effect is much less clear there.

5.4 Conclusions

Analysis of droughts in the simulated recharge and groundwater discharge, shows a much stronger tendency for multi-year droughts for the semi-arid regime (Upper-Guadiana, ES) than for the sub-humid regime (Pang, UK). This is caused by the relatively strong, regular seasonal component in the Pang. This seasonal cycle has two effects on the discharge droughts. First, it prevents pooling of the droughts and thus the formation of multi-year droughts. And second, it causes a large influence of the recharge in winter (or high flow season) on the discharge drought in the following summer (low flow season), because the effect of the decrease in recharge is delayed. For all cases, the attenuation that results from the storage in an aquifer causes the discharge drought deficits to be small for aquifers with very large reservoir coefficients. *So, the major processes influencing the discharge droughts for the semi-arid regime is pooling of the droughts and attenuation, and for the sub-humid regime is delay from winter to summer and attenuation.*

Acknowledgements The authors gratefully acknowledge the help of Dr. Jos van Dam from Wageningen University with the SWAP model. The meteorological data for the Pang catchment were provided by the UK Meteorological Office through the British Atmospheric Data Centre. The simulated recharge for the Upper-Guadiana catchment was provided by CEDEX (ES).

Chapter 6

Propagation of drought through groundwater systems - drought distribution and performance criteria for the Pang catchment¹

Abstract

In order to investigate the propagation of drought through a groundwater system and analyse the performance of groundwater during drought, 10 series of 1000-year time series of recharge and groundwater discharge were generated. The 1000 years of synthetic daily data were generated using Nearest Neighbour resampling based on 37 years of observed daily meteorological data. The root zone was simulated by a non-linear water balance model and the groundwater system by a linear reservoir model. The size and thus the response time of the reservoir was characterised by a reservoir coefficient. Subsequently, the deficit and duration of the droughts were derived from the time series of recharge and groundwater discharge using the threshold level approach. An analysis of the distribution of these droughts shows that for droughts with small return periods, the deficit in the groundwater discharge is smaller than in the recharge. For droughts with large return periods, the deficit in the groundwater discharge is larger than in the recharge. The effect of the changes in distribution of the droughts on the performance of the groundwater discharge was evaluated as a function of the reservoir coefficient using three classical performance criteria (reliability, resilience and vulnerability), a combination of these three criteria (Loucks' sustainability index) and three newly defined overall performance criteria. The newly defined criteria combine the severity and frequency of the droughts, instead of analysing these separately in reliability and vulnerability. Of all the performance criteria used, one of the newly introduced overall performance criteria with a strong emphasis on droughts with a high return period appeared to characterise the groundwater droughts best. This criterion shows a more or less constant performance for low and medium high reservoir coefficients and an increasing performance for higher reservoir coefficients.

¹This chapter is based on the paper 'Peters, E., H.A.J. van Lanen, P.J.J.F. Torfs and G. Bier, submitted. Propagation of drought in groundwater - drought distribution and performance criteria. *J. of Hydrologic Engineering*, submitted '

6.1 Introduction

In many parts of the world groundwater is increasingly exploited as a resource for public water supply and irrigation (Scheidleder *et al.*, 1999; Estrela *et al.*, 1996). This means that the response of groundwater systems to drought and their performance under drought conditions becomes increasingly important (Calow *et al.*, 1999; White *et al.*, 1999). Droughts that affect the groundwater system are called *groundwater droughts*. Groundwater droughts are mainly caused by a lack of recharge and generally occur on a time scale of months to years (van Lanen and Peters, 2000). In Chapter 4, the authors analysed the propagation of a single, synthetic drought event through the groundwater system. They examined the deficit and duration of the drought event in the recharge and in the simulated groundwater discharge. They showed that small droughts in the recharge decrease as a result of the propagation through groundwater, implying that the drought deficit and duration are smaller in the discharge than in the recharge. Severe droughts in the recharge tend to increase in the groundwater discharge in both deficit and duration. However, it is unclear how *long series* of natural drought events propagate through the groundwater system and thus how the overall distribution of droughts changes from recharge to discharge.

Moreover, criteria to characterise the performance of groundwater reservoirs during droughts are not well developed. In general, reservoir performance is identified by three criteria: *reliability*, *resilience* and *vulnerability*, which represent the frequency, duration and severity of failure (Hashimoto *et al.*, 1982; McMahon, 1993). Although these three criteria are used frequently, especially the definition of the vulnerability is inconsistent. Some authors define the vulnerability as the average drought deficit (Vaz, 1986; Loucks, 1997; Kjeldsen and Rosbjerg, 2001), others define it as the maximum drought (Moy *et al.*, 1986). Another problem associated with these criteria is that they are derived independently, whereas the occurrence frequency and severity of droughts are related. Droughts with a short duration and low deficit occur more often and are accepted with a higher frequency than severe droughts (Vaz, 1986; Maier *et al.*, 2001). Finally, the resilience and vulnerability are dimensional, which makes comparison more difficult. Thus a new, overall performance criterion is needed.

Performance criteria have mostly been applied to streamflow. The few studies that investigate the performance of groundwater or base flow use predefined criteria to compare the sensitivity or susceptibility to drought of different areas or rivers (Robins *et al.*, 1997; Uijlenhoet *et al.*, 2001; Demuth *et al.*, 2000; Stahl, 2001). However, they use very different, sometimes even contradictory criteria. Clearly there is no consensus about how to evaluate or define the performance of groundwater during drought.

The overall objective of this study is to investigate the performance of groundwater systems under drought stress. The first step is to analyse the influence of the groundwater system on the distribution of droughts by comparing the distribution of droughts in the recharge and the discharge in long time series. The distribution of the droughts will be identified by return periods. In the second step we introduce several overall performance criteria for groundwater, of which some are newly introduced and use these to investigate the influence of the propagation through groundwater on the overall performance. To achieve these objectives, time series of recharge and discharge are simulated and analysed on drought behaviour. As the observed meteorological time series were not long enough to estimate overall performance criteria and return periods reliably, the observed time series are expanded. Therefore first the generation of a long time series of synthetic data will be described. Later the definition and calculation of the return periods and performance criteria will be discussed.

6.2 Description of data and methods

Procedure The time series that were generated needed to be sufficiently long to estimate return periods of 50 years (which is the maximum return period of interest) and long-term performance criteria. It was chosen to simulate 10 series of 1000 years. Tests showed that this provided stable estimates of the performance criteria. In Figure 6.1 a schematic overview of the procedure for simulating droughts is presented. Because of non-linearity of the recharge model, the recharge was simulated on a daily basis and thus precipitation and evapotranspiration were generated on a daily basis. The daily recharge values were aggregated to monthly values, because this is a more appropriate time step for the analysis of groundwater droughts. Using monthly values avoids large numbers of minor droughts, but still shows sufficient detail. Because of the exploratory nature of the investigations a simple approach was chosen to simulate the groundwater system, namely a linear reservoir. From the time series of recharge and groundwater discharge, droughts were derived, which were then used to calculate the return periods and the performance criteria. In the following all steps will be discussed.

Meteorological data The methods were illustrated using meteorological data from a temperate humid climate. The precipitation data are from Yattendon station in the Pang catchment (UK) (Figure A.1). The Pang catchment is located some 25 km south of Oxford (Chapter 2). Potential evapotranspiration was calculated according to Penman-Monteith with a crop resistance of 70 s m^{-1} (Peters *et al.*, 2001) for Reading station, which is just outside the Pang catchment. In total 37 years of daily data are available. Average annual rainfall and potential evapotranspiration are 690 and 520 mm a^{-1} , respectively.

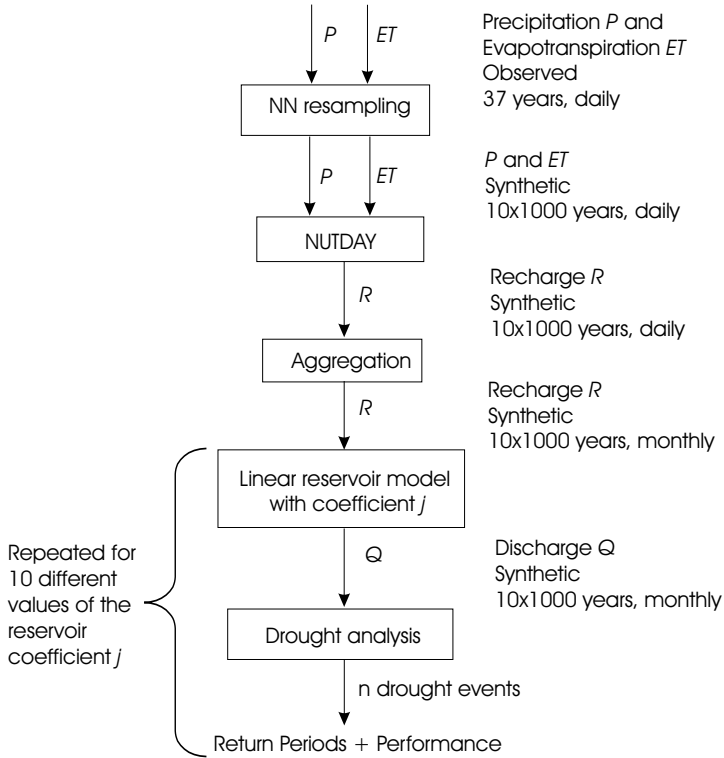


Figure 6.1: Overview of the procedure for estimating the distribution of droughts and the performance criteria

6.2.1 Generating synthetic data

From the 37 years of daily meteorological data, 10 series of 1000 years of daily data were simulated. Several methods are available for generating long time series of daily data, for example Markov chains (Hipel and McLeod, 1994). In this study the Nearest Neighbour resampling (NN resampling) or bootstrap method was used. The principles have been described by Rajagopalan and Lall (1999) and Lall and Sharma (1996). In this chapter the application of the NN resampling technique as described by Wójcik *et al.* (2001) and their recommended parameter values were used. The NN resampling technique has been shown to conserve several statistics well, like for example, average, skewness and correlation structure for daily meteorological data (Brandsma and Buishand, 1998; Rajagopalan and Lall, 1999; Wójcik and Buishand, 2003). Table 6.1 lists some statistics of the observed 37-year data set and the simulated 1000-year data sets. The NN resampling method basically determines from

the whole collection of daily observations those observations, which are most similar to the current value and selects one of those neighbours randomly as the nearest neighbour. The value following on that randomly selected value is the next value in the time series.

To determine the degree of similarity or in other words the distance between neighbours the Mahalanobis distance is used, which takes the covariance structure of the data into account. The distance is calculated for a feature vector, which contains the variables that are used to determine the distance (in this chapter daily precipitation and daily potential evapotranspiration). Sampling from the k nearest neighbours is done using the decreasing kernel defined by Lall and Sharma (1996). For the number of nearest neighbours k a value of 5 was used. For larger values of k the autocorrelation decreases, which is one of the characteristics, which should be preserved as much as possible. The use of smaller values of k is not recommended (Wójcik *et al.*, 2001).

Precipitation and evapotranspiration are resampled simultaneously and unconditionally. Seasonality is preserved by not choosing the entire observation space as potential nearest neighbours, but using a predefined window from which the nearest neighbours can be selected. This moving window is centred at the day of interest and is chosen as 61 d (Wójcik *et al.*, 2001). The simulated and observed values (Table 6.1) show a slight underestimation of the variance and skew for the simulated values. This may decrease the droughts somewhat compared to the original data. However, the overestimation of the number of dry days by 2% may increase the droughts. Especially interesting for groundwater droughts probably is the long-term correlation structure of the precipitation. The autocorrelation coefficient lag 1 for the annual data is -0.20 for the observed data and 0.02 for the simulated data. This means that droughts would be more severe in the simulated series.

6.2.2 Simulation of groundwater recharge and discharge

Recharge The recharge was calculated using a water-balance model for the root-zone, called NUTDAY (Figure 6.1). The model is described more extensively by van Lanen *et al.* (1996) and Peters *et al.* (2001). In NUTDAY the daily balance equation for the root zone can be written as follows:

$$S_{r,t} = S_{r,t-1} + P_t - ET_{a,t} - R_{p,t} \quad (6.1)$$

where $S_{r,t}$ [L] is the soil moisture storage in the root zone at the end of day t , P_t [L] is the precipitation on day t , $ET_{a,t}$ [L] is the actual evapotranspiration on day t and $R_{p,t}$ [L] is the percolation at the bottom of the root zone on day t .

The program NUTDAY does not simulate capillary rise from the saturated zone

Table 6.1: Comparison between daily observed and simulated precipitation P and potential evapotranspiration ET_{pot} data. For the simulated values the average of 10 1000-year series is presented.

	Observed		Simulated	
	37 years		10 x 1000 years	
	P	ET_{pot}	P	ET_{pot}
Mean (mm d^{-1})	1.89	1.43	1.79	1.44
Standard Deviation	4.16	1.25	4.00	1.25
Skewness	4.47	0.98	4.34	0.95
Kurtosis	35.59	0.28	30.78	0.14
Maximum	86.4	8.02	86.4	8.02
Coefficient of Variation	2.20	0.88	2.23	0.87
Autocorrelation lag 1	0.19	0.77	0.21	0.77
Autocorrelation lag 2	0.11	0.73	0.08	0.69
Autocorrelation lag 3	0.07	0.70	0.04	0.64
Autocorrelation lag 4	0.07	0.67	0.02	0.61
Autocorrelation lag 5	0.06	0.66	0.01	0.59
Percentage of dry days	57.1		59.4	

(Figure 6.2). A crop factor f_t is used to calculate potential evapotranspiration for a specific crop from the potential evapotranspiration of a reference crop, being grassland. The reduction from potential to actual evapotranspiration as affected by soil moisture is presented in Figure 6.3. The critical point is defined as the soil moisture storage below which the crop cannot evapotranspire at the potential rate. Percolation at bottom of the root zone $R_{p,t}$ occurs if the soil moisture storage is larger than the soil moisture storage at field capacity. In this study a maximum soil moisture storage of 150 mm was used, which corresponds to a soil with medium high storage capacity. The crop was grassland ($f_t = 1.0$). The recharge R_t was taken equal to the flux through the bottom of the root zone $R_{p,t}$.

Groundwater levels and discharge Groundwater level H and groundwater discharge q were calculated from the recharge R using a linear groundwater model (linear reservoir). The following recursive relations were used (de Zeeuw and Hellinga, 1958):

$$q_t = q_{t-1}e^{-m_t/j} + \frac{R_t}{m_t} \left(1 - e^{-m_t/j}\right) \quad (6.2)$$

$$H_t = H_{t-1}e^{-m_t/j} + \frac{0.001jR_t}{0.8\mu m_t} \left(1 - e^{-m_t/j}\right) \quad (6.3)$$

where m_t [T] is the number of days in a month, μ [-] is the storage coefficient and j [T] is the reservoir coefficient, which represents the recession characteristics

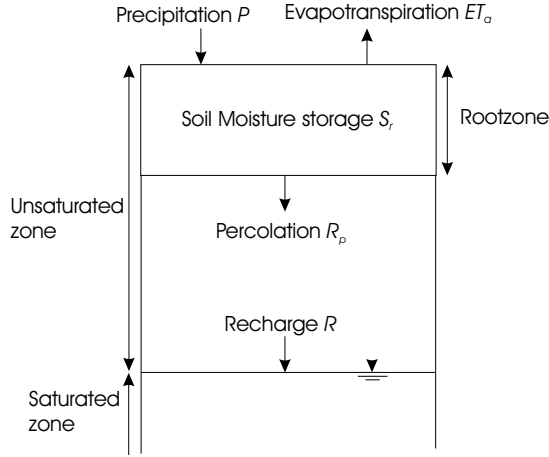


Figure 6.2: Schematisation of the unsaturated zone for NUTDAY

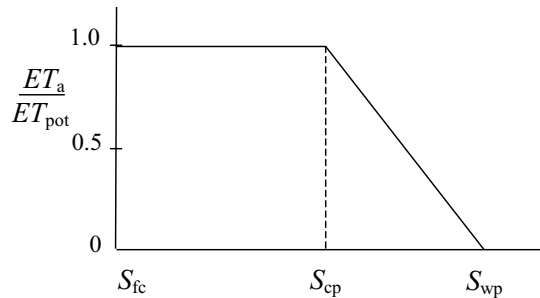


Figure 6.3: The ratio of actual evapotranspiration ET_a to potential evapotranspiration ET_{pot} as a function of soil moisture storage. S_{fc} is soil the moisture storage at field capacity, S_{cp} at critical point and S_{wp} at wilting point

of the reservoir. According to non-linear drainage theory (Krajenhof van de Leur, 1962; Ritzema, 1994), the reservoir coefficient j can be interpreted, in specific cases, as $j = \mu l^2 / \pi^2 k D$, where l [L] is the distance between streams and kD [$L^2 T^{-1}$] is the transmissivity. Values of j of 1 to 20 or 30 d are generally applicable to artificially drained fields and values of 300 to 2000 d to discharge from aquifers (Vereniging Voor Landinrichting, 1992). As the groundwater system is simulated as a linear reservoir, the transient discharge from the reservoir and the storage in the reservoir (represented by the level) are identical, except for a scaling factor and dead storage. Therefore only groundwater discharge was analysed.

6.2.3 Drought event definition

Droughts will be defined using the threshold level approach, which was first described for drought by Yevjevich (1967) and which is illustrated in Figure 6.4. For any hydrologically relevant variable ξ the deficit D below the threshold ξ_T is calculated as:

$$D = \int_{t_b}^{t_e} [\xi_T - \xi(t)] dt \quad (6.4)$$

where t_b and t_e are the start and end date of the drought respectively. The duration L of the drought is calculated as $t_e - t_b$.

The threshold level ξ_T is derived by relating the total deficit below the average to the total deficit below the threshold (Figure 6.4). The threshold function $\xi_T(c)$ is defined by:

$$\int_0^M [\xi_T(c) - \xi(t)]_+ dt = c \int_0^M [\bar{\xi} - \xi(t)]_+ dt \quad (6.5)$$

where $\xi_+ = \begin{cases} \xi & \text{if } \xi \geq 0 \\ 0 & \text{if } \xi < 0 \end{cases}$

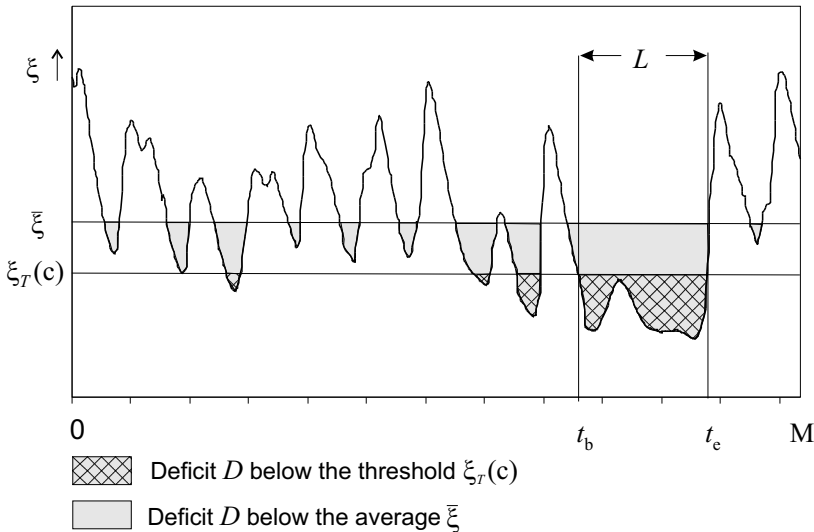


Figure 6.4: Illustration of the definition of droughts and of the threshold level for any hydrologically relevant variable ξ . D is drought deficit, L is drought duration, $\xi_T(c)$ is the threshold dependent on drought criterion c , M is the total length of the time series and t_b and t_e are the start and end date of a drought.

In this chapter, all droughts are derived using $c = 0.3$.

6.3 Return periods and performance

In the final step (Figure 6.1) return periods and performance criteria were derived from the time series of droughts derived from the simulated recharge and groundwater discharge.

6.3.1 Return periods

Return periods (also called recurrence interval or interarrival time) can be understood as a fixed period T in which the expected number of exceedances of the T -year event is exactly 1 (Stedinger *et al.*, 1993). It can also be understood as the average time until the level ξ_T is exceeded (Stedinger *et al.*, 1993; Reiss and Thomas, 1997) or as the average number of time intervals between occurrence of an event $\xi > \xi_T$ (for the right hand tail of a distribution) (Tallaksen, 2000). For independent and identically distributed (iid) events these formulations are equivalent (Fernández and Salas, 1999). In that case the definition of return periods is straightforward and can be calculated from:

$$T(x) = \frac{1}{1 - F(x)} \quad (6.6)$$

where x is an indicator of the severity of a drought (in this chapter the drought deficit) and $F(x)$ is the cumulative distribution function $P(X \leq x)$, which gives the unconditional probability that x is not exceeded. The cumulative distribution function can be estimated from the ranks of x . However, when using Partial Duration Series (collection of events below the threshold), with daily or monthly data, the calculation needs to take into account the expected number of exceedances per year. A second issue is that the drought events may no longer be independent of each other, especially for daily values. Pooling of the dependent droughts is normally used to reduce this problem, however all pooling methods have disadvantages (Tallaksen, 2000). Because dependence of droughts is expected to be a minor problem for monthly values, no pooling has been applied and the droughts are assumed to be independent. For a random iid variable X (here drought deficit or duration) the return periods can be calculated from (Stedinger *et al.*, 1993; Cunnane, 1979):

$$T(x) = \frac{1}{(1 - F(x)) \lambda} \quad (6.7)$$

where $F(x)$ is again the cumulative distribution function of x and λ is the expected number of drought events per year, which is estimated as average number of droughts per year: n/N . Here n is the total number of droughts in the time series and N is the total number of years. This definition is according

to Stedinger *et al.* (1993) and does not take into account the duration of the droughts. Although for surface water droughts, λ is usually larger than 1 (Hisdal *et al.*, 2002), for groundwater it can often become lower than 1. The cumulative distribution function is estimated from the ranked values of x using the Weibull plotting positions (Stedinger *et al.*, 1993):

$$F(x) = P(X \leq x) = \frac{r(x)}{n+1} \quad (6.8)$$

where $r(x)$ is the rank of the drought deficit or duration (ascending order). The exceedance probability can be estimated from the rank because the events are assumed to be independent.

6.3.2 Performance

Before introducing the *overall* performance criteria, first the three *single* performance criteria defined by Hashimoto *et al.* (1982) (reliability, resilience and vulnerability), which address only one aspect of the performance, are discussed. *Reliability* α is the frequency or probability that a system is in a satisfactory state. It is calculated as the period of time when the recharge or groundwater discharge is above the threshold level divided by the total duration. For monthly data this resulted in:

$$\alpha = \frac{12N - n\bar{L}}{12N} = 1 - \frac{\lambda\bar{L}}{12} \quad (6.9)$$

where \bar{L} is the average drought duration. The *resilience* γ describes how quickly a system is likely to recover to a satisfactory state once a failure has occurred. It is calculated as the inverse of the expected drought duration. As the expected drought duration was estimated as the average drought duration \bar{L} , the resilience was calculated as:

$$\gamma = \frac{1}{\bar{L}} \quad (6.10)$$

The *vulnerability* ν is the likely magnitude of a failure if one occurs (Hashimoto *et al.*, 1982). The magnitude of failure was assumed to be the drought deficit as defined using the threshold level approach. The vulnerability was both calculated as the average deficit \bar{D} per drought and as the maximum deficit, because these are predominantly used in literature. As maximum deficit the deficit corresponding to a drought with a return period of 50 years D_{50} ('50-year drought') was used.

Box 6.1: Overview of the performance criteria used in this chapter	
α	Reliability: the probability that the system is not in a drought (Equation (6.9)).
γ	Resilience: the inverse of the expected duration of a drought (Equation (6.10)).
ν	Vulnerability: expected severity of a drought if one occurs, expressed both by the average drought deficit \bar{D} and the deficit of a drought with a 50-year return period D_{50} .
S_L	Sustainability Index (Loucks, 1997), which combines α , γ and ν (Equation (6.11)).
$p_{D,yr}$	Overall performance criterion defined in this chapter based on the average drought deficit per year (Equation (6.14)).
$p_{D,10}$	Overall performance criterion defined in this chapter based on the drought deficit for droughts with return periods larger than 10 years (Equation (6.16)).
$p_{D,Cor}$	Overall performance criterion based on the loss function defined by Correia <i>et al.</i> (1986) (Equation (6.18)).

An overview of the performance criteria used in this chapter is presented in Box 6.1. Loucks (1997) defined a *sustainability index* S_L , which is a combination of the three criteria reliability, resilience and vulnerability.

$$S_{L,i} = \alpha\gamma(1 - r\nu_i) \quad (6.11)$$

where $r\nu_i$ is the vulnerability of scenario i scaled to be between 0 and 1. De term $r\nu_i$ is calculated as:

$$r\nu_i = \frac{\bar{D}_i}{\bar{D}_{\max}}$$

where \bar{D}_i is the average drought deficit of scenario i and \bar{D}_{\max} is the maximum of the average drought deficit. In this chapter, the scenarios represent the range of reservoir coefficients that were used to simulate the groundwater discharge (Figure 6.1). This index does not take into account the relation between severity and frequency as discussed in Section 6.1.

A new, overall performance criterion is proposed in this chapter, which combines the severity of drought events with the probability of their occurrence and which is called *performance p*. It is clear that the performance should decrease with increasing drought severity and with increasing drought frequency. The difficulty is how to combine them. For example, is performance better if we have two droughts in one year with a deficit of 5 units or one drought with a deficit of 10 units? This problem is circumvented by introducing a severity function s , which can then be defined according to the circumstances. The performance p_i of scenario i is now defined as:

$$p_i = 1 - \frac{[\int_0^\infty s(x) \lambda f(x) dx]_i}{[\int_0^\infty s(x) \lambda f(x) dx]_{\max}} \quad (6.12)$$

where x is the drought deficit D or any other variable that is used to indicate drought severity, λ is again the average number of droughts per year and $f(x)$ is the probability distribution of x . Here the drought deficit D is chosen as the appropriate drought indicator. Three possible severity functions, resulting in three performance criteria will be examined:

1. The first severity function is $s(D) = D$ which means that the integral in Equation (6.12) is the average drought deficit per year \bar{D}_{yr} :

$$\bar{D}_{yr} = \lambda \bar{D} = \lambda \nu \quad (6.13)$$

This definition is similar to the definition of risk cost, defined by, for Example, Douglas *et al.* (2002) and an important property is that it is not influenced by persistence. The overall performance criterion $p_{D,yr}$ thus results in:

$$p_{D,yr,i} = 1 - \frac{\bar{D}_{yr,i}}{\bar{D}_{yr,\max}} \quad (6.14)$$

2. The second severity function is:

$$s(D) = \begin{cases} 0 & \text{if } D \leq D_{10} \\ D & \text{if } D > D_{10} \end{cases} \quad (6.15)$$

where D_{10} is the drought deficit corresponding to a return period of 10 years. This function was chosen because it is expected that droughts with a return period of more than 10 years will cause more substantial problems. With $\bar{D}_{yr,10}$ as the average drought deficit per year for droughts with return periods larger than 10 years, the performance criteria $p_{D,10}$ results in:

$$p_{D,10,i} = 1 - \frac{\bar{D}_{yr,10,i}}{\bar{D}_{yr,10,\max}} \quad (6.16)$$

3. The third severity function is the loss function defined by Correia *et al.* (1986) multiplied by -1:

$$s(D) = \frac{-1}{K} \ln \left(1 - \frac{D}{D_{\max}} \right) \quad (6.17)$$

where $K [-]$ is a parameter which describes how fast the maximum value is reached and which must be chosen in advance and x_{\max} is a maximum for scaling purposes. Here $K = 1$ and D_{\max} is the maximum drought deficit in each 1000-year time series (Figure 6.1). The effect of this loss function is to increase the weights of the most severe droughts and decrease the weights for the small and medium severe droughts. Because this loss function already scales the deficit, the scaling factor (denominator) in Equation (6.12) is no longer used. The performance criterion $p_{D,\text{Cor}}$ thus results in:

$$p_{D,\text{Cor},i} = 1 + \int_0^{\infty} \frac{1}{K} \ln \left(1 - \frac{D_i}{D_{\max,i}} \right) \lambda f(x) dx \quad (6.18)$$

6.4 Results

6.4.1 Distribution of droughts

Figure 6.5 shows the number of droughts as a function of the reservoir coefficient j for the temperate humid data set used in this chapter. Except for the recharge drought ($j = 1$ d), this shows a log-linear relation between the number of drought events and the reservoir coefficient j , which characterises the size (amount of delay) of the reservoir. The effect of the propagation of a drought in the recharge (recharge drought) through a groundwater system is also illustrated in Figures 6.6 and 6.7. In these figures the return periods for deficit and duration are plotted using Weibull plotting positions for the recharge droughts and discharge droughts simulated for three values of the reservoir coefficient j . For droughts with low return periods (< 10 years) the deficit and duration of recharge droughts are larger than those for discharge droughts. This means that the propagation through the groundwater system causes a decrease in drought deficit and duration.

For large return periods (> 100 years) the deficit is larger for groundwater discharge than for recharge. For droughts with return periods between 10 and 100 years it depends on the reservoir coefficient, whether the deficit increases as a result of the propagation through the groundwater reservoir or not. The reason why the severe droughts increase in deficit and the smaller droughts decrease in deficit as a result of the propagation through the groundwater

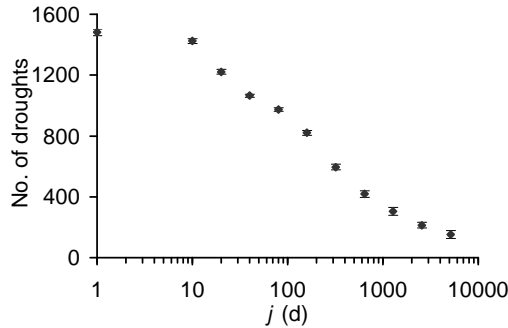


Figure 6.5: Number of droughts per 1000 years for recharge R (plotted for $j = 1$ d) and discharge q for different values of the reservoir coefficient j . The dots indicate the average and the error bars the standard deviation of the 10 runs of 1000 years.

system, was explained using a synthetic case in Chapter 4. Unlike deficit, for duration (Figure 6.7) the drought distributions all cross at around the same point, namely for a return period of 10 years and a duration of 7 to 8 months. This is about the maximum duration that a drought can have that only lasts one summer season. Thus for slowly responding groundwater systems (high j) the number of multi-year droughts increases. Summarising, the effect of the groundwater system is to decrease the number of small droughts and to increase the number of severe droughts. The total number of droughts decreases. The more slowly the groundwater system responds, the stronger these effects become.

6.4.2 Performance

First the results for the single performance criteria are presented, because they are the basis for the first overall performance criterion S_L . Figures 6.8 and 6.9 show the impact of the change in distribution of the droughts as a result of the propagation through the groundwater system on the reliability α , the resilience γ and the vulnerability ν . As could be expected from the strong decrease in the number of droughts (Figure 6.5), α is positively correlated with the reservoir coefficient j . The behaviour of resilience γ is not quite as expected. It was expected that γ would decrease with increasing j because the drought duration increases. However Figure 6.8b shows first a slight increase and later the expected decrease. Further analysis showed that this increase was in fact introduced by the event definition in combination with the seasonality. From Figure 6.7 it was clear that the duration of the minor droughts decreases from recharge to discharge, but that the duration of the severe droughts increases. However, as mentioned before, the maximum duration of a drought lasting one

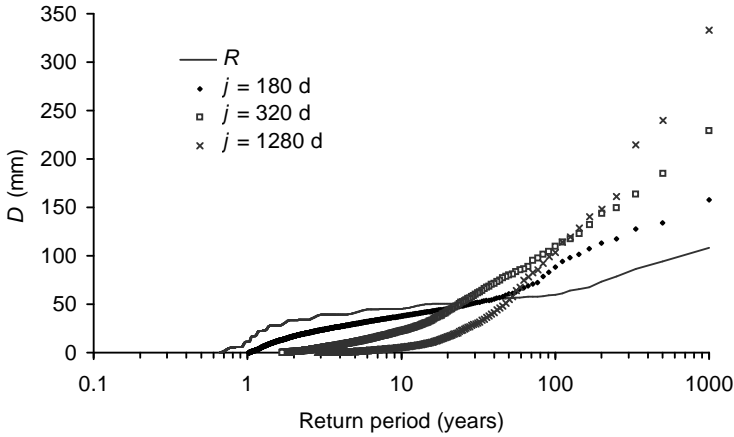


Figure 6.6: Frequency distribution (return periods) of drought deficit D of groundwater recharge R and discharge q for $j = 80$ d, $j = 320$ d and $j = 1280$ d. The average of 10×1000 years is presented. The standard deviation is not presented for clarity reasons and increases with increasing return period.

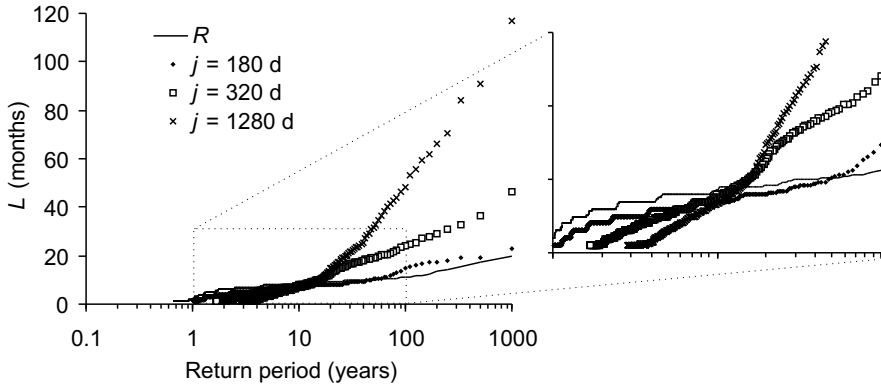


Figure 6.7: Frequency distribution (return periods) of the drought duration L of the groundwater recharge R and discharge q for $j = 80$ d, $j = 320$ d and $j = 1280$ d. The average of 10×1000 years is presented. The standard deviation is not presented for clarity reasons and increases with increasing return period.

summer season is about 7 to 8 months. The duration of a drought event does not increase much in this case until the recharge or discharge during winter is so low that a multi-year drought can develop (Figure 6.4). And thus the average duration of the droughts increases less fast with increasing reservoir coefficient as a result of the seasonality of the recharge.

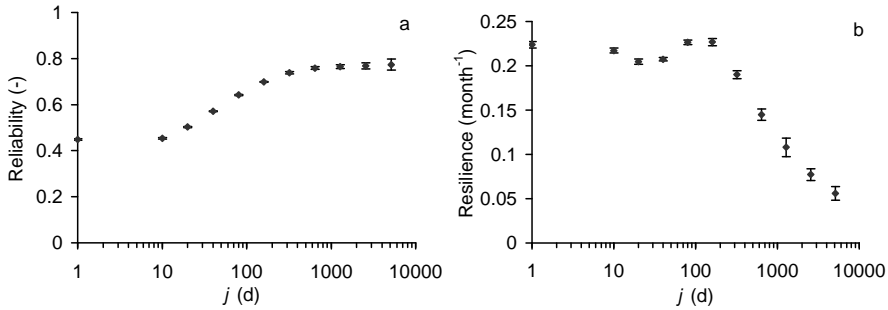


Figure 6.8: a) Reliability (-) and b) Resilience (month^{-1}). For $j = 1$ d the reliability and resilience of the recharge are plotted. The dots indicate the average and the error bars the standard deviation of the 10 runs of 1000 years.

In Figure 6.9 two vulnerability criteria are presented, namely the vulnerability expressed as the average drought deficit \bar{D} and the vulnerability expressed as the deficit of the 50-year return period D_{50} . \bar{D} changes relatively little, from 24.7 mm to 12.5 mm. The maximum occurs for $j = 20$ d, namely = 26.4 mm. D_{50} ranges from 81 to 10 mm, with the maximum at $j = 160$ d. The change in \bar{D} is relatively small because for the small droughts the deficit decreases with increasing reservoir coefficient and for the severe droughts the deficit increases, thus offsetting each other (Figure 6.6). The reason for the occurrence of a maximum value for D_{50} is explained in Chapter 4 (Figure 4.9).

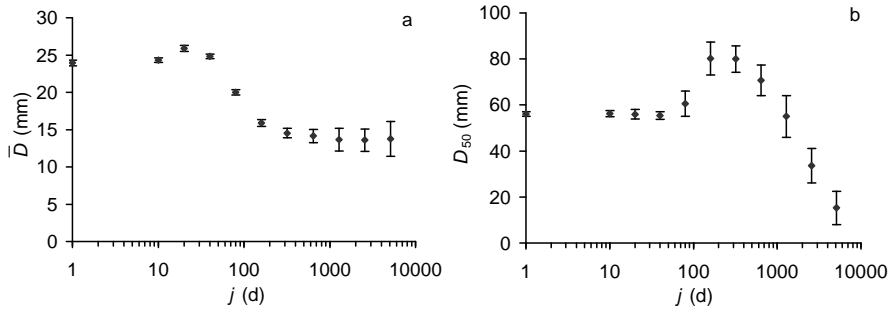


Figure 6.9: Different estimates of vulnerability: a) average drought deficit per drought \bar{D} , b) deficit of a drought with a return period of 50 years D_{50} . For $j = 1$ d the estimates for the recharge are plotted. The dots indicate the average and the error bars the standard deviation of the 10 runs of 1000 years.

S_L (Equation (6.11)) shows a low performance for fast groundwater systems (low j), because the reliability is very small (Figure 6.10). For very slowly responding systems (high j) the performance is low because the resilience is very low. The resilience is low because of the extreme length of droughts

for high j (maximum drought duration is 450 months for $j = 5120$ d). The variation of S_L increases with increasing reservoir coefficient.

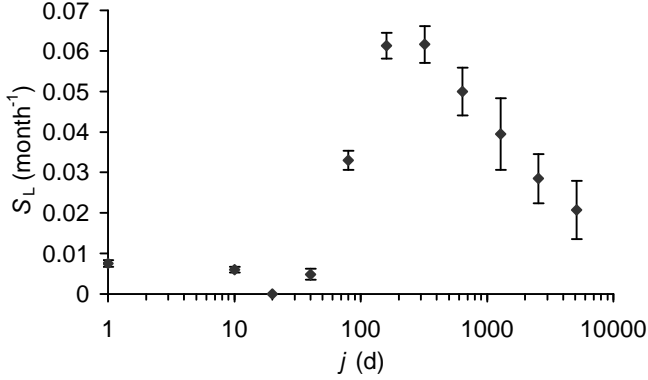


Figure 6.10: Sustainability index S_L according to Loucks (1997) (Equation (6.11)). For $j = 1$ d the estimated of the groundwater recharge are plotted. The dots indicate the average and the error bars the standard deviation of the 10 runs of 1000 years.

The results of the newly introduced overall performance criteria using three different severity functions (Equation (6.12)) are presented in Figures 6.11, 6.12 and 6.13. It is clear that $p_{D,yr}$ and $p_{D,Cor}$ basically show the same behaviour. Both increase monotonously with increasing j . Only $p_{D,Cor}$ starts at a higher value than $p_{D,yr}$ and this value depends on the value of K . Apparently the loss function does not change the weighting of the deficits much. The monotonous increase is the direct result of the drought event definition (Figure 6.4). The drought event definition ensures that the drought deficit below the threshold (and thus also the average drought deficit per year in Equation (6.14)) is a constant fraction of the drought deficit below the average. As the amplitude of the groundwater discharge decreases with increasing reservoir coefficient, the deficit below the average (and with it the deficit below the threshold) decreases with increasing reservoir coefficient. The behaviour of $p_{D,10}$ (Equation (6.16), Figure 6.12) is different. Up to $j = 320$ d the performance is low and does not change much, after that it starts to increase rapidly. For $j = 160$ d the performance is lowest. The behaviour of $p_{D,10}$ can be understood from Figure 6.6. The performance depends on the average deficit per year for droughts with return periods higher than 10 years. For increasing reservoir coefficients the total deficit decreases and shifts to droughts with higher return periods. For $j = 1280$ d, over 90% of the deficit is associated with droughts with return periods higher than 10 years. So, up to $j = 320$ d the decrease in deficit is compensated by the shift and the performance remains more or less constant. For higher values of j the decrease in deficit becomes larger than the shift in deficit and as a result the performance increases.

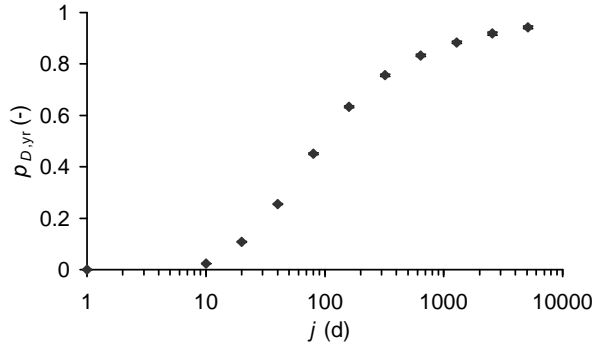


Figure 6.11: Estimates of the performance $p_{D,yr}$ (Equation (6.14)). For $j = 1$ d the estimates of the recharge are plotted. The dots indicate the average and the error bars the standard deviation of the 10 runs of 1000 years.

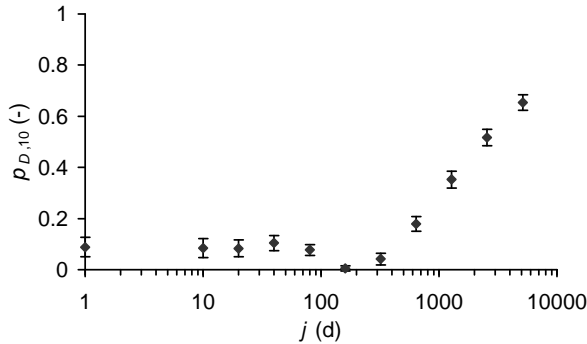


Figure 6.12: Estimates of the performance $p_{D,10}$ (Equation (6.16)). For $j = 1$ d the estimates of the recharge are plotted. The dots indicate the average and the error bars the standard deviation of the 10 runs of 1000 years.

6.5 Discussion

Best overall performance criteria Which of the overall performance criteria (overview in Box 6.1) discussed in the previous section is most useful for groundwater? Looking at performance from a broader perspective we may assume that generally a water resource is experienced as being sensitive or vulnerable to drought (and thus with a low performance) if regularly (with a high frequency) droughts occur whose deficit is considerable in comparison to the resource and of considerable extent in space and time (severe droughts) (Pandey and Ramasastri, 2001; Calow *et al.*, 1999). Based on this concept of performance, the following criteria are used to judge the overall performance criteria:

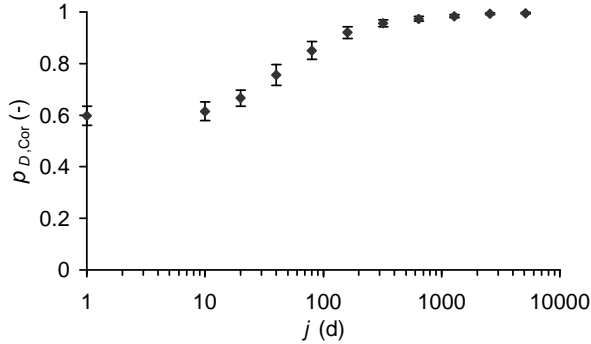


Figure 6.13: Estimates of the performance $p_{D,Cor}$ (Equation (6.18)). For $j = 1$ d the estimates of the recharge are plotted. The dots indicate the average and the error bars the standard deviation of the 10 runs of 1000 years.

- both the frequency and the severity of the droughts should be taken into account;
- severity of a drought should depend both on duration and the drought intensity;
- the criterion should be sensitive to persistence as this is an important aspect of groundwater droughts.

Moreover, the criterion should be robust, it should be between 0 and 1 in order to facilitate comparisons and it should preferably be physically interpretable.

Disadvantages of S_L are the fact that it is dimensional and that it has a rather strong emphasis on duration, which is included in both the reliability and the resilience. Moreover, it is not very robust (large error bars in Figure 6.10) and difficult to interpret physically. Most important, however, is the fact that the relation between severity and frequency of droughts is not addressed. For $p_{D,yr}$ the most important disadvantage is the fact that it is independent of the persistence.

Both $p_{D,Cor}$ (Equation (6.18) and Figure 6.13) and $p_{D,10}$ (Equation (6.16) and Figure 6.12) satisfy the criteria listed above. By weighting droughts with different return periods differently, they include the effects of persistence compared to $p_{D,yr}$. However for $p_{D,Cor}$ only the highest values (return period over 100 years) received a higher weight, so due to their low frequency this had little influence. A disadvantage for both is the introduction of another subjective choice: the pre-defined return period below which the weights are zero for $p_{D,10}$ and K for $p_{D,Cor}$. Overall, $p_{D,10}$ appears to be the best overall performance criterion for the data used in this chapter. Of course a wider range of data sets

would be necessary to get a more complete overview of the behaviour of these performance criteria.

Predefined performance criteria An important use of these overall performance criteria is the possibility to validate the predefined performance or sensitivity criteria for base flow mentioned in Section 6.1. In literature totally different criteria are used: for example response time of the base flow (Uijlenhoet *et al.*, 2001; Demuth *et al.*, 2000) and space-time persistency (Stahl, 2001). Both Uijlenhoet *et al.* (2001) and Demuth *et al.* (2000) state that the performance increases with increasing response time, because the faster the base flow recession, the faster an area or river stretch is in drought. Assuming that the reservoir coefficient j is a measure for the response time, then the performance increases with increasing j . This behaviour was seen for $p_{D,yr}$ (Figure 6.11). So using the response time is correct if you are not interested in the clustering of the droughts. S_L and the resilience (Figures 6.10 and 6.8b) show that the response time is not valid if the interest is in the duration of the droughts.

Stahl (2001) takes an opposite view and assumes that the performance decreases with increasing space-time persistency (or amount of clustering of the droughts), because the risk of very large droughts increases with increasing persistency. This is the behaviour that is seen for very severe droughts. From Figure 6.6, it can for example be derived that for a drought with a return period of 200 years, the drought deficit increases with increasing reservoir coefficient at least up to $j = 1280$ d. However, for a drought with a return period of 10 years, the drought deficit is largest for the recharge in Figure 6.6. So this concept is useful when investigating the sensitivity to extreme events.

6.6 Conclusions

Comparison of the distribution of droughts in the recharge and in the groundwater discharge showed that the propagation of a drought through a groundwater system decreases the number of droughts. The decrease in the number of droughts is mainly the result of the decrease in the number of small droughts. The number of severe droughts increases. Thus the groundwater system causes a shift in the drought distribution from many small droughts in the recharge to fewer, but more severe droughts in the groundwater discharge.

Of the overall performance criteria that were used to summarise these changes in drought distribution, $p_{D,10}$ (Equation (6.16)) was selected as the most suitable for droughts in groundwater discharge for the data from a temperate humid climate used in this chapter. This newly proposed criterion is based on the average drought deficit per year of droughts with a return period of more than 10 years. This criterion shows a low performance with little variation for ground-

water reservoirs with a reservoir coefficient of up to $j = 320$ d. For larger j the performance increases significantly. This behaviour agrees well with the general view that slowly responding systems are less sensitive to drought.

Acknowledgements The assistance of R. Wójcik from the Royal Dutch Meteorological Institute (KNMI, de Bilt) with the implementation of Nearest Neighbour Resampling is gratefully acknowledged. The meteorological data from the Yattendon and Reading stations were kindly provided by U.K. Meteorological Office through the British Atmospheric Data Centre.

Chapter 7

Sensitivity analysis and validation of the linear reservoir concept

This chapter consists of three parts that share the common purpose of validating and extending the results reported in previous chapters:

- An analysis of the influence of recharge characteristics on the propagation of the frequency distribution of the droughts through groundwater.
- An analysis of the influence of non-linearity of the groundwater-discharge relationship on the propagation of drought through groundwater.
- A limited validation of the results so far using observed data.

In the first part the influence of recharge characteristics on the propagation of drought through groundwater is examined by comparing the results from the semi-arid Upper-Guadiana catchment to results based on the recharge from the sub-humid Pang catchment. This was already done to a limited extent in Chapter 5 but is now extended to the results reported in Chapter 6. In the second part the influence of non-linearity in the groundwater-discharge relationship is investigated by comparing the droughts resulting from the propagation through non-linear reservoirs with the droughts in the discharge from a linear reservoir. In the third part observations from the Pang catchment are used for a limited validation.

7.1 Influence of recharge characteristics on the frequency distribution of drought

The influence of recharge characteristics on the propagation of drought could have been examined by generating artificial recharge series with predefined characteristics. However, a major problem in studying the effects of any one characteristic is that the characteristics are interrelated. The effect of a change in one parameter will depend on the values of the others. For example, Douglas *et al.* (2002) show that the influence of the lag-one autocorrelation depends on

the Coefficient of Variation (CV). In natural time series, however, the characteristics do not occur in random combinations. For example, flows with a low CV generally show a high autocorrelation, because often the low variation in flow is the result of storage processes. For that reason, it was decided not to use artificially generated time series, but to extend the results from Chapter 5 using recharge from a second catchment with a different climate: the Upper-Guadiana (Chapter 2). To investigate the influence of the different recharge, for the Upper-Guadiana 10 x 1000 years of recharge and discharge were simulated and the same performance criteria were calculated as in Chapter 6 for recharge from the Pang catchment.

7.1.1 Simulation of recharge for the Upper-Guadiana

To simulate long time series of recharge for the Upper-Guadiana the Nearest Neighbour method was used like in Chapter 6. For the Pang catchment long time series of precipitation P and potential evapotranspiration ET_{pot} were generated by resampling daily observed P and ET_{pot} . This provided satisfactory results. However, for the Upper-Guadiana daily data of P and ET_{pot} were not available, but only 57 years of monthly recharge, simulated from observed monthly P and ET_{pot} using the SIMPA model (Appendix B). Thus the monthly recharge R was resampled with a window width of 1 month and 5 nearest neighbours (see Chapter 6 for explanation about the nearest neighbour resampling technique and the meaning of these variables). As in Chapter 6, 10 time series of 1000 years were generated. Because of the extremely large number of zeros in the months July and August (86 and 77%, respectively), an adjustment was necessary to the resampling algorithm. This high number of zeros caused the selection of nearest neighbours to be limited to the first part of the time series. The problem was solved by starting the selection at each time step at a random point in the time series.

The statistical characteristics of the monthly recharge simulated with the SIMPA model were retained very well (Table 7.1, upper part). However, the statistics of the aggregated annual data were less well reproduced, especially the kurtosis and autocorrelation (AC) (Table 7.1, lower part). This is illustrated in the histogram of the annual data (Figure 7.1). Whereas the 57 years of recharge shows a double peak, this was not retained by the resampled data. The autocorrelation of the 57 years of annual data of 0.25 (Table 7.1) was significant at the 5% level, but not at the 2.5% level (both two-sided). The confidence intervals were generated using a Monte Carlo simulation of the order of the series. From a hydrological point of view, the large annual autocorrelation is not unreasonable for a region with a large carry-over between years. The existence of inter-annual dependence is also seen in the correlation between, for instance, successive Januarys and Februarys. For example, the correlation for

all months of December is 0.16, for January 0.14 and for February 0.11. For March on the other hand the correlation is -0.16, for September it is -0.13. The other months show only small correlations. However, since the time series is rather short to estimate such long-term dependences accurately, the simulated data as presented in Table 7.1 were used, despite their shortcomings.

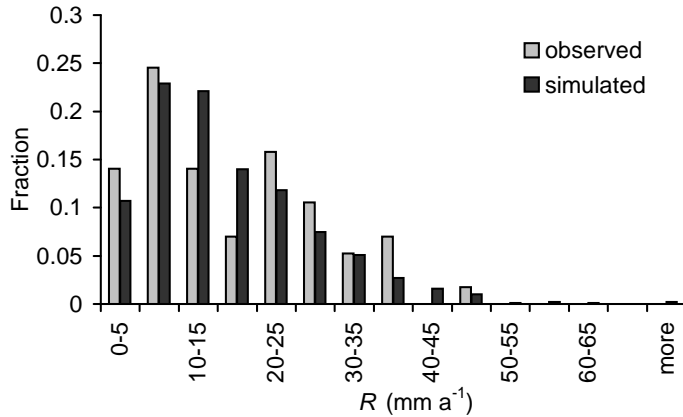


Figure 7.1: Histogram of 57 years of annual recharge R simulated using the SIMPA model and of 10 x 1000 years of resampled recharge.

The discharge was again simulated using linear reservoirs with j ranging from 10 to 10 000 d. The droughts were derived from both the recharge and discharge time series using the same approach as applied in Chapters 4, 5 and 6 with drought criterion $c = 0.3$.

7.1.2 Comparison of droughts for the Pang and Upper-Guadiana

The distribution of the drought deficits is presented in Figure 7.2. In all figures in this section, the results for the Pang from Chapter 6 have been added so that it can be seen easily how the results change as a result of different recharge. Because the recharge (and thus the discharge) for the Pang is much larger, the drought deficit is not expressed in mm, but relative to the annual average recharge. This is called the *relative deficit* D_{rel} . Despite the differences in the recharge between the Pang and the Upper-Guadiana, the distribution of the relative deficit of the recharge droughts was quite similar (Figure 7.2a). For the droughts in the discharge the differences were much larger. For small drought deficits, the deficits for the Pang and Upper-Guadiana were practically identical. However, for increasing return periods, the droughts for the Upper-

Table 7.1: Statistical characteristics of the Upper Guadiana recharge simulated with the SIMPA model and 10 x 1000 years resampled using Nearest Neighbour resampling (AutoCorrelation (AC) for monthly recharge calculated from deseasonalised values).

	Simulated with SIMPA (57 years)	Resampled (10 x 1000 years)
<hr/> MONTHLY DATA <hr/>		
mean (mm month ⁻¹)	1.39	1.40
standard deviation	2.64	2.64
skewness	3.60	3.49
kurtosis	17.47	16.28
maximum	21.46	21.46
AC lag 1	0.20	0.18
AC lag 2	0.07	0.05
AC lag 3	-0.01	0.00
<hr/> ANNUAL DATA <hr/>		
mean (mm a ⁻¹)	16.65	16.76
standard deviation	11.11	11.14
skewness	0.60	1.16
kurtosis	-0.59	1.55
minimum	1.72	0.62
AC lag 1	0.25	0.01
AC lag 2	-0.12	-0.01
AC lag 3	-0.11	-0.01

Guadiana were larger than the droughts with a corresponding return period for the Pang. And the larger the reservoir coefficient j , the sooner (meaning: for lower return periods) this occurred.

The behaviour described above is probably caused by a combination of factors. First, the drought deficit in the recharge is relatively similar, because the larger Coefficient of Variation CV in the Upper-Guadiana (Table 7.2) is compensated for by the lower autocorrelation, which tends to result in many small droughts with low drought deficits. It is not clear whether the similarity in recharge drought deficit is a coincidence or the result of type of model that was used to simulate the recharge (bucket model for both catchments). As a result of the propagation through a reservoir, for the Upper-Guadiana catchment the large number of very small droughts in the recharge can start to pool (Figure 7.3), even for reservoirs with fast response times. For the Pang catchment on the other hand, the pooling of droughts is limited by the seasonal structure. The consistently wet winter prevents the formation of multi-year droughts (Chapter 5).

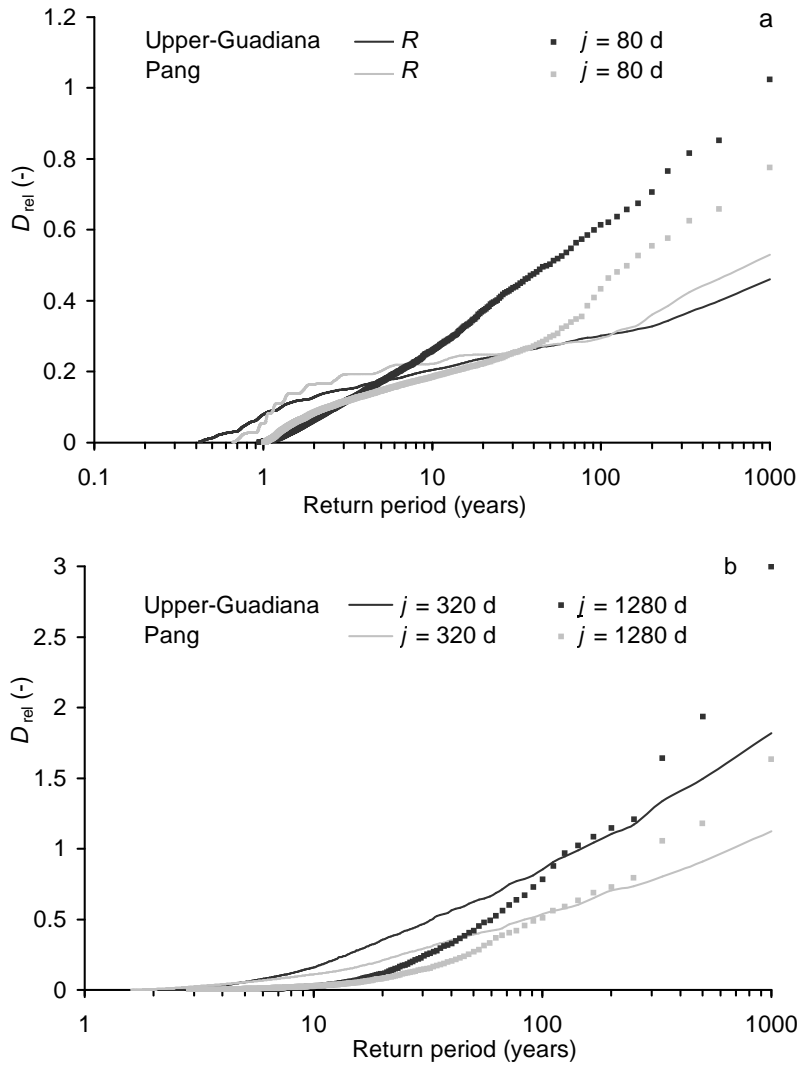


Figure 7.2: Comparison of the frequency distribution of drought deficit D_{rel} for the Pang and Upper-Guadiana for recharge R , and for the discharge from a linear reservoir with $j = 80$ d (a), $j = 320$ d and $j = 1280$ d (b). D_{rel} is expressed as a fraction of the average annual recharge or discharge ($R = q = 204 \text{ mm a}^{-1}$ for the Pang and 17 mm a^{-1} for the Upper-Guadiana). Presented is the average of 10 time series of 1000 years. Droughts are determined using the drought criterion $c = 0.3$.

Table 7.2: Comparison of characteristics of the simulated recharge from Pang and Upper-Guadiana catchment (average of 10 x 1000 years, AutoCorrelation (AC) for monthly recharge calculated from deseasonalised values).

	Annual recharge		Monthly recharge	
	Pang	Upper-Guadiana	Pang	Upper-Guadiana
AC lag 1	0.049	0.005	0.32	0.18
AC lag 2	0.007	-0.006	0.15	0.05
AC lag 3	-0.001	-0.013	0.01	0.00
CV	0.42	0.67	1.48	1.89

The differences between the Pang and Upper-Guadiana recharge are well reflected in the number of droughts (Figure 7.3). For the discharge from reservoirs with small j , the number of droughts was much higher for the Upper-Guadiana than for the Pang. For large j the number of droughts was smaller for the Upper-Guadiana. The resilience (Figure 7.4a; Equation 6.10) shows that the duration of the droughts for the Upper-Guadiana increases fast, unlike for the Pang, where the duration was limited by the seasonality. This means that even more than in the Pang, a change occurred from many, very short droughts to few longer droughts. The reliability (Figure 7.4b), which combines drought frequency and duration, increases somewhat faster for the Pang than for the Upper-Guadiana.

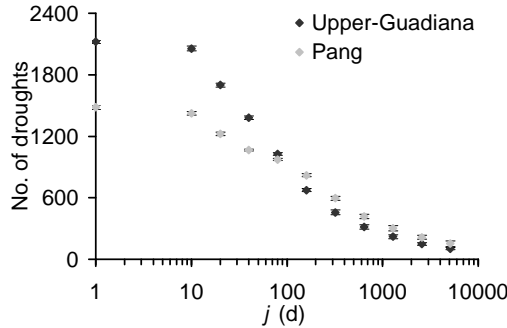


Figure 7.3: Number of droughts for the recharge (plotted for $j = 1$ d) and the discharge for different values of the reservoir coefficient j . The dots indicate the average and the error bars the standard deviation of the 10 runs of 1000 years.

In Figure 7.5 $p_{D,10}$ (Equation 6.16) is shown as the overall measure for the performance. The calculation of $p_{D,10}$ was changed slightly to account for the fact that we are comparing two catchments with very different average recharge. Instead of the deficit, the relative deficit (deficit divided by average recharge or discharge) was used. Both the performance for the Pang and the Upper-

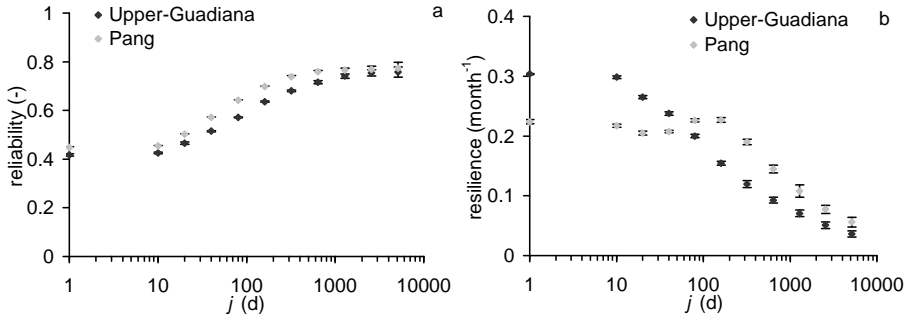


Figure 7.4: a) Reliability and b) Resilience. For $j = 1$ d the reliability and resilience for the recharge is plotted. The dots indicate the average and the error bars the standard deviation of the 10 runs of 1000 years.

Guadiana are scaled to the same maximum, therefore the performance for the Pang is different from that presented in Chapter 6. It is clear that the performance for the Pang catchment is much higher than for the Upper-Guadiana catchment. For very fast and very slowly responding catchments the difference between the catchments is relatively small. The difference is largest around the minimum performance, which occurs for both catchments for reservoirs with $j = 160$ d. The sharp decrease in performance for the Upper-Guadiana between $j = 10$ and $j = 160$ d is probably the combined effect of the comparatively low reliability (Figure 7.4) and high drought deficit (Figure 7.2). For return periods larger than 10 years the drought deficit was consistently higher for the discharge from the Upper-Guadiana than for the Pang.

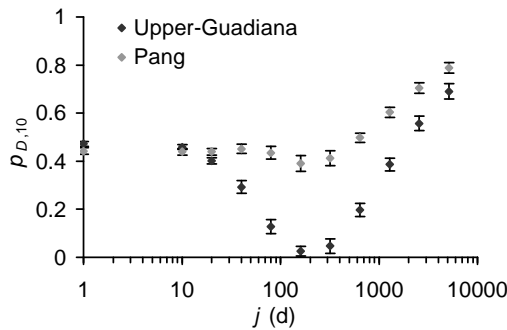


Figure 7.5: Estimates of the overall performance criterion $p_{D,10}$ (Equation (6.16)) calculated with relative deficits. For $j = 1$ d the performance for the recharge is plotted. The dots indicate the average and the error bars the standard deviation of the 10 runs of 1000 years.

7.2 Non-linearity versus linearity of the ground-water reservoir

7.2.1 Simulation of discharge from a non-linear reservoir

Up to now only linear reservoir models have been used to simulate groundwater flow, however, many authors have noted that for many aquifers a non-linear reservoir is theoretically more correct than a linear reservoir. For example, this holds for unconfined aquifers, for aquifers with a drainage pattern which varies with average groundwater level, for partial stream penetration, or for variations in kD (Chapman, 1999; Wittenberg, 1999; Wittenberg and Sivapalan, 1999; Marani *et al.*, 2001; van de Griend *et al.*, 2002). For fast responding systems, non-linearity is important. For more slowly responding systems the non-linearity probably becomes less important, as they can be approximated better by linear reservoirs (Chapman, 1999). However, for drought, non-linearity has an additional importance. According to Eltahir and Yeh (1999) and Marani *et al.* (2001) non-linearity in the groundwater level-discharge relationship increases the persistence on drought in the groundwater system.

To simulate a non-linear reservoir, the approach proposed by van de Griend *et al.* (2002) was followed, where the non-linearity is incorporated in the reservoir coefficient j (Equation (7.1)). For each time step, j is calculated as a function of the discharge q . The storage S is related to q by:

$$S = j(q)q = \frac{a}{q^{1-b}}q \quad (7.1)$$

where a [$L^{1-b}T^b$, if q in [LT^{-1}]] and b [-] are model parameters. For this approach, van de Griend *et al.* (2002) derived the following analytical solution:

$$q(t + \Delta t) = e^{-\beta\Delta t}q(t) + \left(\beta - \beta^2\frac{\Delta t}{2}\right) \int_t^{t+\Delta t} R(r) dr \quad (7.2)$$

where $\beta = \frac{1}{j(q)b}$.

For $b = 1$ a linear reservoir is simulated. $b = 0$ cannot be used, because it causes a singularity in Equation (7.2). Values of $b > 1$ are technically possible, however these values result in physically unrealistic situations, where for high storage, discharge decreases very slowly, whereas for low storage discharge decreases fast. Values for $b < 0$ would result in the impossible situation of increasing discharge with decreasing storage. For very small values of a the solution becomes less accurate. However, comparison of the calculated drought deficit using Equation (7.2) and the analytical solution for a linear reservoir

(Chapter 4) showed that the error for the smallest value of a , that was used ($a = 10$ d) was only 0.33%.

To evaluate solely the effect of the non-linearity, it is important that the linear and non-linear reservoir have comparable storage. In other words, the discharge of a non-linear reservoir should be compared to the discharge from a linear reservoir, which approximates the discharge from the non-linear reservoir best. However, the fact that the units of a change with b , means that the linear and non-linear reservoir cannot be compared using a . Thus a parameter comparable to the reservoir coefficient, which is used for linear reservoirs and with units of time, needs to be derived for non-linear reservoirs. An option would be to optimise a linear reservoir on the output of a non-linear reservoir and use the reservoir coefficient of that linear reservoir as the ‘equivalent reservoir coefficient’ for the non-linear reservoir. However, when optimising on the total series, the peak flows have more weight than the low flows. Moreover, it is inconvenient to run an optimisation for each combination of a and b . Therefore, an alternative approach was chosen, in which the non-linear S - q relationship is approximated by a linear relationship. If the non-linear relationship is approximated at a particular point, the equivalent reservoir coefficient j_1 can be derived from comparing the slopes at that point:

$$\frac{dq}{dt} = \frac{1}{ab}q^{-b} = \frac{-1}{j_1}q \quad (7.3)$$

Thus j_1 can be estimated from:

$$j_1 = \frac{ab}{q^{1-b}} = j(q)b \quad (7.4)$$

The difficulty lies in choosing the right value of q . It could, for example, be the median or the average. A more thorough approach, which was used in this paper, is to base j_1 on two points, for example the 25- and 75-percentile. This is illustrated in Figure 7.6. The equivalent reservoir coefficient j_1 can be determined as:

$$j_1 = \frac{aq_{75}^b - aq_{25}^b}{q_{75} - q_{25}} \quad (7.5)$$

where q_{75} and q_{25} are the 75- and 25-percentile of q respectively.

An additional problem is the presence of large numbers of very small values of q for fast responding catchments (up to 45%). Instead of using different percentiles to determine the linear approximation for the recharge with different reservoir coefficients, these values are removed before determining the

percentiles. For discharge derived from the recharge of the Pang all values below 1 mm month^{-1} were removed, while for the Upper-Guadiana all values below $0.1 \text{ mm month}^{-1}$ were removed.

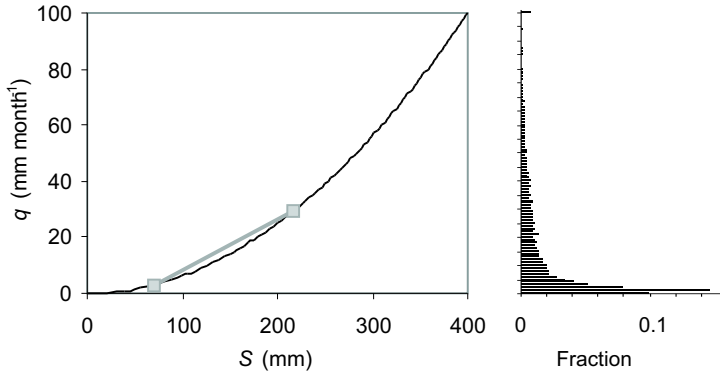


Figure 7.6: Determination of the equivalent reservoir coefficient j_1 (Equation (7.5)) using the 25- and 75-percentiles with $a = 40 \text{ mm}^{0.5} \text{ month}^{0.5}$ and $b = 0.5$. The black line is the non-linear q - S relation, the grey line is the linear approximation. To the right the histogram of q is presented.

The non-linear reservoir approach was mainly examined using long time series as in Chapter 6 and Section 7.1. Occasionally other examples are presented when this improves the understanding. Long time series for both the Pang and Upper-Guadiana catchment were calculated for non-linear reservoirs with b ranging from 0.8 to 0.2 (step 0.2). As in this section the changes compared to the linear solution are most important, only one series of 1000 years was simulated instead of 10.

7.2.2 Results

Although the general effects of non-linearity are well known, it is useful to recall exactly how this non-linearity affects a typical drought situation. In Figure 7.7 the difference in discharge from a non-linear reservoir (Equation (7.2)) and a linear reservoir (Chapter 4) is shown for synthetic recharge data (Equations 4.9 and 4.10) with a decrease in recharge during one year of 60%. This figure illustrates well how small the differences between the non-linear solution and the linear approximation are. At the start of the drought, the discharge decreases less for the non-linear case ($b = 0.5$). Thus, during drought the discharge is lower for the linear reservoir or, in other words, the drought intensity is larger for the linear reservoir ($b = 1$). This would lead us to expect that the drought

deficits for the linear reservoir are larger than the drought deficits for the non-linear reservoir. However, at the end of the drought, the discharge from the non-linear recovers slower than the discharge from the linear reservoir. This causes the drought to be longer and thus more persistent as expected by Eltahir and Yeh (1999).

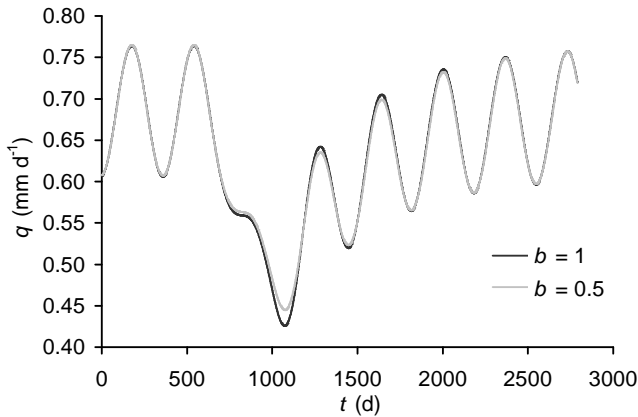


Figure 7.7: Discharge q for continuous, synthetic recharge (Chapter 4) with $a = 500$ d and $b = 1$ ($j_1 = j = 500$ d) and with $a = 828 \text{ mm}^{0.5} \text{ d}^{0.5}$ and $b = 0.5$ ($j_1 = 500.24$ d) ($f_d = 0.4$).

Figure 7.8 shows the overall effect of the non-linearity on the distribution of the drought duration and deficit for the Pang catchment for $j_1 = 80$ d. For higher values of j_1 the difference between the results of linear and non-linear reservoir decreases and for reservoirs with $j_1 > 1000$ d the difference between linear and non-linear reservoirs is practically nil as expected, both for the Pang and Upper-Guadiana (not shown). For small $j_1 (< 500$ d), longer and, mostly, more severe (higher deficit) droughts occur for the non-linear reservoir compared to the linear reservoir. The droughts for the non-linear reservoir were always longer (Figure 7.8b). However, the drought deficit was slightly smaller for non-linear reservoirs for droughts with small return periods. For droughts with larger return periods, the drought deficit was larger for non-linear reservoirs (Figure 7.8a). Because the drought deficit is larger (for the non-linear reservoir), the increase in drought duration is apparently more important than the decrease in drought intensity (Figure 7.7). Only for the smaller droughts in relatively fast responding catchments, the decrease in drought intensity is more important. In other words, the increase in persistency due to non-linearity always results in longer droughts, but not always in droughts with a larger deficit. The Pang and the Upper-Guadiana behave somewhat differently: the part where the drought deficit is smaller for non-linear reservoirs is more pronounced for the Pang than for the Upper-Guadiana (not shown). The transition

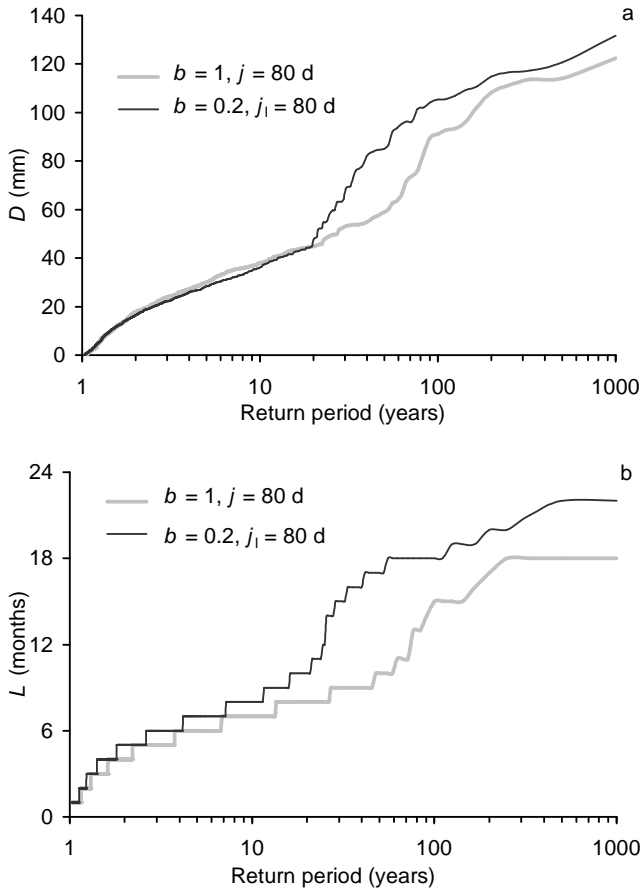


Figure 7.8: Frequency distribution of a) drought deficit D and b) duration L for linear reservoirs ($b = 1$ and $j = 80$ d) and non-linear reservoirs with $b = 0.2$ and $j_1 = 80$ d for recharge from the Pang catchment.

to more severe droughts for the non-linear reservoir occurs for return periods of about 20 years for the Pang and around 6 years for the Upper-Guadiana (for $j_1 = 80$ d).

The transition from within-year droughts to multi-year droughts is clear in both the deficit and the duration in Figure 7.8. For the linear reservoir this transition occurred for return periods of around 60 to 100 years. For a non-linear reservoir with $b = 0.2$, the transition occurred for return periods of around 20 to 30 years.

Because of the increase in drought duration (Figure 7.8b), the resilience (for

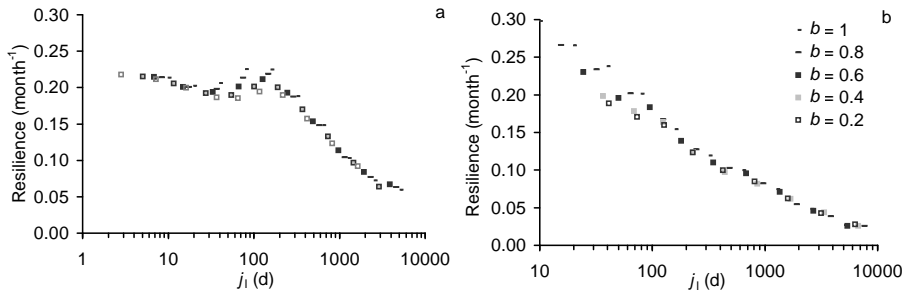


Figure 7.9: Resilience for a) the Pang and b) the Upper-Guadiana catchment for a linear reservoir ($b = 1$) and a series of non-linear reservoirs ($b = 0.8$ to 0.2).

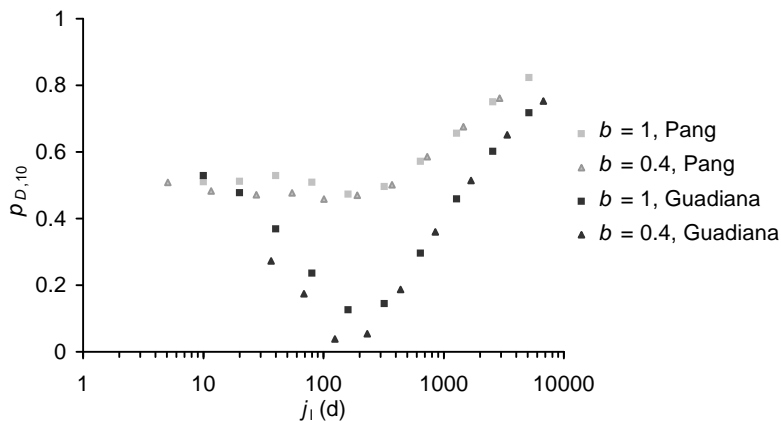


Figure 7.10: Overall performance criterion $p_{D,10}$ for the Pang and Upper-Guadiana catchment for a linear reservoir ($b = 1$) and a non-linear reservoir with $b = 0.4$.

definition see Box 6.1) is smaller for the non-linear reservoirs (Figure 7.9). However, for the Pang this was more the case for intermediately large j_1 -values (30-500 d), whereas for the Upper-Guadiana it was more for small j_1 values (< 300 d). The number of droughts was hardly affected for both the Pang and Upper-Guadiana catchment. The reliability showed the same behaviour as the resilience, namely a decrease for increasing non-linearity (not shown). The performance $p_{D,10}$ is presented in Figure 7.10. The performance for the Pang was affected little. It was slightly lower for the non-linear approach for $j_1 = 10$ to 100 d. Apparently the decrease in reliability is compensated for by the increase in drought deficit (Figure 7.8a). For the Upper-Guadiana, the compensation of the deficit was less and the performance decreased more.

7.3 Validation of the propagation of drought through a linear reservoir using data from the Pang catchment

7.3.1 Approach

In this chapter the results from previous chapters are compared to observations in the Pang catchment. However, the comparison differs from a traditional validation in two ways. First, the purpose of the confrontation in this section is not to test whether or not the (non-)linear reservoir model is a good groundwater model for either the Pang or the Upper-Guadiana catchment. The purpose of examining observed data is to see *whether the (non-)linear reservoir captures the essential influence of a groundwater system on drought*. In other words, it is the transformation of droughts caused by the linear reservoir that is validated. Second, the confrontation is not a comparison of simulated versus observed data, but *a comparison of results from a synthetic model to similar results derived from observed data*. So, droughts in the simulated discharge from a synthetic groundwater system are compared to droughts in base flow derived from observed streamflow, which are called ‘derived observations’.

A further problem for the comparison with observed data is the fact that in the previous chapters drought deficits were examined for a range of reservoir coefficients j , meaning a range of different catchments. Estimates of groundwater recharge, groundwater discharge and reservoir coefficients for large numbers of catchments are, however, not readily available. Moreover, even if they were available, differences in recharge characteristics makes comparison of droughts between catchments difficult. So, the comparison discussed in this section consisted of comparing a range of droughts with different drought deficits for one reservoir coefficient, namely the reservoir coefficient representative for the Pang catchment.

The droughts will be compared in two ways. First, recharge versus discharge droughts for the simulations in Chapter 6 are compared to recharge versus discharge droughts for the ‘derived observations’ (Section 7.3.3). Second, the droughts will be compared by examining the change in frequency distribution as in Chapter 6 (Section 7.3.4). The comparison was not done for the Upper-Guadiana catchment, because of the lack of clear seasons. This makes it very difficult to link a drought in the discharge to a specific drought in the recharge.

The recharge for the ‘derived observations’ is the same as that used in Chapters 5 and 8 (Appendix A). The base flow was only derived at Pangbourne GS (Figure 2.1), because the observations at the other two stations in the Pang catchment are too short. *Base flow was estimated from observed streamflow*

at Pangbourne GS using a new method based on observed groundwater levels, which is fully explained in Appendix C. Instead of one best solution, a range of solutions from a Monte Carlo simulation was accepted (the 250 best runs out of 5000 runs). For each of the 250 accepted time series of discharge the droughts were calculated. Not all droughts occurred for all 250 runs, but these were always minor droughts. Because of the distinct seasonal structure, the droughts could clearly be identified, despite the different numbers of droughts. For each drought, the average duration and deficit was calculated from those runs in which the drought occurred. This means that the number of averaged droughts is larger than the number of droughts in most of the individual runs.

7.3.2 Estimation of the reservoir coefficient j

The reservoir coefficient was estimated for a linear reservoir only. Because the difference between the linear and non-linear response is relatively small compared to the changes caused by different values of the reservoir coefficient (Chapter 7.2), only the results of linear reservoirs will be used in the comparison. Unfortunately, the linear reservoir coefficient cannot be estimated from the results in Appendix C, because the reservoir coefficient was estimated in conjunction with another parameter. So, the reservoir coefficient was estimated using a variety of other methods, which yielded a variety of estimates of the reservoir coefficient. Basically two methods were used: first, direct determination using the correlation method (Tallaksen, 1995) for recessions in discharge, base flow and groundwater levels and second, by inverse modelling.

In Table 7.3 an overview of the results of the different estimation methods is presented. The values for the correlation method are median values for streamflow and base flow derived using the BFI method, because the estimated j -values show approximately a lognormal distribution. For the base flow derived from groundwater levels and for the groundwater levels, initially also the median was used. However, from studying the recessions, it was clear that this was an over-estimation. In Figure 7.11 the estimates of the reservoir coefficient for selected recessions from the base flow derived from groundwater levels are plotted. At the beginning and end of the recessions some recharge occurs and thus the estimated reservoir coefficients are larger. From this figure, the estimate of the reservoir coefficient for the base flow based on groundwater levels resulted in about 150 d (Table 7.3). From a similar figure for observed groundwater levels (not shown) the reservoir coefficient was estimated to be about 215 d. For the groundwater levels, the estimate of j depends on the borehole used and on the reference groundwater level, which was estimated in conjunction with the reservoir coefficient.

Table 7.3: Overview of the estimates for the reservoir coefficient j using the correlation method and inverse modelling. Base flow is estimated using the BFI method and using observed groundwater levels (Appendix C).

Type of data	Correlation method	Inverse model
Observed streamflow	48 d	-
Base flow BFI	96 d	90 d
Base flow based on groundwater levels	150 d	140-150 d
Groundwater levels	215 d	-

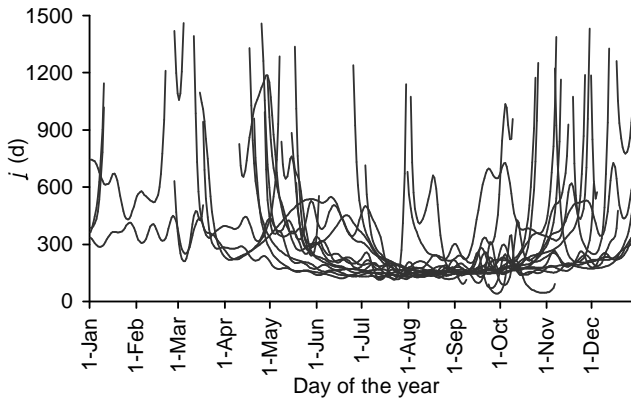


Figure 7.11: Estimation of the reservoir coefficient j using the correlation method for the base flow derived from groundwater levels (Appendix C).

The inverse method used for estimating the reservoir coefficient, consisted of using the recharge as input to a linear reservoir and determining the reservoir coefficient by inverse modelling. The output of the reservoir was fitted to the base flow determined in Appendix C. For the base flow estimated using the BFI method the reservoir coefficient was estimated at approximately $j = 90$ d (Table 7.3). For base flow derived from observed groundwater levels $j = 140$ to 150 d. The difference between reservoir coefficients derived from discharge and groundwater levels is inherent to the discharge process and has also been observed by, for example, Halford and Mayer (2000). In the following the results from a reservoir with $j = 150$ d will be used as an approximation of the groundwater system of the Pang.

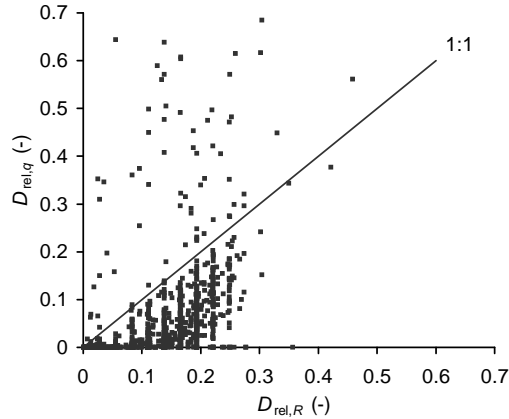


Figure 7.12: Relative drought deficit in the recharge $D_{rel,R}$ and in the simulated groundwater discharge $D_{rel,q}$ as a fraction of mean annual recharge/discharge for a 1000-year time series. Discharge is outflow from a linear reservoir with $j = 150$ d (Drought criterion $c = 0.3$).

7.3.3 Results for droughts in recharge and base flow

In Figure 7.12 the droughts in the recharge and the discharge from a linear reservoir with $j = 150$ d for a 1000-year time series from Chapter 6 are presented. The deficits are expressed as a percentage of mean annual recharge or discharge. This figure shows that overall D_R and D_q are related, but that there is a large variability between individual droughts. For most droughts the deficit in the discharge is smaller than the deficit in the recharge. Only for some droughts (mostly multi-year droughts) the deficit in the discharge is considerably larger. In Figure 7.13 the droughts in the ‘derived observations’ recharge R and base flow Q_s are presented. Although the number of droughts is limited, it shows the a similar pattern as Figure 7.12. Only the difference between the small (low deficit) discharge droughts and the large (high deficit) discharge droughts appears larger than for the linear reservoir with $j = 150$ d. In fact, this behaviour is more like that of a reservoir with a larger reservoir coefficients (data not shown).

7.3.4 Results from the frequency distribution

The second point of the confrontation was the comparison of the frequency distributions of the droughts. In Figure 7.14 the frequency distributions of the droughts from the resampled 1000-year series from Chapter 6 are presented. Only the part with return periods from 1 to 100 years is shown. In Figure 7.15

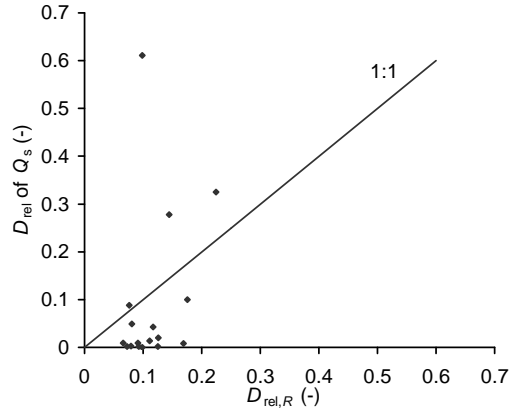


Figure 7.13: Relative drought deficit in the recharge $D_{rel,R}$ and in the base flow D_{rel} in Q_s as a fraction of mean annual recharge/discharge for a 1000-year time series (Drought criterion $c = 0.3$).

the frequency distributions of the droughts derived from the recharge and base flow are presented. The ‘derived observations’ basically show the same behaviour as the results from the linear reservoirs, except for one major difference: the transition to multi-year droughts occurs for lower return periods for the observed data (at a return period of around 8 years, instead of 20 years). It is not clear whether this is a real difference or a result of inaccuracies in R or Q_s . It could also be the result of the shortness of the observed data series. Again, the distribution of the derived observation is more like that of a reservoir with a large reservoir coefficient than 150 d.

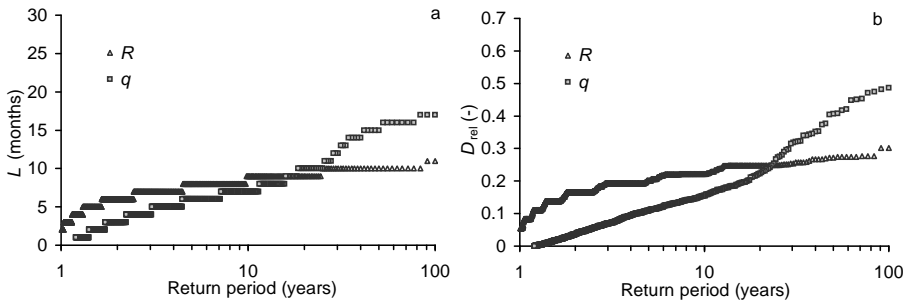


Figure 7.14: Frequency distribution for a) drought duration L and b) relative drought deficit D_{rel} expressed as a fraction of mean annual flux of the recharge R and simulated groundwater discharge q for $j = 150$ d ($c = 0.3$).

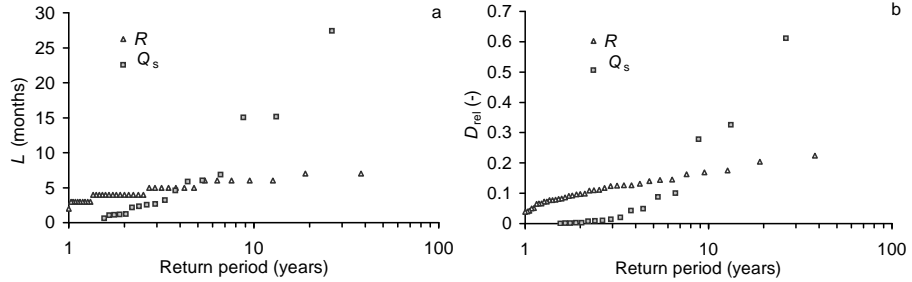


Figure 7.15: Frequency distribution for a) drought duration L and b) relative drought deficit D_{rel} expressed as a fraction of mean annual flux for recharge R (Appendix A) and base flow Q_s (Drought criterion $c = 0.3$).

7.4 Conclusions

The analysis of the influence of the characteristics of the recharge on the propagation of drought through a groundwater reservoir showed that the basic conclusions did not change for different recharge data. Still, the largest drought deficits occur mostly for intermediately large reservoir coefficients ($j = 100$ to 1000 d). However, also differences occur. The effect of the groundwater reservoir on droughts is stronger for the Upper-Guadiana than for the Pang. For a catchment with the semi-arid recharge from the Upper-Guadiana, the number of droughts *decreases* faster with increasing j than for a catchment with the sub-humid recharge from the Pang catchment. The drought duration *increases* faster for a catchment with semi-arid recharge. Whereas the overall performance is nearly identical for the recharge from the Pang and Upper-Guadiana, for the discharge the performance is much lower for the Upper-Guadiana. The most important difference between the two recharge signals appears to be the difference in seasonal structure, which determines the pooling of the drought (see also Chapter 5).

The discharge from a non-linear reservoir deviates in two ways from a linear reservoir: first the flow in periods of low flow is higher and second the recovery after a drought is slower and thus is the flow after a drought lower. The former effect causes the drought deficit to decrease. The latter effect increases the drought duration and from that the drought deficit. For the Upper-Guadiana, the increase in duration is more important and thus the droughts for the non-linear reservoir are generally more severe. For the Pang the underestimation of the flow during low flow is more important for the small droughts (i.e. droughts with small return periods) and thus for these droughts the deficit for the non-linear reservoir is lower. However, for severe droughts (with large return periods) the increase in duration becomes more important and thus the drought

deficit is larger for non-linear reservoirs. This difference in response between the Pang and the Upper-Guadiana can, again, for a large part be contributed to the difference in seasonal cycle. Finally, the influence of the non-linearity is largest for small j and decreases with increasing j .

Two problems complicate the validation of the results of previous chapters with observed data. The first problem for studying the propagation of droughts in a single catchment is that the variability between individual droughts is very large. This means that large numbers of droughts are necessary to observe more general trends. However, as with all extreme events, the number of observations is small. The second problem is the uncertainty associated with the ‘derived observations’: recharge and base flow. Deviations between ‘observed’ and simulated changes in drought (as a result of the propagation through the groundwater system) may also be the result of errors in these ‘derived observations’.

Despite these problems, the conclusions from the simulations appear to be confirmed by the observed values. Apparently most changes in droughts can be explained by the effects of storage. If we look in more detail, however, some deviations occur. The droughts obtained from ‘derived observations’ indicate a larger storage (higher reservoir coefficient), than the discharge from a linear reservoir with the reservoir coefficient derived from base flow. The comparison between the frequency distributions showed that the main difference between the simulated and observed droughts was, that the transition to multi-year droughts occurs for lower return periods for the observed droughts.

Chapter 8

Spatial aspects of drought in a groundwater catchment

8.1 Introduction

In Chapters 4 to 7, the groundwater system has been modelled as a simple linear or non-linear reservoir. So far the spatial extent of a drought, which is an essential aspect (Chapter 1), and the spatial variability in groundwater recharge, levels and discharge has been ignored. In this chapter the effects of the spatial variability on groundwater drought will be examined. So far, very few studies have addressed the spatial distribution of drought in groundwater. One exception is the study by Chang and Teoh (1995), who noticed a clear variation in droughts in 13 wells throughout an aquifer.

Spatial patterns in groundwater It is well-known that the temporal pattern of phreatic groundwater levels is very different for different hydrological and hydrogeological settings (Gehrels *et al.*, 1994; de Vries, 1995). In areas with shallow groundwater levels and high drainage density, groundwater level fluctuations are small and fast. However, in areas with low drainage density and deep groundwater levels (long distance to streams, high drainage resistance) groundwater level fluctuations are slow, the amplitude of the inter-annual fluctuations is larger than the amplitude of the within-year fluctuations (de Vries, 1974). These differences also exist within many catchments, especially those with deep groundwater levels. Close to a stream, the response of the groundwater levels to recharge is fast, because the unsaturated zone is shallow, but the groundwater level fluctuations are limited due to the relatively constant level of the stream. Far away from the stream, the groundwater levels are less constrained, but the recharge is delayed and attenuated by the propagation through thick unsaturated zones. These spatial patterns in the temporal characteristics of groundwater levels have clearly been shown by geostatistical methods for the interpolation of groundwater levels (van Geer, 1994; Stein, 1998; Kumar and Ahmed, 2003).

Spatial patterns in groundwater drought The differences in fluctuations of groundwater recharge, level and discharge influence the spatial distribution of

drought behaviour in a catchment. However, it is unclear how the combination of all the different processes will influence the drought. Yet, it is important to understand how the drought characteristics vary throughout an aquifer, for example, for drought monitoring, interpolation of drought characteristics or comparison of drought severity between catchments, aquifers or within an aquifer.

For the Pang catchment (Chapter 2), some historical droughts will be analysed by examining simulated, spatially distributed recharge, groundwater levels and discharge. Although in the Pang catchment groundwater levels have been observed quite extensively, records with a sufficiently long, common time period are not available in sufficient spatial detail. Thus the groundwater flow had to be simulated. Another reason for simulation of the groundwater flow is the fact that the purpose of this case study is not to analyse the specific flow in the Pang catchment in every detail, but to analyse the spatial aspects of groundwater droughts more generally. The reason for using a real catchment instead of a synthetic catchment is the difficulty of constructing a realistic, consistent synthetic groundwater catchment. A second objective is to evaluate the drought event definition for groundwater levels, as little experience presently exists about the derivation of droughts from groundwater levels (Hisdal *et al.*, 2004). Specifically the use of the threshold level approach (Chapter 3) for groundwater levels will be investigated.

8.2 Simulation of the spatial distribution of groundwater recharge, levels and discharge for the Pang

To simulate the groundwater flow in the Pang catchment the well-known MODFLOW code (McDonald and Harbaugh, 1988, 1996) was used. Detailed processes relating to the stream-aquifer interaction, like bank storage and evapotranspiration from the stream and the riparian area, were not taken into account, as they are beyond the scope of the present study. Groundwater recharge was simulated using the 1D-SWAP model (van Dam *et al.*, 1997)(Appendix A). The distributed recharge was simulated for a grid of cells of 500 by 500 m, which is also the grid used for the MODFLOW model. The MODFLOW model was calibrated using PEST (Watermark Computing, 1998). Because the interest is not in the specific details of the Pang catchment itself, a detailed fit between observed and simulated groundwater levels and discharge is of less importance. So the calibration was relatively limited. The model was calibrated for the time period 1987 to 1997 and run for the period 1960-1997. The model was, of course, calibrated with the abstractions that occurred in the catchment, how-

ever, the results presented here are for model simulations without abstractions. A full description of the MODFLOW model, the calibration and some model simulations is given in Appendix D.

8.2.1 Derivation of droughts

The droughts for groundwater recharge, levels and discharge were extracted from the time series using the threshold level approach described in Chapters 3 and 4. All droughts were derived using drought criterion $c = 0.3$. The recharge and groundwater levels are available on a 500 by 500 m grid and the droughts, and thus the threshold levels, were derived for each grid cell separately. Because the top layer tended to dry up in some areas, the hydraulic heads from the second model layer (Appendix D) were used. They deviated only little from heads of the first model layer. For discharge, the droughts were derived for 3 reaches along the river plus a major karstic spring (the Blue Pool) as shown in Figure 8.1.

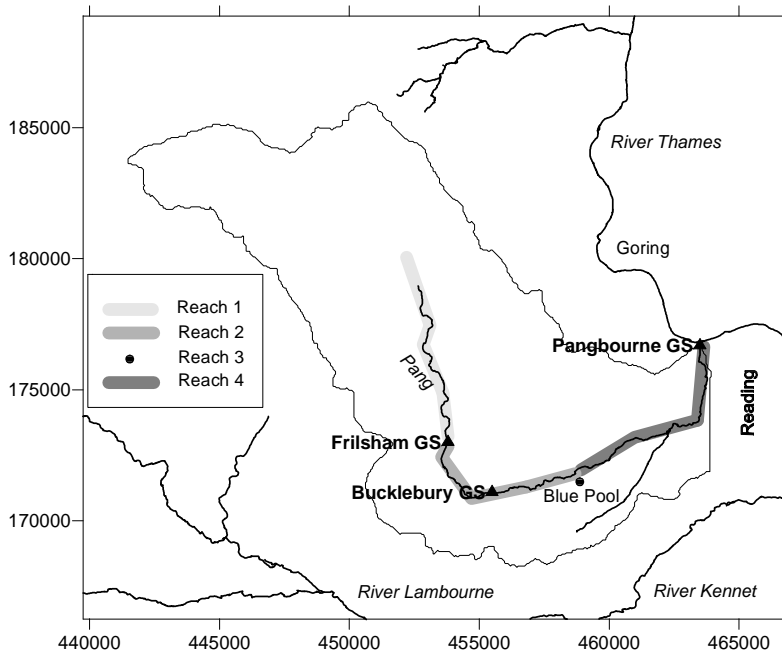


Figure 8.1: River reaches along the Pang for which the discharge and droughts were simulated. From upstream to downstream: reach 1 to 4. Reach 3 is the Blue Pool, a major karstic spring

As stated in the introduction of this Chapter, one of the purposes of this study is to evaluate the use of the threshold level approach for groundwater levels. As groundwater level (or hydraulic head) is a state variable, the deficit has dimension [LT] instead of [L] or [L³], which is the dimension of the drought deficit for recharge and discharge (Section 3.4). When deriving the droughts from the hydraulic heads, a problem became evident: the value of the drought deficit was largely determined by the position in the catchment. The pattern in the drought deficit is probably mainly caused by the variation in the standard deviation, which depends on the spatial variation in the storage coefficient (Figure D.3 in Appendix D) and the distance to a stream or constant head boundary (Figure D.1 in Appendix D). This strong pattern masked any patterns which might result from, for example, variations in recharge or in persistence or skewness in the hydraulic heads. Moreover, the standard deviation is not really influencing drought behaviour, but only serves as a scaling factor. Therefore the deficit needed to be standardised in some way.

Possible standardisations would be to divide by the standard deviation σ , to correct for the influence of the storage coefficient S_y , or to use the distance to the nearest stream (or constant head for model results) as a correction factor. Especially the combination of the last two factors is interesting as it is based on groundwater flow, rather than a purely statistical measure. However, in an exploratory case, the results from the approach based on storage coefficient S_y (which is relatively constant in this model, see Figure D.3) and distance to the stream differed little from the results gained by dividing through σ . Moreover the standardisation using σ is much easier to apply. Thus, it was decided to divide the drought deficit by the standard deviation σ , a procedure which has earlier been proposed for precipitation by Clark (1993). The drought deficit divided by σ is called the *normalised drought deficit* D_{norm} as opposed to the *relative drought deficit*, which is the drought deficit expressed as a fraction of the average annual recharge or discharge (Chapter 7).

8.3 Results

From the record of the period 1960 to 1997, the spatial distribution of two historical droughts with very different characteristics will be investigated: 1976 and 1991-92. The drought in 1976 is a typical example of a short, very severe event in terms of precipitation, whereas the 1991-92 drought was severe mainly because of its long duration.

The 1976 drought The sequence of the winter of 1975-76 followed by the summer of 1976 was extremely dry. The hydrological year 1975 (October 1975 to September 1976) was the year with the lowest precipitation and the highest

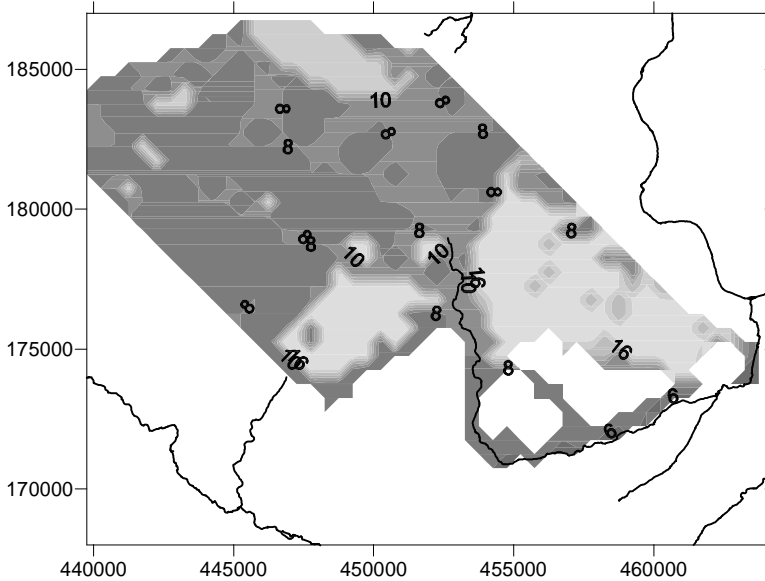


Figure 8.2: Duration (months) of the recharge drought in 1976.

potential evapotranspiration in the period 1960 to 1997 (Chapter 2). The winter of 1976-77 was extremely wet and ended the drought very effectively. Figure 8.2 shows the duration in the recharge droughts. Only the area of interest instead of the whole model area is plotted. The blank areas in the south (Figure 8.2) are areas where the recharge was defined constant below the Tertiary deposits (Appendix D, Figure A.5). Some blank cells in the north and central part of the area are cells which have forest as the dominant land use. The drought for forest lasted much longer than for the other land use types, and has been left out to keep the picture legible. The light colours are the areas where multi-year droughts occur. The multi-year droughts mostly started in June or July 1975 and ended in November to December 1976. The within-year droughts mostly started around April 1976, which is early because of the dry winter. The drought was shortest close to the Pang. In Figure 8.3 the duration of the droughts in the hydraulic heads is plotted, which shows that except for one small area, only within-year droughts occur in the heads. Comparison of the duration of the droughts in the recharge and the heads shows that the few areas of multi-year droughts in the heads are much smaller than the areas of multi-year droughts in the recharge. So, the groundwater system has decreased drought duration. This effect of the groundwater system was also demonstrated in Chapters 4, 5 and 6. The multi-year droughts occur only on the high parts. The drought deficit and the normalised drought deficit in the hydraulic head

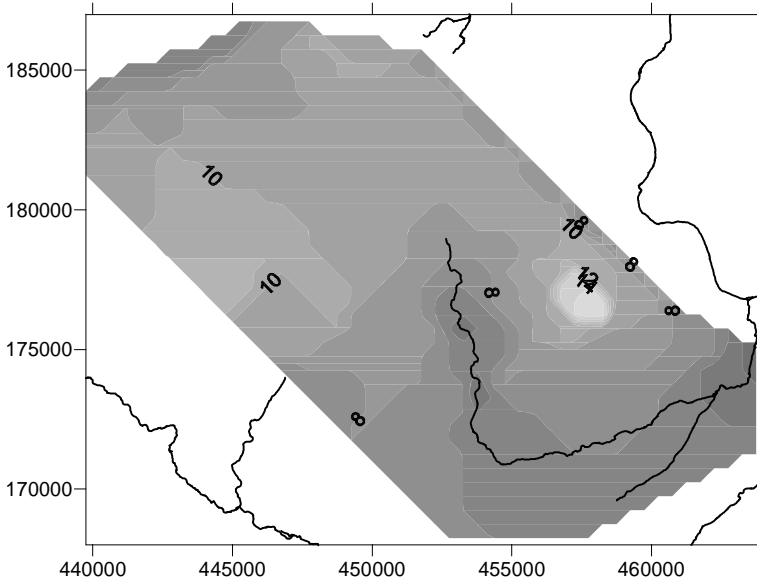


Figure 8.3: Duration (months) of the drought in the hydraulic heads in 1976.

are presented in Figure 8.4. The pattern in the deficit in the hydraulic head (both normal and normalised) hardly resembles the deficit in the recharge (not shown). This might be due to the fact that the threshold level approach for monthly recharge data does not include the decrease in winter recharge compared to the average winter recharge (see for comparison Figure 4.8). However, an exploratory test with droughts derived from annual recharge data, did not improve the relation with the deficit in the heads. The pattern in the normal drought deficit (Figure 8.4a) mostly resembles the pattern of σ (Figure 8.5) or the groundwater level (Figure 2.5). The pattern in the normalised drought deficit (Figure 8.4b) shows that the largest droughts occur near the outlet, and the smallest near the groundwater divide, which is nearly the opposite of the pattern in the normal drought deficit. The most probable explanation of this pattern is that near the groundwater divide, the groundwater system has the longest memory and has dampened this relatively short drought most.

The drought in the groundwater discharge is shown in Figure 8.6 and Table 8.1. Figure 8.6 shows the drought intensity for the incremental flow for the different reaches of the Pang (Figure 8.1). The drought intensity is the difference between the threshold and the discharge at that moment in time (Figure 3.3). Integrated over time the drought intensity gives the drought deficit, which is presented in Table 8.1 for the different reaches of the Pang. The deficit for reach 3 is the discharge from a major karstic spring, named the Blue Pool,

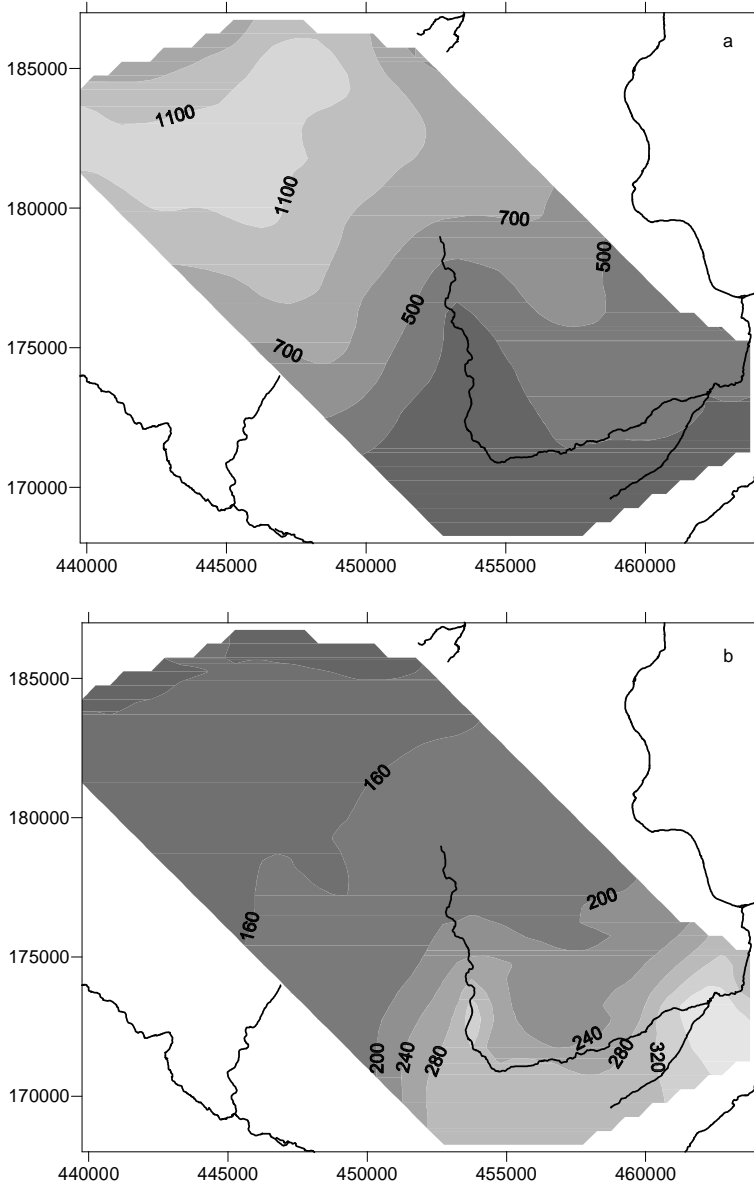


Figure 8.4: a) Drought deficit (md) and b) normalised drought deficit (d) for the drought in the hydraulic heads in 1976.

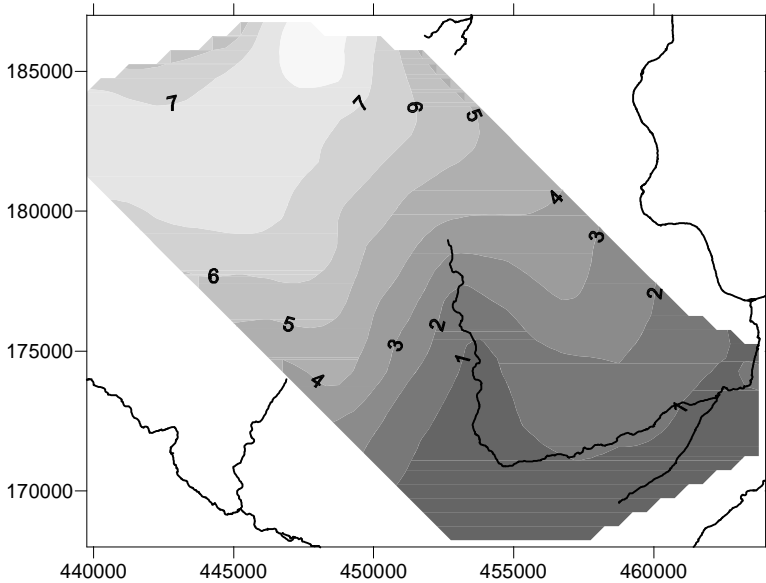


Figure 8.5: Standard deviation σ (m) of the hydraulic heads.

which is discharge from a deeper layer. The spring discharge is very constant throughout the year, and thus provides a relatively small contribution to the deficit, compared to the average discharge. The drought in 1975 was a normal summer drought (see discussion for Figure 3.2 in Section 3.3) after the relatively wet winter of 1974-75. A normal summer drought is a period in summer during which the groundwater discharge is below the (constant) threshold, but near the average summer discharge. The drought in 1975 started earliest for the most downstream reach and last for the most upstream reach. The drought in the most downstream reach ended earlier than the upstream part. The drought in 1976 started earliest in the upstream part, because for this part the hydraulic heads (and thus the groundwater discharge) hardly recovered during the winter. Also in the heads, the drought started earliest on the high parts (data not shown).

The 1991-92 drought The drought in 1991-92 was a typical multi-year drought and was characterised by a sequence of several relatively dry winters, culminating in a two-year drought lasting from summer 1991 to autumn 1992. Both in the recharge and the heads the drought lasted longer than one year for large parts of the catchment (Figures 8.7 and 8.8). But in contrast to the 1976 drought, now the area with multi-year droughts is much larger in the heads than in the recharge. This is the result of the long memory of the groundwater system. The groundwater system integrates the effect of a series

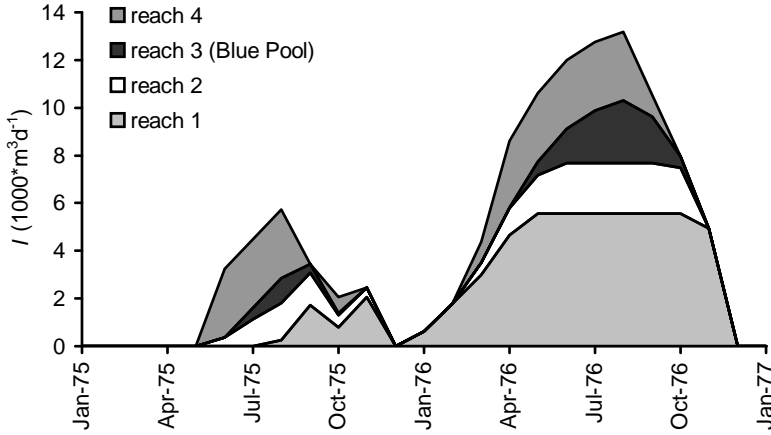


Figure 8.6: Drought intensity I (m^3d^{-1}) for 4 reaches along the Pang (Figure 8.1) during 1975 and 1976.

Table 8.1: Drought deficit D , relative drought deficit D/μ^a and normalised drought deficit $D_{\text{norm}} = D/\sigma$ for the groundwater discharge droughts in 1976 and 1992 for 4 reaches along the Pang (Figure 8.1).

Reach	Period 1960-1997			Drought in 1976			Drought in 1992		
	μ m^3d^{-1}	σ m^3d^{-1}	CV -	D m^3	D/μ d	D/σ d	D m^3	D/μ d	D/σ d
1	11 914	13 543	1.14	1405 874	118	104	2743 574	230	203
2	4 868	4 751	0.98	428 266	89	90	672 669	139	142
3	12 139	1 026	0.08	271 682	22	265	51 093	4	50
4	7 046	6 527	0.93	504 639	72	77	273 954	39	42

^aThe relative drought deficit is expressed here in d rather than as a fraction of annual discharge to facilitate comparison with D_{norm} .

of years with below average recharge. This is reflected in the normalised deficit (Figure 8.9b). The pattern for the 1992 drought is more or less the reciprocal of that for the 1976 drought (Figure 8.4b), with relatively low deficits closer to the outlet and higher deficits near the groundwater divide. In fact it resembles the distribution of the autocorrelation in the heads quite well. The autocorrelation is a measure for the amount of memory and is well-known to increase the drought duration and deficit for severe droughts (Section 3.3). The normalised deficit shows another remarkable feature. Near the upper reaches of the Pang the normalised deficit is very large. This is caused by a combination of drying up of the stream (because the head is lower than the streambed) and a relatively low σ (Figure 8.5), because usually the stream limits the fluctuations of the head (and thus the discharge). The pattern of the normal drought deficit

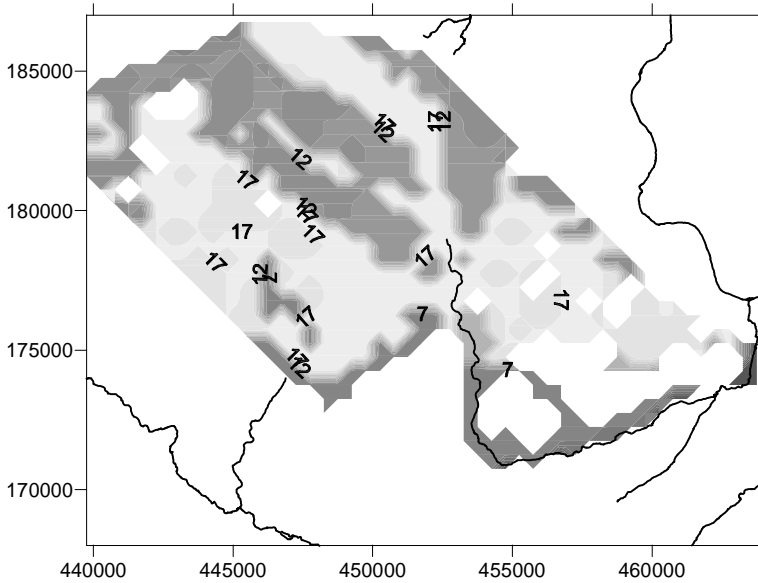


Figure 8.7: Duration (months) of the recharge drought for the 1992 drought.

(compare Figures 8.4a and 8.9a) is only little different for the droughts in 1976 and in 1991-92. That shows how important it is to have some form of standardisation, as explained before in Section 8.2.1.

The drought intensity I along the Pang for the period 1988-1992 is presented in Figure 8.10. Two very dry winters, where the flow in the upper reaches of the Pang remains below the threshold, can be identified in this period: the winter of 1988-89 and the winter of 1991-92. The winter of 1990-91 was only slightly wetter. Like for the drought in 1975, the droughts from May 1988 to March 1989 and from May to December 1990, which both followed on a relatively wet period, started first closest to the outlet. After a dry period (winter 1988-89 and winter 1990-91), the drought started at more or less at the same time over the entire length of the Pang, whereas for the drought of 1976 the drought started first in the most upstream part. The difference in response time is also illustrated during the winter of 1991-92. The flow in the more downstream reaches of the Pang recovered to above the threshold level, but not in the two most upstream reaches. The drought intensity of the most upstream reach (reach 1) in Figure 8.10 also illustrates that the drought deficit in dry years tends to be similar each year, because the flow cannot be lower than zero. Only by increasing the duration, the deficit can increase. Indeed it is a well-known fact that drought deficit and duration in streamflow are highly correlated (Yevjevich, 1967; Sharma, 1997).

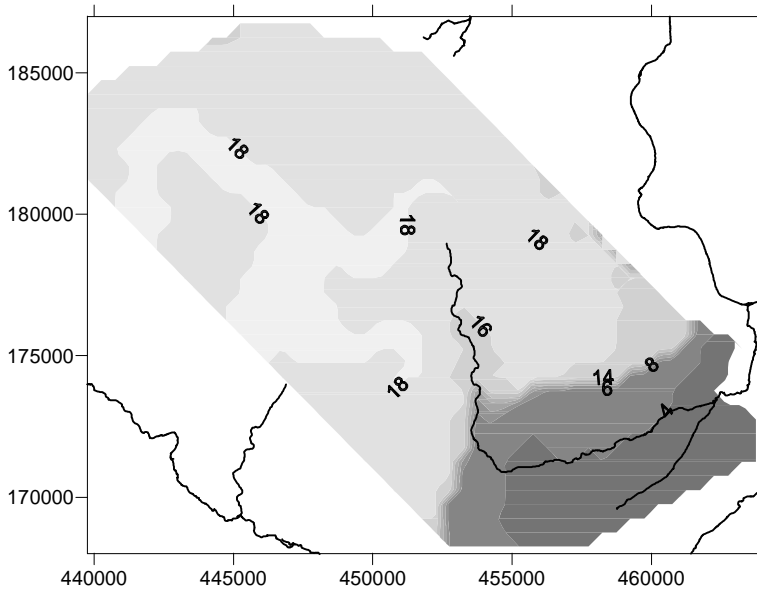


Figure 8.8: Duration (months) of the drought in the hydraulic heads for the 1992 drought.

8.4 Discussion

Influence of persistence on groundwater levels From the results presented above it is clear that the variations in memory throughout an aquifer or groundwater catchment are very important for droughts, because they change the drought behaviour fundamentally. This has some interesting consequences. Consider, for example, the flow in a homogeneous medium between two parallel streams with a constant recharge. To most people, the severity of the drought derived from groundwater levels would seem identical for the whole groundwater system, irrespective of the distance to the stream. However this is not true. Even if the droughts are caused by the same recharge drought, the drought severity changes with distance to the stream, because of the change in the persistence of the groundwater levels. The variations in persistence cannot be standardised in the event definition as has been done for the standard deviation of the groundwater levels, because of the strong non-linearity of the relation between the persistence and the drought deficit. Due to increasing persistence some droughts become more severe and others become less severe. This is illustrated in Figure 8.11 which shows the frequency distribution of the drought deficits in the hydraulic head with increasing distance to the Thames for the period 1960 to 1997. The return periods were estimated according to

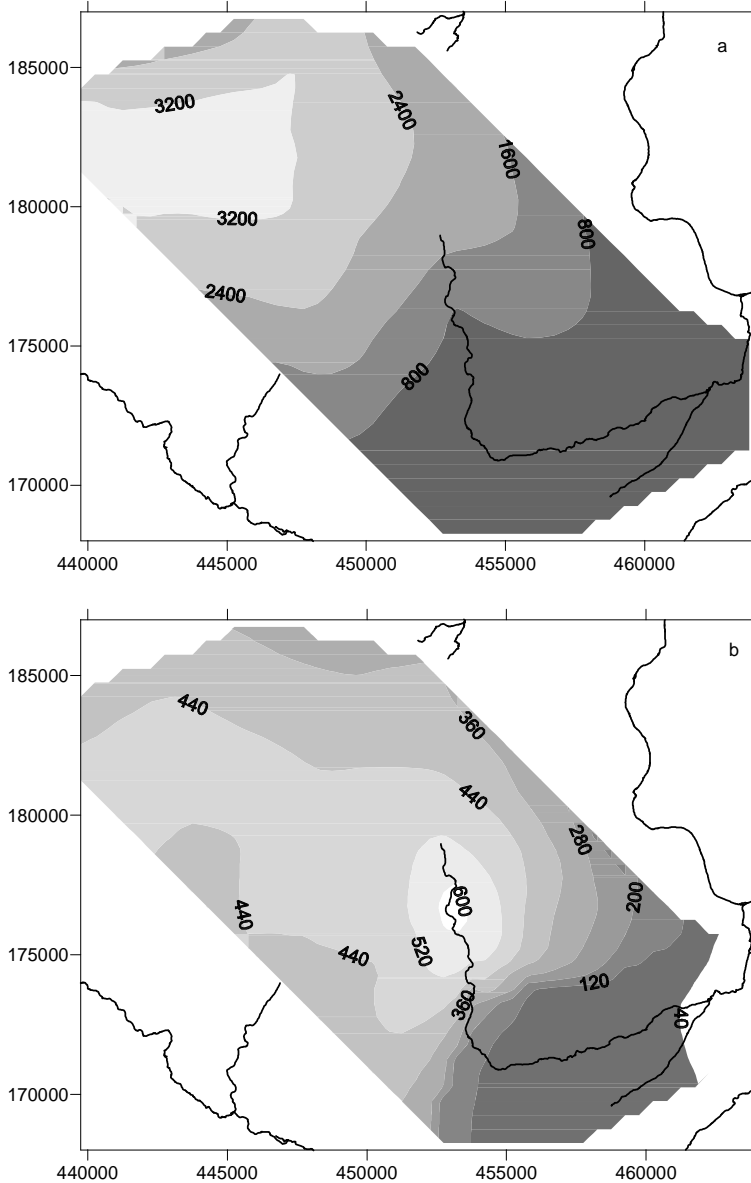


Figure 8.9: a) Drought deficit (md) and b) normalised drought deficit (d) for the drought in 1976 for the groundwater levels.

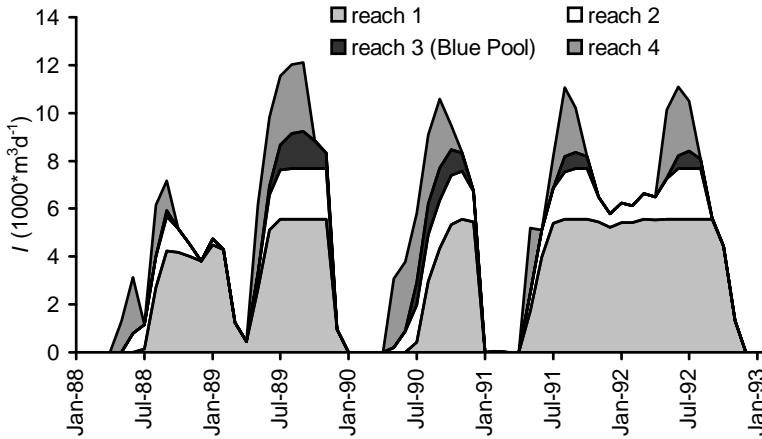


Figure 8.10: Drought intensity I (m^3d^{-1}) for 4 reaches along the Pang (Figure 8.1) for the period 1988 to 1992.

Equation (6.7). The location of the three points is at 500, 2300 and 4100 m from the Thames. The transect was taken at the Thames instead of the Pang to avoid any influence of drying up of the stream that might occur for the Pang. In Figure 8.11 it is clear that with increasing distance the frequency distribution becomes steeper. In fact, when compared with the results from Chapters 6 and 7, it is clear that the change is similar to the output from linear reservoirs with increasing reservoir coefficient. The main difference between the output from linear reservoirs and the hydraulic head with increasing distance from a stream is that for the discharge from the linear reservoir the variance decreases with increasing reservoir coefficient and for the head the variance increases with increasing distance to the stream.

In this study it was found that the interaction between the saturated groundwater flow and the stream was more important in determining the drought deficit than the drought in the recharge. However, Gehrels *et al.* (1994) found that recharge was the most important factor in determining the groundwater level fluctuations. The difference may be caused by the difference in catchment size (the area investigated by Gehrels *et al.* (1994) is much larger), because the relative importance of the stream probably decreases with increasing distance to the stream. Also the difference in characteristics of the unsaturated zone might cause the difference. The groundwater levels in the Chalk in the Pang catchment respond fast to the recharge (Appendix A), whereas Gehrels *et al.* (1994) noticed that the unsaturated zone of sandy soils caused a very strong delay.

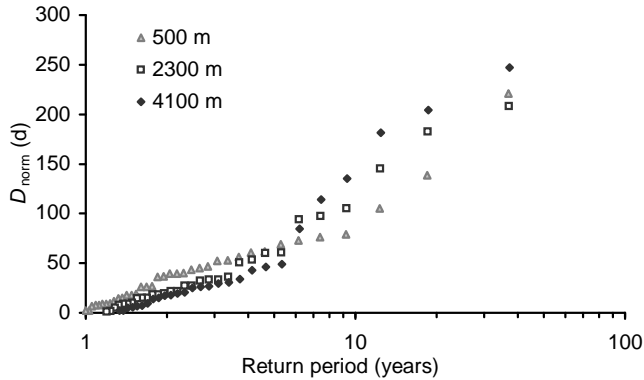


Figure 8.11: Frequency distribution of the normalised drought deficit D_{norm} in the hydraulic head for the period 1960-1997 in a transect perpendicular to the Thames. The hydraulic heads were taken at 500, 2300 and 4100 m distance from the Thames.

Influence of persistence on groundwater discharge The effect of increasing persistence in the groundwater levels with increasing distance to the stream is also reflected in the groundwater discharge. The droughts in the groundwater discharge in the upstream reach of the Pang showed a more delayed response than downstream (except for the discharge from the spring, the Blue Pool). This becomes more obvious when the frequency distribution of the normalised drought deficit of the groundwater discharge droughts along the Pang is investigated (Figure 8.12). The change in shape of the distribution of the droughts is as would be expected from a change in persistence. The autocorrelation of the groundwater discharge (deseasonalised in average and standard deviation) changes from 0.88 for reach 1 to 0.77 for the discharge at the outlet. The autocorrelation of the discharge of the most downstream reach (reach 4) is only 0.33. This is also reflected in the number of drought in the 38 years that were simulated: 35 for reach 1, 38 for the discharge at the outlet and 51 for the discharge from reach 4. In comparison, the number of droughts in the groundwater level in the upstream part is only around 20¹. The change in persistence in downstream direction corresponds to the general idea of a catchment getting less wide and with shallower groundwater levels near the outlet. The change in persistence also implies that the minimum flow decreases in downstream direction. This is probably only valid for relatively small catchments, because generally the specific minimum streamflow increases with increasing catchment size for natural catchments (Fuchs and Rubach, 1983; Gottschalk and Perzyna, 1989, 1993).

¹The difference in the number of droughts in the groundwater levels and discharge is possibly caused by non-linearity in the storage-discharge relationship. However, the analysis in Chapter 7 to determine the influence of the non-linearity in the storage-discharge relationship

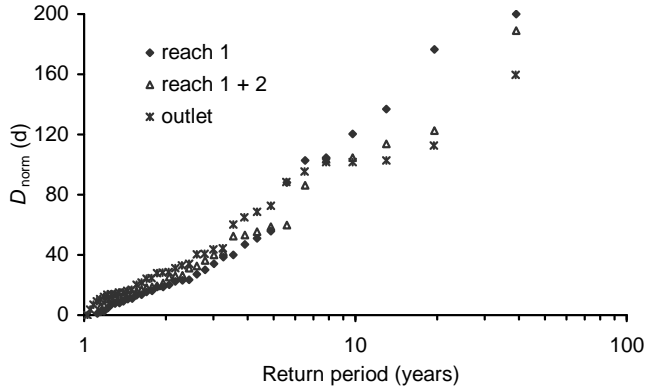


Figure 8.12: Frequency distribution of the normalised drought deficit D_{norm} of the droughts in the simulated groundwater discharge from the Pang in the period 1960-97.

The variation of the drought deficit within an aquifer also has some consequences for operational hydrology. For example, this makes it difficult and maybe even useless to characterise the drought status of an aquifer with one borehole, as one might do for a surface water reservoir. Even the total volume of groundwater stored has limited meaning, if it is not known how the storage is distributed. The spatial variations are also important for monitoring of groundwater levels for drought-early-warning systems. Some droughts start near streams and rivers in areas with shallow groundwater level, whereas other start earliest near the groundwater divide. Short, acute droughts in the dry period tend to start earliest in the shallow areas near rivers. Longer, less acute droughts, with the main decrease in precipitation and recharge during wet periods tend to start near to the groundwater divide. Hence, the location of the monitoring wells depends on the type of drought one is interested in.

Finally, it should be remembered that the analyses in this chapter are based on the results of a groundwater flow model and not on measurements, so the results and conclusions have to be viewed with some caution. The groundwater model is not only a simplified representation of reality, but also a distorted representation. The simplifications are not necessarily negative. They have the advantage of making the results easier to interpret. A model shows the fundamental behaviour of the system rather than all details. The distortions of the reality (errors in the model representation) are more important. The most important errors in this study are probably the boundary conditions, especially the constant head boundaries (Appendix D). These impose restrictions on the temporal fluctuation in the head which are not present in reality. This means that all results close to constant head boundaries should be interpreted with

showed little influence on the number of droughts

caution. However, because the model area was larger than the area of interest this problem is mitigated.

8.5 Conclusions

The analysis of the spatial distribution of groundwater drought characteristics in groundwater recharge, levels and discharge shows a clear spatial variation for all three variables. The main time series characteristic that determines the characteristics of the droughts and that is changed throughout a groundwater system is the persistence. The absolute amount of recharge or discharge is less important because in this thesis relative thresholds are used. The variance is important for the recharge and the discharge, but varies less than the persistence. For the groundwater levels, the variance is merely a scaling factor caused by the distance to the stream and is therefore corrected for. The impact of increasing persistence is to change a time series with many, but small droughts, to a time series with few droughts, but with a higher probability for severe, long droughts.

The variation in persistence is mainly controlled by the thickness of the unsaturated zone and the distance to streams. Close to streams, the unsaturated zone is usually shallow and thus the attenuation and persistence in the recharge are small. The fluctuations in the groundwater level are however constrained by the relatively constant level of the stream. Further away from streams, groundwater levels are deeper and consequently the recharge is usually more dampened and with a higher persistence. Also further away from the stream, the groundwater level can move more freely vertically. This results in larger (interannual) fluctuations and a higher persistence. So both as a result of the flow in the saturated zone and depth of flow through the unsaturated zone, the persistence is lower near streams than near the water divide. This also means that throughout an aquifer the severity of the same drought will vary. Short droughts will generally be more severe near the streams, as they are dampened further away. Whereas long periods of below average recharge will have more effect near the groundwater divide.

The droughts in the groundwater discharge show a change in behaviour in downstream direction. More upstream, the discharge droughts behave more like droughts in the groundwater levels further away from the stream, while more downstream the discharge is faster responding, implying more, but shorter and less severe droughts. Even in the most upstream part of the Pang, the groundwater discharge is less dampened than the groundwater levels, which is reflected in the number of droughts in the groundwater discharge (35 in reach 1) compared to that in the groundwater levels (around 20).

Groundwater levels near intermittent streams show special behaviour, which can lead to very high normalised drought deficits. When the groundwater level is above the streambed, the stream obviously is flowing and the level is constrained by the surface water level. However, when the groundwater level falls below the bottom level and river infiltration is small or absent, the level can drop freely and the normalised drought deficit can be unexpectedly large.

Chapter 9

Summary and conclusions

9.1 Conclusions

Droughts are dynamic phenomena which can affect all parts of the hydrological cycle and which are variable both in space and time. Depending on which part of the hydrological system is affected, meteorological droughts, soil moisture droughts and hydrological droughts can be identified (Figure 1.1). Hydrological droughts can be subdivided in streamflow droughts and groundwater droughts. Droughts propagate through the hydrological system from precipitation, via soil moisture to groundwater and surface water. The primary objective of this thesis is to improve *the understanding of the transformation of drought in groundwater systems*. The secondary objective is to develop the concept and definition of groundwater drought. The study has been conducted using data from two catchments, namely the sub-humid Pang catchment in southern England and the semi-arid Upper-Guadiana catchment in central Spain.

Like other types of droughts, groundwater droughts are mainly caused by a decrease in the amount and/or effectiveness of the precipitation, often in combination with high evapotranspiration. The primary effects of a groundwater drought are lower groundwater levels and a decreased discharge to the surface water system. Secondary effects include dried-up streams, reduced crop yields and damage to terrestrial and aquatic ecosystems.

In this thesis, groundwater droughts are defined as *a decrease in water availability (with or without negative impacts) caused by the variability of the weather*. Drought *events* are derived from time series using the threshold level approach (Figure 3.3). The duration of a drought is the time period between a down crossing of the threshold and a subsequent up crossing. The drought deficit is the accumulated departure below the threshold between crossings. The drought intensity is the difference between the threshold and the actual value. In order to be able to use a *consistent* event definition throughout the analyses, a new way of defining the threshold level has been introduced in Chapter 4, which relates the accumulated deficit of all droughts in a time series to the deficit below the average (Figure 4.1).

It is well known that the groundwater reservoir acts as a low-pass filter, remov-

ing high frequency variability, increasing the delay and persistence and decreasing the variance because of the attenuation. Thus, as a result of the propagation through the groundwater system, the number of droughts should decrease (less high frequency variations), the duration of droughts should increase (persistence) and the deficit should decrease (attenuation). However, it is unclear how these changes, when combined, affect the propagation of droughts. From data from the Pang catchment, it is clear that droughts with different characteristics propagate differently through the groundwater system (Figure 3.2). Some droughts are mitigated as a result of the propagation through groundwater, others become more severe.

The main result of this thesis is a *systematic and extensive investigation of the transformation of droughts as a result of the propagation through a wide range of groundwater systems*. This result is described in Chapters 4, 6 and 8 and will be summarised first. In Chapters 5 and 7, some extensions are presented, like for example the influence of different types of recharge and a validation of some of the results in Chapters 4 and 6.

Propagation of single droughts through linear reservoirs In Chapter 4, the propagation of a *single* drought from groundwater recharge to discharge has been investigated. The recharge is synthetic and based on a sine function and a drought is simulated as a decrease in recharge during one year. The groundwater system was modelled as a linear reservoir that is characterised by a reservoir coefficient j . This reservoir coefficient can be derived from the physical properties of the area for specific cases and is closely related to the response time of the catchment. An *analytical solution* has been derived that describes the deficit and duration of the discharge drought as a function of the decrease in recharge, the reservoir coefficient j and the drought criterion which represents the height of the threshold level. The analytical solution has been used to analyse the propagation of drought through *a wide range of groundwater systems* defined by different j -values ($10 < j < 10000$) for *a range of different drought severities*.

The results show that the attenuation and delay caused by the groundwater system have opposing effects on the droughts. The attenuation causes the variance and thus the drought deficit to decrease. The delay causes an increase in the drought deficit in two ways. First, by delaying the decrease in recharge from the peak to the subsequent low flow period and second by increasing the persistence and thus the duration of the droughts. In most cases, this resulted in a larger deficit and duration of the discharge drought (i.e. drought in groundwater discharge) than of the recharge drought (Figures 4.9, 4.10 and 4.11). Only for small droughts the deficit of the discharge drought was smaller. The increase in deficit was generally larger for more severe droughts and for lower threshold levels. In most cases, the largest increase in deficit occurred

for groundwater systems with $j \approx 200$ d.

Propagation of the distribution of droughts through linear reservoirs

In Chapter 6, the changes in the *frequency distribution* of drought deficit and duration due to the propagation from groundwater recharge to discharge have been investigated for a range of groundwater systems. The frequency distributions of the drought deficit and duration have not been derived by using a theoretical probability distribution function, but from large numbers of drought events derived from long time series of simulations of recharge and discharge. The long time series of recharge (10 x 1000 years) have been simulated for *observed* meteorological data from the Pang catchment (UK), using Nearest Neighbour resampling. The recharge has been used as input to a range of linear reservoirs with reservoir coefficients $10 \leq j \leq 5120$ d to simulate time series of discharge.

As a result of the propagation through the groundwater system, the cumulative frequency distribution of the drought deficit changes its shape (Figures 6.6 and 6.7). For *small* return periods (< 50 years), the cumulative frequency distribution of the *recharge droughts* is convex, while for droughts in the *discharge* from reservoirs with j larger than approximately 300 d, the distribution is concave. For the *higher* return periods, the cumulative frequency distribution is steeper for the discharge than for the recharge, and it becomes steeper with increasing j . The change in shape is the combined effect of attenuation and delay. The variance and thus the drought deficit decreases, which translates the cumulative frequency distribution of the drought deficit *downwards*. Because of the increase in persistence, which increases the duration and pooling of the droughts, the cumulative frequency distribution becomes *steeper*, which means a decrease in the number of small droughts and an increase in the probability of severe droughts. The delay of the decrease in recharge from the peak to the subsequent low flow period (Chapter 4), appears to be less important. Possibly, because sometimes also the decrease in recharge is delayed from a drier to a wetter period.

The change in shape also means that the frequency distributions of the drought deficit for droughts in groundwater recharge and discharge cross and they cross for ever higher return periods for discharge from reservoirs with higher j -values. For the drought duration, which is much less affected by the attenuation, the distributions cross for much lower return periods. For example, for a drought with a return period of 50 years, the highest drought deficit occurs for a reservoir with j around 200 to 300 d. For a return period of 100 years, the highest deficit occurs for j around 500 to 600 d. The maximum drought *duration* for droughts with return periods of more than 20 years occurs for the slowest responding reservoirs in the analysis ($j = 5120$ d).

To characterise the behaviour of a groundwater system with respect to drought

by one number instead of the whole frequency distribution, a *new performance criterion* (Equation (6.12)) is introduced, which estimates the overall performance of a catchment with respect to drought. This criterion takes into account the whole frequency distribution of the drought deficit and uses a weight function to weigh different parts of the distribution differently. The most useful weight function in this case is a weight function, which weighs all droughts with a return period higher than 10 years equally (Equation (6.16)). The overall performance was lowest for intermediately fast responding groundwater systems (minimum for $j = 160$ d) and highest for very slowly responding groundwater systems (Figure 6.12).

Spatial distribution of droughts In Chapter 8 the propagation of single droughts in a spatially distributed groundwater system has been examined and especially the *spatial distribution in groundwater levels*. To that purpose the groundwater flow in the Pang catchment was simulated using a spatially distributed groundwater flow model. The spatially distributed drought deficit in the recharge is difficult to relate to the spatially distributed drought deficit in the groundwater levels, because the processes in the saturated groundwater system dominate the drought deficit in the groundwater level. In groundwater levels, both the persistence and the variance increase with increasing distance to the stream, which means that the deficit of droughts of all severities increases rapidly with increasing distance to the stream. After normalising the drought deficit in the groundwater levels using the standard deviation, the persistence is the main time series characteristic determining the spatial pattern in drought severity. The cumulative frequency distribution of the normalised drought deficit becomes steeper with increasing distance to the stream. *Thus throughout an aquifer, even for systems as simple as flow between parallel streams, the severity of a drought will vary.* Short droughts will generally be more severe near the streams, as they are dampened further away, whereas long periods of below average recharge will have more effect near the groundwater divide. Similar differences can be observed in the groundwater discharge: upstream, the cumulative frequency distribution of the drought deficit is steeper than downstream. Near intermittent streams, the normalised drought deficit in the groundwater level can be very large, because under normal circumstances the groundwater level is close to the stream, but once the stream has dried up, the groundwater level can drop considerably.

Different climatic regimes To examine the influence of the recharge characteristics on drought propagation, recharge from two different catchments was used as input to a range of linear reservoirs: the sub-humid Pang catchment (UK), from which the results have been discussed so far and the Upper-Guadiana catchment (ES) which has a semi-arid climate (Chapters 5 and 7). The droughts have been compared using the relative drought deficit, which is

the drought deficit divided by the average recharge or discharge. The relative droughts in the recharge differ little between the two catchments, except for a high number of very small droughts in the Upper-Guadiana, which does not occur for the Pang. In the discharge droughts, the relative drought deficit is mostly larger for the Upper-Guadiana (Figure 7.2). The overall performance for the droughts in the recharge is about the same for the two catchments, but for the droughts in the discharge it is much lower for the Upper-Guadiana than for the Pang (Figure 7.5). The lowest value of the performance occurs for the same j (160 d) for both catchments. The main characteristic causing these differences between the two catchments is the seasonality. The difference between the seasons compared to the variance is much larger for the Pang than for the Upper-Guadiana. This means that the increase in persistence as a result of the propagation through groundwater has a much larger effect for the Upper-Guadiana. For the recharge from the Upper-Guadiana, the large number of small droughts decreases fast through pooling, creating relatively severe discharge droughts, which are even more severe because the coefficient of variation is larger for the Upper-Guadiana than for the Pang. For the Pang pooling of droughts is prevented by the consistently wet winter. Also, because of the strong seasonality, the deficit of droughts with low return periods (< 10 years) is relatively large. For *individual* discharge droughts in the Pang catchment the delay of the decrease in recharge from a peak flow period (winter) to a subsequent low flow period can be important.

The influence of non-linearity Because many groundwater systems can be described better by a non-linear model than a linear one, the influence of non-linearity has been examined. Because of non-linearity in the relation between groundwater levels and discharge, droughts become longer and get a lower intensity. Whether the drought deficit increases or not depends on the relative importance of the two effects. In most cases, the increase in duration is more important than the decrease in drought intensity and thus the drought deficit increases (Figure 7.8). However, the drought deficit decreases for droughts with small return periods (< 20 years) in discharge from fast responding reservoirs ($j < 100$ d) for the Pang catchment.

(Im-)possibilities of a validation In Chapter 5, a limited validation was carried out for the results of Chapter 4. The recharge from the Pang and Upper-Guadiana catchments was used as input to a range of linear reservoirs. The results showed that the synthetic recharge was an adequate approximation of real-world recharge. In Chapter 7 an attempt has been made to validate the results of Chapters 4, 5 and 6 more thoroughly using observed data from the Pang catchment. Several problems complicated the validation. First, neither groundwater recharge nor discharge was observed, which means that they needed to be simulated or derived from other observations. Second, when they

were derived, they were available for one value of j only. Third, the number of events was too small in a record of 37 years.

Groundwater recharge was simulated and groundwater discharge was approximated by base flow, which was derived from observed streamflow for the Pang catchment (Appendix C). The base flow (in this thesis defined as that part of the observed streamflow that is derived from saturated groundwater) was derived using a *new method based on observed groundwater levels*. The results of the validation appear to support the results. Only the crossing of the probability distributions of the groundwater recharge and discharge occurs for smaller return periods for the observed data than for the simulated values (Figure 7.15). This may be the effect of inaccuracies in the simulated recharge or derived base flow or it may be that the variance is relatively larger in the estimated base flow than in the simulated output from the linear reservoirs.

Drought event definition The definition of drought events has a large influence on the results. First, it is important to realise that a *relative threshold* was used throughout this thesis. A relative threshold means that for the discharge time series from each groundwater system a new threshold is derived. So for increasing j , also the threshold increases. In most drought analyses a relative threshold is used, because drought is a deviation from normal conditions. If the same threshold had been used for the discharge from all reservoirs, the fastest responding systems would have had the droughts with the highest deficits. Probably the output for the groundwater reservoirs with very high j would have had no droughts at all.

In Chapter 3 it was stated that the skewness changes as a result of the propagation through the groundwater system. However, because of the derivation of threshold level, this has not been discussed in the remainder of the thesis. The threshold level was derived in such a way that it becomes higher with increasing skewness and this reduces the influence of skewness. If the height of the threshold level had been derived based on exceedance percentiles as is done in many drought studies, the drought deficit from fast responding groundwater systems would be much smaller. In fact the threshold would be zero for recharge unless a very low exceedance percentile (e.g. 40-percentile) had been chosen.

Not only the choice of the threshold level, also the choice for a particular event definition influences the results. Therefore, in Chapter 4 the effect of the propagation through the groundwater system on the *minimum flow* in the groundwater discharge was examined. This showed that although the minimum flow increases with increasing reservoir coefficient, the difference in minimum flow between a non-drought year and a drought year was largest for intermediately fast responding groundwater reservoirs ($j = 225$ d) (Figure 4.13). This corresponds well with the observations that the largest droughts deficit occurred for

reservoirs with j around 200 d.

Concept of groundwater drought The concept of groundwater drought as used in this thesis included groundwater recharge, levels and discharge as possible variables to identify groundwater droughts. However, in the course of this thesis it has become clear that this statement should be interpreted with caution. When recharge is used to define groundwater drought, the influence of the (saturated part of the) groundwater system is not taken into account. Therefore, it is difficult to relate the drought deficit in the recharge to the deficit in the groundwater levels (Chapter 8). For groundwater levels it was shown that they provide local information, rather than information about the state of the aquifer. Disadvantages of using groundwater discharge to define groundwater drought, is that it can give information predominantly about the area close to the stream and that the groundwater level-discharge relationship may be strongly non-linear. Thus all variables can be used to define drought, but it should be realised that they provide limited information on the state of the groundwater system as a whole. In other words, trying to capture a dynamic event such as a groundwater drought in one static definition will always result in a loss of information.

9.2 Recommendations for future research, perspectives

The thesis provides a clear overview of the effect of groundwater systems on drought, however, it is not complete. A useful extension would be to examine how e.g. abstractions influence and interact with groundwater droughts. Also, the influence of the details of the stream-aquifer interaction (e.g. bank storage) on drought have not been studied, but might have considerable impact on the drought behaviour of groundwater discharge. The impact of the unsaturated zone (including the vegetation) on drought could be studied, using a water balance approach similar to the one used in this study. An extension which can probably be applied quite easily, is to use the empirical probability distributions (as estimated in Chapters 6 and 7), to estimate the parameters of theoretical models, like the Generalised Extreme Value model or Generalised Pareto Distribution. The changes in these parameters as a result of the propagation through the catchment might prove to be interesting. These parameters could also be compared to the parameters of physically-based probability distributions (Gottschalk and Perzyna, 1989; Gottschalk *et al.*, 1997).

Groundwater-discharge relation The relation between groundwater levels and discharge was discussed on several occasions in this thesis (e.g. Chapter 7

and 8 and Appendix C). Many factors influence this relation, like drainage density, depth of penetration of the stream, relief, properties of the aquifer, type of flow (fracture or porous medium). Qualitatively, the many forms in which the relation between groundwater and discharge can occur, have been described well (for example by Domenico and Schwartz (1998)). Quantitatively the description is often limited to a stationary situation, except for the most simple 1-dimensional case. Few studies have investigated how the different groundwater-discharge interactions influence the temporal variability of the groundwater discharge. Some exceptions are, for example, Rorabaugh (1964), who investigated the influence of bank storage on the recession curve and Singh (1968), who did the same for evapotranspiration, a flux to a deeper layer and recharge. More recently, Halford and Mayer (2000) analysed the difference between recessions in groundwater levels and discharge in a range of different catchments. Marani *et al.* (2001) showed the influence of a decreasing drainage density on the persistence in the groundwater discharge. However, an overview is lacking. To improve our knowledge about the groundwater level-discharge relation, a possible approach would be to describe the characteristics of the groundwater-discharge relationship that influence the temporal variability of the groundwater discharge and to investigate how they influence the relationship for each characteristic separately. In a second step, the interaction might be studied.

Estimation of return periods for mixed streamflow Several authors have observed that the frequency distribution of droughts in streamflow show droughts from different populations (Gottschalk and Perzyna, 1989; Woo and Tarhule, 1994; Hisdal *et al.*, 2002; Kjeldsen *et al.*, 2000). However, to fit a theoretical probability distribution to the observed frequency distribution, a homogeneous population of droughts is necessary. To make the population of droughts homogeneous, Gottschalk and Perzyna (1989) and Hisdal *et al.* (2002) used only the droughts above a certain predefined threshold. Woo and Tarhule (1994) have divided the estimated droughts in different groups and estimated the return periods for these groups separately. Kjeldsen *et al.* (2000) have estimated the return periods using a two-component distribution. However, the separation between droughts was based only on drought deficit and not on physical characteristics of the flow from which the droughts were derived, nor was the reason for the separation in these different groups of droughts clearly examined. The reason could be that the discharge is derived from different sources, however in this thesis an alternative cause has been identified, namely a strong seasonality in the data. Strong seasonality in the recharge from the Pang catchment, made it look as if the frequency distribution had a break, especially at the transition from within-year to multi-year droughts (Chapter 6). On the other hand, the frequency distribution of the droughts of the total streamflow from the Pang, which is clearly derived from two different sources (Appendix C

and Chapter 2), does not show a break (Figure 9.1). The distribution is less steep than the distribution of the droughts in the base flow (Appendix C and Figure 7.15), but shows no evidence of the presence of streamflow from the two totally different sources (groundwater discharge from the Chalk aquifer and direct runoff from low-permeability, Tertiary deposits).

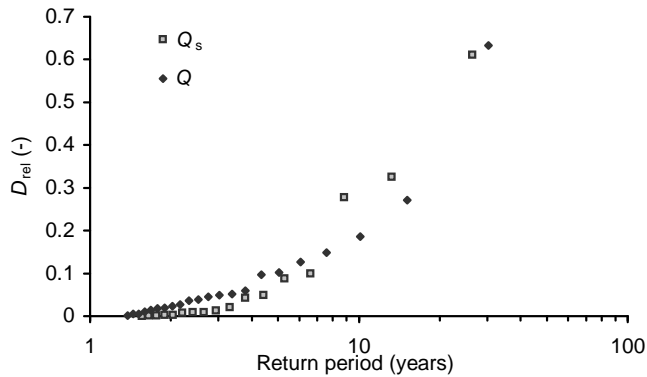


Figure 9.1: Cumulative frequency distribution for the relative drought deficit D_{rel} expressed as a fraction of the annual average discharge of the observed streamflow Q at Pangbourne gauging station (Figure 2.1) and base flow Q_s (drought criterion $c = 0.3$).

Future research might be directed at investigating the causes for these apparent or real breaks in the frequency distribution of drought. Also, the interrelation between the return periods for different groups might be addressed. Some approaches do exist which allow distribution functions to be combined and the return period to be estimated for inhomogeneous data, for example by Yamaguchi and Hatada (2001). It would be useful to attempt the application of their method to droughts.

Samenvatting

Droogtes zijn, anders dan de meeste natuurrampen, zich langzaam ontwikkelende gebeurtenissen, waarvan begin en einde moeilijk te definiëren zijn. Droogtes zijn ook zeer dynamische gebeurtenissen, die zich op verschillende tijdstippen, in verschillende delen van het hydrologische systeem zoals bodemvocht, oppervlaktewater en grondwater kunnen ontwikkelen (Figuur 1.1). Bij een droogte in het grondwater spreken we van een grondwaterdroogte. Een droogte is in tegenstelling tot verdroging een tijdelijk fenomeen. Droogtes planten zich voort door het hydrologische systeem van neerslag, naar bodemvocht en vervolgens naar grondwater en oppervlakte water. De voornaamste doelstelling van dit proefschrift is het verbeteren van het begrip van de verandering van de eigenschappen van een droogte als gevolg van de voortplanting door het grondwatersysteem. De tweede doelstelling is om het concept van grondwaterdroogte verder te ontwikkelen.

Net als andere typen droogtes, worden grondwaterdroogtes veroorzaakt door een afname in de hoeveelheid en/of effectiviteit van de neerslag, vaak in combinatie met een hoge evapotranspiratie. De voornaamste effecten van een grondwaterdroogte zijn het verlagen van de grondwaterstand en de grondwaterafvoer naar het oppervlaktewatersysteem. Secundaire effecten omvatten onder andere het opdrogen van beken en rivieren, een afname van de gewasopbrengst en schade aan terrestrische en aquatische ecosystemen.

In dit proefschrift zijn grondwaterdroogtes gedefinieerd als *een afname van de hoeveelheid beschikbaar water (met of zonder negatieve gevolgen), die veroorzaakt wordt door de temporele variabiliteit van het weer*. Een *droogteperiode* wordt geselecteerd uit een tijdserie door middel van de drempel methode (Figuur 3.3). De duur van een droogte is de periode tussen een overschrijding van de drempel naar beneden toe en de daaropvolgende opwaartse overschrijding. Het deficit van een droogte is gedefinieerd als het geïntegreerde volume beneden de drempel tussen de twee overschrijdingen. Om te waarborgen dat de drempel waarmee de droogtes bepaald worden op een consistente wijze kan worden afgeleid voor alle analyses, wordt in Hoofdstuk 4 een nieuwe methode geïntroduceerd om de drempel af te leiden. Deze methode relateert het gezamenlijke deficit van alle droogtes aan het geaccumuleerde volume beneden het gemiddelde (Figuur 4.1).

Het is een bekend feit dat het grondwatersysteem de invloed van een low-pass filter heeft, waarbij de variaties met hoge frequentie worden uitgedempt, de vertraging en de persistentie nemen toe en door de demping neemt de variantie

af. Hieruit kan worden afgeleid dat als gevolg van de voortplanting door het grondwatersysteem, het aantal droogtes zou moeten afnemen (door de afname van de variaties in de hoge frequenties), de duur van de droogtes zou moeten toenemen (door de toename in persistentie) en het droogtedeficit zou moeten afnemen (door de demping). Het is echter onduidelijk hoe de combinatie van deze veranderingen de voortplanting van droogtes beïnvloedt.

Het voornaamste resultaat van dit proefschrift is een *systematisch en uitgebreid overzicht van de verandering van droogtes als gevolg van de voortplanting door een reeks van grondwatersystemen*. Dit is beschreven in Hoofdstukken 4, 6 en 8 en zal eerst besproken worden. In de Hoofdstukken 5 en 7 komen enkele uitbreidingen aan bod, zoals de invloed van de eigenschappen van de grondwateraanvulling en een validatie, die daarna besproken worden.

Voortplanting van een individuele droogte door lineaire reservoirs

In Hoofdstuk 4 wordt de voortplanting van een *individuele* droogte van grondwateraanvulling tot grondwaterafvoer gesimuleerd. De grondwateraanvulling is synthetisch en gebaseerd op een sinus functie. Een droogte is gesimuleerd als een afname in de grondwateraanvulling gedurende 1 jaar. Het grondwatersysteem is gesimuleerd door middel van een lineair reservoir, dat gekarakteriseerd wordt door de reservoir coëfficiënt j . De reservoir coëfficiënt kan onder bepaalde omstandigheden berekend worden uit de fysische karakteristieken van het gebied en is nauw gerelateerd aan de reactietijd van het stroomgebied. Via een *analytische oplossing* wordt het deficit van de droogtes in de grondwaterafvoer uitgedrukt als een functie van de afname in de grondwateraanvulling, j en het droogtecriterium dat de hoogte van de drempel bepaalt. De analytische oplossing wordt gebruikt om de voortplanting van een *reeks van droogtes met verschillende zwaarte door een reeks van grondwaterreservoirs* te analyseren.

De resultaten laten zien dat de demping en vertraging die door het reservoir veroorzaakt worden een tegengesteld effect op de droogte hebben. De demping veroorzaakt een afname in de variantie en dus een afname in het droogtedeficit. De vertraging verhoogt het droogte deficit op twee manieren. Ten eerste wordt de afname in de grondwateraanvulling vertraagd van de piek in de afvoer naar de periode met lage afvoer. Ten tweede neemt de persistentie en daarmee de duur van de droogtes toe. In de meeste gevallen resulteerde dit in een groter deficit van de droogte in de grondwaterafvoer dan van de droogte in de grondwateraanvulling (Figuren 4.9, 4.10 en 4.11). Alleen voor kleine droogtes was het droogtedeficit groter in de grondwateraanvulling dan in de grondwaterafvoer. De toename in deficit was in het algemeen groter voor ernstigere droogtes en voor droogtes bepaald met een lagere drempel. In veel gevallen treedt het grootste deficit op voor reservoirs met een middelmatig snelle reactietijd ($j = 200$ d).

Voortplanting van de verdeling van droogtes door lineaire reservoirs In Hoofdstuk 6 wordt de voortplanting van de *frequentieverdeling* van droogtes van grondwateraanvulling naar grondwaterafvoer onderzocht. De frequentieverdeling van het droogte deficit en de duur van de droogtes is niet afgeleid van een theoretische verdeling maar van grote aantallen gesimuleerde droogtes, afgeleid uit gesimuleerde tijdreeksen van grondwateraanvulling en grondwaterafvoer. Deze lange tijdreeksen (10 x 1000 jaar) zijn gesimuleerd voor het stroomgebied van de Pang (UK), gebruikmakend van de techniek van Nearest Neighbour resampling. De grondwateraanvulling is gebruikt als invoer voor een reeks van lineaire reservoirs met j variërend van 10 tot 5120 d om de tijdreeksen van grondwaterafvoer te simuleren.

Door de voortplanting door het grondwatersysteem verandert de cumulatieve frequentieverdeling van vorm (Figuren 6.6 en 6.7). Voor *kleine* herhalingsstijden (< 50 jaar) is de cumulatieve verdeling van de droogtedeficiten in de *grondwateraanvulling* convex, terwijl de verdeling van de droogtedeficiten in de *grondwaterafvoer* van reservoirs met $j > 300$ d concaaf is. Voor *hogere* herhalingsstijden is de cumulatieve verdeling van de droogtes in de grondwaterafvoer steiler dan van de droogtes in de grondwateraanvulling. Deze verandering van vorm is het gevolg van de combinatie van demping en vertraging. Door de afname in de variantie, neemt het droogtedeficit af en daarmee wordt de cumulatieve frequentieverdeling van het droogtedeficit *naar beneden* verplaatst. Door de toename in persistentie worden meer droogtes samengevoegd, waardoor het aantal kleine droogtes afneemt, terwijl de kans op ernstige droogtes toeneemt. Hierdoor wordt de cumulatieve frequentiedistributie steiler. De vertraging van de afname in de grondwateraanvulling van de piek in de afvoer naar de periode met lage afvoer lijkt minder belangrijk te zijn. Mogelijk, omdat soms ook de afname in de grondwateraanvulling vertraagd wordt van een drogere periode naar een nattere periode.

Door de verandering van vorm kruisen de cumulatieve frequentieverdelingen voor de droogtes in de grondwateraanvulling en de grondwaterafvoer, bovendien kruisen ze voor hogere herhalingsstijden voor afvoer van reservoirs met grotere j . Voor de duur van de droogtes kruisen de cumulatieve frequentieverdelingen voor lagere waarden van j , omdat die minder verlaagd worden door de demping. Voor een droogte met een herhalingsstijd van 50 jaar, treedt het grootste droogtedeficit op voor de afvoer uit een reservoir met j ongeveer 200 tot 300 d. Voor een droogte met een herhalingsstijd van 100 jaar, treedt het grootste deficit op bij j ongeveer 500 tot 600 d. De *langste* droogte treedt vrijwel altijd (herhalingsstijd van meer dan 20 jaar) op voor het meest traag reagerende reservoir dat gesimuleerd is ($j = 5120$ d).

Om het gedrag van een stroomgebied met betrekking tot droogte met één getal te karakteriseren in plaats van met de hele frequentieverdeling, is een nieuw prestatie criterium geïntroduceerd, dat de totale prestatie van een stroomge-

bied met betrekking tot droogte samenvat. Dit criterium houdt rekening met de hele frequentiedistributie en maakt gebruik van een gewichtfunctie om verschillende delen van de frequentieverdeling verschillende gewicht te geven. De beste gewichtsfunctie in dit geval, bleek een gewichtsfunctie waarbij alle droogtes met een herhalingstijd groter dan 10 jaar een gelijk gewicht kregen. De totale prestatie was het laagste voor middelmatig snel reagerende systemen (minimum voor $j = 160$ d) en het hoogste voor zeer traag reagerende systemen (Figuur 6.12).

Ruimtelijke verdeling van droogtes In Hoofdstuk 8 wordt de voortplanting van een droogte door een ruimtelijk verdeeld grondwater systeem bestudeerd, waarbij met name gelet is op de ruimtelijke verdeling van droogtes in grondwaterstanden. Hiervoor is de grondwaterstroming in het stroomgebied van de Pang gemodelleerd met ruimtelijk verdeeld grondwatermodel. De ruimtelijke verdeling van het droogtedeficit in de grondwateraanvulling is moeilijk te relateren aan het deficit in de grondwaterstanden, omdat in het stroomgebied van de Pang de processen in het verzadigde grondwatersysteem de grootte van de droogtedeficiten grotendeels bepalen. In de grondwaterstand neemt zowel de variantie als de persistentie sterk toe met toenemende afstand tot rivier of beek. Daardoor neemt het droogtedeficit sterk toe met toenemende afstand tot de rivier. Nadat het droogtedeficit genormaliseerd is met de standaard deviatie van de grondwaterstanden, is de persistentie de factor die de ruimtelijke verdeling van het droogtedeficit bepaalt. Hierdoor wordt de cumulatieve frequentieverdeling van het genormaliseerde droogtedeficit steiler met toenemende afstand tot de rivier. *Dit betekent dat in een aquifer, zelfs voor een simpel systeem als stroming tussen twee evenwijdige waterlopen, de hevigheid van een droogte varieert.* Minder ernstige, korte droogtes zullen over het algemeen heviger zijn vlak bij een rivier, aangezien ze verder van de stroom af afgezwakt worden. Langdurige droogtes zullen juist heviger zijn ver van de stroom af. Vergelijkbare verschillen zijn terug te vinden in de grondwaterafvoer: bovenstrooms is de cumulatieve frequentieverdeling steiler dan meer benedenstrooms. In de buurt van droogvallende beken kan het genormaliseerde droogtedeficit zeer groot worden, doordat onder normale omstandigheden de grondwaterstand dicht bij de beek is (en daarmee is de variantie klein), terwijl de grondwaterstand ver weg kan zakken als de beek eenmaal is drooggevallen.

Verskillende klimaten Om de invloed van de karakteristieken van de grondwateraanvulling op de voorplanting van droogtes te bekijken, is de grondwateraanvulling van twee stroomgebieden met een verschillend klimaat gebruikt: het stroomgebied van de Pang (UK), waarvan de resultaten tot nu toe besproken zijn en het stroomgebied van de Upper-Guadiana (ES) met een semi-aride klimaat (Hoofdstuk 5 en 7). De droogtes zullen vergeleken worden met behulp van het *relatieve* droogtedeficit, wat het droogtedeficit gedeeld door de

gemiddelde grondwateraanvulling of -afvoer is. De droogtes in de grondwateraanvulling verschillen vrij weinig van elkaar, met uitzondering van een grote hoeveelheid zeer korte droogtes met een laag deficit voor de Upper-Guadiana. Het relatieve droogtedeficit voor de droogtes in de grondwaterafvoer is over het algemeen veel groter voor de Upper-Guadiana dan voor de Pang (Figuur 7.2). Hierdoor is de totale prestatie van de Upper-Guadiana met betrekking tot droogtes in de grondwaterafvoer veel kleiner. De laagste waarde van het prestatie criterium treedt overigens voor beide stroomgebieden voor dezelfde waarde van j op. De voornaamste tijdreeks karakteristiek die dit verschil tussen de Pang en de Upper-Guadiana veroorzaakt is de seizoensmatigheid. Voor de Pang is het verschil tussen de seizoenen vergeleken met de variantie veel groter dan voor de Upper-Guadiana. Dit betekent dat de toename in de persistentie een veel groter effect heeft in de Upper-Guadiana. Voor de Pang wordt het samengaan van droogtes tegengegaan door de consistent natte winter, terwijl voor de Upper-Guadiana de grote aantallen kleine droogtes gemakkelijk samen kunnen smelten tot lange, hevige droogtes. Bovendien is de variantie voor de grondwateraanvulling van de Upper-Guadiana relatief groter, waardoor de droogtes een relatief groter deficit krijgen. Een bijkomend effect van de sterke seizoensmatigheid voor de grondwateraanvulling van de Pang is dat er vrijwel elk jaar 1 droogte optreedt, waarbij het droogte deficit voor relatief natte jaren, relatief groot is. Voor *individuele* droogtes in het stroomgebied van de Pang kan de vertraging van de afname in de grondwateraanvulling van piek naar de daaropvolgende periode met lage afvoer ook van belang zijn.

Invloed van niet-lineariteit Aangezien veel grondwatersystemen beter met een niet-lineair dan een lineair model beschreven kunnen worden en tot nu toe alleen de lineaire modellen gebruikt zijn, is de invloed van niet-lineariteit op de voortplanting onderzocht. Niet-lineariteit in de relatie tussen grondwaterberging en -afvoer, veroorzaakt langere droogtes, maar deze droogtes hebben tevens een lagere intensiteit. Het hangt dus van het relatieve belang van deze twee veranderingen af, of het droogte deficit toeneemt of afneemt. In de meeste gevallen is de toename in de duur van de droogte belangrijker en neemt het droogte deficit toe (Figuur 7.8). Echter, voor droogtes met een kleine herhalingsjijd (< 20 jaar), voor grondwaterafvoer van reservoirs met een relatief snelle reactie ($j > 100$ d) voor het stroomgebied van de Pang, is de afname in intensiteit belangrijker en neemt het droogte deficit af door de invloed van de niet-lineariteit.

(On-)mogelijkheid van een validatie In Hoofdstuk 5 is een beperkte validatie uitgevoerd van de resultaten in Hoofdstuk 4. De grondwateraanvulling gebaseerd op de gemeten waarden van de stroomgebieden van de Pang en Upper-Guadiana zijn gebruikt als invoer voor een reeks van lineaire reservoirs. De resultaten laten zien dat de synthetische grondwateraanvulling die gebruikt

was in Hoofdstuk 4, een goede benadering was voor de meer realistische grondwateraanvulling. In Hoofdstuk 7 is een poging gedaan om de resultaten van Hoofdstuk 4, 5 en 6 grondiger te valideren gebruikmakend van metingen in het stroomgebied van de Pang. Verscheidene problemen compliceren de validatie. Ten eerste, zijn noch grondwateraanvulling, noch grondwaterafvoer gemeten, hetgeen betekent dat beide gesimuleerd moeten worden of uit metingen moeten worden afgeleid. Ten tweede, zijn de grondwateraanvulling en -afvoer beschikbaar voor maar één waarde van j . Ten derde, is het aantal droogteperiodes in de periode van 37 jaar te klein.

De grondwateraanvulling is gesimuleerd, terwijl de grondwaterafvoer is benaderd door de basisafvoer, die afgeleid is uit metingen van de afvoer. De basisafvoer (dat deel van de afvoer dat is afgeleid van het verzadigde grondwater) is afgeleid van de gemeten afvoer, *gebruikmakend van gemeten grondwaterstanden via een nieuwe methode*. De validatie lijkt de voorgaande resultaten te bevestigen. Echter de cumulatieve frequentieverdelingen snijden elkaar voor een lagere waarden van de herhalingstijd (Figuur 7.15). Dit kan het resultaat zijn van onnauwkeurigheden in de berekende grondwateraanvulling en -afvoer, maar het kan ook zijn dat de variantie in de geschatte basisafvoer groter is dan in de gesimuleerde grondwaterafvoer.

Definitie van de droogteperiodes De wijze van definiëren van de droogteperiodes heeft een grote invloed op de resultaten. Ten eerste is het belangrijk te realiseren dat de drempel die in dit proefschrift gebruikt is om de droogteperiodes af te leiden, een *relatieve drempel* is. Dit betekent dat voor elke tijdreeks van grondwateraanvulling of -afvoer een aparte drempel is afgeleid. Bijvoorbeeld voor toenemende j , neemt ook de hoogte van de drempel toe. Indien voor alle tijdreeksen dezelfde drempel was gebruikt, dan zou de afvoer van de grondwatersystemen met de kleinste j altijd de langste droogtes met de grootste deficiten hebben gehad. Waarschijnlijk zouden er in de afvoer van reservoirs met zeer hoge j in het geheel geen droogteperiodes geïdentificeerd zijn.

In Hoofdstuk 3 was vastgesteld dat de scheefheid van de frequentieverdeling verandert als gevolg van de voortplanting door een grondwatersysteem en dat de droogte-karakteristieken veranderen als gevolg van veranderingen in de scheefheid. Echter in de rest van het proefschrift is dat niet verder aan bod gekomen. De reden hiervoor is de keuze van de drempel. Deze is op zodanige wijze afgeleid, dat hij hoger wordt naarmate de scheefheid toeneemt en daardoor wordt het effect van de scheefheid verminderd. Indien de drempel bepaald zou zijn met de veelgebruikte methode van de percentielen, dan zou het effect veel groter geweest zijn. In dat geval zouden de droogtes van snel reagerende grondwatersystemen veel kleiner geweest zijn. Voor de recharge zouden waarschijnlijk geen droogtes geïdentificeerd zijn, omdat die een zeer hoog percentage

nullen heeft.

Niet alleen de keuze van de drempel, ook de keuze voor een bepaald type droogtedefinitie heeft invloed op de resultaten. In Hoofdstuk 4 is het effect van de voortplanting door het grondwatersysteem op de *minimum afvoer* onderzocht. Hieruit bleek enerzijds dat de minimum afvoer toeneemt met toenemende j , anderzijds was het verschil tussen de minimum afvoer van een droogte jaar en een normaal jaar het grootste voor middelmatig-snel reagerende grondwatersystemen ($j = 225$ d). Dit komt goed overeen met het resultaat dat de grootste droogtedeficiten optreden voor grondwaterreservoirs met j ongeveer 200 d.

Concept van grondwaterdroogte Het concept van grondwaterdroogte zoals dat in dit proefschrift gebruikt is, maakt gebruik van grondwateraanvulling, -standen en -afvoer om grondwaterdroogtes te definiëren. Echter, de ervaringen opgedaan in dit proefschrift laten zien, dat hierbij voorzichtigheid geboden is. Grondwateraanvulling geeft uiteraard geen informatie over de veranderingen die nog in het verzadigde grondwatersysteem optreden, terwijl dit wel nog een grote invloed op de droogtes heeft. Grondwaterstanden geven alleen lokale informatie, terwijl de ruimtelijk variatie van de droogtes in het grondwatersysteem groot is. Grondwaterafvoer geeft weliswaar een geïntegreerd beeld, maar alleen van de zone dicht bij de rivier. Feitelijk is grondwater droogte een dermate dynamisch begrip dat het onmogelijk is om het aan de hand van één enkele reeks te definiëren. Het is waarschijnlijk beter om het als ‘kapstok’ te zien, en bij de praktische definitie te spreken van een droogte in de grondwateraanvulling, -stand of -afvoer.

Appendix A

Simulation of recharge for the Pang catchment with the SWAP model

A.1 Simulation of the recharge

The recharge was simulated with the SWAP model (van Dam *et al.*, 1997) for the period 1960-1997, where 1960 was used as the initialisation year. The SWAP model simulates the water flow in the unsaturated zone by solving Richards' equation in a heterogeneous, 1-D soil column taking, for example, into account changing root water uptake. The recharge was not calibrated. The SWAP model needs precipitation and potential evapotranspiration, land use and soil characteristics and information on the position of the 1-D column in the hydrological system as input. Of the available output (i.a. actual evapotranspiration, soil moisture pressure head, drainage and recharge) only the recharge was used.

A.1.1 Calculation Procedure

The recharge is used as input for the groundwater flow model (Appendix D) for each 500 x 500 m cell and time step. The recharge was not calculated for each cell separately, but a limited number of physiographic units was identified. Each physiographic unit represents a unique combination of the following spatially-variable land characteristics:

- land use,
- soil type,
- subsoil,
- bottom boundary condition for SWAP and
- precipitation.

Other input, like for example the meteorological input data necessary for the calculation of the potential evapotranspiration was assumed to be constant over

the entire model area. It was possible to reduce these five characteristics to three by assigning one specific subsoil and one bottom boundary condition to each soil type. This reduced the number of combinations significantly.

For each of the three remaining characteristics, grids with a spatial resolution of 500 m were compiled. These grids were then combined to determine the unique combinations of land use, soil type and precipitation per cell. In more detail the procedure to derive a physiographic unit for each MODFLOW cell is as follows:

- The land use types defined on the land cover map provided by Institute of Terrestrial Ecology (@CEH, Wallingford, UK) were more detailed than could be simulated with the SWAP model. Therefore they were reclassified to a smaller number of land use types, of which the main types are grassland, tilled land and deciduous woodland.
- The grid files of land cover (25 x 25 m) and soil type (digitised 1:250 000 soil map of South East England (Soil Survey of England and Wales, 1983); 31.8 x 31.8 m) have been combined to produce one map with unique land use-soil combinations.
- For each MODFLOW cell (500 x 500 m), the distribution of the unique land use-soil combinations was determined. The land use-soil combination that occurred most in a cell was assigned as the representative land use-soil combination for that cell.
- To reduce the number of land use-soil combinations, 10% of the cells, which had the least numerous combinations were interpolated using nearest neighbour interpolation. Also 1.85% of the surface area classified as urban, were reclassified using nearest neighbour interpolation.
- The model area was divided into five polygons with spatially-uniform rainfall in each polygon.
- The rainfall polygons were then combined with the land use-soil combinations to identify for each cell the proper physiographic unit.

In total 7 types of land use, 24 soil types and 5 rainfall zones were defined. The maximum number of physiographic units is thus 840. With the procedure described above the number of physiographic units was reduced to 84, which can be divided into three groups:

1. locations on Chalk with an unsaturated zone exceeding 10 m. The large thickness of the unsaturated zone means that the interaction between the water table and the root zone does not have to be included in the

modelling (no capillary rise). This group consists of 48 physiographic units and covers 69.4% of the model area.

2. locations on Chalk or alluvium with shallow groundwater tables and thus near-potential evapotranspiration. These are 19 physiographic units, which cover 10.3% of the model area.
3. locations on deposits from the Tertiary (Figure 2.3). These deposits have a low conductivity and the recharge to the chalk aquifer through these deposits is therefore low. This is 20.3% of the model area and it includes 17 physiographic units.

For group 1, recharge was calculated using SWAP. The input for this group will be discussed below. For group 2, recharge was calculated assuming that the evapotranspiration is potential. Therefore for this group only rainfall and potential evapotranspiration data depending on land use were necessary. Calculation of the recharge for group 3 was a problem, because hardly any information is available about the hydraulic properties of the Tertiary deposits. Therefore a constant recharge was assumed in this area. The area was first subdivided into two parts: one part in the south where the deposits are thick and a second part in the north where the deposits are thinner. For the first part the recharge was estimated as 10 mm a^{-1} (Soley and Heathcote, 1998), while for the second part it was estimated as 30 mm a^{-1} .

A.1.2 Description of the input

Meteorological data Four rainfall stations in the model area (Yattendon, Priors Court, Wantage (Kitford gardens) and Pangbourne PS (Figure A.1)) with less than 10% missing data in the period 1961-1997 were selected to be used for the calculation of the recharge. However, these stations are not divided equally over the catchment. In the highest part of the catchment no station with sufficient data is available. From observations at stations with insufficient data (Peasemore (over 25% missing data) and Catmore (less than 14 years of data), Figure A.1), however, it is clear that the precipitation is higher in this area than at any of the four selected stations. The precipitation for this area was derived from a nearby station with sufficient data (Priors Court) and high correlation with the Peasemore station ($\rho = 0.944$) using a simple weighing factor (1.065). The polygons for the five stations were not derived with a standard Thiessen approach, because in that approach no additional information can be included. The polygons were derived based on expert judgement using the correlation structure between the rainfall stations, the isohyetal map and the elevations above sea level. Missing values were filled in using multiple linear regression.

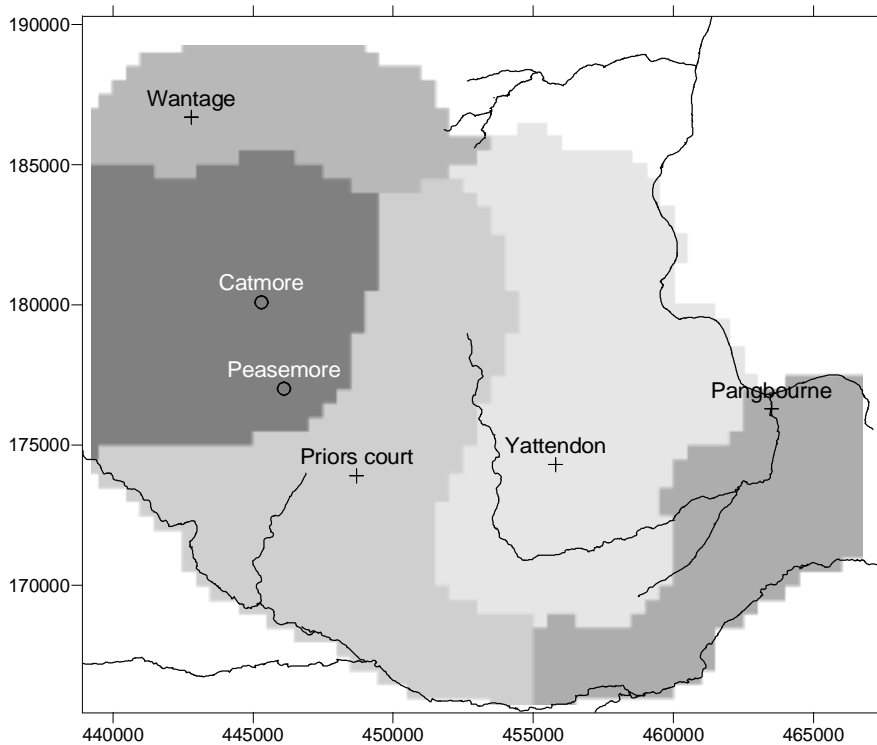


Figure A.1: Location of the rainfall stations and the 5 rainfall zones into which the model area (Appendix D) has been divided.

Data for 1960 from Reading (see next paragraph) was added to the time series as run-in period.

The data necessary for the calculation of potential evapotranspiration in SWAP (maximum and minimum daily temperature, wind speed, air humidity and solar radiation) were taken from Reading meteorological station. The station is named Reading University, Whiteknights no. 3 and is located about 7 km east of the model boundary. The station was relocated in 1968. Before 1968 the station name was Reading University. The data were tested for a step trend in the average and variance for all variables, which revealed a significant break for the wind speed and to a lesser extent humidity for the daily data. The break in the average of the wind speed was corrected for by decreasing the wind speed in the period before 1968 with a constant value. The solar radiation was calculated from observations of sunshine duration (Vereniging Voor Landinrichting, 1992).

Land use Only three main types of land use (tilled land, grassland and deciduous forest) remained after following the procedure described above. To calculate the recharge for tilled land the most common type of land use (cereals, mostly spring wheat/barley) was used. The calculation for grassland was performed for permanent grassland (not ley grassland). In order to calculate the recharge for deciduous forest, the interception module of SWAP had to be adapted. Interception is calculated in SWAP using an empirical relation between rainfall and interception, which is derived for arable crops and grassland. Therefore the interception module of SWAP was extended to enable the calculation of interception according to Gash (1979) on a daily basis. In Table A.1 the most important input values for crops are listed and in Table A.2 the input for the interception module is listed.

Table A.1: Input values for the SWAP model for grass, cereals and deciduous forest (van Dam *et al.*, 1997; Dolman and Moors, 1994; Kroes *et al.*, 1998; Boons-Prins *et al.*, 1993; Hough, 1990; Jackson *et al.*, 1996)

	Grass	Cereals	Deciduous Forest
Maximum canopy height (m)	0.1	0.8	10
Maximum rooting depth (m)	0.8	0.8	1.5
Minimum canopy resistance (s m^{-1})	70	30	150
Maximum Leaf Area Index	5.5	5.5	5
Length of growing season	365	10 April to harvest (latest: 18 August)	365
Light extinction coefficient (diffuse visible light)	1.0	1.6	1.6
Light extinction coefficient (direct visible light)	0.75	0.8	0.8

The input values for the free throughfall coefficient and the storage capacity of the canopy were mostly taken from Dolman and Moors (1994) and later verified by comparing the calculated daily interception with interception calculated on an hourly basis with data from Bracknell, Beauford park meteorological station. Average precipitation and evaporation intensity were calculated from the same hourly data set as used for verification.

Soil and subsoil To model the soil in SWAP the following information for each soil type is necessary:

- description of layering of soil,
- characteristics for each soil layer, including: saturated hydraulic conductivity, relation between the unsaturated hydraulic conductivity, the soil

Table A.2: Input values for the Gash model to compute interception for deciduous forest (daily basis). The term ‘Linear interpolation’ for autumn and spring values means that the values are derived using a linear interpolation between the summer and winter values.

	Summer	Winter	Autumn/spring
	Jul, Aug, Sept	Dec, Jan, Feb and Mar	Apr, May, Jun and Oct, Nov
Free throughfall coefficient (-)	0.3	0.8	Linear interpolation
Stem flow coefficient (-)	0	0	0
Storage capacity of the canopy (mm)	0.8	0.3	Linear interpolation
Average precipitation intensity (mm h ⁻¹)	1.4	1.4	1.4
Average evaporation intensity from wet canopy during rainfall (mm h ⁻¹)	0.3	0.2	Linear interpolation

moisture content and the pressure head, textural composition, organic matter content, bulk density and porosity.

The relation between the unsaturated hydraulic conductivity, the soil moisture content and the pressure head is described through the van Genuchten model (van Dam *et al.*, 1997). Most of this information is available through the SEISMIC database (Soil Survey and Land Research Center, 1995), which lists this information for all major soil types in England for all layers. Only the shape parameter for the unsaturated hydraulic conductivity (van Dam *et al.*, 1997) was derived using the pedotransfer functions listed in Wösten *et al.* (1998). The spatial extent of the different soil types was derived from the 1:250 000 soil map of South East England (Soil Survey of England and Wales, 1983).

For each soil type on the Chalk (group 1), a representative subsoil and a bottom boundary condition were derived. Most soils are developed directly on the Chalk, however in some places a drift deposit or a clay-with-flints deposit occurs between the soil and the bedrock. Because of their poor description these deposits have not been taken into account. So for all soils in group 1, the subsoil is composed of chalk. The bottom boundary condition was taken as the depth to the groundwater table. As most soil types have a relatively constant position with respect to the ground water table, a representative groundwater depth can be derived for each soil type. The representative thickness of the unsaturated zone was derived from the digitised soil map, the isohypse map of August 1976 (low groundwater levels) and of March 1995 (high levels). The results are presented in Table A.3.

Table A.3: Representative water table depth for soil types on the Chalk in the Pang model area.

Soil type	Representative groundwater table depth (m)
Hornbeam	55
Andover	50
Coombe	20
Frilsham	17
Wantage	17
Upton	50
Charity	20
Newmarket	20

The same information that was needed for the soil, is also necessary for the chalk. However, because this is not routinely available, it was derived from various sources, mostly from (Gregory, 1989; Geake and Foster, 1989; Downing *et al.*, 1993; Price *et al.*, 2000). As explained in Chapter 2, the Chalk is a dual-permeability medium. However, most of the flow is expected to go through the matrix, which has a saturated hydraulic conductivity in the order of 1 to 4 mm d⁻¹. Only for very high intensity rainfall events, the fissures are probably filled with water. The saturated hydraulic conductivity (both fissures and matrix) is in the order of 1 to 10 m d⁻¹. The matrix has a very uniform pore size distribution, with an approximate pore throat diameter in the range of 0.1-1 μm (Downing *et al.*, 1993) and is expected to be nearly saturated even for very deep water tables. The total porosity is generally up to 40% (Table 2.2). To simulate these characteristics in SWAP the equivalent continuum approach (Altman *et al.*, 1996) was used. In this concept flow is assumed to take place both in the matrix and the fissures, with instantaneous pressure equilibrium between the matrix and the fissures. In Figure A.2 the hydraulic properties for the chalk as they were used in SWAP are presented. The sharp drop in θ is determined by the uniform pore throat diameter. The two parts with decreasing k represent the fissures and the matrix respectively.

A.2 Recharge results

In Figure A.3 the recharge for the groundwater catchment of the Pang (Chapter 2) is presented for annual periods from August to July. The period August-July was used because the recharge is nearly always minimal in this period. In Figure A.4 an example of the monthly recharge as computed with the SWAP model for a common physiographic unit on the Chalk is presented. Both time

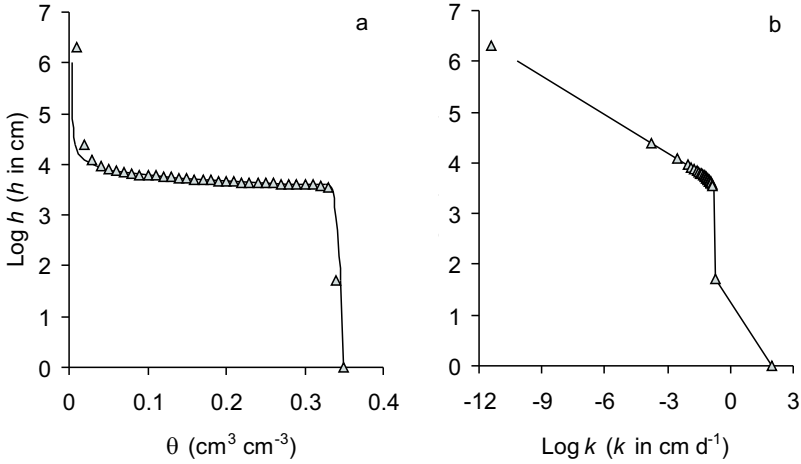


Figure A.2: Relation between the pressure head h and a) the soil moisture content θ and b) the unsaturated hydraulic conductivity k (b) for the unsaturated zone of the Upper Chalk. The continuous line indicates the relation based on literature, the symbols indicate the relation as it was applied in SWAP.

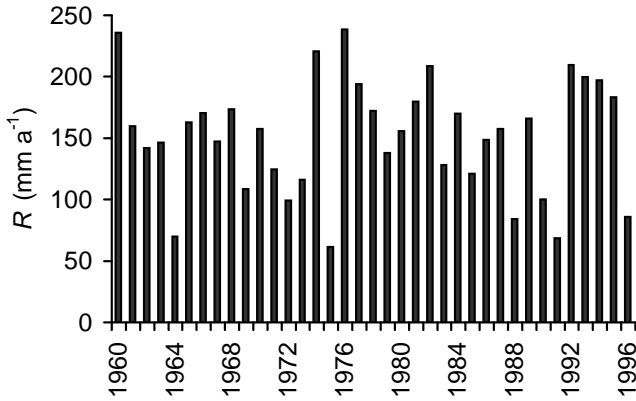


Figure A.3: Recharge R for the groundwater catchment of the Pang for annual periods from August to July.

series show dry years in 1964, 1975 and around 1990. The monthly recharge in Figure A.4 does not fall below 10 mm month^{-1} , because of the outflow from the thick unsaturated chalk matrix. During periods with very high recharge also the fissures start conducting water.

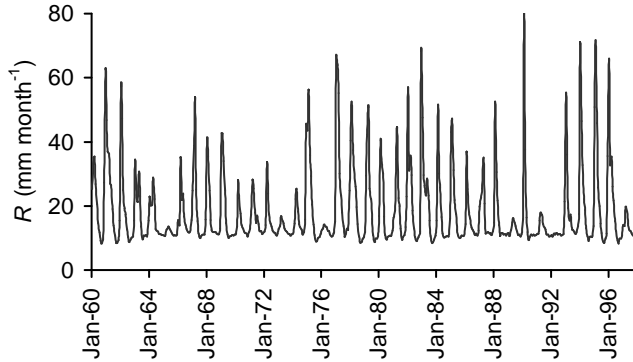


Figure A.4: Monthly groundwater recharge R simulated by the SWAP model for a cereal crop on Hornbeam soil, with precipitation of the polygon on the high part of the catchment (without station), which is one of the most common physiographic units. Average R is 221 mm a^{-1} .

In Figure A.5 the average annual recharge for each cell is presented. In the southern part of the catchment, the constant recharge below the Tertiary deposits is obvious (group 3). Along the Thames a few locations with negative recharge occur. These are locations with shallow water tables, where evapotranspiration is assumed to be potential (group 2). For the remainder of the catchment, the dominant feature is the soil type. In the valleys (both with stream and dry) the recharge is lower than in the higher areas. The highest recharge occurs on shallow soils on chalk (Andover soils, Chapter 2).

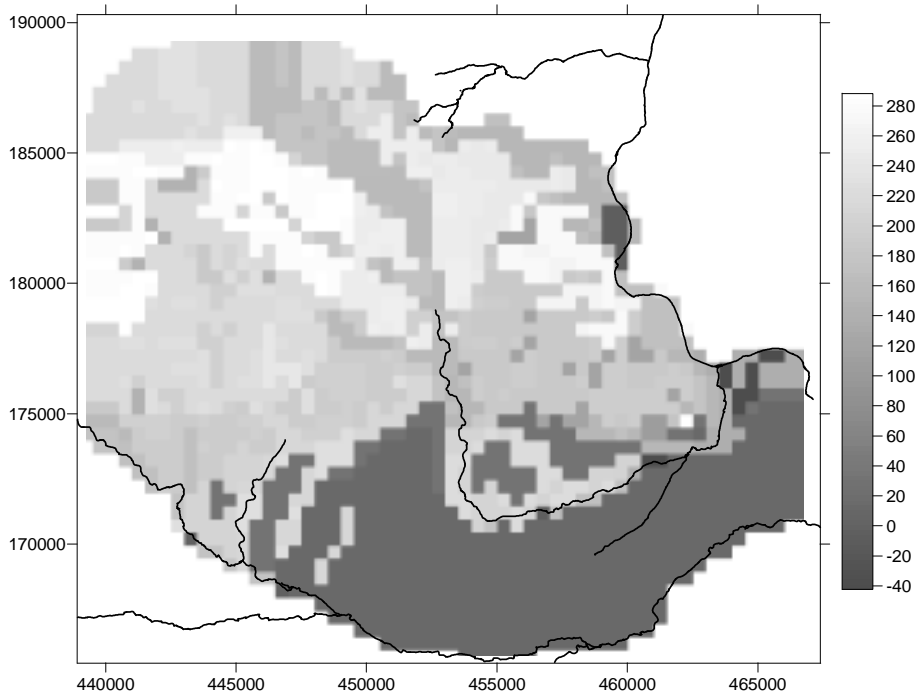


Figure A.5: Spatially-distributed average annual recharge model over the period 1960-1997 for all model cells.

Appendix B

Simulation of recharge for the Upper-Guadiana catchment with the SIMPA model

B.1 Simulation of the recharge

The monthly recharge was simulated for the Upper-Guadiana catchment by the Centro de Estudios y Experimentación de Obras Públicas (CEDEX, Spain) using the SIMPA model. This appendix only gives a short description of their work. A full description of the model and its application to the Upper-Guadiana catchment is provided by Ruiz García (1998) in Spanish. Shorter descriptions in English are provided by Estrela *et al.* (2000b) and Peters *et al.* (2001). For a description of the model only see Estrela and Quintas (1996). The SIMPA model is a spatially-distributed rainfall-runoff model based on a raster Geographical Information System (GIS). For each cell the water balance is simulated. The aggregated discharge from all cells in a catchment is calibrated using observed streamflow. Groundwater is accounted for through a linear reservoir approach, where the surface water catchment and the aquifer do not need to overlap. For each cell the following information is required:

- precipitation P and potential evapotranspiration ET_{pot} ;
- maximum infiltration rate, which controls the partitioning between infiltration into the aquifer (recharge) and surface runoff;
- maximum soil water storage capacity;

Also the aquifer recession coefficient, which determines the discharge rate from the aquifer, is required.

The model was run for a grid of 2.5 by 2.5 km cells covering the catchment of the Upper-Guadiana (Ruiz García, 1998). However, only for those areas (cells) overlying aquifers, recharge was calculated. P was interpolated using multiple linear regression. ET_{pot} was calculated from observed and subsequently interpolated temperatures using the Thornthwaite method. ET_{pot} was corrected

for local variations through corrector maps, which were derived by comparing ET_{pot} from the Thornthwaite method with that from the Penman-Monteith method. The maximum infiltration rate was derived from the lithology. Maximum soil storage capacity depends on the slope (derived from a Digital Terrain Model), soil texture and land use. Also the presence of wetlands was taken into account, because of the high potential for evapotranspiration in those areas. The aquifer recession coefficient depends on the aquifer characteristics and was derived directly from recession curves measured at gauging stations.

The model was calibrated with data from 11 streamflow gauging stations for the period from October 1940 to September 1971 (Ruiz García, 1998). The period after 1971 was not used because of high aquifer abstractions, which hamper parameter estimation. The maximum soil water storage capacity varies between 200 mm and 500 mm. The highest values occur in the flat regions. The wetlands also have high values in order to account for the high actual transpiration. The maximum infiltration rate varies between 150 and 600 mm month⁻¹. The largest values of the aquifer recession constant, i.e. 1.10^{-1} d^{-1} , occur in the Mancha Occidental unit (Groundwater and River Resources Action Programme (GRAPES), 1998). Once the calibration for the period before 1971 provided satisfactory results, the SIMPA model was run for the period 1940/41 to 1996/97 to obtain the recharge in the natural regime (i.e. without abstractions).

B.2 Recharge results

In Figure B.1 the annual recharge for the whole Upper-Guadiana catchment (to all aquifers in the catchment) is presented. The variability of the annual recharge is larger than for the Pang catchment (Figure A.3 and Table 7.2). The dry periods are mainly at the beginning of the time series (several dry years up to 1956) and at the end (1992-94). The recharge is also highly variable in space. The average recharge for the three major aquifer units (Figure 2.6) presented in Table B.1, shows that the recharge for the central, flat area is very low. The main amount of recharge occurs on the hilly parts in the south of the catchment (Campo de Montiel region).

Table B.1: Overview of the simulated groundwater recharge of the major aquifer units (Figure 2.6) of the Upper-Guadiana catchment.

	Surface area (ha)	Recharge (mm a^{-1})
Sierra de Altomira	233 750	14.1
Mancha Occidental	456 875	3.5
Campo de Montiel	223 125	58.8
Total	1148 750	16.6

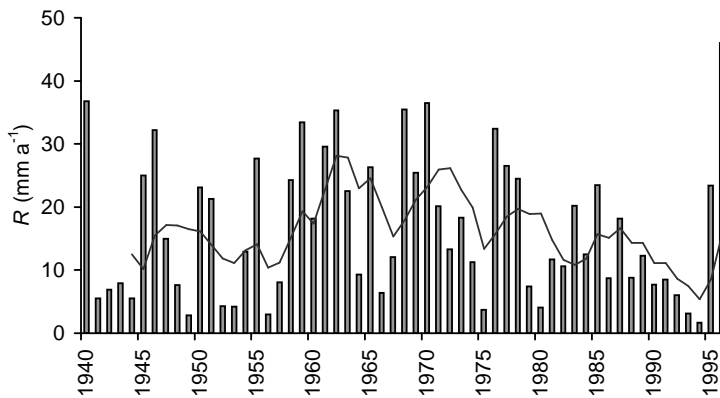


Figure B.1: Groundwater recharge R for the Upper-Guadiana catchment for hydrological years (October-September) and the 5-year moving average.

Appendix C

Separation of base flow from streamflow using groundwater levels - illustrated for the Pang catchment (UK)¹

Abstract

A new filter to separate base flow from streamflow was developed, which uses observed groundwater levels. To relate the base flow to the observed groundwater levels a non-linear relation was used, which is suitable for unconfined aquifers with deep groundwater levels that do not respond to individual rainfall event. Because the filter was calibrated using *total* streamflow, also an estimate of the direct runoff was needed. The direct runoff was estimated from precipitation and potential evapotranspiration using a water balance model. The parameters for the base flow and direct runoff were estimated simultaneously using a Monte Carlo approach. Instead of one best solution, a range of satisfactory solutions was accepted. The filter was applied to data from two nested gauging stations in the Pang catchment (UK). Streamflow at the upstream station (Frilsham) is strongly dominated by base flow from the main aquifer, whereas at the downstream station (Pangbourne) also a significant component direct runoff occurs. The filter appeared to provide satisfactory estimates at both stations. For Pangbourne, the rise of the base flow was strongly delayed compared to the rise of the streamflow. However, base flow exceeded streamflow on several occasions, especially during summer and autumn, which might be explained by evapotranspiration from riparian vegetation. To evaluate the results, the base flow was also estimated using three existing base flow separation filters: arithmetic filter (BFI), a digital filter (Boughton, 1993) and another filter based on groundwater levels (Kliner and Kněžek, 1974). Both the BFI and Boughton filters showed a much smaller difference in base flow between the two stations. The filter by Kliner and Kněžek (1974) gave consistently lower estimates of the base flow. Differences and lack of clarity in the definition of base flow complicated the comparison between the filters. An advantage of the method introduced in this paper is the clear interpretation of the separated components. A disadvantage is the high data requirement.

¹This appendix is based on the paper ‘Peters, E. and H.A.J. van Lanen. Separation of base flow from streamflow using groundwater levels - illustrated for the Pang catchment (UK). Accepted for publication in *Hydrological Processes*’

Keywords: base flow separation, digital filter, BFI, calibration, uncertainty analysis, Monte Carlo simulation, Pang catchment

C.1 Introduction

Many methods exist to estimate the base flow or groundwater contribution to streamflow (e.g. reviews by Hall (1968); Tallaksen (1995)). However, the separation of streamflow in two or more runoff components is fraught with difficulties. First, the definition of the different components of streamflow (base flow, interflow and overland flow or alternatively base flow and quick flow) is not straightforward (Dingman, 2002; Ward and Robinson, 2000; Nathan and McMahon, 1990; Chapman, 1999; Halford and Mayer, 2000). Some define base flow as the component of streamflow that cannot directly be explained from precipitation (streamflow minus quick flow). Often, however, base flow is interpreted as the outflow from stored sources like groundwater, lakes and glaciers and does not include interflow (Nathan and McMahon, 1990; Vogel and Kroll, 1996; Wittenberg and Sivapalan, 1999; Furey and Gupta, 2001). In this study, the latter definition is used. The second problem, which arises for base flow separation, is that many methods are based on base flow recessions, for which the recession constants are notoriously difficult to estimate. The recessions are influenced by many aspects, for example evapotranspiration, bank storage, the occurrence of several storage reservoirs instead of one, recharge from a thick unsaturated zone, variations in recharge, variations in aquifer thickness, stream penetration and antecedent rainfall (Brutsaert and Nieber, 1977; Tallaksen, 1995; Vogel and Kroll, 1996; van de Griend *et al.*, 2002). The third problem is that for continuous separation the base flow during peak flow has to be decided upon (Yu and Schwartz, 1999; Shukla *et al.*, 2000; Mizumura, 2001).

Early methods for base flow separation included many graphical methods, which were cumbersome in their application and included many subjective choices (Hall, 1968; Brutsaert and Nieber, 1977; Vogel and Kroll, 1996). To overcome the subjectivity and cumbersome application of these methods, digital filters were introduced (Nathan and McMahon, 1990; Chapman, 1999; Furey and Gupta, 2001). However, these methods suffer from a lack of physical interpretability. Relating to the evaluation of some automated filters, Nathan and McMahon (1990) state that ‘the methods do not attempt to simulate actual base flow conditions, but rather they are aimed at deriving an objective index related to base flow response’.

To derive more meaningful separations, many attempts have been made to use additional sources of information. The most important contribution in this respect has been made by using geochemical and isotope tracers (Buttle, 1994; Kendall and McDonnell, 1998; Burns, 2002). This has led to some important

insights, most notably the fact that during stormflow much more of the water is pre-event water than hitherto was considered. However, pre-event water and groundwater are not necessarily identical (Chapman, 1999; Holko *et al.*, 2002) and it is not clear yet how these results should be translated into separation algorithms for the continuous separation of streamflow. There have also been some attempts to develop physically-based methods to separate base flow from streamflow (Chapman, 1999; Furey and Gupta, 2001; Mizumura, 2001; Pauwels *et al.*, 2002). These methods are mostly based on formulating relations to describe hillslope runoff as a function of precipitation, evapotranspiration and slope characteristics.

To date, another source of information, namely observed groundwater levels, has been used to a far lesser extent. Hall (1968) discusses some early attempts to relate streamflow to groundwater levels. A limited number of authors have used groundwater levels to derive base flow or to support other separation methods (Rorabaugh, 1964; van Lanen *et al.*, 1993; Holko *et al.*, 2002; Hertzler, 1939; Olin, 1995; Halford and Mayer, 2000; Mizumura, 2001). Only the method used in the first three references really use groundwater levels to separate base flow from streamflow. Rorabaugh (1964) uses a theoretically derived linear relationship between base flow and groundwater level to examine the influence of bank storage. Holko *et al.* (2002) and van Lanen *et al.* (1993) both use the same method, which they cite as first being described by Kliner and Kněžek (1974). In this method an empirical relationship between base flow and groundwater level is derived. Holko *et al.* (2002) concludes that the method provides realistic results in five European basins.

In this paper it will be further investigated how observed groundwater levels can be used for separating streamflow. A new filter is developed which estimates the base flow continuously from observed streamflow, groundwater levels and excess precipitation. The filter will be demonstrated using data from the Pang catchment (UK). To evaluate the result of the new filter, they will be compared to the results of other separation filters, namely the arithmetic BFI method (Institute of Hydrology, 1980), the Boughton two-parameter digital filter (Boughton, 1993) and the method proposed by Kliner and Kněžek (1974).

C.2 Derivation of the filter equations

It is not straightforward to relate observed groundwater levels in a catchment to the base flow at the outlet (Hall, 1968). The first problem is the fact that in principle the flow rate from groundwater to the stream is determined by the difference in potential between the stream and the groundwater close to the stream. After precipitation, at the start of a recession, the decrease of the groundwater flow rate into the stream is strongly non-linear (Kraijenhof

van de Leur, 1962; Polubarinova-Kochina, 1962). However, after a sufficiently long time, the recession can be described by the outflow from a reservoir and then the groundwater flow to the stream is related to the groundwater level at some distance from the stream. If it can be assumed that the transmissivity is constant in time (Kraijenhoff van de Leur, 1958) as in the case of an aquifer with a large saturated thickness or a confined aquifer (Wittenberg, 1999) the recession can be described by the outflow from a linear reservoir. For an unconfined aquifer for which the transmissivity decreases with falling water table, the groundwater flow into the stream can be described after a sufficiently long time by the outflow from a second-order storage reservoir (Brutsaert and Nieber, 1977; Troch *et al.*, 1993; Tallaksen, 1995; Wittenberg, 1999; Halford and Mayer, 2000). Additional causes for non-linearity in the recession are flow convergence, changes of the hydraulic conductivity with depth, changes in the length of the drainage system and non-fully penetrating stream channels (Wittenberg, 1999; Marani *et al.*, 2001; van de Griend *et al.*, 2002).

A second problem for relating groundwater levels to base flow is the hysteresis effect caused by rising and falling groundwater tables, which means that there are no fixed relations between base flow and groundwater levels (Kraijenhoff van de Leur, 1958). The rise in groundwater table occurs first closest to the stream and thus the base flow for a rising water table is higher than for a falling water table for an identical groundwater level at some distance from the stream. The third problem are the effects of the translation of the base flow through the stream on the base flow: flow time, re-infiltration of stream water, bank storage and evapotranspiration from the stream and the riparian area are some of the reasons why the base flow at the outlet may be different from the groundwater flow to the stream.

To derive filter equations to separate the streamflow, it is assumed that the groundwater levels do not respond to individual rainfall events and thus that the non-linear response shortly after a rainfall event does not need to be taken into account. This is generally reasonable for areas with deep groundwater levels. Second, the hysteresis in the groundwater level-base flow relationship is not taken into account and third, the flow processes in the stream mentioned above are not taken into account. It was not assumed beforehand whether the groundwater level-base flow relationship is linear or non-linear.

The filter equations consist of two parts: base flow Q_s and direct runoff Q_f , where direct runoff incorporates both overland flow and interflow. An estimate of the direct runoff is needed, because the calibration is done with total observed streamflow, which includes direct runoff. The relation for the *base flow* was derived assuming a non-linear relationship between the storage and the base flow of the form (Wittenberg, 1999; Wittenberg and Sivapalan, 1999):

$$S_s = aQ_s^b \quad (\text{C.1})$$

where S_s is groundwater storage [L^3], Q_s is base flow [L^3T^{-1}] and a and b are model parameters that need to be calibrated. Units of a depend on the value of b and are [$L^{3-3b}T^b$]. Groundwater level H [L] is related to storage by:

$$\frac{dS_s}{dt} = c \frac{dH}{dt} \quad (C.2)$$

where t stands for time and c is a model parameter [L^2]. Parameter c theoretically equals storativity times the surface area of the aquifer. Both storativity and surface area may alter with changing height of the water table. However, this is not taken into account. Equations (C.1) and (C.2) are combined to define the following recursive relationship to estimate base flow:

$$Q_{s,t+1} = Q_{s,t} + \Delta t \left. \frac{dQ_s}{dt} \right|_t = Q_{s,t} + \Delta t Q_{s,t}^{1-b} \left. \frac{c}{ab} \frac{dH}{dt} \right|_t \quad (C.3)$$

where Δt is the time step of the calculation (in this paper 1 d) and $\left. \frac{dH}{dt} \right|_t$ was derived from observed groundwater levels.

The *direct runoff* was described by the outflow from a linear reservoir with two thresholds using a two-step approach:

Step 1:

$$S_{f,t+1/2} = S_{f,t} + \Delta t (P_t - ET_{pot,t}) \quad (C.4)$$

with $S_{f,t+1/2} \geq 0$

$$\begin{aligned} Q_{f,t} &= 0 & \text{if } S_{f,t+1/2} \leq S_{f,tr} \\ Q_{f,t} &= \frac{A_f}{j} (S_{f,t+1/2} - S_{f,tr}) & \text{if } S_{f,tr} < S_{f,t+1/2} \leq S_{f,fc} \\ Q_{f,t} &= S_{f,t+1/2} - S_{f,fc} + \frac{A_f}{j} (S_{f,fc} - S_{f,tr}) & \text{if } S_{f,t+1/2} > S_{f,fc} \end{aligned} \quad (C.5)$$

Step 2:

$$S_{f,t+1} = S_{f,t+1/2} - \frac{\Delta t}{A_f} Q_{f,t} \quad (C.6)$$

where $Q_{f,t}$ [L^3T^{-1}] is the direct runoff at time t [T], $S_{f,t}$ and $S_{f,t+1}$ [L] are the storage of the direct runoff reservoir at time t and $t + 1$, respectively, $S_{f,t+1/2}$ [L] is the storage at the intermediate step, $S_{f,tr}$ and $S_{f,fc}$ [L] are the threshold values of the storage below which no runoff occurs and above which all input immediately becomes runoff, A_f [L^2] is the surface area contributing to direct runoff, j [T] is the reservoir coefficient and P_t [LT $^{-1}$] and $ET_{pot,t}$ [LT $^{-1}$] are the precipitation and potential evapotranspiration at time t , respectively. Excess precipitation is defined as $P_t - ET_{pot,t}$. The evapotranspiration is potential as long as $S_f > 0$, and becomes zero when $S_f = 0$. The approximation in Equations (C.4)-(C.6) is adequate as long as the time step is not too large compared to the reservoir coefficient.

During the calibration procedure, several different simple formulations for direct runoff were tested. However, these had only a minor influence on the base flow estimate (data not shown). During the separation the estimated base flow was not constrained to be smaller than the observed streamflow, in order to evaluate the total behaviour of the filter (Furey and Gupta, 2001). Both the estimated base flow and direct runoff were constrained to be larger than or equal to zero. Thus, it was assumed that the stream is always draining.

C.3 Data and methods

The Pang catchment is a softly undulating catchment some 25 km south of Oxford (UK) (Figure C.1). Annual average precipitation and potential evapotranspiration are 690 and 600 mm a⁻¹, respectively. The main aquifer underlying the area consists of Upper-Cretaceous Chalk. The Chalk deposits are sloping in a southerly direction. In the south of the catchment the aquifer is covered by low-permeability deposits from the Tertiary. Where the Chalk aquifer is covered with Tertiary deposits it is confined, for the rest it is unconfined. The Chalk aquifer is known to have large variations in hydraulic conductivity both in horizontal and vertical direction. The main water flow is assumed to occur in the top 50 m. For a more elaborate description of the catchment see Acreman *et al.* (2000); Peters *et al.* (2001); Bradford (2002). The streamflow of the Pang is observed at three gauging stations. The gauging station (GS) at the outlet (Pangbourne GS, Figure C.1) has been in operation since 1968. The flow ranges from 0.074 to 5.97 m³s⁻¹, with an average of 0.6 m³s⁻¹. The Pang at this point discharges both base flow from the Chalk aquifer and direct runoff (overland flow and interflow) from the Tertiary deposits in the south (Bradford, 2002; Neal *et al.*, 2000; Estrela *et al.*, 2000b). Bradford (2002) estimates the direct runoff for the Pang at Pangbourne at 0.1 – 0.3 m³ s⁻¹ during seasonal high flow conditions. The other two stations (Frilsham and Bucklebury GS, Figure C.1) have been in use since 1992. At Frilsham GS mostly base flow discharges, whereas at Bucklebury GS a small component direct runoff is added. The flow at both stations is intermittent, however for the analyses only a period with continuous above-zero flow was used. The streamflow at Frilsham GS ranges from 0 to 0.8 m³s⁻¹, with an average of 0.19 m³s⁻¹ in the period from 1993 to 1997. In the following, only Pangbourne GS and Frilsham GS will be analysed.

In the Chalk aquifer, over 50 boreholes are available. Many of these have only been observed irregularly or during short periods. One borehole (SU47/141) was selected which represents the response of the aquifer well and which had a long, relatively uninterrupted record. The borehole was chosen at some distance of the stream, so as to avoid direct influence of the stream on the borehole

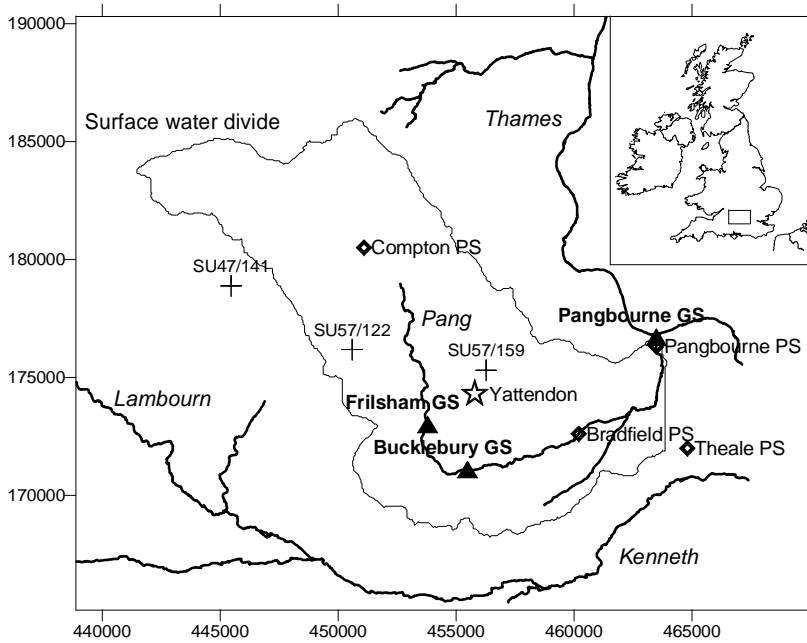


Figure C.1: Location map of the Pang catchment. Indicated are the locations referred to in the text. (PS: Pumping station, GS: Gauging station, SU: Observation Boreholes, Yattendon: rainfall station, coordinates according to British National grid)

(Rorabaugh, 1964). The borehole is located just outside the surface water catchment, however, it is located within the groundwater catchment, which does not coincide with the surface water catchment. Observations for this borehole started in 1973. The base flow was estimated for the period July 1973 to December 1997 on a daily basis. Because the groundwater level data were not observed on a daily basis, but on a weekly basis, they were interpolated using cubic splines. Occasional observations on intervals shorter than a week show little short-term (< 1 week) variation. The term $\frac{dH}{dt}$ in Equation (C.3) was initially approximated by $\frac{\Delta H}{\Delta t}$ derived from the interpolated daily groundwater levels. The time step of the observed groundwater levels (weekly) was too coarse for the non-linear equation. However, also for the daily values, the solution showed a drift and thus a Runge-Kutta scheme was used to solve Equation (C.3) with $\frac{dH}{dt}$ again approximated by $\frac{\Delta H}{\Delta t}$ of the interpolated groundwater levels. Figure C.2 shows the resulting relation between H and Q_s . The stability of the relation shows that the solution using the Runge-Kutta scheme was adequate.

Precipitation and potential evapotranspiration are needed to simulate the direct runoff. Precipitation is observed at several stations in the Pang catchment.

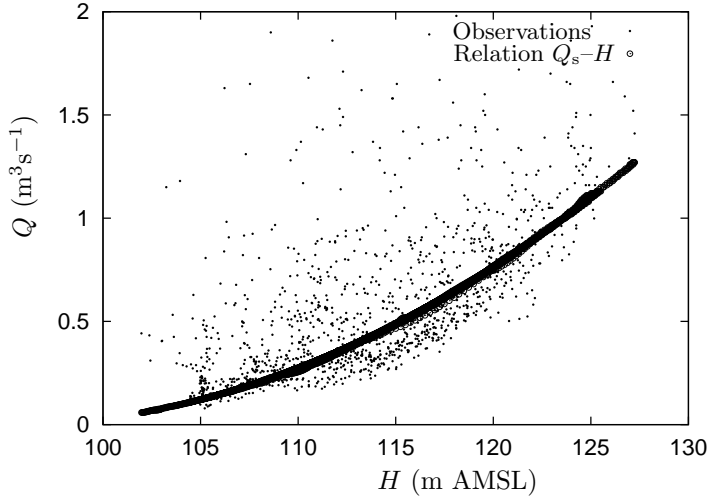


Figure C.2: Observed streamflow Q at Pangbourne gauging station versus the observed groundwater level H in borehole SU47/141 and the relation between base flow Q_s and groundwater level H resulting from solution of Equation (C.3).

Data from one station (Yattendon) in the central part of the catchment with a long and uninterrupted observation record were selected for use in this paper (Figure C.1). The potential evapotranspiration was calculated according to Penman-Monteith (Feddes and Lenselink, 1994) with crop resistance r_s is 70 s m^{-1} . The necessary data to calculate the potential evapotranspiration have not been observed in the Pang catchment. Therefore, data from a nearby station (Reading, about 7 km east of the catchment boundary) were used.

The assumptions for which the filter equations were derived, are fulfilled quite well by the Pang catchment. Because of thick unsaturated zones and a sparse drainage network, the direct response to precipitation is limited, certainly for the flow at Frilsham GS. From groundwater observations it is known that the groundwater levels in the Chalk aquifer in most places do not respond to individual rainfall events. With regard to the hysteresis in the groundwater level-base flow relationship, no structural difference in timing could be observed between groundwater level observations relatively close to the stream and those further away. Because the Pang is only a short river, the travel time in the stream is probably negligible. However, it is unknown whether the other processes in the stream channel have a significant influence. For the direct runoff no distinction was made between the flow generated on the low permeability deposits in the south of the catchment and any direct runoff that might originate on the Chalk.

C.4 Parameter estimation

The parameters in Equations (C.3) and (C.4)-(C.6) were estimated from daily time series of observed streamflow. The parameters a , b and c were not estimated separately, but the combined parameters c/ab and $1 - b$ were estimated. Because the optimisation problem is essentially multi-objective and because of possible variability of the parameters, which was not taken into account, a set of solutions was accepted instead of one ‘best’ solution (Beven and Binley, 1992; Gupta *et al.*, 1998; Savenije, 2001; Hall and Anderson, 2002). This set of solutions was the best 5% from a Monte Carlo simulation of 5000 runs. The parameter sets for the 5000 runs of the Monte Carlo simulation were determined by latin hypercube sampling from uniform distributions within predefined ranges. The performance of the simulations was evaluated by plotting the performance as a function of parameter value (scatterplots according to Freer *et al.* (1996)). The criteria used to determine the performance were: Nash-Sutcliffe model efficiency R^2 , model efficiency during June, July and August R_{JJA}^2 , bias B_s and the cross-correlation coefficient between the observed and simulated streamflow (ρ). The period June - August was analysed separately because during this period hardly any direct runoff is expected to occur. The bias was used in two ways. First, the bias for each individual parameter set should be below the performance limit and second, the average bias of all the accepted runs should be close to zero. The latter is to avoid a systematic error in the estimated base flow.

The initial parameter ranges for the Monte Carlo simulations were chosen to be rather wide. For some parameters the performance varied considerably over the parameter range. Thus the parameter ranges were determined iteratively, where the final ranges showed no clear (not quantified, subjective) performance differences over the range.

The set of solutions accepted in this paper should in no way be interpreted as an actual uncertainty interval. In the first place the width of the interval is rather arbitrary, because it depends on the number of runs in the Monte Carlo simulation, the parameter ranges and the performance criteria used. Second, only part of the uncertainty is incorporated, namely uncertainty about the model parameters. Not included is uncertainty about the representativeness of the selected borehole or about the model concepts.

The results of the Monte Carlo runs were also used to determine the information content contained in the observations per parameter (Weerts *et al.*, 2001; Vrugt *et al.*, 2001; Musters and Bouten, 2000). Weerts *et al.* (2001) determine the information content as follows: first the model is run once using a reference parameter set. This reference parameter set is a more or less arbitrary parameter set, which gives reasonable results. Subsequently, a large number of

parameter sets is generated. For each set and for each observation the simulated streamflow is compared to the simulated streamflow from the reference run. If the simulated streamflow falls within a specified range (e.g. 5%) from the streamflow in the reference run the parameter set is accepted, otherwise it is rejected. From the accepted runs the information content is calculated according to:

$$I_m(a) = 1 - \frac{\max(a)_m - \min(a)_m}{\max(a)_b - \min(a)_b} \quad (\text{C.7})$$

where $I_m(a)$ is the information content of an individual measurement point m (in this paper daily streamflow) with respect to parameter a , $\max(a)$ and $\min(a)$ are the maximum and minimum values of the accepted parameter values, and subscript b denotes the pre-defined parameter range of the reference run. If $I_m(a)$ is close to zero, the information content of measurement point m for parameter a is small, if $I_m(a)$ is close to one, the information content is large.

C.5 Results

In Table C.1 the parameter ranges are presented that were used for the Monte Carlo simulation. In Figures C.3 and C.4 the information content for the parameters determining the base flow at Pangbourne are given. In general, the information content was quite sensitive to changes in either the reference parameter set or the parameter ranges. For example, in initial simulations (when the parameter ranges were still rather wide) the information content for the parameter b (Equation (C.1)), which determines the non-linearity of the groundwater reservoir, was very low. Also the information content during recessions was quite low, while it was high during peak flow. However, with increasing accuracy of the parameter ranges and the reference parameter set, b became increasingly sensitive and the information content increased. Finally, the information content for parameter b (Figure C.4) is mostly concentrated in drought periods, e.g. 1991-1992. In Figure C.3 the information content for the first parameter pertaining to base flow (c/ab) is clearly concentrated during the recession parts of the total streamflow. Additional analyses showed that the maximum in the information content mostly coincides with the peak in the groundwater levels or comes just after it (data not shown).

From the Monte Carlo simulation (5000 runs) with the parameter ranges in Table C.1, the best-performing 5% were selected using the performance limits in Table C.2. For R^2 , R_{JJA}^2 and ρ this performance limit is the lower boundary. For the bias B_s this is the upper boundary. The selected 250 runs resulted in the simulated base flow range presented in Figure C.5 for Frilsham GS and in Figure C.6 for Pangbourne GS. For clarity reasons only part of the time

Table C.1: Parameter ranges for the final Monte Carlo simulation.

	Pangbourne GS	Frilsham GS
$Q_{s,0}$ (m^3s^{-1})	0.25–0.30	0.175–0.195
c/ab ($\text{m}^{3b-3}\text{s}^{-b}$)	0.05–0.10	0.07–0.12
$1-b$ (-)	0.4–1.0	0.4–0.8
$S_{f,0}$ (mm)	1–130	1–150
$S_{f,\text{tr}}$ (mm)	90–125	1–100
$S_{f,\text{fc}}$ (mm)	200–300	150–300
j (d)	10–20	5–25
L (m) ¹	4250–5250	1000–1500

¹ $L^2 = A_f$ (Equation (C.5))

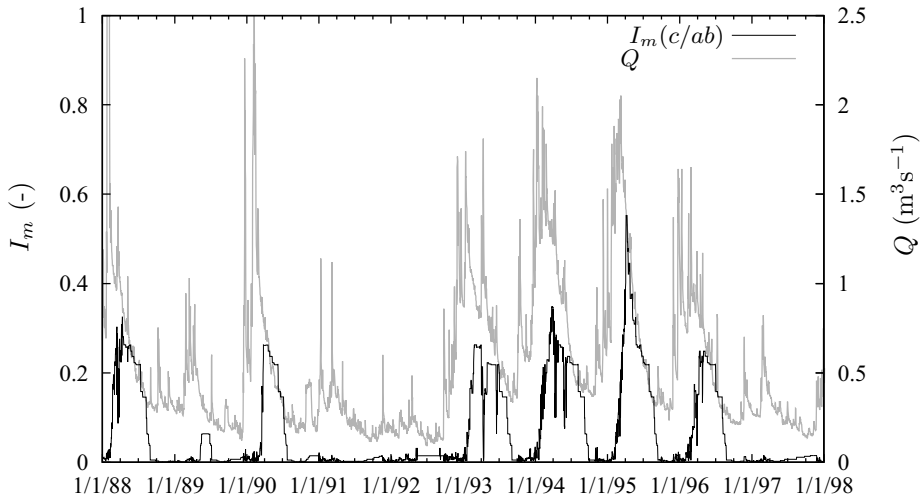


Figure C.3: Information content I_m of daily observations from Pangbourne GS with respect to parameter c/ab (Equation (C.7)) and observed streamflow Q at Pangbourne GS.

series is given for Pangbourne GS. The base flow component for Frilsham is estimated at 88.5 to 98.6% of the total streamflow and for Pangbourne at 67.3 to 77.4% (Table C.3). As expected the base flow component from the Chalk is considerably higher at Frilsham than at Pangbourne. The range width for Frilsham (Figure C.5) varies from 9.7 to 281.1%, expressed as a percentage of the estimated average base flow per day. The median width of the range is 14.9%. The largest absolute range widths occur during peak flow, while the largest relative range width occurs during droughts. The range width for Pangbourne varies from 15.9 to 110.5% and the median width is 18.4%. The maximum relative range width is reached during a severe drought in 1976.

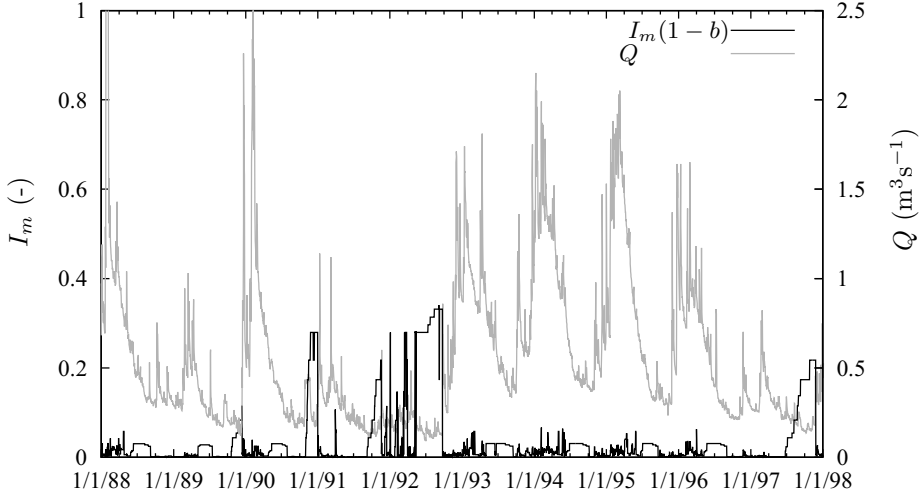


Figure C.4: Information content I_m of daily observations from Pangbourne GS with respect to parameter $1-b$ (Equation (C.7)) and observed streamflow Q at Pangbourne GS.

Table C.2: Performance limits for the acceptance of base flow simulations. All values were calculated by comparing simulated and observed *total* streamflow.

	Pangbourne GS	Frilsham GS
R^2 (-)	0.795	0.9418
R^2_{JJA} (-)	0.996	0.9997
$ B_s $ (m^3s^{-1})	0.031	0.0110
ρ (-)	0.891	0.9718

Figures C.5 and C.6 clearly show the difference in response between the flow at Frilsham GS and Pangbourne GS that was expected from the geology. The flow at Frilsham is dominated by base flow with a small component direct runoff. The peak in the estimated base flow at Frilsham coincides with the peak in observed streamflow. However, at Pangbourne GS on average about 28% (32.7 - 22.6%) of the flow is direct runoff from the low permeability deposits in the south. The major part of this direct runoff is concentrated in winter. In this period, the base flow is clearly smaller than the observed streamflow and the rise in the base flow is later than in the observed streamflow. In other words, the direct runoff at Pangbourne GS is simulated to have a large seasonal component, which discharges earlier than the base flow. In summer and autumn the estimated base flow is sometimes larger than the observed streamflow, because it was not constrained as explained earlier.

Table C.3: Overview of the base flow as a percentage of the total streamflow estimated by different methods.

	Pangbourne GS (1973-1997)	Frilsham GS (1993-1996)
This paper	67.3–77.4%	88.5–98.6%
BFI (Institute of Hydrology, 1980)	87.0%	94.3%
Boughton (1993) 2-parameter	77.5%	88.2%
Kliner and Kněžek (1974)	54.8%	72.9%

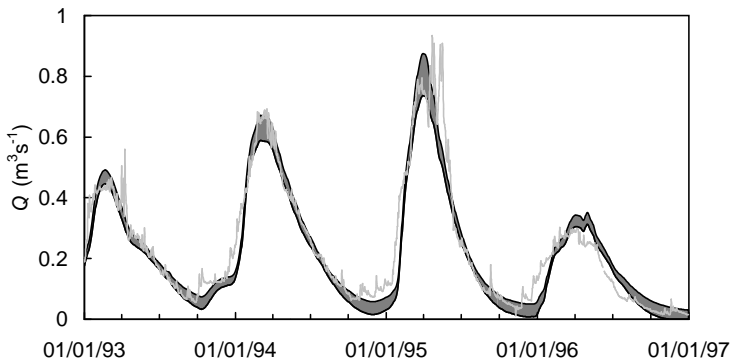


Figure C.5: Simulated base flow (range) and observed streamflow (line) at Frilsham GS.

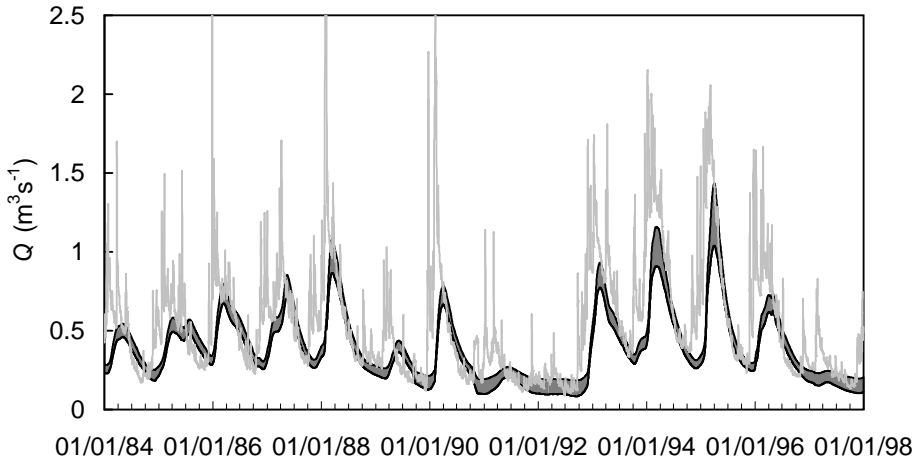


Figure C.6: Simulated base flow (range) and observed streamflow (line) at Pangbourne GS.

The uncertainty due to the selected representative borehole was examined by estimating the base flow using other boreholes. The base flow for Frilsham was estimated using a borehole closer to the stream (SU57/122, Figure C.1), but not in the direct vicinity of the stream. This resulted in a base flow estimate of 87.4 to 97.2% for Frilsham GS. The daily base flow was very similar (data not shown). The main difference was a decrease in estimated base flow in the autumn of 1996 for SU57/122 compared to SU47/141. For Pangbourne the base flow was also estimated using a borehole at the opposite side of the stream closer to the outlet (SU57/159, Figure C.1). This resulted in a base flow estimate of 66.3 to 77.1% for Pangbourne GS, which is almost identical to the estimate using borehole SU47/141. Again, no systematic differences occurred between the two estimates of the daily base flow.

C.6 Comparison of base flow separation methods

As base flow was not measured directly, the only way of evaluating the performance of the filter is by comparing the results of the filter proposed in this paper to results of other filters. The following methods were selected for comparison: the BFI method (Institute of Hydrology, 1980), a two-parameter digital filter (Chapman, 1999; Boughton, 1993) and the method developed by Kliner and Kněžek (1974) which also uses groundwater levels (Holko *et al.*, 2002; van Lanen *et al.*, 1993).

C.6.1 BFI filter

The BFI method is a purely arithmetic method to obtain an estimate of the base flow contribution on a long time scale, mainly as a time-independent catchment characteristic. The separation rules are described in Institute of Hydrology (1980), and they are based on selecting base flow turning points from 5-day minima. The method was developed for streams like the Pang and it is in fact illustrated for data from Pangbourne GS in Institute of Hydrology (1980). The base flow derived using this procedure is not the base flow derived from groundwater, but ‘the proportion of the river’s runoff that derives from stored sources’ (Institute of Hydrology, 1980). It is not elaborated what these stored sources are. The BFI for the Pang at Pangbourne GS is 0.870 (87% base flow) and at Frilsham is 0.943 (94.3% base flow)(Table C.3). For the streamflow at Frilsham GS, which was only derived from the Chalk, the BFI estimate is well in the range of base flow estimates by the method proposed in this paper. For Pangbourne, the BFI estimate is considerably larger than

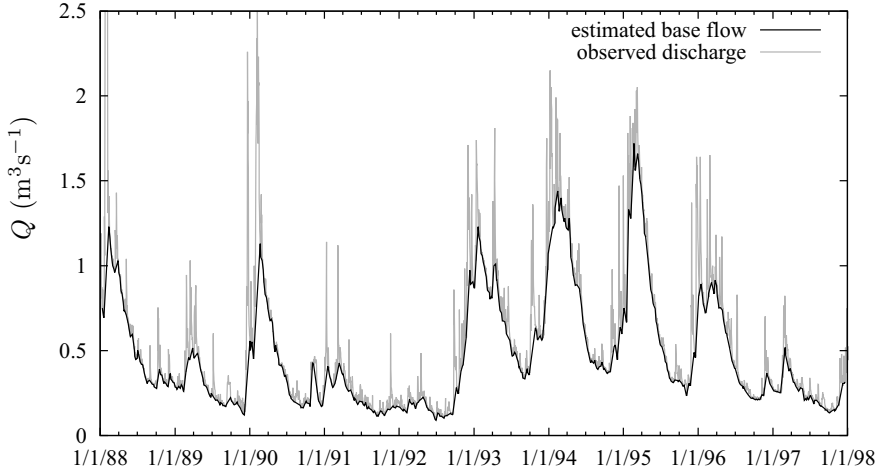


Figure C.7: Estimated base flow for Pangbourne GS using the BFI method (Institute of Hydrology, 1980) and observed streamflow.

the estimate of the method proposed in this paper. Figure C.7 presents the base flow at Pangbourne GS as determined by the BFI method. The largest difference between the BFI method and the method presented in this paper occurs during early winter. According to the method proposed in this paper, which is based on observed groundwater levels, it is unlikely that the majority of the streamflow during early winter is derived from the Chalk aquifer. According to the BFI-method, however, this flow is derived from stored sources and thus was not directly linked to precipitation. In other words, this flow during early winter is neither base flow from the Chalk aquifer nor overland flow produced by precipitation, but interflow from the low-permeability deposits in the south of the catchment.

C.6.2 Boughton filter

The second method used is the 2-parameter filter described by Boughton (1993). The Boughton-filter (Equation (C.8)) gave the most reasonable results out of three digital filters according to Chapman (1999) and is written as:

$$Q_{s,t} = \frac{k}{1+C}Q_{s,t-1} + \frac{C}{1+C}Q_t \quad (\text{C.8})$$

where Q_t is the total streamflow at time t [L^3T^{-1}] and k and C are the filter parameters. The filter can be interpreted as follows: the base flow is simulated as outflow from a linear reservoir with recession constant k [-]; the streamflow

exceeding the outflow from the reservoir ($Q_t - kQ_{s,t-1}$) is divided between recharge to the groundwater store and direct runoff with a constant partitioning factor $1/(1 + C)$ [-]. This last assumption is a gross simplification of reality. It is not quite clear how base flow is interpreted in this approach. On the one hand base flow is simulated as the outflow from a groundwater reservoir, on the other hand interflow is not explicitly accounted for.

The filter was used with one forward pass only, although Spongberg (2000) in general advises to use two passes in order to minimise the phase-shift caused by the filter. However, in this study using a second pass resulted in an unrealistically early base flow response. Unfortunately, the filter parameters k and C cannot be calibrated on observed streamflow straightforwardly. Chapman (1999) suggests (citing Boughton (1994), personal communication) basing the calibration 'mainly on the endings of surface runoff, particularly in big runoff events'. Furey and Gupta (2001) use the number of exceedances of the base flow over the streamflow π_1 and the deviation from the annual minimum π_2 in order to evaluate the performance of different filters.

In this paper the filter parameters were calibrated by maximising the base flow component while at the same time minimising π_1 , π_2 and the rate of rise of the base flow. The latter criterion was necessary to prevent the parameter C from getting very large, which results in $Q_{s,t} \approx Q_t$. The maximisation of the base flow was necessary, because using only the other three criteria resulted in unrealistically low base flow estimates for Frilsham GS. The weights of the four criteria were first tested for Frilsham, where it is known that the percentage of base flow should be large (probably $> 90\%$). The resulting base flow estimates were quite sensitive to the weights and should thus be interpreted with caution. The estimated parameters k and C are 0.988 and 0.0424 for Pangbourne GS and 0.968 and 0.239 for Frilsham GS. The values for k are well within the range for base flow recession constants given by Klaassen and Pilgrim (1975).

The overall unconstrained base flow estimates ($\frac{C}{1+C-k}$) for this filter were 77.5 and 88.2% of total streamflow for Pangbourne and Frilsham, respectively (Table C.3). When the base flow is constrained to be below the total streamflow the resulting estimates are 77.4 and 88.1%, respectively. Figure C.8 shows that the base flow according to the Boughton filter shows behaviour which is intermediate between the BFI estimate (Figure C.7) and the method proposed in this paper (Figure C.6), although the percentage base flow was only just outside the range estimated for the method proposed in this paper. The Boughton filter does recognize more direct runoff than the BFI method, but the timing of the direct runoff differs considerably with method proposed in this paper (Figure C.6).

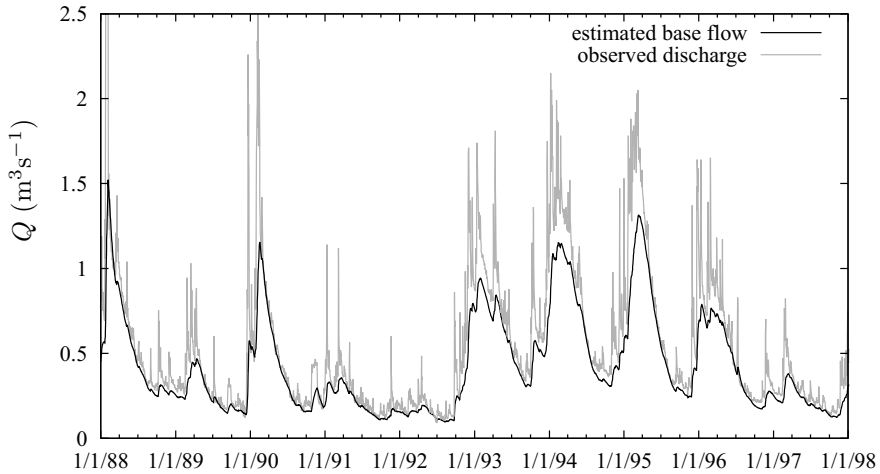


Figure C.8: Estimated base flow for Pangbourne GS using the Boughton two-parameter filter (Boughton, 1993) and observed streamflow.

C.6.3 Kliner and Kněžek filter

The third method used to compare was that developed by Kliner and Kněžek (1974). This method assumes that the lowest flow observed for a certain groundwater level is the base flow, thus providing a minimum estimate of base flow. In principle the level difference with the river stage should be used. However, by assuming that the river stage is constant or constant compared to the variations in groundwater level, the groundwater level can be used. The groundwater level data from borehole SU47/141 (Figure C.1) was used again. The relationship between base flow and groundwater level is derived by plotting total streamflow versus groundwater level and fitting an envelope as shown in Figure C.9. The difference between the Q_s-H relation for this method and the method introduced in this paper is clear when Figure C.2 and Figure C.9 are compared. For the Kliner and Kněžek method a piece-wise linear envelope was fitted to all data. It is also possible to fit an envelope to the data from each year separately (Holko *et al.*, 2002). Usually this results in higher base flow estimates. The envelope in Figure C.9 is clearly non-linear. For a linear reservoir the relationship between the groundwater level and base flow would be linear. The different parts of the envelope have been interpreted as different flow routes (base flow, interflow and overland flow) by Holko *et al.* (2002), as discharging to different levels of the drainage system (Querner, 1997) and as a sign of inherent non-linearity of the discharge process (Wittenberg, 1999). The latter is the most probable explanation of the shape of the envelope in this case. In fact, the shape is quite close to the theoretical shape for the outflow

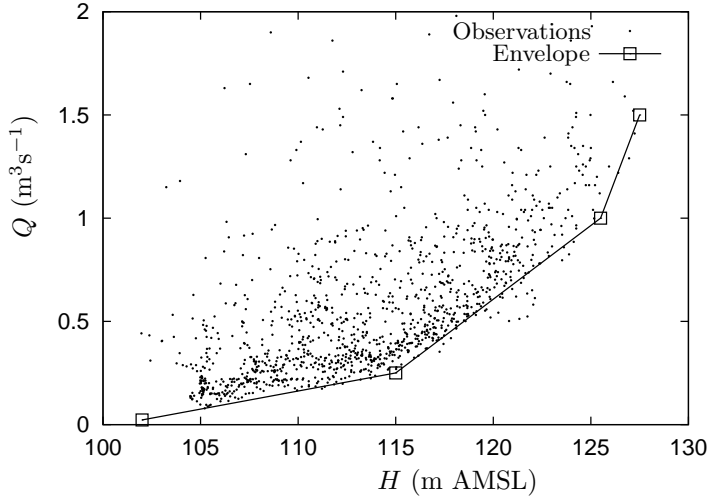


Figure C.9: Relationship between the streamflow Q at Pangbourne GS and the groundwater level H in borehole SU47/141. The envelope gives the relationship used to estimate the minimum base flow. For clarity reasons, flows larger than $2 \text{ m}^3\text{s}^{-1}$ are not plotted.

from an unconfined aquifer ($Q \sim H^2$, (Wittenberg, 1999; Troch *et al.*, 1993)), except for the highest flows ($Q > 1 \text{ m}^3\text{s}^{-1}$).

In Figure C.10 the base flow according to the Kliner and Kněžek filter is presented for Pangbourne GS. The proportion base flow was estimated at 54.8% (Table C.3), which is considerably lower than any of the other methods. For Frilsham the percentage base flow was estimated at 72.9%, which is also very low. The assumption that the lowest streamflow associated with a particular groundwater level is the base flow, ignores the large variability in recessions. Possible solutions could be fitting an envelope which excludes the lowest 5% of the observations (Troch *et al.*, 1993) and fitting an envelope for each year as mentioned before.

C.7 Discussion

The differences between the base flow estimates for Pangbourne GS are considerable, especially the differences in the temporal evolution (Figures C.6, C.7, C.8 and C.10). This can largely be explained from differences in the concept of base flow. Whereas the BFI method incorporates the interflow into the base flow, the two methods based on observed groundwater levels (this study and

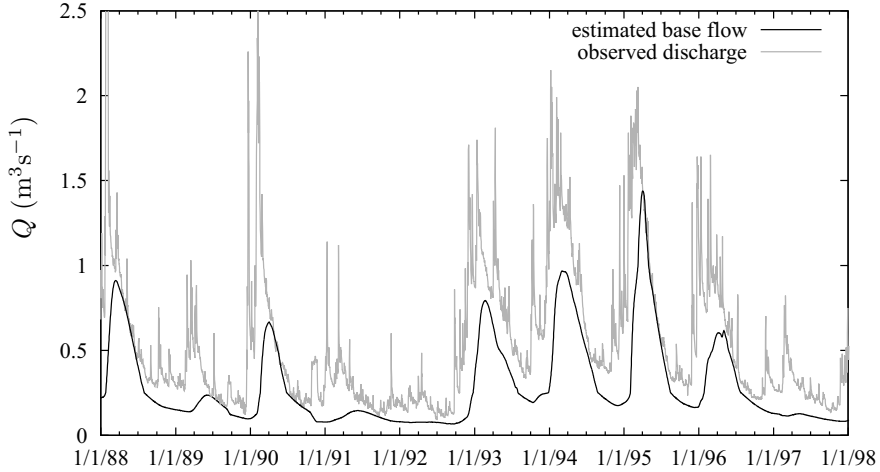


Figure C.10: Estimated base flow for Pangbourne GS using the method by Kliner and Kněžek (1974) and observed streamflow.

Kliner and Kněžek filter) do not incorporate interflow into base flow. This means, however, that care should be taken when interpreting the base flow estimates from the BFI method as derived from the saturated groundwater as has happened in the past (Bradford, 2002), because the base flow can include water from many different sources with very different response times.

As mentioned before, the base flow estimate from the method proposed in this study quite often exceeds the observed streamflow in late summer to early autumn (mostly July-August), especially for Pangbourne. If the base flow was constrained to be equal or lower than the observed streamflow, the average base flow at Pangbourne would decrease by about 3%. This overestimation can be caused by some of the processes in the stream channel, which were not taken into account, like evapotranspiration ET (Wittenberg and Sivapalan, 1999; Bond *et al.*, 2002) or bank storage (Rorabaugh, 1964; Fernald *et al.*, 2001). Considering that the periods during which the base flow is larger than observed streamflow occurs mainly during periods of quite high potential ET and recessions, ET may be responsible for the deviation. Wittenberg and Sivapalan (1999) estimate ET as 25% of the base flow in a semi-arid catchment. Bond *et al.* (2002) give estimates of 1 to 6% for a temperate marine climate with a pronounced summer season. Rough estimates show that for Frilsham, ET probably has little influence ($< 0.01 \text{ m}^3\text{s}^{-1}$), but for Pangbourne it may be noticeable at the maximum of roughly $0.04 \text{ m}^3\text{s}^{-1}$. This amount is large enough to explain many of the occasions where base flow is larger than observed streamflow.

Probably the strongest limitation or source of error in the method proposed in this paper is the reliance on one representative borehole. The groundwater level variations of this representative borehole must represent the 3-dimensional groundwater table surface. Possibly this can be approached by using the average of several boreholes (Merriam, 1948; Holko *et al.*, 2002). However, the sensitivity analysis with two other boreholes showed that in this case the selection of another borehole had little effect. A second limitation is the need for optimisation of the model parameters. First, this forces the need for simulation of the direct runoff and thus for observations of precipitation and evapotranspiration. Second, the optimisation method used in this paper includes subjective choices, for example, the parameter ranges and the number of Monte Carlo runs. Test calibrations using least-squares optimisation showed that correlation between the parameters posed a significant problem for this type of optimisation. A third limitation can be the presence of temporally variable abstractions, which change the relationship between groundwater levels and base flow. In the Pang catchment, abstraction of groundwater occurs at several locations (Pumping Stations (PS) in Figure C.1). The abstractions at Compton PS influence the base flow at Frilsham GS most. However, during the period 1993-1997 (for which the analyses were done for the Frilsham GS), the abstractions from Compton were very small. For Pangbourne GS the influence of the abstractions at Compton were estimated at around $0.1 \text{ m}^3\text{s}^{-1}$ (Estrela *et al.*, 2000b). The abstractions at Bradfield and Theale are small. The abstractions at Pangbourne PS are quite large (25 to 30 Ml d^{-1} or around $0.3 \text{ m}^3\text{s}^{-1}$). Fortunately they are rather constant over the period of analysis. Also their influence on the base flow is expected to be small compared to the amount of groundwater abstracted, because of induced recharge from the Thames and because part of the abstracted water probably comes from outside the catchment (Estrela *et al.*, 2000b).

C.8 Conclusions

Comparison of the results of four different filters shows that for the upstream station Frilsham GS (homogeneous groundwater catchment with a high component base flow) three out of four filters gave reasonably consistent estimates (88.2 - 98.6% of total streamflow). However, for the downstream station Pangbourne GS the BFI filter does not recognise that a considerable part of the flow in early winter is generated by a different source than the base flow from the Chalk aquifer, as is indicated by the filters based on groundwater levels. The BFI filter excludes the flow with very high response times from the bulk of the flow, even if the bulk is derived from sources with very different response times. The Boughton filter filter recognizes some interflow, but very differently from the filters based on groundwater levels. The two methods based on groundwa-

ter levels show that the rise of the base flow is considerably delayed compared to the total flow for Pangbourne GS. This implies that the BFI and to some extent also the Boughton filter include a component interflow in the base flow during winter. The main difference between the two methods using groundwater levels is that, unlike the method proposed in this paper, the method by Kliner and Kněžek gives a minimum value for the base flow. Thus, the base flow estimates by the Kliner and Kněžek filter are consistently lower. Drawbacks of the method introduced in this paper are the high data requirements and the need for calibration. The need for groundwater level measurements with sufficient spatial and temporal resolution may particularly limit its use.

The method introduced in this paper can separate streamflow into base flow and direct runoff, especially for non-homogeneous catchments. Despite the promising results, more tests in different hydro(geo)logical conditions are necessary to investigate if the method provides good results consistently. The role of evapotranspiration from riparian vegetation and bank storage on the base flow should also be investigated more thoroughly.

Acknowledgements The meteorological data for the Pang basin were provided by the UK Meteorological Office through the British Atmospheric Data Centre. The flow data were supplied by the Environment Agency (England and Wales). The help of Dr. L. Holko (Institute of Hydrology, Slovak Academy of Sciences) with the application of the Kliner and Kněžek method is gratefully acknowledged. The research was carried out under the Programme of the Wageningen Institute of Environment and Climate Research (WIMEK-SENSE).

Appendix D

Description of the groundwater flow model for the Pang catchment

The groundwater flow model for the Pang catchment was developed in the well-known MODFLOW code. For a description of MODFLOW see McDonald and Harbaugh (1988, 1996). The simulation period is 1960 to 1997, where 1960 is only the run-in year. The model was calibrated using PEST (Watermark Computing, 1998) for the period 1987-1997 and validated for the period 1961-1986. The recharge used as input for the model is described in Appendix A. In the following, first the model will be described, next the calibration and finally some results will be presented.

D.1 Definition of the groundwater flow model

D.1.1 Hydrogeological schematisation and discretisation

Definition of model layers The Chalk was modelled with two layers: one layer with high hydraulic conductivity representing the zone with high fissuring and a second layer representing the less fissured lower part of the aquifer. For the part of the aquifer with unconfined flow, the boundary between the two layers is assumed to be around the minimum groundwater level. Below the streams and in that part of the aquifer where it is covered by Tertiary deposits (Chapter 2), the thickness of the top layer is assumed to be 40 m. A third (bottom) layer represents the Upper Greensand. The Tertiary deposits were not included in the model, because little groundwater flow occurs in these deposits. All layers have been defined as variably confined/unconfined with a variable transmissivity and storage. The thickness of the layers was mostly determined from the hydrogeological map from the area (Institute of Geological Sciences and Thames Water Authority, 1978).

Spatial and temporal discretisation For the spatial discretisation a uniform square grid with cells of 500 by 500 m was chosen. The discretisation (Δx) was based on error functions derived by Lal (2000). The required cell size

can be estimated from:

$$\Delta x = 0.5 \sqrt{\frac{kD\varepsilon_d}{\omega S_y}} \quad (\text{D.1})$$

where kD is the transmissivity (m^2d^{-1}), ε_d is the maximum discretisation error (%), ω is the frequency of the disturbance (d^{-1}) and S_y is the specific yield (-). Using values of 100 to 500 m^2d^{-1} for kD , 5% for ε_d , 0.1 d^{-1} for ω and 0.005 to 0.03 for S_y , a cell size of 500 x 500 m was estimated as appropriate for the Pang catchment. The appropriate time step is a few days. Therefore a calculation time step of 3 d was chosen. The stress period (i.e. the period over which the boundary conditions are constant) is one month. A possibility to increase the accuracy would be to enhance the spatial resolution in those areas where high groundwater gradients occur, for example along the Pang. This was not done, however, because the first goal is to get a satisfactory overall performance of the model and not to get a detailed model of the Pang. Also the temporal and horizontal resolution are too coarse in comparison.

Boundaries Because of uncertainty about the extent of the groundwater catchment it was decided that the model had to be large enough to encompass the groundwater catchment in all situations. In general, the model boundaries are located as much as possible near streams, rivers or springs. In the north the boundary is chosen in the area, where several springs occur in the Lower Chalk (Figure D.1). The boundary in the south is along the rivers Kennet and Lambourn, in the east along the Thames. In the west the boundary is at the groundwater divide between the Pang and Lambourn. The location of this groundwater divide was checked for dry, wet and normal conditions and was found to be reasonably constant.

For the *top layer* the boundary conditions are defined as follows: the Rivers Pang, Lambourn and Winterbourne and the springs in the north and the Blue Pool are modelled as drains. This means that when the groundwater level drops below the bottom level of the drain, the stream or spring falls dry and no flow from the stream or spring to the aquifer will occur. For the springs and the intermittent parts of the stream this is conceptually right, but in the perennial part of the streams some infiltration might occur. However, this is not expected to be significant. The River Thames is modelled as a river, because the discharge of the Thames is constant enough to allow infiltration if the groundwater level drops below the river stage. In the confined area in the south, below the Kennet, a constant head boundary is specified based on observed groundwater levels. The heads were assumed constant in time. Unfortunately, because of the limited number of observations in this area the accuracy of this boundary is low. For the western boundary and the area between the springs in the north no flow conditions prevail.

For the *second model (middle) layer* no flow boundaries are specified for all

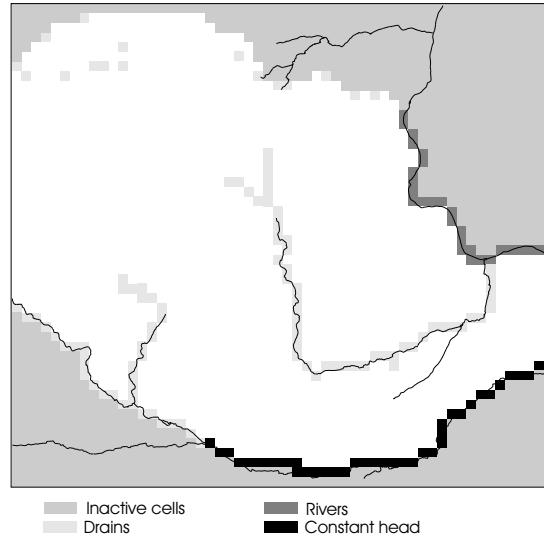


Figure D.1: Boundaries for the top layer of the groundwater flow model for the Pang catchment.

boundaries except where springs occur to this depth and in the south below the Kennet. The springs are again modelled as drain cells. In the confined zone below the Kennet again a constant head boundary was assumed. For the *bottom layer* (which represents the Upper Greensand formation) the number of boreholes is scarce, especially in the southern part of the catchment. Overall, a northwest-southeast flow is expected in this layer. Therefore part of the boundary was assigned a constant head based on the sparse observations, the remaining boundaries are no flow boundaries.

D.1.2 Input data MODFLOW

Hydraulic conductivity The values for the hydraulic conductivity for all three layers were determined during the calibration. As initial values, values in the range described in Chapter 2 (Table 2.2) were used (D.1). The hydraulic conductivity of the bottom layer and middle layer were assumed to be constant. The final zonation of the hydraulic conductivity in the top-layer is presented in Figure D.2.

Storage properties Two different types of parameters are necessary to describe the storage properties. One which represents the changes in storage under unconfined conditions (specific yield S_y (-)) and the other which repre-

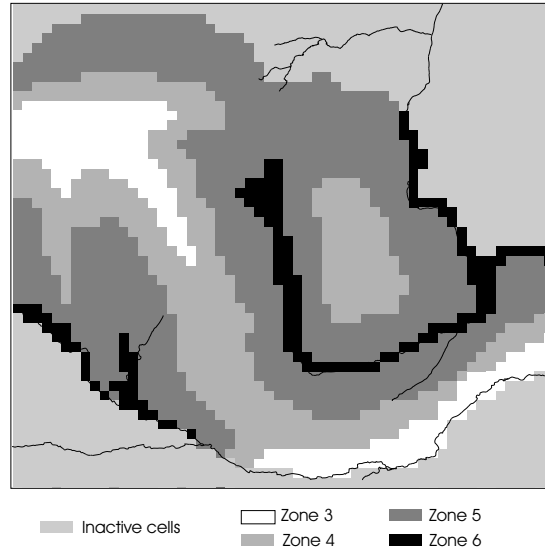


Figure D.2: Zonation of the hydraulic conductivity k of the top layer of the Pang catchment model after calibration.

sents the storage under confined conditions (specific storage S_s (m^{-1})). The specific yield follows approximately the same pattern as the hydraulic conductivity. It is higher in the river valleys than on the interfluvies. The specific yield is divided in two zones in the top layer and is constant for the two lower layers. In Figure D.3 the zonation of the specific yield for the top layer is presented. The specific yield of the top and middle layer were included in the calibration. The specific yield of the bottom layer was assumed to be constant at 0.001 and was not included in the calibration because unconfined conditions hardly ever occur in this layer. The specific storage S_s is constant throughout the model and has a value of 1.10^{-5} m^{-1} .

Rivers, streams and springs All the river and drain boundaries need a level and conductance as input data. For the drain cells the level is the bottom of the stream, for the river cells it is the surface water level. These levels have been derived from different sources. For the Lambourn and Winterbourne the levels were derived from the 1:50 000 Ordnance Survey map from 1993/94 with a contour interval of 10 m. The values for the Thames were derived from a Digital Terrain Model (from the former Institute of Hydrology, Wallingford, UK) with a horizontal resolution of 50 m and a vertical resolution of 0.1 m. The level data for the Pang were derived from fieldwork, three survey maps from the NRA and the 1:25 000 Ordnance Survey map from 1985 and 1990 with a contour interval of 5 m.

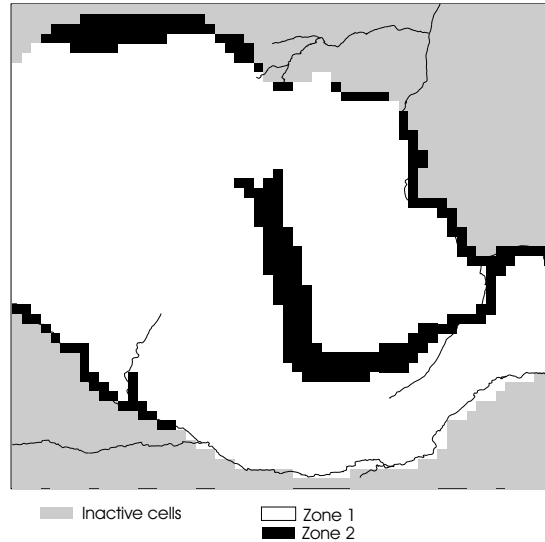


Figure D.3: Zonation for the specific yield S_y for the top layer of the Pang catchment model.

The streams that are in direct hydraulic contact with the Chalk were assumed to have a high conductance (up to $3000 \text{ m}^2 \text{ d}^{-1}$). These are the Lambourn, the Winterbourne and the upper reaches of the Pang. In the valleys of the lower reaches of the Pang low-permeability Tertiary deposits are expected in the alluvium. Therefore the lower reaches of the Pang (and other areas where the valley fillings have a lower conductivity) have a lower conductance of $1500 \text{ m}^2 \text{ d}^{-1}$. The conductance of the river Thames was taken to be around $500 \text{ m}^2 \text{ d}^{-1}$ depending on the length of the river in that particular cell. The springs in the north which were modelled as drain cells were assumed to have a conductance of $1000 \text{ m}^2 \text{ d}^{-1}$.

Abstractions In Figure C.1 the location of the abstraction wells is presented. Only the main pumping stations, which are located in the model area, were incorporated in the model: Pangbourne, Compton and Bradfield. In Chapter 2 the historical abstraction rates were discussed. All pumping stations abstract groundwater from the Chalk aquifer. The abstractions from Gatehampton and Cleeve were not incorporated in the model, because it is expected that these have only a small influence on the groundwater flow in the catchment. The abstractions at Pangbourne pumping station were not entered in the model for the full amount but only 75% of the total amount. This was done, because the pumping station is very close to the model boundary and it is likely that the pumping station draws part of its water from outside the model area. The

Table D.1: Overview of the parameters optimized during the calibration. The zonation of the conductivity and the specific yield are presented in Figures D.2 and D.3

Name	Transformation	Initial value	Range	Final value
K3 (m d ⁻¹)	log	1	0.1-50	4.6
K4 (m d ⁻¹)	log	4	0.1-100	4.0
K5 (m d ⁻¹)	log	25	1-100	17.9
K6 (m d ⁻¹)	log	30	5-200	24.6
Km (m d ⁻¹)	log	2	0.01-50	0.074
Kb (m d ⁻¹)	log	1	0.01-50	0.36
Sy1 (-)	log	$2 \cdot 10^{-3}$	10^{-15} -0.5	$4.0 \cdot 10^{-3}$
Sy2 (-)	log	$2 \cdot 10^{-3}$	10^{-15} -0.5	$2.0 \cdot 10^{-2}$
Sym (-)	log	$2 \cdot 10^{-3}$	10^{-15} -0.5	$7.9 \cdot 10^{-2}$

amount of 75% was selected because the model boundary is on one of the four sides of the cell in which the abstractions are located.

D.2 Calibration

The transient groundwater model was calibrated using PEST for the period 1987-1997. The period 1961-1986 was used for validation. Because the interest in this study is not in the specific details of the Pang catchment itself, a detailed fit between observed and simulated groundwater levels and discharge is of less importance.

D.2.1 Input for PEST

The following parameters were optimised during the calibration:

- hydraulic conductivity of all zones for all layers. The parameters for layer 1 (top layer) are called K3 to K6 following the zone numbering in Figure D.2. The name for layer 2 (middle layer) is Km, for layer 3 (bottom layer) it is Kb.
- specific yield of first two layers. The parameters are called Sy1 and Sy2 for layer 1 (see Figure D.3 for the zones). For layer 2 it is Sym.

In Table D.1 some important values are listed for these parameters.

The following observations were used to calibrate the model:

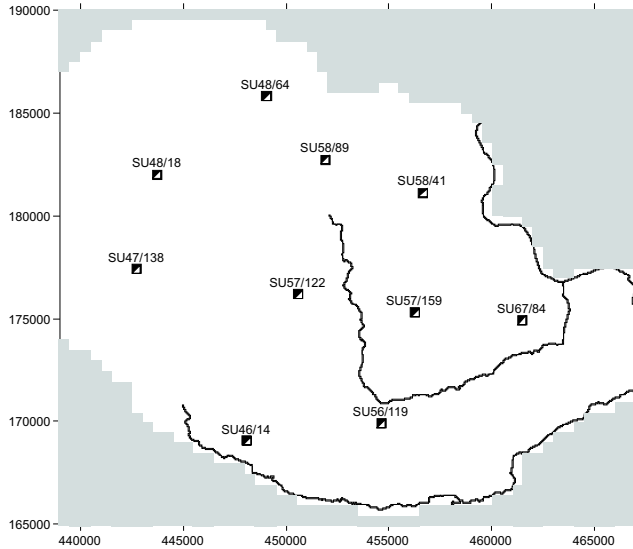


Figure D.4: Location of the 10 observation boreholes used for calibration of the groundwater model. Grey indicates inactive cells.

- groundwater level at 10 locations (Figure D.4);
- discharge Q at Frilsham GS (Gauging Station) (Figure 2.1);
- prior information that the hydraulic conductivity is larger near the stream than near the interfluves.

Only the discharge at Frilsham GS was used, because the discharge at this gauging station is mostly groundwater discharge (Appendix C). The prior information regarding the hydraulic conductivity was used to ensure that the hydraulic conductivity decreases from the stream to the groundwater divide. In Table D.2 presents how this is implemented in PEST.

Because of the difference in standard deviation and the difference in the number of observations, the observations and prior information needed to be weighted. Different weighting schemes were explored during the calibration. Initially the groundwater levels, discharge and prior information were weighted as 45 (4.5 per head observation location), 45 and 10 (100 in total). However, the weights for the prior information appeared to be too high and were decreased to 1 each, bringing the total weights to 93. In Table D.2 the weights used in the final optimisation run are presented. The following equation was used to

Table D.2: Weighting of the observations and prior information.

Name	Number of observations	σ	Weight
SU46/14	524	1.16 m	$7.4 \cdot 10^{-3} \text{ m}^{-1}$
SU47/138	553	5.19 m	$1.6 \cdot 10^{-3} \text{ m}^{-1}$
SU48/18	113	3.54 m	$1.1 \cdot 10^{-2} \text{ m}^{-1}$
SU48/64	100	3.98 m	$1.1 \cdot 10^{-2} \text{ m}^{-1}$
SU56/119	545	0.85 m	$9.7 \cdot 10^{-3} \text{ m}^{-1}$
SU57/122	114	3.77 m	$1.0 \cdot 10^{-2} \text{ m}^{-1}$
SU57/159	558	3.28 m	$2.5 \cdot 10^{-3} \text{ m}^{-1}$
SU58/41	38	4.73 m	$4.0 \cdot 10^{-2} \text{ m}^{-1}$
SU58/89	548	2.94 m	$1.7 \cdot 10^{-3} \text{ m}^{-1}$
SU67/84	112	2.01 m	$2.0 \cdot 10^{-2} \text{ m}^{-1}$
Q at Frilsham	119	$17447 \text{ m}^3\text{d}^{-1}$	$2.2 \cdot 10^{-5} \text{ m}^{-3}\text{d}^1$
Prior 1	1	K3:K4 = 1:2	1
Prior 2	1	K3:K5 = 1:4	1
Prior 3	1	K3:K6 = 1:6	1

calculate the weights per groundwater level observation:

$$w_i = \frac{4.5}{n_i \sigma_i} \quad (\text{D.2})$$

where w_i is the weight per observation for borehole location i , n_i is the number of observations for location i and σ_i is the standard deviation for location i . And for the discharge:

$$w = \frac{45}{n\sigma} \quad (\text{D.3})$$

During the calibration process the zonation of the hydraulic conductivity and storage was adapted to improve the model fit, but only as far as seemed reasonable from the literature. For example, between the Thames and the Pang the simulated heads were consistently too high. Initially the hydraulic conductivity around the Thames was not particularly high. However, it is reasonable to assume that a large river has a large zone of widened fissures and thus the conductivity near the Thames was increased. The boundary between the top and middle layer was slightly modified in some places. During initial calibration runs, it appeared that the aquifer was essentially isotropic (both horizontally and vertically) and thus anisotropy was not taken into account in the final optimisation runs. The conductivity of the drains and rivers was not included in the automatic calibration, but the conductivity of the Pang was varied to assess the sensitivity. The initial values for all parameters were varied, but this had little influence on the final result.

D.2.2 Results of the calibration and validation

During the final calibration run the parameters showed low correlations. The highest correlation was -0.69 and occurred between K5 (hydraulic conductivity zone 5 in Figure D.2) and Kb (hydraulic conductivity of the bottom layer). The second highest was -0.55 between K4 and Km. The sensitivity of most parameters was quite stable from run to run. The most sensitive parameter was K5, followed by Sy1 (specific yield of most of the top layer). The parameter with the lowest sensitivity was Sym (specific yield of the middle layer).

In Table D.3 the overall performance for the final run is presented. First the contribution to the objective function ϕ is presented. In the other columns the Nash-Sutcliffe efficiency criterion R^2 , the bias B_s and the cross-correlation coefficient between the observed and simulated values ρ are presented. For those observation series with sufficient data, the series has been divided in two parts: the calibration part 1987 to 1997 and the validation part 1960 to 1986. To avoid influence of the starting value, both for the calibration and the validation the first year has not been taken into account for determining the performance.

For borehole SU58/41 (Figure D.4), the contribution to the objective function is particularly high, namely around 45% of the total contribution of the hydraulic heads to the objective function (Table D.3). As discussed before, groundwater levels in this area between the Pang and the Thames were overestimated. Increasing the hydraulic conductivity reduced the error. However, further increase of the hydraulic conductivity did not seem reasonable. Possibly, the number of springs at the boundary north of this area was underestimated. Moreover in the observations a very strong local gradient is observed in this area, for which no explanation is known. This can be seen by comparing the bias for SU58/41 and SU58/89.

For most of the boreholes the observed groundwater level is overestimated (positive bias), while the discharge at Frilsham GS is slightly underestimated. The model efficiency for most boreholes is very low. Partially this is explained because many boreholes show a bias, which strongly decreases the model efficiency. The correlation shows a much better fit between simulated and observed. For model efficiency and bias, the model performs about equally well in the calibration and validation period. However, for the correlation the performance is consistently better in the calibration period.

The simulated average groundwater discharge at Pangbourne GS for the whole simulation period is $0.32 \text{ m}^3\text{s}^{-1}$, which is too low compared to the base flow estimates in Appendix C, which are 0.40 to $0.46 \text{ m}^3\text{s}^{-1}$. The simulated average discharge of the Blue Pool was $0.14 \text{ m}^3\text{s}^{-1}$, whereas the observed average discharge is around $0.2 \text{ m}^3\text{s}^{-1}$ (Chapter 2).

Table D.3: Model fit: contribution to the objective function ϕ (-), model efficiency R^2 , bias B_s (-) and cross-correlation coefficient ρ for the calibration period 1988-97 and the validation period 1961-86.

Name	ϕ (-)	R^2 (-)		B_s		ρ (-)	
		1961-86	1988-97	1961-86	1988-97	1961-86	1988-97
SU46/14	0.15	-5.3	-5.8	2.4 m	2.5 m	0.82	0.91
SU47/138	0.04	-0.4	-0.1	4.6 m	4.2 m	0.84	0.93
SU48/18	0.57	-3.8	-4.6	0.4 m	0.6 m	0.63	0.83
SU48/64 ^a	0.42		-4.6		-4.0 m		0.48
SU56/119	0.48	-7.8	-8.4	2.3 m	2.5 m	0.43	0.74
SU57/122	0.06	0.4	0.6	-0.3 m	0.5 m	0.76	0.92
SU57/159	0.01	0.7	0.6	1.1 m	1.2 m	0.87	0.92
SU58/41	1.83	-4.4	-2.4	5.7 m	3.9 m	0.75	0.72
SU58/89	0.08	-2.3	-1.3	-6.1 m	-5.7 m	0.57	0.90
SU67/84	0.53	0.1	-0.7	0.4 m	-2.0 m	0.51	0.53
Q (Frilsham)	3.49		0.76		-0.03 m ³ s ⁻¹		0.89
Prior 1-3	0.13						

^aData only available from 1990 to 1997

D.3 Simulated hydraulic heads and discharge

In this section some examples of the temporal variation of the simulated discharge and hydraulic heads are shown. In Figure D.5 the simulated and observed discharge at Frilsham GS are shown. In the years 1993 and 1994, following on the drought in 1988-1992 the discharge appears to be underestimated. In 1996 and 1997 the discharge is somewhat overestimated.

In Figure D.6 two examples of time series of observed groundwater levels and simulated hydraulic heads are shown. Figure D.6a (SU47/138) is a boreholes where the groundwater level is reproduced reasonably well. The temporal variation of the simulations is very close to the temporal variation of the observations. The absolute level of the groundwater level is overestimated. Figure D.6b shows an example where the temporal variation of the groundwater level is represented particularly bad, although the average simulated head is close to the average observed head for the total series. It is not clear why the observed groundwater level at this borehole shows this strong inter-annual variability. The borehole is quite close to the abstraction boreholes at Pangbourne, but shows little relation with the abstractions there.

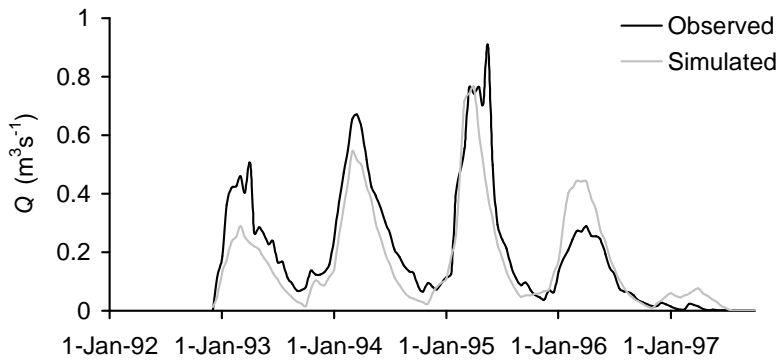


Figure D.5: Comparison of simulated and observed discharge Q at Frilsham GS for the period 1992-97.

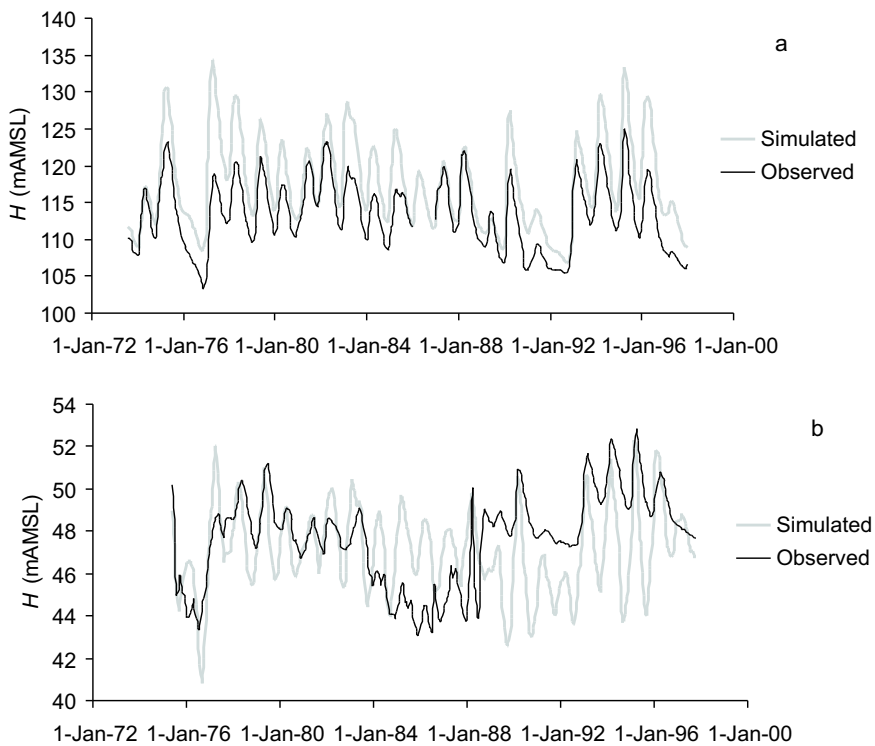


Figure D.6: Comparison of simulated and observed head H (m AMSL) at two locations: a) SU47/138 and b) SU 67/84.

Bibliography

- Acreman M, Almagro J, Alvarez J, Bouraoui F, Bradford R, Bromley J, Crooks S, Cruces J, Dolz J, Dunbar M, Estrela T, Fernandez-Carrasco P, Fornes J, Gustard A, Haverkamp R, de la Hera A, Hernández-Mora N, Llamas R, Cortina LM, Papamastorakis J, Ragab R, Sánchez M, Vardavas I, Webb T, 2000. *Technical Report to the European Union - Groundwater and River Resources Programme on a European Scale (GRAPES)*. Institute of Hydrology, Wallingford, UK.
- Ahn H, 2000. Modeling of groundwater heads based on second-order difference time series models. *J. of Hydrology* **234**: 82–94.
- Allen DJ, Brewerton LJ, Coleby LM, Gibbs BR, Lewis MA, Macdonald AM, Wagstaff SJ, Williams AT, 1997. *The Physical Properties of Major Aquifers in England and Wales*. British Geological Survey and Environment Agency.
- Altman SJ, Arnold BW, Barnard RW, Barr GE, Ho CK, McKenna SA, Eaton RR, 1996. *Flow Calculations for Yucca Mountain, Groundwater Travel Time (GWTT-95)*. Tech. rep., Sandia report SAND96-0819.
- Banks D, Davies C, Davies W, 1995. The Chalk as a karstic aquifer: evidence from a tracer test at Stanford Dingley, Berkshire, UK. *Quart. J. of Engineering Geology* **28**: 31–38.
- Beran M, Rodier JA, 1985. *Hydrological Aspects of Drought*. Studies and Reports in Hydrology 39, UNESCO-WMO, Paris, France.
- Beven K, Binley A, 1992. The future of distributed models: Model calibration and uncertainty prediction. *Hydrological Processes* **6**: 279–298.
- Birtles AB, Wilkinson WB, 1975. Mathematical simulation of groundwater abstraction from confined aquifers for river regulation. *Water Resources Research* **11**(4): 571–580.
- Bloomfield J, 1996. Characterisation of hydrogeologically significant fracture distributions in the Chalk: An example from the Upper Chalk of southern England. *J. of Hydrology* **184**: 355–379.
- Bloomfield JP, Brewerton LJ, Allen DJ, 1995. Regional trends in matrix porosity and dry density of the Chalk of England. *Quarterly J. of Engineering Geology* **28**: 131–142.
- Bond B, Jones JA, Moore G, Phillips N, Post D, McDonnell JJ, 2002. The zone of vegetation influence on baseflow revealed by diel patterns of streamflow and vegetation water use in a headwater basin. *Hydrological Processes* **16**: 1671–1677.
- Boons-Prins ER, de Koning GHJ, van Diepen CA, Penning de Vries FWT, 1993. *Crop-Specific Simulation Parameters for Yield Forecasting Across the European Community*. Tech. rep., CABO-TT, Wageningen.
- Boughton WC, 1993. A hydrograph-based model for estimating the water yield of ungauged catchments. In *Hydrology and Water Resources Symp., Institution of Engineers Australia, Newcastle, NSW*. 317–324.
- Bradford RB, 2000. Drought events in Europe. In Vogt JV, Somma F (eds) *Drought and Drought Mitigation in Europe*. Kluwer Academic Publishers, 7–20.
- Bradford RB, 2002. Controls on the discharge of Chalk streams of the Berkshire Downs, UK. *The Science of the Total Environment* **282-283**: 65–80.
- Brandsma T, Buishand TA, 1998. Simulation of extreme precipitation in the Rhine basin by nearest-neighbour resampling. *Hydrology and Earth System Sciences* **2**(2): 195–209.
- Bras RL, Rodriguez-Iturbe I, 1985. *Random Functions and Hydrology*. Addison-Wesley: Reading.
- Bredehoeft J, 1997. Safe yield and the water budget myth. *Ground Water* **35**(6): 929.
- Bredehoeft J, 2002. The water budget myth revisited: Why hydrogeologists model. *Ground*

- Water* **40**(4): 340–345.
- Brutsaert W, Nieber JL, 1977. Regionalized drought flow hydrographs from a mature glaciated plateau. *Water Resources Research* **13**(3): 637–643.
- Bryant SJ, Arnell NW, Law FM, 1994. The 1988-92 drought in its historical perspective. *J. Institution Wat. Env. Man.* **8**(1): 39–51.
- Burns DA, 2002. Stormflow- separation based on isotopes: The thrill is gone - what's next. *Hydrological Processes* **16**: 1515–1517.
- Buttle JM, 1994. Isotope hydrograph separations and rapid delivery of pre-event water from drainage basins. *Progress in Physical Geography* **18**: 16–41.
- Calow R, Robins N, Macdonald A, Nicol A, 1999. Planning for groundwater drought in Africa. In *Proceedings of the international conference on integrated drought management: lessons for Sub-Saharan Africa*. IHP-V, Technical Documents in Hydrology, No. 35, 255–270.
- Caruso BS, 2002. Temporal and spatial patterns of extreme low flows and effects on stream ecosystems in Otago, New Zealand. *J. of Hydrology* **257**: 115–133.
- Chang TJ, Kleopa XA, 1991. A proposed method for drought monitoring. *Water Resources Bulletin* **27**(2): 275–281.
- Chang TJ, Teoh CB, 1995. Use of the kriging method for studying characteristics of ground water droughts. *J. of the American Water Resources Association* **257**: 1001–1007.
- Changnon S, 1987. *Detecting Drought Conditions in Illinois*. Illinois State Water Survey Circular 164-87.
- Changnon SA, Huff FA, Hsu CF, 1988. Relations between precipitation and shallow groundwater in Illinois. *J. of Climate* **1**(12): 1239–1250.
- Chapman TG, 1999. A comparison of algorithms for stream flow recession and base flow separation. *Hydrological Processes* **13**(5): 701–714.
- Charalambous AN, Buckle DJE, Sage R, Aldous PJ, 1995. Contribution of river flow seepage to borehole yields and its implication for source protection zone definition. In Younger PL (ed) *Modelling River-Aquifer Interactions*. 147–164.
- Chiew FHS, McMahon TA, 2002. Global ENSO-streamflow teleconnection, streamflow forecasting and interannual variability. *Hydrological Sciences J.* **47**: 505–522.
- Clark C, 1993. How dry is a drought? *Crossosoma* **19**(2): 37–48.
- Correia FN, Santos MA, Rodrigues RR, 1986. Risk, resilience and vulnerability in regional drought studies. In Valadares Tavares L, Evaristo Da Silva J (eds) *Systems Analysis Applied to Water and Related Land Resources. Proceedings of the IFAC Conference, Lisbon, Portugal, 2-4 October 1985*. Pergamon Press, Tarrytown, N.Y.
- Cramer H, Leadbetter MR, 1967. *Stationary and Related Stochastic Processes : Sample Function Properties and their Applications*. Wiley, New York.
- Cunnane C, 1979. A note on the poisson assumption in partial duration series models. *Water Resources Research* **15**(2): 489–494.
- Custodio E, 2000. *The Complex Concept of Overexploited Aquifer*. Proyecto Aguas Subterráneas. Serie A, El Uso Intensivo de Las Aguas Subterráneas, Fundación Marcelino Botín, Madrid.
- Day JBW, Rodda JC, 1978. The effects of the 1975-76 drought on groundwater and aquifers. *Proc. R. Soc. London* **363**: 55–68.
- de Vries JJ, 1974. *Groundwater Flow Systems in the Netherlands. A Groundwater-Hydrological Approach to the Functional Relationship Between the Drainage System and the Geological and Climatological Conditions in a Quarternary Accumulation Area*. Ph.D. thesis, Free University of Amsterdam.
- de Vries JJ, 1995. Seasonal expansion and contraction of stream networks in shallow groundwater systems. *J. of Hydrology* **170**: 15–26.
- de Zeeuw JW, Hellinga F, 1958. Precipitation and runoff (original title: Neerslag en afvoer). *Landbouwkundig Tijdschrift* **70**: 405–422. (in Dutch).
- Delworth T, Manabe S, 1989. The influence of soil wetness on near-surface atmospheric

- variability. *J. of Climate* **2**: 1447–1462.
- Demuth S, Lehner B, Stahl K, 2000. Assessment of the vulnerability of a river system to drought. In Vogt JV, Somma F (eds) *Drought and Drought Mitigation in Europe*. Kluwer Academic Publishers, 209–219.
- Demuth S, Young A, Hisdal H, Tallaksen LM, 2004. Regional estimation methods. In Tallaksen LM, van Lanen HAJ (eds) *Hydrological Drought: Processes and Estimation Methods for Streamflow and Groundwater*, Elsevier, chap. 8.
- Deutscher Verband Für Wasserwirtschaft und Kulturbau (ed) 1998. *How to Work Out a Drought Mitigation Strategy: An ICID Guide*. DVWK, Bonn. Comp. by L. Vermes.
- Dingman SL, 2002. *Physical Hydrology*. Prentice-Hall, New Jersey.
- Dolman AJ, Moors EJ, 1994. *Hydrology and Water Resources of Woodlands in the Netherlands. Phase 1: Testing Instrumentarium (Original Title: Hydrologie en Waterhuishouding van Bosgebieden in Nederland. Fase 1: Toetsing Instrumentarium)*. Tech. rep., DLO-Staring Centre, Wageningen.
- Domenico PA, Schwartz FW, 1998. *Physical and Chemical Hydrogeology*. John Wiley and sons, New York. 2nd ed.
- Dooge JCI, 1973. *Linear Theory of Hydrologic Systems*. Agricultural Research service, Washington DC. Reproduced by European Geosciences Union, 2003.
- Douglas EM, Vogel RM, Kroll CN, 2002. Impact of streamflow persistence on hydrologic design. *J. of Hydrologic Engineering* **7**(3): 220–228. DOI: 10.1061/(ASCE)1084-0699(2002)7:3(220).
- Downing R, Price M, Jones GP, 1993. *The Hydrogeology of the Chalk of North-West Europe*. Clarendon Press, Oxford.
- Dracup JA, Lee KS, Paulson Jr EG, 1980. On the definition of droughts. *Water Resources Research* **16**(2): 297–302.
- Driessen PM, Dudal R, 1991. *The major soils of the world, lecture note on their geography, formation, properties and use*. Wageningen Agricultural University and Katholieke Universiteit Leuven.
- Eltahir EAB, Yeh PJJ, 1999. On the asymmetric response of aquifer water level to floods and droughts in Illinois. *Water Resources Research* **35**(4): 1199–1217.
- Entekhabi D, 1994. A simple model of the hydrological cycle and climate: 1. model construct and sensitivity to the land surface boundary. *Adv. In Water Resources* **17**: 79–91.
- Estrela T, Bradford R, Vardavas I, 2000a. Catchment management planning. In Acreman *et al. Technical Report to the European Union ENV4 - CT95-0186 - Groundwater and River Resources Programme on a European Scale (GRAPES)*, Institute of Hydrology, Wallingford (UK), chap. 3. 149–245.
- Estrela T, Crooks S, Croke B, 2000b. Conceptual groundwater/surface water modelling. In Acreman *et al. Technical Report to the European Union ENV4 - CT95-0186 - Groundwater and River Resources Programme on a European Scale (GRAPES)*, Institute of Hydrology, Wallingford (UK), chap. 2.2. 91–117.
- Estrela T, Marcuello C, Iglesias A, 1996. *Water Resources Problems in Southern Europe*. European Environment Agency.
- Estrela T, Quintas L, 1996. A distributed model for water resources assessment in large basins. In *Proc. Of 1st Int. Conf. On Rivertech 96. IWRA. Chicago, USA, September 1996*. 861–868.
- Feddes RA, Lenselink KJ, 1994. Evapotranspiration. In Ritzema HP (ed) *Drainage Principles and Applications*. 145–174. ILRI Publication no. 16.
- Federal Emergency Management Agency, 1995. *National Mitigation Strategy, Partnerships for Building Safer Communities*. Tech. rep., Federal Emergency Management Agency, Washington DC.
- Fernald AG, Wigington Jr PJ, Landers DH, 2001. Transient storage and hyporheic flow along the Willamette river, Oregon: Field measurements and model estimates. *Water Resources Research* **37**(6): 1681–1694.

- Fernández B, Salas JD, 1999. Return period and risk of hydrological events, II: Applications. *J. of Hydrologic Engineering* **4**(4): 308–316.
- Foster S, 2000. *Sustainable Groundwater Exploitation for Agriculture; Current Issues and Recent Initiatives in the Developing World*. Proyecto Aguas Subterráneas. Serie A, El Uso Intensivo de Las Aguas Subterráneas, Fundación Marcelino Botín, Madrid.
- Freer J, Beven K, Ambrose B, 1996. Bayesian estimation of uncertainty in runoff prediction and the value of data: An application of the GLUE approach. *Water Resources Research* **32**(7): 2161–2173.
- Fuchs L, Rubach H, 1983. Low water analysis under the special consideration of a regional prediction (original title: Niedrigwasseranalyse unter besonderer berücksichtigung einer regionalen aussage). *Wasser und Boden* **35**(1): 13–17.
- Furey PR, Gupta VK, 2001. A physically based filter for seperating base flow from streamflow time series. *Water Resources Research* **37**(11): 2709–2711.
- Garanganga BJ, 1999. Role of regional climate system monitoring and prediction in drought management. In *Proceedings of the International Conference on Integrated Drought Management: Lessons for Sub-Saharan Africa. 20-22 September 1999, Pretoria, South-Africa*. IHP-V, Technical Documents in Hydrology, No. 35, 255–270.
- Gash JHC, 1979. An analytical model of rainfall interception by forests. *Quarterly J. Royal Meteorological Society* **105**: 43–55.
- Geake AK, Foster SSD, 1989. Sequential isotope and solute profiling in the unsaturated zone of British chalk. *Hydrological Sciences J.* **34**: 79–95.
- Gehrels JC, van Geer FC, de Vries JJ, 1994. Decomposition of groundwater level fluctuations using transfer modelling in an area with shallow to deep unsaturated zones. *J. of Hydrology* **157**: 105–138.
- Gottschalk L, Perzyna G, 1989. A physically based distribution function for low flow. *Hydrological Sciences J.* **34**(5): 559–573.
- Gottschalk L, Perzyna G, 1993. Low flow distribution along a river. In Kundzewicz ZW, Rosbjerg D, Simonovic SP, Takeuchi K (eds) *Extreme hydrological event: floods and droughts (proceedings of the Yokohama symposium, July 1993)*. IAHS, Wallingford, UK.
- Gottschalk L, Tallaksen LM, Perzyna G, 1997. Derivation of low flow distribution functions using recession curves. *J. of Hydrology* **194**: 239–262.
- Gregory PJ, 1989. Depletion and movement of water beneath cereal crops grown on a shallow soil overlying chalk. *J. of Soil Science* **40**: 513–523.
- Groundwater and River Resources Action Programme (GRAPES), 1998. *Second annual report to the European commission*. Tech. rep., Institute of Hydrology, UK.
- Guerrero-Salazar P, Yevjevich V, 1975. *Analysis of Drought Characteristics by the Theory of Runs*. Colorado State University, Fort Collins, Colorado.
- Gupta HV, Sorooshian S, Yapo PO, 1998. Toward improved calibration of hydrologic models: Multiple and noncommensurable measures of information. *Water Resources Research* **34**(4): 751–763.
- Halford KJ, Mayer GC, 2000. Problems associated with estimating ground water discharge and recharge from stream-discharge records. *Ground Water* **38**(3): 331–342.
- Hall F, 1968. Base-flow recessions - a review. *Water Resources Research* **4**(5): 975–983.
- Hall J, Anderson M, 2002. Handling uncertainty in extreme or unrepeatable hydrological processes - the need for an alternative paradigm. *Hydrological Processes* **16**: 1867–1870.
- Hashimoto T, Stedinger JR, Loucks DP, 1982. Reliability, resiliency, and vulnerability criteria for water resources system performance evaluation. *Water Resources Research* **18**(1): 14–20.
- Headworth HM, Owen M, Skinner A, 1983. River augmentation schemes using groundwater. *British Geologist* **9**(2): 50–54.
- Hertzler RA, 1939. Engineering aspects of the influence of forests on mountain streams. *Civil Engineering* **9**: 487–489.

- Hipel KW, McLeod AI, 1994. *Time Series Modelling of Water Resources and Environmental Systems*. Developments in Water Science, 45. Elsevier Science, Amsterdam.
- Hisdal H, Clausen B, Gustard A, Peters E, Tallaksen L, 2004. Event definitions and indices. In Tallaksen LM, van Lanen HAJ (eds) *Hydrological Drought, Processes and Estimation Methods for Streamflow and Groundwater*, Elsevier, chap. 5.
- Hisdal H, Tallaksen LM, 2000. *Drought event definition*. ARIDE Technical Report No. 6, University of Oslo, Oslo, Norway.
- Hisdal H, Tallaksen LM, Frigessi A, 2002. Handling non-extreme events in extreme value modelling of streamflow droughts. In van Lanen HAJ, Demuth S (eds) *FRIEND2002 Bridging the Gap between Theory and Practice*. IAHS Publication no. 274, 281–288.
- Hisdal H, Tallaksen LM, Peters E, Stahl K, Zaidman M, 2001. Drought event definition. In Demuth S, Stahl K (eds) *Assessment of the Regional Impact of Droughts in Europe. Final Report to the European Union ENV-CT97-0553*, Institute of Hydrology, University of Freiburg, chap. 3. 17–26.
- Holko L, Herrmann A, Uhlenbrook S, Pfister L, Querner EP, 2002. Groundwater runoff separation - test of applicability of a simple separation method under varying natural conditions. In van Lanen HAJ, Demuth S (eds) *FRIEND2002 Bridging the Gap between Theory and Practice*. IAHS Publication no. 274, 101–108.
- Hough MN, 1990. *Agrometeorological Aspects of Crops in the United Kingdom and Ireland : A Review for Sugar Beet, Oilseed Rape, Peas, Wheat, Barley, Oats, Potatoes, Apples and Pears*. Tech. rep., Commission of the European Communities, Luxembourg.
- Illston BG, Basara JB, 2003. Analysis of short-term droughts in Oklahoma. *EOS* **84**(17): 157,161.
- Institute of Geological Sciences and Thames Water Authority, 1978. *1:100 000 Hydrogeological Map of the South West Chilterns and the Berkshire and Marlborough Downs*. Natural Environment Research Council.
- Institute of Hydrology, 1980. *Low Flow Studies*. Tech. rep., Institute of Hydrology, Wallingford, UK.
- Jackson RB, Canadell J, Ehleringer JR, Mooney HA, Sala O, Schulze E, 1996. A global analysis of root distributions for terrestrial biomes. *Oecologia* **108**: 389–411.
- Kašpárek L, Novický O, 1997. Application of a physically based model to identify factors causing hydrological drought in western and central European basins. In Gustard A, Blazkova S, Brilly M, Demuth S, Dixon J, van Lanen H, Llasat C, Mkhani S, Servat E (eds) *FRIEND'97-Regional Hydrology: Concepts and Models for Sustainable Water Resource Management*, IAHS Publication no. 246.
- Kendall C, McDonnell JJ, 1998. *Isotope Tracers in Catchment Hydrology*. Elsevier science Publishers, Amsterdam.
- Kendy E, 2003. The false promise of sustainable pumping rates. *Ground Water* **41**(1): 2–4.
- Kjeldsen TR, Lundorf A, Rosbjerg D, 2000. Use of a two-component exponential distribution in partial duration modelling of hydrological droughts in Zimbabwean rivers. *Hydrological Sciences J.* **45**(2): 285–298.
- Kjeldsen TR, Rosbjerg D, 2001. A framework for assessing the sustainability of a water resources system. In Schumann A (ed) *Regional Management of Water Resources (Proceedings of a Symposium Held During the Sixth IAHS Scientific Assembly at Maastricht, The Netherlands, July 2001)*. IAHS Publication No. 268, 107–113.
- Klaassen B, Pilgrim DH, 1975. Hydrograph recession constants for New South Wales streams. *Civil Engineering Transactions* **CE17**: 43–49.
- Klemeš V, 2000. Tall tales about tails of hydrological distributions II. *J. of Hydrologic Engineering* **5**(3): 232–239.
- Klemeš V, Srikanthan R, McMahon TA, 1981. Long-memory flow models in reservoir analysis: What is their practical value? *Water Resources Research* **17**(3): 737–751.
- Klinck BA, Hopson PM, Lewis MA, Macdonald DMJ, Inglethorpe SDJ, Entwisle DC, Harrington JF, Williams L, 1998. *The Hydrogeological Behaviour of the Clay-with-Flints of*

- Southern England*. British Geological Survey.
- Kliner K, Kněžek M, 1974. The underground runoff separation method making use of the observation of groundwater table (Original title: Metoda separace podzemního odtoku při využití pozorování hladiny podzemní vody). *J. Hydrol. and Hydrodynamics* **XXII**(5): 457–466.
- Kogan F, 2002. World droughts in the new millenium from AVHRR-based vegetation health indices. *EOS* **83**(48).
- Kraijenhof van de Leur DA, 1962. Some effects of the unsaturated zone on nonsteady free-surface groundwater flow as studied in a sealed granular model. *J. Geophysical Research* **67**(11): 4347–4362.
- Kraijenhoff van de Leur DA, 1958. A study of non-steady groundwater flow with special reference to a reservoir coefficient. *De Ingenieur* **70**: 87–94.
- Kroes JG, van Dam JC, Huygen J, Vervoort RW, 1998. *User's Guide of SWAP Version 2.0*. Tech. rep., DLO-Staring Centre, Wageningen.
- Kumar D, Ahmed S, 2003. Seasonal behaviour of groundwater level in a granitic aquifer in monsoon climate. *Current Science* **84**(25): 188–196.
- Lal AMW, 2000. Numerical errors in groundwater and overland flow models. *Water Resources Research* **36**(5): 1237–1247.
- Lall U, Sharma A, 1996. A nearest neighbor bootstrap for resampling hydrologic time series. *Water Resources Research* **32**(3): 679–693.
- Leonard R, 1999. Climate change and groundwater, predicting how changes in the hydrological cycle affect water resources. *The Aquifer* **14**(2).
- Lewis MA, Jones HJ, Macdonald DMJ, Price M, Barker JA, Shearer TR, Wesselink AJ, Evans DJ, 1993. *Groundwater storage in British aquifers: Chalk*. National Rivers Authority.
- Lloyd-Hughes B, 2002. *The Long-Range Predictability of European Drought*. Ph.D. thesis, University College London.
- Loucks DP, 1997. Quantifying trends in system sustainability. *Hydrological Sciences J.* **42**(4): 513–530.
- Maier HR, Lence BJ, Tolson BA, Foschi RO, 2001. First-order reliability method for estimating reliability, vulnerability and resilience. *Water Resources Research* **37**(3): 779–790.
- Marani M, Eltahir E, Rinaldo A, 2001. Geomorphic controls on regional base flow. *Water Resources Research* **37**(10): 2619–2630.
- Marsh TJ, Monkhouse RA, Arnell NW, Lees ML, Reynard NS, 1994. *The 1988-92 Drought*. Institute of Hydrology, Wallingford, UK.
- McDonald MG, Harbaugh AW, 1988. *A Modular Three-Dimensional Finite Difference Ground-Water Flow Model*. United States Geological Survey.
- McDonald MG, Harbaugh AW, 1996. *User's Documentation for MODFLOW-96, an Update to the U.S. Geological Survey Modular Finite-Difference Ground-Water Flow Model*. United States Geological Survey.
- McMahon TA, 1993. Hydrologic design for water use. In Maidment DR (ed) *Handbook of Hydrology*, McGraw-Hill, chap. 27.
- McNab AL, Karl TR, 1991. Climate and droughts. In Paulson RW, Chase EB, Roberts RS, Moody DW (eds) *National Water Summary 1988-89 - Hydrological Events and Floods and Droughts: U.S. Geological Survey Water-Supply Paper 2375*. 89–98.
- Melloul AJ, Collin ML, 2002. Israel's 1999 drought: Its impact on groundwater and environmental systems. CWST (Center for water science and technology), Ben-Gurion University of Negev. <http://www.bgu.ac.il/cwst/water/israeldrought.htm>; access date: 30 December 2002.
- Merriam CF, 1948. Ground-water records in river-flow forecasting. *Transactions, American Geophysical Union* **29**(3): 384–386.
- Millan J, Yevjevich V, 1971. *Probabilities of Observed Droughts*. Colorado State University, Fort Collins, Colorado.

- Mizumura K, 2001. Determination of component of ground-water flow from rainfall data. *J. of Hydrologic Engineering* **6**(3): 243–250.
- Montaseri M, Adeloye AJ, 1999. Critical period of reservoir systems for planning purposes. *J. of Hydrology* **224**: 115–136.
- Moy WS, Cohon JL, ReVelle CS, 1986. A programming model for analysis of the reliability, resilience and vulnerability of a water supply reservoir. *Water Resources Research* **22**(4): 489–498.
- Musters PAD, Bouten W, 2000. A method for identifying optimum strategies of measuring soil water contents for calibrating a root water uptake model. *J. of Hydrology* **227**: 273–286.
- Nathan RJ, McMahon TA, 1990. Evaluation of automated techniques for base flow and recession analyses. *Water Resources Research* **26**(7): 1465–1473.
- National Drought Mitigation Center, 2003. Understanding your risk. [Http://www.drought-unl.edu/risk/risk.htm](http://www.drought-unl.edu/risk/risk.htm); acces date: 12 May 2003.
- Neal C, Neal M, Wickham H, Harrow M, 2000. The water quality of a tributary of the Thames, the Pang, southern England. *The Science of the Total Environment* **251-252**: 459–475.
- Olin M, 1995. Estimation of base level for an aquifer from recession rates of groundwater levels. *Hydrogeology J.* **3**(2): 40–51.
- Owen M, Robinson VK, 1978. Characteristics and yield in fissured chalk. In *Thames Ground-water Scheme, Proceedings of the Conference Held at Reading University on 12-13 April, 1978*. Institution of Civil Engineers, London.
- Pandey RP, Ramasastry KS, 2001. Relationship between the common climatic parameters and average drought frequency. *Hydrological Processes* **15**: 1019–1032.
- Panu US, Sharma TC, 2002. Challenges in drought research: Some perspectives and future directions. *Hydrological Sciences J.* **47**: s19–s30.
- Pauwels VRN, Verhoest NEC, de Troch FP, 2002. A metahillslope model based on an analytical solution to a linearized Boussinesq equation for temporally variable recharge rates. *Water Resources Research* **38**(12): 33–1–33–4. DOI: 10.1029/2001WR000714.
- Pelletier JD, Turcotte DL, 1997. Long-range persistence in climatological and hydrological time series: Analysis, modeling and application to drought hazard assessment. *J. of Hydrology* **203**: 198–208.
- Peters E, van Lanen HAJ, 2001. Environmental impact. In Demuth S, Stahl K (eds) *Assessment of the Regional Impact of Droughts in Europe. Final Report to the European Union*, Institute of Hydrology, University of Freiburg, chap. 4.5. 40–45.
- Peters E, van Lanen HAJ, 2003. Propagation of drought in groundwater in semi-arid and sub-humid climatic regimes. In Servat E, Najem W, Leduc C, Shakeel A (eds) *Hydrology of the Mediterranean and Semi-Arid Regions*. IAHS Publication no. 278, 312–317.
- Peters E, van Lanen HAJ, Bradford RB, Cruces de Abia J, Martinez Cortina L, 2001. Droughts derived from groundwater heads and groundwater discharge. In Demuth S, Stahl K (eds) *Assessment of the Regional Impact of Droughts in Europe. Final Report to the European Union*, Institute of Hydrology, University of Freiburg, chap. 4.4. 35–39.
- Polubarinova-Kochina P, 1962. *Theory of Groundwater Movement*. Princeton University Press, Princeton, N.J. Translated from Russian by R.J.M. De Wiest.
- Price M, Low RG, McCann C, 2000. Mechanisms of water storage and flow in the unsaturated zone of the Chalk aquifer. *J. of Hydrology* **233**: 54–71.
- Price M, Robertson AS, Foster SSD, 1977. Chalk permeability - a study of vertical variation using water injection tests and borehole logging. *Water Services* : 603–610.
- Querner EP, 1997. Description and application of the combined surface and groundwater model MOGROW. *J. of Hydrology* **192**: 158–188.
- Querner EP, van Lanen HAJ, 2001. Impact assessment of drought mitigation measures in two adjacent Dutch basins using simulation modelling. *J. of Hydrology* **252**: 51–64.
- Rajagopalan B, Lall U, 1999. A k-nearest-neighbor simulator for daily precipitation and

- other variables. *Water Resources Research* **35**: 3089–3101.
- Reiss RD, Thomas M, 1997. *Statistical Analysis of extreme values, from insurance, finance, hydrology and other fields*. Birkhäuser Verlag, Basel.
- Rice SO, 1954. Mathematical analysis of random noise. In Wax N (ed) *Selected Papers on Noise and Stochastic Processes*, Dover, New York. 133–294.
- Ritzema HP (ed) 1994. *Drainage Principles and Applications*. ILRI Publication no. 16.
- Robins NS, Calow RC, Macdonald AM, Macdonald DMJ, Gibbs BR, Orpen WRG, Mtembezeka P, Andrews AJ, Appiah SO, Banda K, 1997. *Final Report - Groundwater Management in Drought-Prone Areas of Africa*. Tech. Rep. BGS Report WC/97/57, British Geological Survey.
- Rodriguez-Iturbe I, Valdez JB, 1979. The geomorphologic structure of hydrologic response. *Water Resources Research* **15**(6): 1409–1420.
- Rorabaugh MI, 1964. Estimating changes in bank storage and ground-water contribution to streamflow. In *Symposium on Surface Waters*. International Association of Scientific Hydrology, 432–441.
- Ruiz García JM, 1998. *Desarrollo de un Modelo Hidrológico Conceptual Distribuido de Simulación Continua Integrado con un SIG (Development of a Distributed Conceptual Hydrological Model for Continuous Simulation Integrated with a GIS)*. Ph.D. thesis, Universidad Politécnica de Valencia, Valencia, Spain.
- Rushton KR, Connorton BJ, Tomlinson LM, 1989. Estimation of the groundwater resources of the Berkshire Downs supported by mathematical modelling. *Quarterly J. of Engineering Geology* **22**: 329–341.
- Santos MJ, Goncalves-Henriques A, 1999. Characterisation of meteorological drought in Mozambique. In *Proceedings of the International Conference on Integrated Drought Management: Lessons for Sub-Saharan Africa. 20-22 September 1999, Pretoria, South-Africa*. IHP-V, Technical Documents in Hydrology, No. 35, 99–109.
- Savenije HHG, 2001. Equifinality, a blessing in disguise? *Hydrological Processes* **15**: 2835–2838.
- Scheidleder A, Grath J, Winkler G, Stärk U, Koreimann C, Gmeiner C, Nixon S, Casillas J, Gravesen P, Leonard J, Elvira M, 1999. *Groundwater Quality and Quantity in Europe*. European Environment Agency.
- Schneider RL, 2001. Watershed approaches to ameliorating floods and droughts: The U.S. perspective. In van Es H, Húška DH (eds) *Environmental Management of the Rural Landscape in Central and Eastern Europe*, Slovak Agricultural University, Nitra, Slovakia.
- Schürch M, Buckley D, 2002. Integrating geophysical and hydrochemical borehole-log measurements to characterize the Chalk aquifer, Berkshire, United Kingdom. *Hydrogeology J.* **10**: 610–627. DOI: 10.1007/s10040-002-0220-x.
- Seely M, 1999. Climate variability: Implications for sustainable natural resource management. In *Proceedings of the International Conference on Integrated Drought Management: Lessons for Sub-Saharan Africa. 20-22 September 1999, Pretoria, South-Africa*. IHP-V, Technical Documents in Hydrology, No. 35, 123–132.
- Sharma TC, 1997. A drought frequency formula. *Hydrological Sciences J.* **42**(6): 803–814.
- Sharma TC, 1998. An analysis of non-normal Markovian extremal droughts. *Hydrological Processes* **12**: 597–611.
- Sherlock RL, 1960. *London and Thames Valley*. H.M.S.O., London (UK).
- Sherman LK, 1932. The relation of hydrographs of runoff to size and character of drainage basins. *Amer. Geophys. Union Trans* : 332–339.
- Shiva V, 1991. *Ecology and the politics of survival, conflicts over natural resources in India*. United Nations University Press, Sage Publications, New Delhi.
- Shukla S, Mostaghimi S, Petrauskas B, Al-Smadi M, 2000. Multivariate technique for baseflow separation using water quality data. *J. of Hydrologic Engineering* **5**(2): 172–179.
- Singh KP, 1968. Some factors affecting base flow. *Water Resources Research* **4**(5): 985–999.

- Smakhtin VU, 2001. Low flow hydrology: a review. *J. of Hydrology* **240**: 147–186.
- Soil Survey and Land Research Center, 1995. *SEISMIC user manual*. Soil Survey and Land Research Center, Cranfield University, Silsoe, UK.
- Soil Survey of England and Wales, 1983. Soils of south-east England. Sheet 6 of the 1:250,000 soil map series.
- Soley RWN, Heathcote JA, 1998. Recharge through the drift: A study of contrasting Chalk catchments near Redgrave Fen, UK. In Robins NS (ed) *Groundwater Pollution, Aquifer Recharge and Vulnerability*. Geological Society, London, Special Publications, 129–141.
- Sophocleous M, 1997. Managing water resources systems: Why "safe yield" is not sustainable. *Ground Water* **35**(4): 561.
- Spongberg ME, 2000. Spectral analysis of base flow separation with digital filters. *Water Resources Research* **36**(3): 745–752.
- Stahl K, 2001. *Hydrological Drought - a Study Across Europe*. Ph.D. thesis, Institut für Hydrologie der Universität Freiburg i. Br., Freiburg, Germany.
- Stedinger JR, Vogel RM, Foufoula-Georgiou E, 1993. Frequency analysis of extreme events. In Maidment DR (ed) *Handbook of Hydrology*, McGraw-Hill, chap. 18.
- Stein A, 1998. Geostatistical procedures for analysing spatial variability and optimizing collection of monitoring data. In van Lanen HAJ (ed) *Monitoring of Groundwater Management in (Semi-)Arid Regions*. United nations educational, scientific and cultural organization, Paris, 91–106.
- Svoboda M, Lecomte D, Hayes M, Heim R, Gleason K, Angel J, Rippey B, Tinker R, Palecki M, Stooksbury D, Miskus D, Stephens S, 2002. The drought monitor. *Bulletin of the American Meteorological Society* **83**(8): 1181–1190.
- Swistock B, 2002. Penn state groundwater expert urges 'take drought seriously'. Pennstate News, February 26, 2002. [Http://aginfo.psu.edu/News/february02/drought.html](http://aginfo.psu.edu/News/february02/drought.html); access date: 30 December 2002.
- Tallaksen LM, 1995. A review of baseflow recession analysis. *J. of Hydrology* **165**: 349–370.
- Tallaksen LM, 2000. Streamflow drought frequency analysis. In Vogt JV, Somma F (eds) *Drought and Drought Mitigation in Europe*. Kluwer Academic Publishers, 103–117.
- Tallaksen LM, van Lanen HAJ, 2004. *Hydrological Drought: Processes and Estimation Methods for Streamflow and Groundwater*. Elsevier.
- Thompson N, Barrie IA, Ayles M, 1981. *The Meteorological Office Rainfall and Evaporation Calculation System: MORECS*. Meteorological Office, UK.
- Troch P, de Troch F, Brutsaert W, 1993. Effective water table depth to describe initial conditions prior to storm rainfall in humid regions. *Water Resources Research* **29**(2): 427–434.
- Uijlenhoet R, de Wit MJM, Warmerdam PMM, Torfs PJJF, 2001. *Statistical Analysis of Daily Discharge Data of the River Meuse and its Tributaries (1968-1998): Assessment of Drought Sensitivity*. Sub-department Water Resources, Wageningen University, Wageningen, The Netherlands.
- van Dam J, Huygen J, Wesseling J, Feddes RA, Kabat P, van Walsum P, Groenedijk P, van Diepen CA, 1997. *Theory of SWAP, Simulation of Water Flow, Solute Transport and Plant Growth in the Soil-Water-Atmosphere-Plant Environment*. Wageningen. Tech. rep., Department of Water Resources, WAU and DLO Winand Staring Centre.
- van de Griend AA, de Vries JJ, Seyhan E, 2002. Groundwater discharge from areas with a variable specific drainage resistance. *J. of Hydrology* **259**: 203–220.
- van Geer FC, 1994. *Spatial Variability in the Groundwater Head in Areas with a Controlled Surface Water Level (Original Title: Ruimtelijke Variabiliteit in de Grondwaterstand in Gebieden Met Een Beheerst Peil)*. Tech. Rep. OS 92-111A, Instituut voor Grondwater en Geo-Energie.
- van Lanen HAJ, Clausen B, Kašpárek L, 1993. Interaction between low flows and hydrogeology. In Gustard A (ed) *FRIEND, Volume I Hydrological Studies*. Institute of Hydrology, Wallingford, 21–55.

- van Lanen HAJ, Peters E, 2000. Definition, effects and assessment of groundwater droughts. In Vogt JV, Somma F (eds) *Drought and Drought Mitigation in Europe*. Kluwer Academic Publishers, 49–61.
- van Lanen HAJ, Peters E, 2002. Temporal variability of recharge as an indicator for natural groundwater droughts in two climatically contrasting basins. In van Lanen HAJ, Demuth S (eds) *FRIEND2002 - Regional Hydrology: Bridging the Gap Between Research and Practice*. IAHS Publication no. 274, 101–108.
- van Lanen HAJ, Weerts AH, Kroon T, Dijkema R, 1996. Estimation of groundwater recharge in areas with deep groundwater tables using transient groundwater flow modelling. In *Proc. Int. Conf. On 'Calibration and Reliability in Groundwater Modelling', September 1996, Golden, USA*. 307–316.
- Vaz AC, 1986. Reliability in water resources planning. In Valadares Tavares L, Evaristo Da Silva J (eds) *Systems Analysis Applied to Water and Related Land Resources. Proceedings of the IFAC Conference, Lisbon, Portugal, 2-4 October 1985*. Pergamon Press, Tarrytown, N.Y.
- Vereniging Voor Landinrichting, 1992. *Cultuurtechnisch Vademecum*. Vereniging Voor Landinrichting, Werkgroep Herziening Cultuurtechnisch Vademecum, Utrecht. (in Dutch).
- Vogel RM, Kroll CN, 1992. Regional geohydrologic-geomorphic relationships for the estimation of low-flow statistics. *Water Resources Research* **28**(9): 2451–2458.
- Vogel RM, Kroll CN, 1996. Estimation of baseflow recession constants. *Water Resources Management* **10**: 303–320.
- Vrugt JA, Bouten W, Weerts AH, 2001. Information content of data for identifying soil hydraulic parameters from outflow experiments. *Soil Science Society Am. J.* **65**: 19–27.
- Ward RC, Robinson M, 2000. *Principles of Hydrology*. McGraw-Hill, Maidenhead, UK.
- Warren GD, 1994. Drought in the south - implications for the management of groundwater resources. In Reeve C, Watts H (eds) *Groundwater - Drought, Pollution and Management*. Balkema, Rotterdam (NL).
- Watermark Computing, 1998. *PEST, Model Independent Parameter Estimation (Users Manual)*. Watermark Computing.
- Weerts AH, Huisman JA, Bouten W, 2001. Information content of time domain reflectometry waveforms. *Water Resources Research* **37**(5): 1291–1299.
- White I, Falkland T, Scott D, 1999. Droughts in small coral islands: Case study, South Tarawa, Kiribati. IHP-V, Technical Documents in Hydrology, No. 26.
- Willhite DA, 1999. Drought preparedness in the sub-Saharan Africa context. In *Proceedings of the International Conference on Integrated Drought Management: Lessons for Sub-Saharan Africa. 20-22 September 1999, Pretoria, South-Africa*. IHP-V, Technical Documents in Hydrology, No. 35, 22–36.
- Willhite DA, 2000. *Droughts, a Global Assessment*. Hazards and Disasters: A Series of Definitive Major Works, Routledge, New York.
- Willhite DA, Glantz MH, 1985. Understanding the drought phenomenon: The role of definitions. *Water International* **10**: 111–120.
- Wittenberg H, 1999. Baseflow recession and recharge as nonlinear storage processes. *Hydrological Processes* **13**(5): 715–726.
- Wittenberg H, Sivapalan M, 1999. Watershed groundwater balance estimation using streamflow recession analysis and baseflow separation. *J. of Hydrology* **219**: 20–33.
- Wójcik R, Beersma JJ, Buishand TA, 2001. *Rainfall Generator for the Rhine Basin. Multi-Site Generation of Weather Variables for the Entire Drainage Basin*. Dutch Royal Meteorological Society (KNMI), De Bilt.
- Wójcik R, Buishand TA, 2003. Simulation of 6-hourly rainfall and temperature by two resampling schemes. *J. of Hydrology* **273**: 69–80.
- Woo MK, Tarhule K, 1994. Streamflow droughts of northern Nigerian rivers. *Hydrological Sciences J.* **39**(1): 19–34.
- Wösten JHM, Lilly A, Nemes A, Le Bas C, 1998. *Using Existing Soil Data to Derive*

- Hydraulic Parameters for Simulation Models in Environmental Studies and in Land Use Planning*. Tech. rep., DLO-Staring Centre, Wageningen.
- Wyness AJ, Rippon PW, Wardlaw RB, 1994. Application of an integrated model to Chalk catchments. In Reeve C, Watts H (eds) *Groundwater - Drought, Pollution and Management*, Balkema, Rotterdam (NL).
- Yamaguchi M, Hatada Y, 2001. Stratified sampling technique in the extreme value analysis. In van Gelder P, Roos A, Vrijling H (eds) *Risk-Based Design of Civil Structures*. Proceedings of a One-Day Workshop at the Subfaculty of Civil Engineering on January 11, 2000.
- Yevjevich V, 1967. *An objective approach to definition and investigations of continental hydrologic droughts*. Hydrology Papers, No. 23, Colorado State University, Fort Collins.
- Yevjevich V, 1968. Misconceptions in hydrology and their consequences. *Water Resources Research* **4**(2): 225–232.
- Younger PL, 1989. Devensian periglacial influences on the development of spatially variable permeability in the Chalk of southeast England. *Quart. J. of Eng. Geology* **22**: 343–354.
- Yu Z, Schwartz FW, 1999. Automated calibration applied to watershed-scale flow simulations. *Hydrological Processes* **13**: 191–209.
- Zaidman MD, Rees HG, Young AR, 2001. Spatio-temporal development of streamflow droughts in north-west Europe. *Hydrology and Earth System Sciences* **5**(4): 733–751.
- Zecharias YB, Brutsaert W, 1988. The influence of basin morphology on groundwater outflow. *Water Resources Research* **24**(10): 1645–1650.

Curriculum Vitae

Elisabeth Peters, 24 december 1973, Nijmegen

- | | |
|--------------------|---|
| 1986-1992 | VWO, 'SERVIAM' R.K. scholengemeenschap
Lyceum-Havo te Sittard |
| 1992-1998 | Studie Bodem, water en atmosfeer, specialisatie
Hydrologie en Waterbeheer, Wageningen Universiteit |
| 6-1998 t/m 10-1998 | Project-medewerker bij RIZA (Rijksinstituut voor
Integraal Zoetwaterbeheer en Afvalwaterbehandeling),
Afdeling Watersystemen. |
| 11-1998 t/m 8-2003 | AIO vakgroep Waterhuishouding,
Wageningen Universiteit. |